The University Of Sheffield.

Wheel/Rail Contact Tribology: Characterising Low Adhesion Mechanisms and Friction Management Products

Luke Evelyn Buckley-Johnstone

May 2017

Thesis submitted for the Degree of Doctor of Philosophy

Department of Mechanical Engineering

Summary

Friction management and control of adhesion at the wheel/rail interface is vital for an efficient and cost effective railway network. The understanding of how the friction management products (grease and friction modifiers) work and effectively test these products is necessary to improve the performance of a railway network.

The papers presented concern the effective benchmarking of wayside curve lubricants (grease) in a twin disc test rig. They compare the effectiveness of several greases in respect to adhesion, wear protection and retentivity (number of cycles of adequate lubrication). A new method for assessment of grease carry down has been trialled in the field. The modified pendulum was able to detect the difference between a dry and lubricated rail gauge face.

Top of rail friction modifiers (TOR-FMs) have been tested at two different laboratory test scales. The results showed the difference in operational behaviour of the chosen TOR-FM when used in a laboratory versus the field.

The ‘wet-rail’ phenomena, where low adhesion as a result of water on the rail head, has been investigated at two scales of laboratory test and results have been used to generate a model to predict adhesion coefficients for a range of water and iron oxide mixtures. The results presented show how the addition of small amounts of water to a wheel/rail contact can cause reduced adhesion to ‘low/ultra-low’ levels when combined with third body materials (iron oxides, wear debris etc.).

A novel treatment method to protect the rail head using hydrophobic solutions was investigated using twin disc and pendulum testing. Tests showed that these products, when sufficiently diluted, do not reduce friction to dangerous levels or isolate the vehicle from the track circuit. However, the benefits of use in the field are questioned.

Thanks

First and foremost I would like to thanks Professor Roger Lewis who supported me and made this thesis possible.

For those who helped in every aspect of this piece of work; Dave Butcher Stephen Lewis, Hiroyuki Suzuki, Matt Harmon, Guiseppe Tronci, Martin Evans, Klaus Six, Gerald Trummer and Petr Voltr, Apologies to those I have missed.

To my partner Erin for all her support and guidance without which I would have been at a loss.

To my family; my pops Nicolas, my mum Barbara (I love and miss you), my brothers Edward, Jacob and Benedict, my Granddad John, Big John, Judith and Aphra, my Aunt Mog and Uncle Dick, my Aunt Janet and Uncle Ed, my Aunt Maureen and Uncle Bruce.

Again, to my pops Jed who raised me and guided me. You are the best.

To my friends Alex Keyte, Liam Power, Greg Kirkham, Stefan Bird, Tom Sara, Tom Facer, Tim Beech, Rob Wannop, Tom Reeves, Alex Buckman, Emily Nix, Richard Jeffs, and Jonathan Stephenson. Cheers guys, you are all great people.

Table of contents

1. Introduction

Increasing demands on the United Kingdom's (UK) rail network, as well as those worldwide, have led to more pressure on the infrastructure to deliver consistent and safe transport. To meet these demands, a more predictable network must be created by extending maintenance intervals, increasing component life (particularly of rail and wheels), reducing energy consumption, reducing acceleration and braking distances whilst improving reliability. These goals can be achieved by improving one component of a railway system: the wheel/rail contact.

Since the 1970s, the new passenger type vehicles that have been introduced on the UK network have increased in weight per meter (Network Rail, 2011). All forces that are required to start, stop and steer trains are transmitted through the contact patch formed by a steel-wheel on a steel-rail, which is roughly the size a coin (1 cm^2) (Lewis, 2006a). The contact is highly variable and depends on many factors such as wheel/rail profile, vehicle type (weight) and curve radii creating highly variable conditions of contact. All damage, instantaneous or gradual, to the wheel/rail is related to this open tribological-system.

Rail transport is more energy efficient and has lower CO_2 emissions than the road alternatives for both passenger and freight transportation. This can be attributed to the low energy required at the contact interface between the wheel and rail when compared to a rubber tyre on a Tarmac road. However, unlike rubber tyres, which are able to maintain contact with the road surface through the tyre's tread, this contact can be easily affected by the introduction of a small amount contaminant.

It is the control of this tribological system that can be used to manage the wheel/rail contact. This can be done through the design of wheel/rail profiles, material selection and introduction of third body materials (grease, sand, friction modifiers) to control friction. The control of friction can be used to reduce wear, increase tractive/adhesive forces in braking and acceleration, reduce noise and control rolling contact fatigue (RCF). As this is an open system, a number of unwanted or uncontrollable factors can have a considerable affect. For example, oil on the top of rail may cause a wheel slide during braking.

Contaminants that are found in a wheel/rail contact have been previously grouped into three categories: *climatic, operational* and *transported* bodies (Descartes, 2005). *Climatic* bodies include water and leaves. *Operational* bodies include lubricating oils, sand and ballast material. *Transported* bodies include any products that are carried on freight. Additionally, Descartes has separated the *'natural'* contaminants arising from the wheel rolling over the rail, such as consistently present wear debris (Descartes, 2008). These contaminants form the *third body layer* on the rail head and can be both advantageous and detrimental in the management of the railway (Lewis, 2012).

Friction management is a part of a whole systems approach to the systematic management of the wheel/rail interface. This approach to managing the

wheel/rail contact includes the materials of the wheel and rails, the vehicle dynamics and the contact mechanics as visualized in Figure 1(Kalousek, 1996).

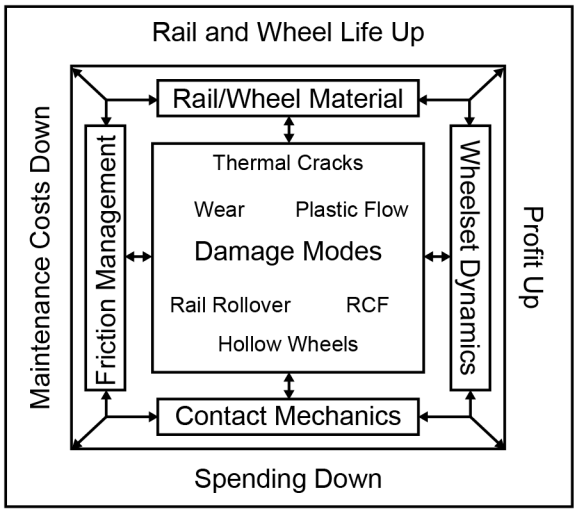

Figure 1: Visualisation of a systematic approach to wheel/rail interface management (Kalousek, 1996).

“Friction modifiers” is a broad term used in the railway industry to describe products that are designed to be used to treat rail heads to reduce energy consumption and suppress noise by controlling the friction at the wheel/rail interface (Stock, 2016).

1.1. Aims and objectives

The objective of this thesis is to explore the effects that third body materials have on the tribological system of the wheel-rail contact. Four different third body materials have been investigated separately and are each dealt with individually. The broad theme between all conducted experiments has been how to best select appropriate tribological test methods to investigate behaviour of specific third bodies; what the applicable tribological performance data needed to be gathered is and how this information can be used to inform railway operators in the selection of appropriate course of action for wheel/rail interface management.

Laboratory and field-testing of applied products (grease and friction modifiers) were carried out to help better understand and improve product selection.

1. Wayside greases

The currently standards for railway grease do not require tests that accurately represent the conditions the grease will be subjected to in the field. It is necessary to select an appropriate test method that can analyse the key tribological features for wheel/rail gauge corner contact. Experiments have been completed using a twin disc test set-up to compare the performance of several commercially available greases. This is used to define a standardize

laboratory test methodology able to differentiate between several commercially available products.

Additionally, grease performance in the field is poorly quantified. Measurements of rail profile change can be readily made over multiple site visits and wear can be monitored to give a grease performance over time. However, these measurements give no information on whether grease is present on the rail at the time. The aim was to develop a device to improve the measurement of grease performance in the field over the current visual inspection through gauge corner friction measurements.

2. Top of rail friction modifiers

The aim was to design a test methodology to examine the frictional development of a top of rail friction modifier (TOR-FM) (a product designed to give intermediate friction levels at tread contact) when subjected to repeated axle passes. The performance requirements of a TOR-FM require an intermediate friction level to be sustained on the railhead for multiple train passes and understanding how these product develop in the laboratory is critical to informing their use in the field.

The objective is to measure and understand the effects that test scale has on the performance of a TOR-FM using a full-scale wheel/rail test stand and a scaled wheel/rail contact in a twin disc test rig.

3. Water and iron oxides

The aim was to develop experiments to investigate the hypothesis that water, in combination with iron oxides, can severely reduce adhesion between the wheel/rail and to understand and define the conditions that promote adhesion reduction to define possible mitigation options.

Laboratory test of oxide water mixtures in a highly controllable laboratory High Pressure Torsion (HPT) rig recently commissioned at the University of Sheffield. The tests compared adhesion between wheel/rail specimens in the presence of different ratios of water-iron oxide mixtures. Results were used to better understand the shearing process of these mixtures and an adhesion model developed.

Using the information from HPT tests and the adhesion model a set of full-scale tests were defined and conducted. This allowed adhesion measurement on a fully representative wheel/rail contact. Water flow rates were varied to investigate these water and iron oxide mixtures.

In parallel a wheel/rail adhesion model was developed using the test data and a paper detailing this is included for clarity and context.

4. Hydrophobic solutions

Finally, an investigation into alternative solutions to mitigate against low adhesion using hydrophobic solutions to treat the rail head has been completed. Two sets of tribological test set-ups have been used to investigate adhesion and adhesion change over time.

1.2. Thesis layout

Several papers are presented to further academic and industrial knowledge of the wheel/rail interface and effects of third body materials on adhesion/traction. These papers can be broadly spilt between the following hierarchical topics:

1. Benchmarking of applied products used to treat the rail head
2. Causes and mitigation of low adhesion

Paper 1 and a section of Paper 2 examine the performance of railway-specific grease. The first paper examines the use of scaled laboratory testing to evaluate a variety of greases. The second paper measures the presence of a lubricant on the gauge face of the rail head using a new adapted pendulum test rig has been tested in both laboratory and field settings.

These papers form part of a series of tests evaluating the whole life of grease against standards when used to lubricate the rail gauge face. Other work has been completed at the University of Sheffield to examine pumpability (ability of the grease to be readily pumped out of an applicator bar and remain in place over a range of temperatures), pick-up (the effect of lateral shift and wheel flange-grease bulb interaction and transfer) and carry-down (how far the grease is deposited along the high rail of a curve).

These test methods have been developed to contribute to product approval standards for Network Rail. In addition to the laboratory test methods, two field investigations were carried out to assess the use of an adapted pendulum test foot as a measure of grease/oil presence and carry down. This new method has been shown to be useful as an indicator of gauge face friction when making an assessment of lubricant carry down.

Paper 3 examines friction modification products and the methods of assessing and benchmarking products and completed using different scales of test method. Comparison between products tested on different laboratory test scales showed comparable rankings of product performance; however, the absolute values of adhesion were not the same.

Papers 4, 5 and 6 are part of a work package to investigate the ‘wet rail’ phenomenon, building and understanding of low adhesion due to water in the wheel/rail contact. Paper 4 details the use of a newly developed High Pressure Torsion (HPT) test rig at the University of Sheffield to investigate the effect of low amounts of water and water/iron oxide mixtures. An adhesion model was used to understand the difficulties experienced when replicating low adhesion in the laboratory. Paper 5 details laboratory testing in a full-scale tram wheel rig to investigate the findings from HPT and adhesion model. Paper 6 presents the final adhesion curve model created to model water and oxide mixtures in the wheel/rail contact.

Finally, a novel low adhesion mitigation method using hydrophobic fluids has been investigated in Paper 7.

Full details of the listed papers are given in Table 8, which can be found after the literature review. The table details the author’s contributions to each body of work.

2. Literature review

The worked outlined in this thesis will look at effective ways to benchmark the operationally applied products in a laboratory setting and the cause of low adhesion and its mitigation. The literature review will include standards currently in use for the selection of grease and friction modifiers for use on the UK network. In addition, the causes of low adhesion and conditions that contribute to adhesion loss will also be reviewed.

2.1. Wheel/rail contact

The UK network has a standard gauge of 1435 mm and rails inclined at 1:20, as shown in Figure 2. The inclined rail, along with rail and wheel profile design, ensures forces are transmitted through the web of the rail. Many different wheel and rail profiles with varying run-in states can be found in the UK, which leads to difficulty in defining a standard wheel/rail contact.

Cant is often introduced between the two rails in a curve to reduce lateral acceleration experienced by passengers, chance of a vehicle over turning and lateral force exerted on the rail. Cant is measured as the super elevation in millimetres and defined as the height difference between the rail heads across the wheelset gauge. In a curve, the inner rail is called the low rail and the outer rail the high rail.

All vehicles in the UK operate with fixed axles, meaning that the wheels do not rotate independently. The ‘steering’ of a vehicle is a product of the coned wheel profiles. This profile, coupled with a fixed rail gauge, produces different contact patches between the two wheel/rail contacts when a lateral shift is introduced during a curve.

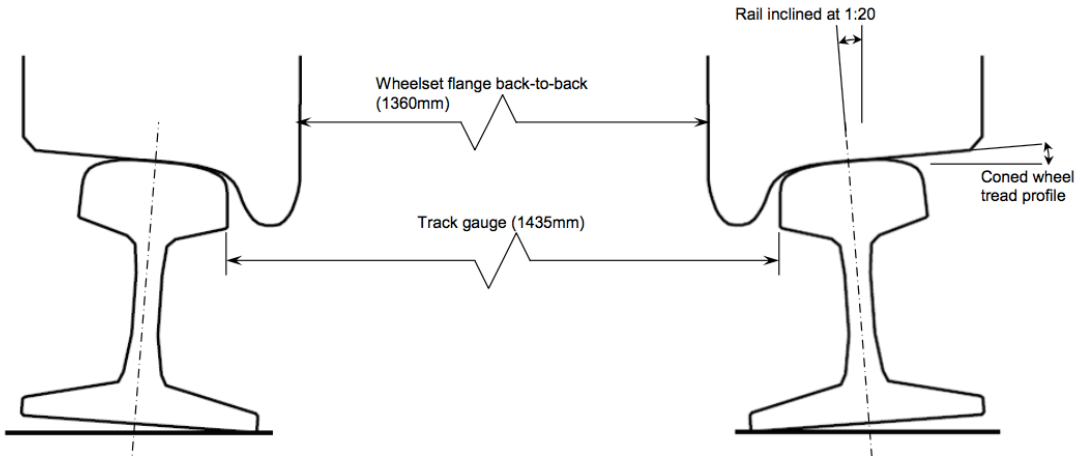

Figure 2: UK railway specifications showing track gauge and rail inclination (Burstow, 2011).

To explain the different contact zones and the method of a fixed axle navigating, a curve the following generalised scenario has been used. Figure 3 shows the affect of a lateral shift on the rolling radius difference (RRD) and how a wheelset navigates a fixed radius curve. Steering forces are the function of the wheel/rail profile, track curvature and lateral shift experienced

as the vehicle travels down the track. As a wheelset has mirror symmetry, this lateral shift causes the effective radius of one wheel to increase and the other to decrease.

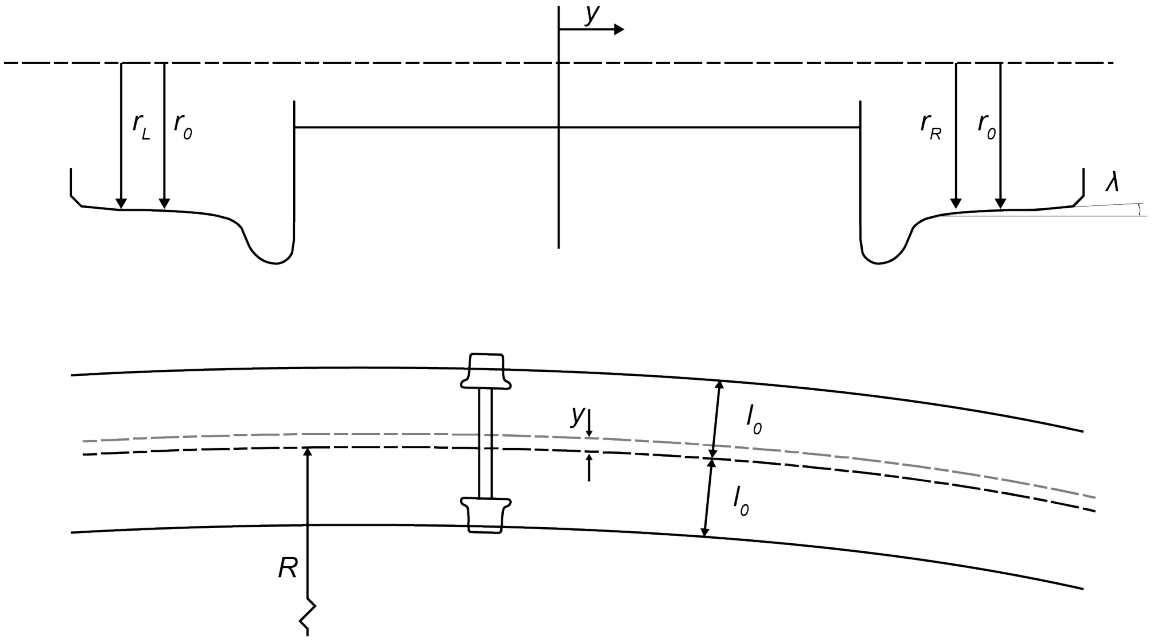

Figure 3: Lateral shift and rolling radius difference in steering a curve.

A simple calculation resulting in Equation 1 can be made to estimate the lateral shift required to produce a RRD sufficient to navigate a curve of a given radius.

$$r_L = r_0 - \lambda y$$
$$r_R = r_0 + \lambda y \quad (1)$$
$$Rolling\ radius\ difference = r_R - r_l = 2\lambda y$$

where, r_0 is the nominal radius, $r_{L/R}$ are the rolling radius of the left and right wheel resulting from a lateral shift y, R is the radius of the curve, and λ is the conicity (for example a 1:20 cone would have a conicity of 0.05).

Calculating the lateral displacement (y) results in Equation 2 and is required for a specific radius curve R:

$$y = \frac{r_o l_o}{\lambda R} \quad (2)$$

where, l_0 is distance from an imaginary centre line between the contact patches with zero lateral shift (the wheelset gauge).

The introduction of the RRD allows the outer wheel to travel further than the inner wheel. It must be noted that in practice, wheelset displacement is also a function of whether the axle is leading or trailing, as leading axles produce different contact forces than trailing axles.

2.1.1. Contact zones

As stated, the contact between a wheel and rail can be highly variable. Tournay categorised three main types of contact zone (Tournay, 2001), as shown in Figure 4. The shift between zones is depended on the wheel/rail profiles, degree of curvature and whether wheel is on the high or low rail.

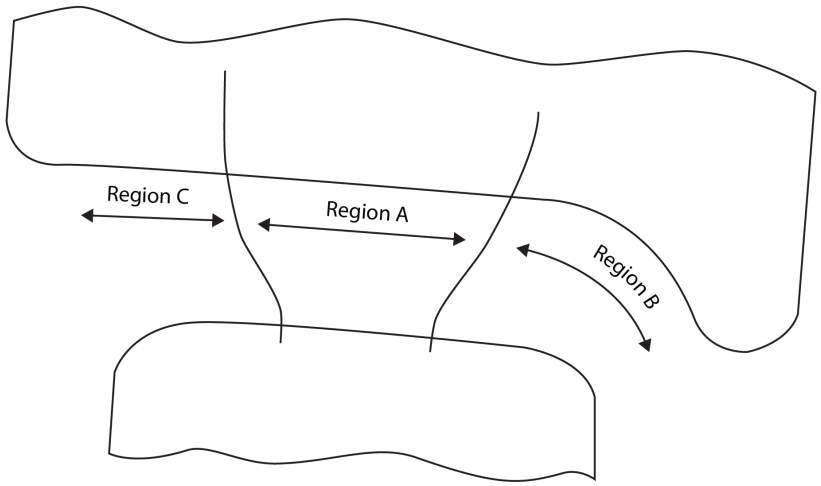

Figure 4: **Schematic representation of wheel/rail contact zones of the wheel/rail contact. Drawing adapted by Lewis (2007) from Tournay (2001)**

- Region A - Wheel tread/rail head;
- Region B - Wheel flange/rail gauge face;
- Region C - Field side.

Contact conditions vary with each contact region, where some produce contact over more than a single point. Contact region 'A' is the typical contact as a train moves along tangent track. This zone produces the lowest contact stresses and small lateral forces. In tangent tracks both wheel/rail contacts across a wheelset will likely fall into region A

Contact region 'B' occurs on tight radius curves between the rail gauge and wheel flange of the high rail and produces a more severe contact stresses due to a reduction in contact area and significantly higher wear rates. Two-point contact can occur in region 'B' if wear is too severe. Contact region 'C' occurs least often and can lead to high wear due to the contact size being small.

The UK network has many vehicle types using the network, meaning highly variable contact conditions with different vehicle sizes and wheel profiles in different stages of profile degradation. Wear of both wheel and rail form different worn-in profiles which affects the contact zone and other contact parameters.

2.1.2. Contact pressure

The shift between contact regions leads to a change in the contact dimensions owing to the wheel/rail profiles. This means that different levels of stress and contact pressures are associated with each of the contact regions.

Wheel/rail contact pressures have been plotted against sliding speeds by Jendel (2000). Figure 5 shows contact pressures and sliding velocities of the first and second wheels calculated for a specific curve using Medyna dynamics software. This figure highlights the difference in contact pressures between the three possible regions of contact from Figure 4, with Region C conditions being far more severe, both in terms of contact pressure and sliding speed.

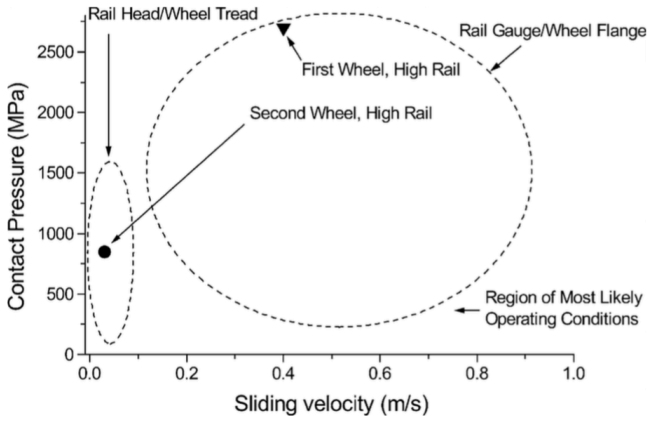

Figure 5: Contact pressures and sliding velocities of typical contact zones in the wheel/rail contact (Jendel, 2000)

Much research has been conducted into the analysis and prediction of the wheel/rail contact area and pressures through numerical methodologies Telliskivi carried out a comparison between different contact models (Telliskivi, 2001), as shown in Figure 6.

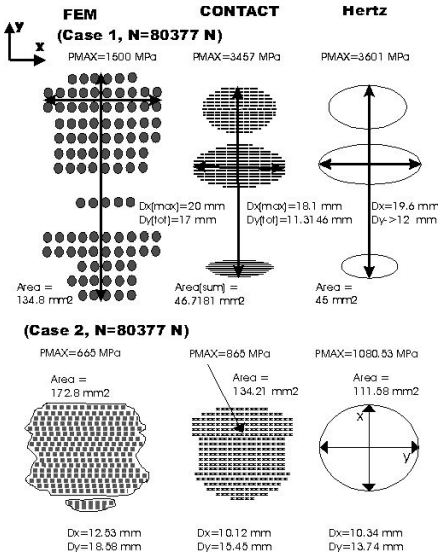

Figure 6: Comparison of contact models of wheel/rail contacts (Telliskivi, 2001)

Differences in predicted contact areas, and subsequently pressures, has been found between models. Large differences can be seen between models which predict for gauge corner contact (Case 1 in Figure 5), where the contact stresses are predicted to be dramatically lower when using finite element modeling (FEM). It has been suggested that these differences arise in part due to the Hertz contact being limited by the elastic half-space assumption, where other models factor the displacement.

2.1.3. Friction and creep

Sinclair proposed a set of *ideal* friction levels by region of contact (Sinclair, 2004), shown in Figure 7. These are the levels of friction that need to be met in friction management. These friction levels are specified by region because what is right for one may be detrimental to another. Low friction between the wheel flange and rail gauge is needed to reduce wear but intermediate friction between the wheel tread and rail head is required to achieve braking and traction. That being said, these levels exceed those expected in pure rolling. The requirements of the friction coefficient for the adhesion levels required in braking and acceleration have been given as μ = 0.1 and μ = 0.25, respectively.

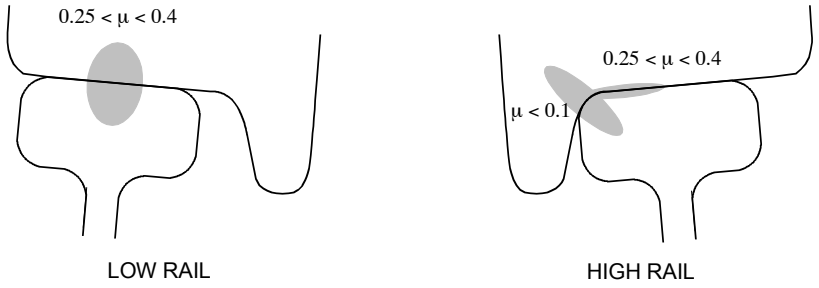

Figure 7: Ideal friction coefficients in the wheel/rail contact (Sinclair, 2004).

The friction coefficient could be, and often is, more correctly called the *traction coefficient*. This is due to the wheel/rail contact patch being a combination of a rolling/sliding interaction. For consistency, the term *friction coefficient* will be used throughout this thesis.

The friction coefficient between two bodies in contact is the percentage of normal force, *mg*, required to initiate motion of that body whilst the other remains stationary. More accurately, this is the *static friction coefficient*, as it is the friction force required to initiate movement. The *dynamic friction coefficient* is the ratio of the normal force to friction force required to sustain the sliding motion.

The sliding friction coefficient, *μ*, is therefore simply given by Equation 3:

$$\mu = \frac{F}{N} \tag{3}$$

where *F* is the friction force*, and N* is the normal force both measured in Newtons*.*

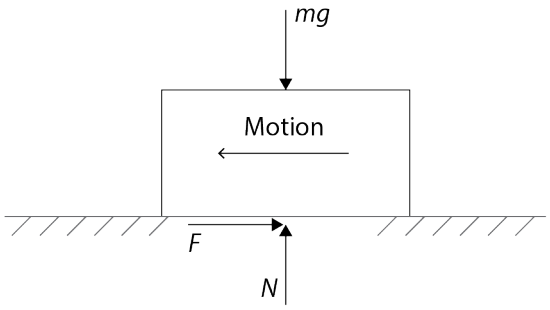

Figure 8: Friction block sliding over a stationary surface.

In a rolling contact, friction forces at the contact are generated through the difference in the forward velocity of the body and its rotational velocity, as shown in Figure 9.

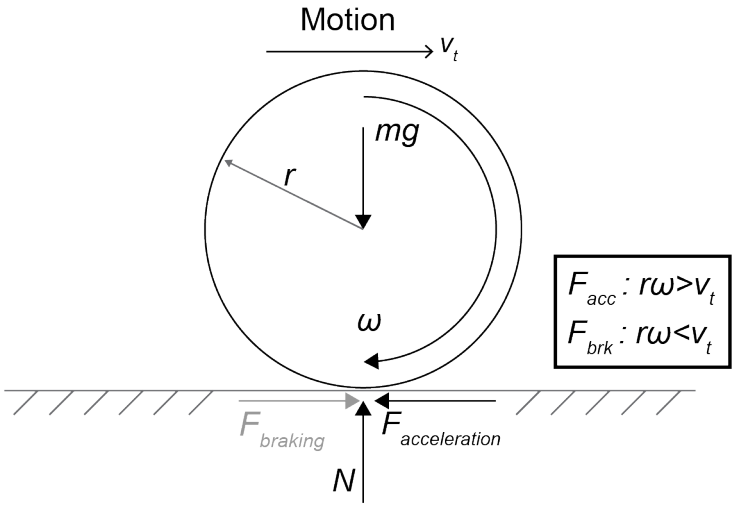

Figure 9: Free body diagram of a rolling-sliding contact showing forces in both traction and braking on the wheel.

In a pure rolling contact where the translational and rotational velocities of the wheel are equal, friction will be virtually zero. This is not entirely correct as some deformation in the contact will occur; however, low rolling resistance is one of the reasons rail travel is energy efficient. When a velocity difference is present, the ratio between these speeds is called the *creepage* or *slip* and is given by Equation 4.

$$\gamma(\%) = 100\frac{v_{rotational} - v_{translational}}{v_{translational}} = 100\frac{r\omega - v_{vehicle}}{v_{vehicle}} \tag{4}$$

where, γ is the creepage, v the velocity in m/s, r the wheel radius and ω the rotational speed of the wheel.

As a result of this equation, the contact patch is divided into areas of stick and slip. A snap shot of a contact would show the leading edge of the contact having stick, as would be found in a pure rolling, and followed by an area of

sliding. The amount of slip determines the proportions of contact in slip and stick.

Therefore, the traction coefficient is the combined frictional forces, expressed using Equation 5.

$$\mu = \frac{F_{stick} + F_{slip}}{N} \tag{5}$$

During braking, the wheel is rotating slower than the translational speed to generate a frictional force that is greater or equal to the torque being applied by the brake on the wheel, tread brake or otherwise. In acceleration, it is the rotational speed of the wheel that exceeds the translation velocity and the torque exerted multiplied by the effective radius of the wheel must not exceed the traction coefficient multiplied by the normal load of the vehicle.

This increase in slip/creep gives rise to an increase in the tractive forces (and vice versa) up until a point where the contact becomes saturated, as seen in Figure 10.

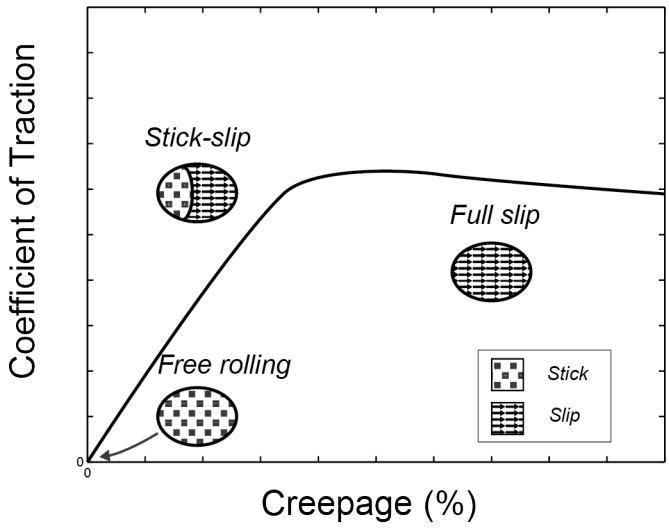

Figure 10: Slip/creepage in the wheel/rail contact against traction.

As the wheel/rail contact has a wide range of pressures (through profile design, axle load, etc.), the effect on traction is important. Several authors have produced results showing an increase of contact pressure is accompanied by the reduction of coefficient of traction (Olofsson, 2006; Zhang, 2002). This reduces the saturation point on the creep curve, as shown in Figure 11.

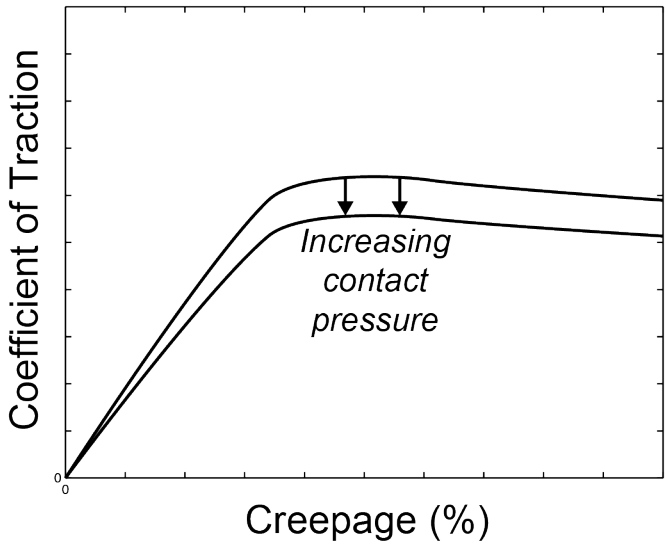

Figure 11: Schematic of the affect on the coefficient of traction by varying contact pressure.

A low friction coefficient will allow the contact conditions to stay within the elastic region of the shakedown graph. This can be done by limiting creep to avoid saturation of the contact, where the contact tractive forces are greatest, or reducing friction through lubrication in high creep contact zones (i.e. the gauge corner in low radius curves).

The creep curve is highly dependent on the third body layer and any contamination in the wheel/rail contact. Figure 12 shows an example of the effect contaminants have on the creep curve. When velocity is sufficiently increased, this can be further exacerbated and will be discussed in Section 2.3.

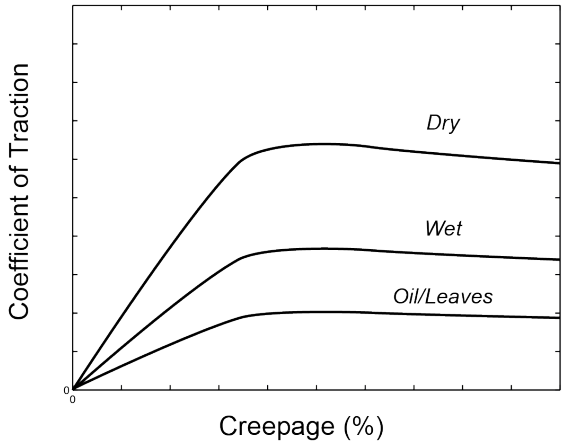

Figure 12: The effect of contamination on the coefficient of traction with variable slip.

2.1.4. Wear

Wear of both the wheel and rail has been extensively investigated and the most recent results have shown three distinct regimes of wear of the wheel/rail contact, each with a different characteristic and cause. These regimes have been catagorised as *mild*, *severe* and *catastrophic* (Lewis, 2004) and are linked to the slip within the contact (Figure 13). This chart can be compared to the creep curve saturation point (see Figure 10), where there is transition from mild to severe wear.

The transition from the severe to catastrophic has been linked with an increase in contact temperature that affects the mechanical properties of the materials in contact. The mild regime is dominated by oxidative wear that leaves an oxide layer on the rail head. The severe regime is characterised by ratcheting, where strain accumulates from small increments of plastic deformation over a number of cycles and the ductility is exceeded which leads to material's removal (Kapoor, 1994).

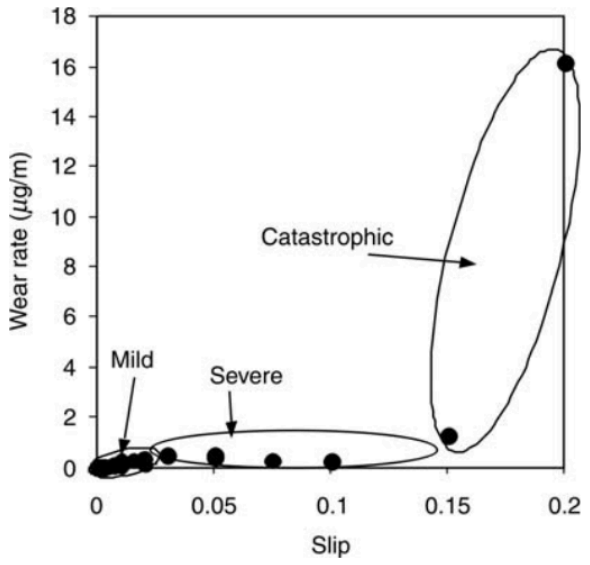

Figure 13: **Wear types in the wheel/rail contact for R8T rail steel (Lewis, 2004)**

There is a variety of strategies for reduction of wear, including wheel profile modification, friction modification and lubrication. Table 1 shows the advantages of using gauge face lubrication to reduce wear.

Table 1: **Wear reduction factors by choice of lubrication policy. Rail wear factor is the ratio of wear to dry wear. (Schmid, 2010)**

Gauge face lubrication policy	Rail wear factor
Dry	1
Inconsistent	2
Intermittent	5
Consistent	>10

2.1.5. Isolation

Railway networks are often spilt into discrete sections to monitor vehicle locations on the network. These sections can vary in length, especially in the UK where the lengths depend on the historical use of line. Branch lines will tend to have more irregular section distances than the mainline. Sections of track are divide by insulated rail joints and a simple electrical track circuit (Figure 14).

When a train enters a section, it shorts the track circuit by virtue of the metal-metal wheel/rail contact and disrupts the circuit between the transmitter and detector. When a vehicle travels from one section to another, it must be entering a section without another vehicle present, which is indicated by an untripped track circuit. As the vehicle crosses the insulated joint, the new section circuit is tripped whilst the old returns to a vacant section.

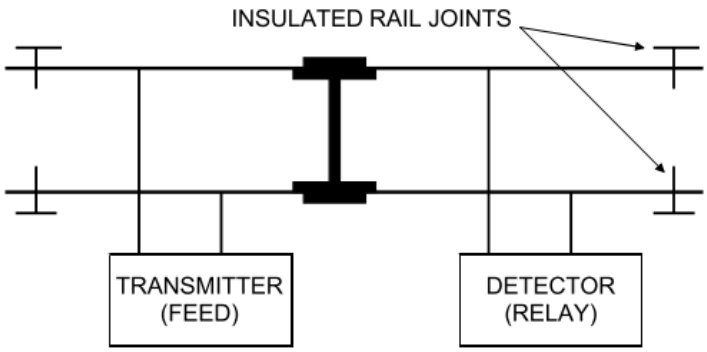

Figure 14: Schematic of railway track circuit (Lewis, 2012)

If there is sufficient build up of non-conductive material between the wheel/rail contacts and there is no longer a sufficient metal-metal contact, a section can falsely display that there are no vehicles in that section with potential for detrimental consequences.

Leaves can build up on the rail head and form a tough coating that can cause isolation (Lewis, 2006). This same study found that some products, such as railway sand often used as a traction enhancer to mitigate leaves, could also cause isolation.

2.2. Third body contaminants

Third body contaminants are any additional materials that can be found in the wheel/rail contact. These materials have previously been divided into three categories (Godet, 1984), but more recently an additional fourth category has been added (Descartes, 2008). These categories are:

- Climatic contaminants
- Operational contaminants
- Products transported
- Natural third body layer

Each category has a host of different subcategories with their own unique third body characteristics. Climatic bodies include leaves and water, and

operational bodies include ballast and any products that are applied to the rail or wheel, including oil, grease and friction modifier. Transported products include any product that is carried by freight, such as cereals or coal. To further complicate the situation these materials can, and often do, interact with one another to alter the third body layer yet again.

The natural third body layer is a 15-micrometre thick layer that is present on the rail head, which is generated by the contacting conditions and corrosion products from exposure to the open environment (Descartes, 2005). The layer consists of iron oxides and oxyhydroxides particles, mixed with unoxidised wear debris (Lewis, 2012a).

2.2.1. Iron oxides

Rail and wheel materials are both susceptible to electrochemical corrosion that produces oxides or rust. A range of oxides are generated due to the variance in conditions of wheel/rail contact (high pressure and high temperature during sliding) and rail location (coastal sea spray).

Examples of iron oxides are Fe_3O_4 (magnetite) and Fe_2O_3 (haematite) and oxyhydroxides, generated under moist conditions, which include goethite, akaganeite and lepidocrocite (α-FeOOH, β-FeOOH and γ-FeOOH, respectively) (Lewis, 2012). Some general properties of these are given in Table 2.

Table 2: Properties of iron oxides and oxyhdroxides that are found on the rail head (Godfrey, 1996) and the impact on friction (Ishida, 2005)

Name	Formula	Colour	Crystal Structure	Magnetic	Impact on friction
Haematite	Fe_2O_3	Red	Trigonal	No	Increase[1]
Magnetite	Fe_3O_4	Black	Cubic	Yes	Decrease
Geothite	α-FeOOH	Yellow-brown	Orthorhombric	No	Decrease
Akageneite	β-FeOOH	Yellow-brown	Monoclinic	No	Decrease[2]
Lepidocrocite	γ-FeOOH	Orange	Orthorhombric	No	

It has been theorized that iron oxides can cause low adhesion (Beagley, 1976) because oxides, which form naturally on the rail head, mix with water to form a solution that is viscous enough lubricate the wheel/rail contact (Beagley, 1975b). This theory comes from anecdotal evidence from train drivers when using a dampened line that has not been used for a while, braking becomes compromised.

[1] (Godfrey, 1999)
[2] (Ishida, 2005)

The oxidation products on the rail head can be highly transient and, as such, it can be difficult to analyse the exact composition of iron oxides/oxyhydroxides that caused low adhesion between wheel and rail. In the UK, samples of rail head debris are taken after a low adhesion event but this can be hours after the actual event has occurred. It is highly possible that the conditions that cause low adhesion exist for only a short amount of time (Lewis, 2012).

Researchers have used *in situ* spectroscopy techniques to analyse rail head debris with some success (Sone, 2008). X-ray diffraction (XRD) is one of the most reliable techniques for composition anlaysis, where the crystalline structure of iron oxide is determined. However, the iron oxide must be removed from the original specimen and ground into a fine powder prior to analysis and the detection threshold for oxides is quite high. Zhu (2013) used XRD to establish the oxide composition on both lightly and heavily oxidised sample, but was only able to detect oxides on the heavily oxidised sample.

In recent years there has been a shift back to focusing on how iron oxides may play a role in the low adhesion problem. There has been limited research investigating the possible low adhesion effect of iron oxides in the wheel/rail contact. Researchers have previously found differences in friction between different oxides but these have not generated low adhesion (Lewis, 2012b; Zhu, 2013).

2.2.2. Leaves

Leaves have been a source of trouble for the rail industry for a number of years. When steam trains were prevalent, line-side trees were felled to ensure they did not catch fire. Since the move to electric and diesel locomotives, there was a reduction in line-side tree management. Leaves can become entrained both when a train passes and as airflow drags the leaves under the train into contact. This is a constant source of headache for the rail network management, particularly during the autumn when the leaf fall season has begun. Solutions to address this have been designed, such as leaf guards that protect the rail, but the problem still persists.

Once crushed in the contact, leaves are known to reduce adhesion by a large amount. It is crushed by the contact and after a number of cycles, a black Teflon-like material can be found on the rail head. In this state, the traction coefficient can be reduced to below 0.05, seriously affecting the braking distance. Moisture on the rail head can reduce this further (Pearce, 1987)

Many researchers have experimented with various methodologies for assessment of how leaves reduce traction in the wheel/rail contact. Cann (2006) used a mini-traction-machine (MTM) to investigate the affect of leaf layers on adhesion. Arias-Cuevas used the twin-disc tests machine to measure the adhesion of crushed leaf material when in contact (Arias-Cuevas, 2010). Sand has been shown to be an affective adhesion mitigation strategy when treating the rail head against leaf film formation.

2.2.3. Water

A number of rail researchers have measured low adhesion in the laboratory (Ohyama, 1991; Chen, 2006; Chen, 2008). Chen has both numerically and experimentally investigated the influence of water on adhesion in the wheel/rail contact (Chen, 2002; Chen, 2005; Chen, 2006; Chen, 2008; Chen, 2011). Experimentally the influence of contact conditions (load, slip, surface roughness, speed) and water temperature were examined.

The numerical models were compared with three separate field measurements of adhesion under wet conditions using Japanese Shinkansen vehicles. The models show a good fit with the data under specific conditions; however, only at speeds above 100 km/h (62.5 mph) does adhesion fall within the specific low adhesion range (Chen, 2002; Chen, 2011). Furthermore, the model only reproduced the results by adjusting the boundary lubrication coefficient appropriately.

The laboratory investigation showed water temperature had an effect on adhesion. A reduction in temperature from 50ºC to 5ºC produced a fall in adhesion from 0.14 to 0.08 (as read from the steady state friction for creep curve at 100 km/h). The effect of surface roughness had a more pronounced effect on adhesion with the smoothest surfaces, giving adhesion below 0.06.

The water used in testing was applied at four litres per minute. It was suggested that a reduction in water would lead to an increase in adhesion. This is contrary to heavy rain being seen as adhesion improving in results by other authors (Baek, 2007). Ohyama (1991) also investigated speed, load and roughness effects. They found a decrease in adhesion with a decrease in roughness. Only at higher speeds was the adhesion reduced into the low range.

The application of a small amount of water and allowing the contact to dry out has previously been tested. Arias-Cuevas tested the effect of applying a single drop of water to a dry contact at varying levels of slip in a twin disc test rig (Arias-Cuevas, 2010). They compared the recovery time against tests with two different friction modifiers. At low slip (0.5%) the dry baseline adhesion was marginally reduced (0.25 to 0.2). At slip of 1% and 2% the baseline was reduced by 50%, but the recovery time was reduced. At no point did the adhesion level go below 0.2 for all slip values tested.

Beagley and Pritchard showed a difference in adhesion for the application frequency of water (Beagley & Pritchard, 1975a) with tests using an Amsler twin disk rig at constant slip (3.3%). They found that a ‘constant slow’ application of water reduced adhesion to 0.2 from a dry value of 0.6. A subsequent bulk application of water was found to increase adhesion from this minimum. They investigated debris and water mixtures and only found reduction into ultra-low adhesion levels when the test disks were rusted and slightly wet ($\mu \approx 0.05$).

Several authors have investigated water and additional contaminants. Cann (2006) investigated water and leaf mixtures using a MTM with control of speed and slip. Slip values of 1% and 50% were investigated against speed. Adhesion was measured at minimums of 0.05 and 0.18 for 1% and 50%,

respectively. It was not postulated as to why such low adhesion was found with water alone.

Only the roughness of one contacting bodies was measured and was much lower than would be expected of a wheel or rail (Ra = 15 nm). Hardwick et al. (2013) investigated the effect of salt and water mixes alongside pure water. They found that water alone did not lower adhesion into the low range but with an increase of salt present, the adhesion was drastically lowered.

It is worth noting, that although pure water may have been the only 'contaminant' introduced in a laboratory, tribological tests inherently make debris free testing difficult (Beagley, 1975b). In the field, there will always be to some extent a third body layer on the rails and the wheels (Niccolini, 2005).

A new concept in the rail industry is the 'wet rail syndrome', where adhesion is lost when there is little water, has come in to railway parlance. (RSSB, 2014). This research has defined the 'wet rail syndrome' as

> *"poor adhesion conditions caused when low levels of moisture are present at the wheel/rail interface. These conditions are associated with dew on the rail head; very light rain, misty conditions and the transition between dry and wet rails at the onset of rain. These conditions are not associated with continuous rain*"

This research showed that low adhesion events that could not be attributed to 'leaves on the line' often occurred around the time when dew, or a minute amount of water, was likely to be found on the rail head. From the literature search, it has been seen that only tests have been conducted with relatively large amounts of water being applied to the contact.

2.3. Low adhesion

"Low adhesion" is the blanket term used when wheel/rail adhesion falls below values useful for braking or acceleration. This loss of adhesion can cause increased stopping distances which leads to station overruns and signals passing at danger which impact both the safety and punctuality of the railway network. Low adhesion can also cause damage to wheel/rail material through wheel slip during acceleration and wheel slide during braking. Cost estimates of low adhesion to the UK network have been made at £50 million (Adhesion Working Group, 2001).

For the purposes of this work, the following definitions of adhesion levels were taken (Vasic, 2008):

- Medium low: $0.1 < \mu < 0.15$
- Low: $0.05 < \mu < 0.1$
- Exceptionally low: $0.02 < \mu < 0.05$

Fulford and Tunna (2010) have categorised these low adhesion events by type of rail and environment conditions where *'medium low'* occurs on damp rails with a small amount of contamination;,'*low*' occurs on typical autumn mornings where the rail is damp and rust could have formed over night and '*exceptionally low*' occurs on severely contaminated rails, most typically but not limited to leaf contaminants.

British Rail Research (Fulford, 2010) conducted a survey to map the frequency of adhesion levels on the railway as shown in Figure 15. The survey shows a high percentage of measurements have levels of adhesion exceeding the values defined as low adhesion, indicating how infrequent '*low'* and '*exceptionally low'* adhesion levels occur on track.

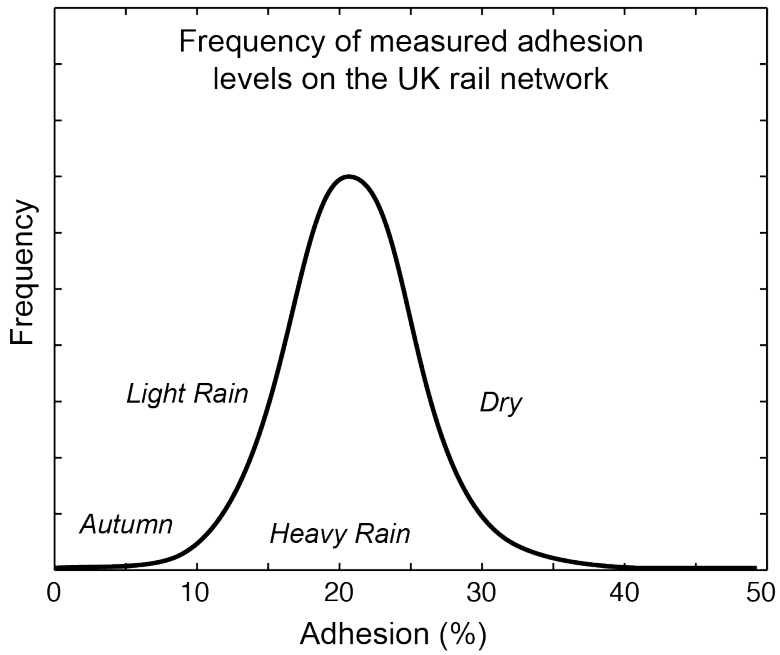

Figure 15: **Diagrammatic representation of the distribution of adhesion measurements on the UK rail network (Schmid, 2010).**

Values of adhesion are expressed as a percentage in Figure 15 This is a common, though outdated, method of expressing adhesion levels and is approximately equivalent to the deceleration/acceleration rate the wheel is subjected to, either through the brake or motor. Braking rates can be used to indicate available levels of friction. For example, a braking rate of 1.2 m/s^2 is equivalent to 12 %g or a friction coefficient of 0.12. This approximation is most commonly employed during rail accident investigations using data collected by the trains onboard management system at the time of an incident (RAIB, 2007).

In the UK, braking systems vary by vehicle type. The difference between tread and disc braked vehicles susceptibility to low adhesion has been recently been investigated by the Rail Safety and Standards Board (RSSB) using similar historic traction data obtained by train management systems.

Drivers have set options for braking levels ranging from a light brake to an emergency brake that is used in an event of low adhesion, where there is often an application of sand to the contact. For example, a Class 375 Electrical Multiple Unit (EMU) has a 4-step brake system with designed braking rates shown in Table 3. The braking force must be less or equal to the adhesion force at the contact point.

Table 3: **Designed braking rates for a 4 step braking system (RAIB, 2011).**

Brake step	Designed retardation (% g)	Minimum coefficient of adhesion
1	3	0.03
2	6	0.06
3	9	0.09
Emergency	12	0.12

2.4. Wheel/rail friction management

Friction management is the practice of controlling the friction levels to provide optimal levels of adhesion for improved service. Improvements in service can be both from reducing the adhesion, i.e., reducing wear to extend rail/wheel grinding intervals, to increasing adhesion, i.e., providing adequate traction in braking.

The friction management products include:

- Flange lubricants (grease, oil)
- Top of rail friction modifiers (providing intermediate friction levels)
- Traction enhancers (sand, traction gels)

It is the responsibility of the engineer to introduce the use of any additional friction management products to improve the system as a whole. Ultimately the goal of friction control in the wheel/rail contact is to avoid:

- Excessive wear
- Rail damage (RCF, corrugations)
- Wheel slide (loss of traction in braking)
- Wheel spin (loss of traction in acceleration)
- Reduction of noise (curve squeal)

For the purpose of this thesis, the main focus of the literature review is focused on grease for wayside lubrication and top-of-rail friction modifiers designed to produce intermediate rail head friction.

2.4.1. Grease

Grease has been used to lubricate the contact between the rail gauge face and wheel flange, as they experience the most severe contact conditions of the wheel/rail contact. This contact can have peak contact pressures of more than of the tread contact with increased sliding speeds, known as high creepages.

The lubrication of the high rail in a curve using a track based applicator system (Figure 16) is common practice. The advantages grease applicators can include:

- Reduction of wear for both rail and wheel
- Prevention of freshly ground wheels climbing

- Reduction of force, resulting in less gauge corner cracking and rolling contact fatigue
- Reduction curve noise

Figure 16: MC4 grease distribution unit in the field.

Shown in Figure 17, these track based flange lubricators supply the lubricant to the gauge face of the high rail, which is then picked up by the wheel flange upon passing. There are no set guidelines for the placing of these lubricators, but they are commonly located the transition to a curve prior to evidence of flange contact or wear. Initial set-up is within the manufacturers guidelines and then observation of the GDU during use is made to ensure effective placement. Adjustments can be made to accommodate dominant traffic types for specific lines. These adjustments can fall outside manufactures guidelines, but must not exceed maximum tolerances. For example, a LBFoster MC4 lubricator should sit between 20 and 25 mm below the top of rail.

There is either a mechanical or hydraulic application of grease, triggered by the passing of a wheel over a plunger located at or in advance of the applicator bars, called grease distribution units (GDUs). For grease pick-up to be effective, the grease columns must be transferred to wheel flange, as shown in Figure 17.

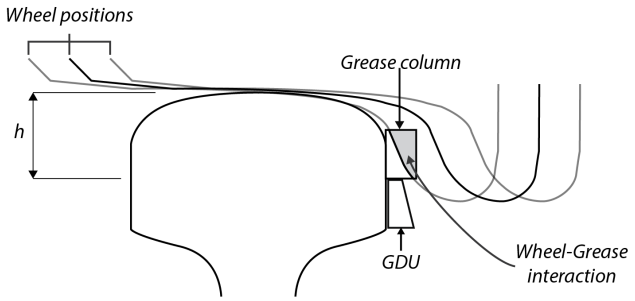

Figure 17: Schematic of grease bulb and wheel flange interaction showing the effect of lateral shift on amount grease pick-up.

The initial pick-up and transfer of grease from the rail gauge face to the wheel, followed by the deposition of grease along the gauge face of the rail around

the curve, is important for the effective and efficient lubrication of a rail curve. The distance that grease is deposited around a curve has been termed the "carry-down distance".

Grease will be consumed during the lubrication of the wheel/rail contact and, thus, has a finite life span. The duration that grease remains effectively reducing the frictional forces within the contact is termed the "retentivity".

Currently, there are two greases approved for use on the UK network, according to Network Rail standard NR/L3/TRK/3530/A01 (Track lubricants: curve lubricants). These are shown in Table 4.

Table 4: Manufacture product effectiveness claims

	Description	Carry down	Application rate (g/port/axle)
Supreme (RSClare)	Non toxic, readily biodegradable curved rail lubricant with EP/anti-wear properties		0.007
BioRail EP1.5 (Whitmore)	Bio-Semi-Synthetic Blend Lubricant	6400	0.007

The claims made by manufacturers of pick-up, retentivity and carry-down are often based on field experience, meaning there is no rail-specific standardised laboratory test that can be used to compare greases for the improvement of products.

Mota, using an Amsler test rig, investigated the effect of grease composition on wear for a number of different greases (Mota, 2009). Grease is often composed of extreme pressure additives in the form of solid lubricants, such as molybdenum disulfide or fine particles of graphite and thickeners of metallic salts of a fatty acid, such as lithium stearate. An increase in base-oil viscosity, percentage soap concentration and addition of extreme pressure additives reduced wear in a rolling-sliding contact, which was attributed to the promotion of full-film lubrication and a reduction in adhesion. Several researchers have used bespoke test equipment to characterize the rententivity (Wilson, 2006) and grease carry-down (Chen, 2013) with some success.

2.4.2. Friction modifiers

For the purpose of this thesis the term "friction modifiers" has been used to describe the class of products that are applied to the top of rail and are designed to provide an intermediate level of friction. These products have been termed top of rail friction modifiers (TOR-FMs).

TOR-FMs are used to treat the top of rail and provide a level of friction between 0.3-0.4, which is a reduction from the dry top of rail friction (0.5-0.6) Stock, 2016). TOR-FMs are used to treat a wide variety of railway network issues from this reduction in tread traction. These include improving fuel consumption and reducing RCF (Eadie, 2008; Stock, 2009), short-pitch rail corrugations (Eadie, 2002), wheel squeal and noise (Eadie, 2003; Eadie,

2005). Two common TOR-FMs and the performance claims made by manufacturers are shown in Table 5.

TOR-FMs are supplied to the track via wayside applicator bars as shown in Figure 18. The product is automatically pumped onto the top of the rail as a train passes and transferred to the wheel tread, where it is subsequently deposited along the track.

Figure 18: Top of rail applicator bar for liquid friction modifiers (LBFoster).

Table 5: Manufacturers product effectiveness claims of TOR-FMs

	Description	Friction Coefficient	Carry down (m)	Wear	Application rate
Keltrack (LBFoster)	Water based polymer suspension	0.3 – 0.4[3]	1600-3200[3,4]		0.035 to 0.06 litres/mile/rail[3]
RailGuard (Whitmore)	Petroleum Hydrocarbon, Soft paste/Grease[1]	"Ideal range"[2]	1600	"75% reduction[2]"	

[1] RailGuard MSDS, [2]Railguard technical data sheet, [3] Product website information

Thin film TOR-FMs are known to suppress noise (Eadie, 2003; Eadie, 2005) and reduce rolling contact fatigue and wear (Eadie, 2008). These products are water based and work in combination with the third body layer that is present on the rail head. The polymer components of the water-based TOR-FM combine with the third body layer (wear debris, iron oxides, etc.) as a consequence of the wheel/rail contact. Once effectively combined, the adhesion between wheel/rail is lowered from the dry level through the modified shear properties of the mixture of TOR-FM and the third body layer.

Friction modifiers are designed to give either neutral or positive friction as shown in Figure 19. This helps to mitigate stick-slip as 2 creepage levels at the same coefficient of friction (Stock, 2016). Without the friction modifiers

these oscillations in creepage cause short pitch rail corrugations and wheel squeal (Eadie, 2002; Eadie, 2008).

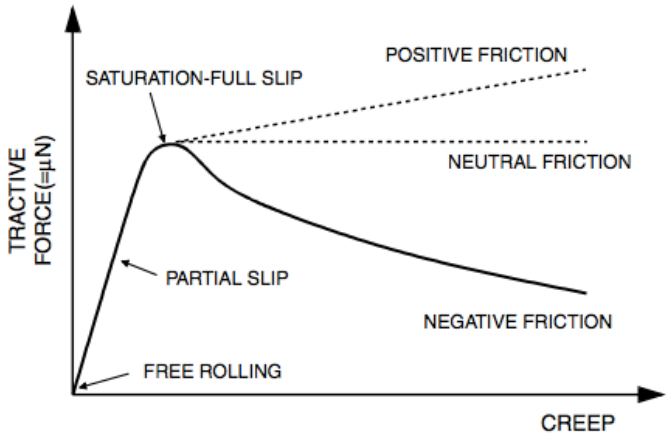

Figure 19: Schematic of friction modifiers affect on the tractive forces against creep showing the positive friction behavior (Eadie, 2002).

Currently the approval of friction modifiers used on the UK rail network is governed by Network Rail standard NR/L3/TRK/3510 (Rail Friction Management). There is no directive to use any particular friction modifier on the network and anecdotal evidence suggests that different routes across the UK have preferences to one or the other, based on past user experience.

2.5. Tribological testing of the wheel/rail contact

2.5.1. Contact scaling

Due to the complicated and ever evolving contact between the wheel and rail, simplifications of the contact geometry are made for analytical and experimental purposes. The wheel/rail contact may not satisfy all requirements for the use of Hertzian approximation of a contact. However, they are useful when approximating contact shape, size and pressures and removes the need for complicated computer modelling.

Under the Hertzian contact, several assumptions are made:

- Non-conformal bodies touch over an area that is small relative to the overall dimensions (the wheel/rail contact mostly satisfies this)
- Surfaces are frictionless
- Bodies are isotropic
- Contacting surfaces are clean and free of any contaminant.

The contacting shapes that are appropriate to represent the wheel/rail contact are, in descending order of accuracy,

- Elliptical point contact (cross contacting cylinders)
- Line contact (parallel contacting cylinders)
- Point contact (pin-on-disc/ball-on-flat).

Table 6 shows the Hertzian equations required to convert a contact pressure into a contact geometry and vice versa.

Table 6: **Hertzian contact calculations for point, line and cross-cylinder contacts.**

Contact shape	Point	Line	Elliptical
Reduced radius, R'	$\left(\frac{1}{R_1}+\frac{1}{R_2}\right)^{-1}$	$\left(\frac{1}{R_1}+\frac{1}{R_2}\right)^{-1}$	$\left(\frac{1}{R_x}+\frac{1}{R_y}\right)^{-1}$
Contact half width, a	$\sqrt[3]{\frac{3PR'}{4E^*}}$	$\sqrt{\frac{4PR'}{\pi LE}}$	$\sqrt[3]{\frac{3k^2\mathbf{E}PR'}{\pi E^*}}$
Maximum contact pressure, p_o	$\frac{3P}{2\pi a^2}$	$\frac{2P}{aL\pi}$	$\frac{3P}{2\pi ab}$
Contact pressure distribution, $p(x)$	$p_o\sqrt{1-\frac{r^2}{a^2}}$	$p_o\sqrt{1-\frac{x^2}{a^2}}$	$p_o\sqrt{1-\frac{x^2}{a^2}-\frac{y^2}{b^2}}$
Average contact pressure, p_{avg}	$\frac{P}{\pi a^2}$	$\frac{P'}{2a}$	$\frac{P}{2\pi ab}$
Maximum shear stress, τ_{max}	$0.31p_0$	$0.3p_0$	
Depth of maximum shear stress, z	$0.57a$	$0.78a$	
Other contact dimensions			$b=\sqrt[3]{\frac{3\mathbf{E}PR'}{\pi kE^*}}$

The nomenclature is similar for all three conditions with some additions. Shared units are: R' the reduced radius of contact (note $R_{y,x} = (1/(R_{1y,x} + R_{2y,x})^{-1}$ where x and y are the effective radii in the two contact bodies in perpendicular planes); E* the reduced elastic modulus (Nm^{-2}); a the contact half width (for a point contact a = b in the elliptical case); P the normal load (N); p contact pressure (Pa) and p_o the maximum contact pressure (Pa). For the line contact P′ is the load per unit length (Nm^{-1}). For the elliptical contact k is the ellipticity parameter, and **E** an elliptical integral both found in tables or from approximate solutions.

Figure 20 shows the difference in size of contact area for equivalent contact pressures when using Hertzian calculations.

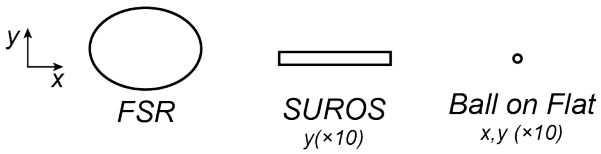

Figure 20: **Comparison of contact size for different scales of laboratory test equipment (maximum Hertzian contact pressure 1.5 GPa). From left) Full-scale wheel on rail rig (FRS) based on elliptical contact calculations; Twin disc (SUROS) rig based on crossed cylinders; and Ball-on-flat.**

This simplification is for statically loaded contacts. For a rolling contact, the pressure/stress distribution under the surface from the tractive forces is shifted towards the contacting surface as traction increases.

Creep within the contact is present in three directions of longitudinal, lateral and spin. For the purpose traction, it is the longitudinal creep that is usually varied, as this is a controllable variable in twin disc testing, and is the creep in the direction of travel.

At the laboratory-level of testing, there is a spread in types of test methods that have been used to characterise the wheel/rail contact. An understanding of the advantages and disadvantages, as well as the capabilities of each of the test methods, is key in informing the selection process when designing the experiments to be performed.

Prior to discussion of different test types, a word on the adhesion results from tests at different scales. Gallardo-Hernandez (2008) collated the results from several studies of the wheel/rail contact under in analogous contact conditions on different scales of test rig. Table 7 replicates what was previously published and shows how comparable adhesion measurements can be.

Table 7: Measured adhesion using tribometers of different scale (Gallardo-Hernandez, 2008)

Author	Test Apparatus	Load/Contact Pressure	Rolling Speed (km/h)	Test Conditions	Peak μ	Slip at Peak μ [%]	Stable μ [5% slip]
Zhang (2002)	Full-scale roller rig (using an actual bogie)	44 kN	10-70	Dry	0.5-0.57	2	0.5-0.57
		67 kN	10-70	Dry	0.44-0.55	1-2	0.44-0.52
		44 kN	120-240	Wet	0.07-0.13	0.5-1	0.065-0.12
		67 kN	80-240	Wet	0.05-0.11	0.5-1	0.05-0.105
Jin (2004)		67 kN	140-300	Oil	0.045-0.055	1	0.044-0.052
		135 kN	140-300	Oil	0.04-0.05	1	0.037-0.048
Harrison (2002)	Triborailer (used on actual rail)			Dry	0.52	1	0.5
	Push tribometer			Dry	0.7	2-5	0.7
Nagese (1989)	Instrumented bogie on test vehicle (run on test track and actual routes)	Variable	Variable	'Dry'	Range of μ: 0.2-0.4		
				Wet	Range of μ: 0.05-0.2		
				Oil	Range of μ: 0.05-0.07		
				Leaves	Range of μ: 0.025-0.10		
Gallardo-Hernandez (2008)	Twin disc	1500 MPa/7.7 kN	3.54	Dry	0.6	2	0.54
			3.54	Wet	0.2	1	0.17
			3.54	Oil	0.07	1	0.06

2.5.2. Field testing

Field experiments are performed to ensure the contact between the wheel and rail is fully characterised, including actual contact pressures, areas and creepage, amongst others, and often involves instrumented wheel sets on trains. An instrumented train has been used to assess wheel flats, using an axle that had a separate braking system to lock up the wheel and cause a skid. Data obtained from these experiments included axle rotation velocity, train speed and braking system forces which could be then post-processed to calculate a friction coefficient. This information can be used to assess power generated at the contact surface.

Other methods of field assessment include instrumenting the rail itself in areas of particular interest. Egana (2005) performed experiments on a specific 250m long curve (radius 200m) to assess the effect a liquid high positive friction (HPF) modifier had on track corrugations. Though direct measurement of loading forces did not occur, acceleration measurements in the lateral and transverse directions were taken and compared measurements taken with and without the HPF. A reduction in acceleration forces was recorded but due to the long time scales of corrugation, it was suggested that experiments should be carried out on a section of track where corrugation develops rapidly.

The issues with field testing are wide and varied, as it often delays research due to several factors that include track access, test approval and costs, amongst others. Cost is of particular concern as it can often be particularly high due to staffing costs and train hire, which are essential to run a single experiment. To mitigate these concerns, field assessments are often performed using equipment that can be brought onto track to make various measurements over a period of time. This allows a variable to be controlled, such as type of rail material, and measurements over the time that variable is ‘on/off’ to be compared. Eadie (2008) performed a field study on a HPF modifier to assess corrugations on a section of track, making comparisons between corrugation rates when no HPF modifier was used on the line to when a HPF modifier system was installed.

Tribometers are often used on tracks to assess the coefficient of friction on the rail head at a particular point of interest (Broster,1974). Tribometers consist of a spring-loaded wheel that is rolled along the wheel until gross slip occurs, as it’s been calibrated to give a corresponding coefficient of friction for the particular level of gross slip. Tribometers can also use gravity loading, but this restricts the measurements to top of the rail head.

These measurements are often done on track that has shown particular problems with low adhesion. Harrison also compared two types of tribometer; a hand push tribometer and one designed to be pushed along track via a separate vehicle (Harrison, 2002). The hand push tribometer works under the action of a spring and was able to take measurements on both the rail head and gauge face, unlike previous versions. More recently, an improved push tribometer has been designed to work more accurately in the low creep regime (Harrison, 2008).

A larger on-track tribometer is the TriboRailer developed by Salient Systems to take measurements on a larger area of track which was previously limited by the hand push tribometer (Harrison, 2002). The new version was designed to provide four simultaneous measurements of friction via integral load cells and could travel at up to 60 kilometers per hour, although at this speed issues in reading noise occurred. The saturation creep level for the Triborailer was 2.5%, whilst estimations of creep levels for the hand pushed were based off the measured wheel speed at zero slip.

Though there are benefits of collecting data *in situ*, field tests are subjected to many varying and uncontrollable conditions. It should be used to finalise testing of a product or procedure, allowing a full field assessment as it is difficult at this point to attribute a change in performance to a single factor. These issues highlight a need for laboratory experiments to test the effects of a particular point on the wheel/rail contact.

2.5.3. Laboratory testing of the wheel/rail contact

Laboratory testing is extensively used to assess the wheel/rail contact when loading, creep, or contamination is altered. Testing comes in many different forms from twin disc testing with scaled profiles, offering the ability to precisely control and measured creepage, to pin-on-disc testing where full sliding is constant throughout. These tests are preformed at a scale down from the field testing and allow for far more control of variables with a rapid evolution in results, comparisons and conclusions as to how these tests would be utlised in the field.

2.5.4. Full-scale rigs

Full-scale rigs have been used to assess adhesion/wear and can vary in size and scope. Zhang (2002) used a full-scale rig that consisted of a bogie mounted on four rollers. Torque measurements were taken on the wheelsets, and the corresponding rollers that had a UIC60 rail profile. This allowed assessment of adhesion levels under different loading, velocity and contamination conditions. Stock (2011) used a full-scale wheel/rail rig to assess the effect of friction modifiers on rolling contact fatigue. Instead of using a whole bogie and rollers, a freight wheel was loaded against a length of rail that could move back and forth under hydraulic action. The rig also allowed for lateral loading and cant adjustment, which allowed for the simulation of curving and changes in angle of attack and replicated conditions found *in-situ*.

A method that has been widely adopted for testing wheel/rail contacts is that of twin disc testing - essentially two rotating discs loaded together, because full-scale testing can be time consuming and the consumables are expensive due to the requirement of full-scale wheels.

2.5.5. Twin disc

One of the most common types of laboratory rig is the twin disc machine, the most basic of which consist of two fixed axle discs rotating in contact used to measure wear and adhesion These rigs can vary in complexity but most are

capable of running tests at fixed slip rates with loads approximate to those found in the field.. Most rigs are able to run at different levels of slip which means tests can be run to produce creep curves.

The Amsler machine is a basic version of the twin disc test set-up. It consists of two discs loaded together, which are driven at a fixed gear ratio. The diameters of the disc are able to introduce different creep ratios. The test rig can be used to assess adhesion levels and can produce creep curves for various contaminant contact conditions. Amsler rigs were commonly used by British Rail Research in the 1970s and 1980s (Beagley, 1975a; Beagley,1975b).

More complex twin disc experiments allow many aspects to be controlled and manipulated, with simultaneous measurement of many factors including adhesion, wear, RCF and isolation. Fletcher modified established twin disc testing to include the control of creep at the contact between the two tests specimens (Fletcher, 2000a) and more recently introduced variable creep control during testing (Fletcher, 2013).

For the case of wheel/rail research, the two discs are manufactured from full size wheel and rail into several discs. The twin disc test-rig at the University of Sheffield, dubbed the SUROS rig (Sheffield University ROlling & Sliding), has been used to experimentally determine many different issues from low adhesion from leaves through to isolation as a consequence of sanding (Fletcher, 2000b; Fletcher, 2000c; Arias-Cuevas, 2010a; Arias-Cuevas, 2010b; Arias-Cuevas, 2011; Hardwick, 2012; Hardwick, 2013a; Hardwick, 2013b; Lewis, 2003; Lewis, 2004a; Lewis, 2004b; Lewis, 2006b; Lewis, 2009; Lewis, 2010a; Lewis, 2011a; Lewis, 2012a; Li, 2009).

Twin disc set-ups can vary design. For example, Chen (2008) used a twin disc test rig with larger discs to allow higher velocities to be reached (30-100km/h). The rig used two DC motors to drive the discs and measured the torque on the wheel disc shaft. Load cells above the wheel disc housing were used to measure the radial loading or normal force between the two discs. Again, such rigs are extensively used to investigate many of the issues mentioned above (Ishida, 1998; Baek, 2007; Baek, 2008; Chen, 2002; Chen, 2005; Chen; 2006; Chen, 2011; Nakahara, 2011).

2.5.6. Mini Traction Machines

Mini traction machines (MTM) have also been used to carry out wheel/rail contact studies. The MTM consists of a rotating ball loaded against a spinning disc that is mounted to a drive shaft with a torque meter attached. This system allows for creep to be altered, even during an experiment. The ability to control creep throughout the experiment allows traction versus creep curves to be built up in a single test. Using MTMs, Zhu (2012) has studied the effects of temperature and humidity and Cann (2006) ushas investigated adhesion reduction due to leaves on the line.

2.5.7. Pin-on-disc

Pin-on-disc testing is traditionally used for wear testing of sliding contacts. A steel pin is loaded at a right angle against a rotating disc, with a load cell

placed to measure the tangential loads. The normal load is set using a dead weight system, enabling friction measurements to be taken. Wear volumes can be calculated from mass loss and displacement can be measured in the vertical direction during testing (assuming a horizontal rotating disc).

Currently, few researchers have used the pin-on-disc assessment, as full slip can only be observed. It does not represent a roll-slide contact. The researchers whom have used this test method also include the use of a pin-on-disc rheometer to assess the shear strength of a friction modifier layer (Lu, 2005). However, pin-on-disc experiments in an environmental chamber allow for investigation into the affect of temperature and humidity on adhesion and wear. Several researchers have effectively used a pin-on-disc test set-up to investigate the influence of humidity and temperature on adhesion (Zhu, 2015), friction modifiers (Lewis, 2012b), leaves (Olofsson, 2004) and iron oxides (Zhu, 2013; Lyu, 2015).

2.5.8. Other laboratory tribological test methods

Using a method employed in other tribological applications, Lewis (2011) investigated the slip between a rubber pad and the floor. The contact of a spring-loaded pendulum foot and the floor is measured over a pre-set length. The distance the pendulum arm travels post-contact allows for the calculation of the friction coefficient.

Lewis modified the pendulum so it could be used on track in the field. Results measured in field were compared with those measured in the laboratory. These values were then evaluated against those obtained through other experimental methods. It was found that even though the contact is a fully sliding contact rather and a roll-slide one the results were comparatively useful. The modified pendulum test provided rapid assessment of rail head adhesion using simple, portable testing equipment.

Research has shown that the pin-on-disc rheometer results can be useful in material selection tests for friction modifiers (Harrison, 2002). This allows the shear properties of the interfacial layer to be assessed over time.

There are many other test rigs found in literature which include modifications to existing test rigs or are bespoke for a specific area of interest. Descartes (2011) used a modified unidirectional wheel/rail test rig to investigate wheel flange/rail gauge contact lubrication. A large-scale rig was re-commissioned by Wilson (2006) also to investigate the properties of curve lubricants. These rigs are often highly specialised and lack the previous test data to bridge the gap between laboratory and field.

2.6. Summary

The literature review has shown a wide variety of issues that can afflict the wheel/rail contact and methods currently employed by the railway network for adhesion management. The network must consider how to effectively use products currently in service and how to assess new products to be introduced to the network. It is also critical that the network understands the conditions that cause low adhesion and the possible mitigation techniques.

2.6.1. Benchmarking of railway grease

Specifically in a railway context, there is a lack of standards governing the use of grease as a wayside lubricant. The need for a specific standard is particularly important when considering the high contact pressures and creepages that grease can be subjected to in the wheel/rail contact. Within the standards, retentivity and carry down of grease must be considered.

Paper 1: Development of a standardised test method for comparing greases effectiveness and establishing a benchmark for future grease products.

Paper 2: Development of a simple method of assessing how far grease has been carried-down a rail curve

2.6.2. Friction modifier in the laboratory

Friction modification products are used in the rail head to provide intermediate friction levels. Evaluation of the factors that affect the performance of friction modifiers in the laboratory compared to the field is critical to improve the understanding of their effectiveness.

Paper 3: Comparison of friction modifiers when testing at different scales of laboratory test rig.

2.6.3. Low adhesion

It is essential that low adhesion be attributed to more than just a “leaves on the line” problem. The literature review highlighted research from Beagley (1976) showing iron oxide and water mixtures could be a cause of low adhesion, but no laboratory tests were able to confirm this hypothesis. More recently, there is renewed interest in the problem from the UK’s RSSB with the publication of studies showing prevalence of low adhesion events at the dew point. To learn more about low adhesion, investigations need to determine whether a small amount of water alone or water and iron oxide mixtures produce low adhesion, and if so what are the conditions that cause this case to occur.

Paper 4: Development of a simplified and repeatable laboratory test method to investigate small amounts of water and iron oxide in the wheel/rail contact.

Paper 5: Towards generating repeatable tests conditions that produce low adhesion in a full-scale test set-up.

Paper 6: A model produced to predict the effects of water and iron oxide mixtures in the wheel/rail contact as a function of water flow rate

2.6.4. Low adhesion mitigation

The suppression of iron oxide generation on the rail head reduces low adhesion events using novel solutions from areas outside of the railway industry. If iron oxides are one of the causes of low adhesion, what are the possible mitigation methods?

Paper 7: Twin disc testing of hydrophobic liquids for treatment of the rail head.

Table 8: Thesis papers and the author's contributions.

ID	Paper title	Contribution
1	Assessment of railway grease performance using a twin disc tester	Secondary author. Contributed to SUROS testing, microscopy and specimen analysis. Additional work on Network rail standard for grease pumpability completed as supplementary work towards a railway grease standard.
2	Field trials of a new method for the assessment of gauge face condition using a modified Pendulum test rig	First author. All work is authors own.
3	A comparative study of twin disc and full scale experimentation methods of the wheel/rail contact – assessment of friction modifiers	First author. Specified and carried out all full-scale and SUROS testing at the University of Sheffield. Presented work at Leeds-Lyon tribology symposium 2013.
4	Assessing the impact of small amounts of water and iron oxides on adhesion in the wheel/rail interface using High Pressure Torsion testing	First author. Led and performed all High Pressure Torsion (HPT) tests. Worked with group to understand significance of HPT test data, which led to the development of an adhesion model to better understand the third body layer effects at the interface.
5	Full-scale testing small amounts of water in the wheel/rail interface	First author. Designed and specified full-scale tram wheel tests, and worked with a team to carry out tests.
6	Wheel-rail creep force model for predicting water induced low adhesion phenomena	Secondary author. This paper details the final model generated from the HPT and full-scale tram wheel tests. Restates and uses full-scale test data for model development. It has been included to highlight the water induced low adhesion phenomena.
7	Investigation of the isolation and frictional properties of hydrophobic products on the rail head, when used to combat low adhesion	Co-author. Collaborated with partner to Assisted in SUROS testing of hydrophobic solutions. Led pendulum testing including test specifications, data generation and analysis.

2.7. References

Adhesion Working Group (AWG), 2001, “Managing Low Adhesion”, London, UK

Arias-Cuevas, O., Li, Z. and Lewis, R., 2010a, “Laboratory investigation of some sanding parameters to improve the adhesion in leaf-contaminated wheel–rail contacts.” Journal of Rail and Rapid Transit Proceedings of IMechE Part F, 224, 3, pp.139–157

Arias-Cuevas, O., Li, Z. and Lewis, R., 2010b, “Investigating the lubricity and electrical insulation caused by sanding in dry wheel–rail contacts,” Tribology Letters, 37, 3, pp. 623–635, 2010

Arias-Cuevas, O., Li, Z. and Lewis, R., 2011. “A laboratory investigation on the influence of the particle size and slip during sanding on the adhesion and wear in the contact.” Wear, 271, 1-2, pp.14–24

Baek, K.S., Kyogoku, K. and Nakahara, T., 2007, “An experimental investigation of transient traction characteristics in rolling-sliding wheel/rail contacts under dry-wet conditions.” Wear, 263, 1-6, pp.169–179

Baek, K.S., Kyogoku, K. and Nakahara, T., 2008, “An experimental study of transient traction characteristics between rail and wheel under low slip and low speed conditions”, Wear, 265, 9-10, pp.1417–1424

Beagley, T.M. & Pritchard, C., 1975a, “Wheel/rail adhesion — the overriding influence of water.” Wear, 35, 2, pp.299–313

Beagley, T.M., McEwen, I.J. & Pritchard, C., 1975b. “Wheel/rail adhesion — the influence of rail head debris.” Wear, 33, 1, pp.141–152

Beagley, T.M., McEwen, I.J. & Pritchard, C., 1975c, “Wheel/rail adhesion — Boundary lubrication by oily fluids.” Wear, 31, 1, pp.77–88

Beagley, T.M., 1976. “The rheological properties of solid rail contaminants and their effect on wheel/rail adhesion.” Proceedings of the Institution of Mechanical Engineers, 190, 39, pp.259–266

British Standard, 2012, “BS EN 16028:2012— Wheel / rail friction management — Lubricants for trainborne and trackside applications,”

Broster, M., Pritchard, C. and Smith, D.A., 1974. “Wheel/rail adhesion: its relation to rail contamination on British railways.” Wear, 29, pp.309–321

Burstow, M., 2011 “Vehicle/Track Interaction: Part 1 – Railway vehicle dynamics, conicity and stability” MEC6429: Mechanical Engineering of Railways, University of Sheffield, Sheffield

Cann, P.M., 2006. “The ‘leaves on the line’ problem - A study of leaf residue film formation and lubricity under laboratory test conditions.” Tribology Letters, 24, 2, pp.151–158

Chen, H. et al., 2002. Adhesion between rail/wheel under water lubricated contact. Wear, 253, 1-2, pp.75–81

Chen, H., Ishida, M. & Nakahara, T., 2005. “Analysis of adhesion under wet conditions for three-dimensional contact considering surface roughness.”

Wear, 258, 7-8, pp.1209–1216

Chen, H. et al., 2006. “Effect of water temperature on the adhesion between rail and wheel.” Proceedings of the Institution of Mechanical Engineers, Part J: Journal of Engineering Tribology, 220, 7, pp.571–579

Chen, H. et al., 2008. “Experimental investigation of influential factors on adhesion between wheel and rail under wet conditions”,

Chen, H. et al., 2011. “Estimation of wheel/rail adhesion coefficient under wet condition with measured boundary friction coefficient and real contact area. Wear, 271, 1-2, pp.32–39

Descartes, S., Desrayaud, C., Niccolini, E. and Berthier, Y., 2005, “Presence and role of the third body in a wheel-rail contact”, Wear, 258, 7–8, pp. 1081–1090

Descartes, S., Desrayaud, C. and Berthier, Y., 2008, “Experimental identification and characterization of the effects of contaminants in the wheel-rail contact” Journal of Rail and Rapid Transit Proceedings of IMechE Part F, 222, 2, pp. 207–216

Descartes, S. Saulot, A., Godeau, C., Bondeux, S., Dayot, C. and Berthier, Y., 2011, “Wheel flange/rail gauge corner contact lubrication: Tribological investigations.” Wear, 271, 1-2, pp.54–61

Gallardo-Hernandez, E. A., and Lewis, R., 2008, “Twin disc assessment of wheel/rail adhesion”, Wear, vol. 265, no. 9–10, pp. 1309–1316

Eadie, D.T., Kalousek, J. and Chiddick, K.C., 2002. “The role of high positive friction (HPF) modifier in the control of short pitch corrugations and related phenomena”. Wear, 253, 1-2, pp.185–192

Eadie, D.T., Santoro, M. and Powell, W., 2003 “Local control of noise and vibration with Keltrack friction modifier and Protector trackside application: An integrated solution”. Journal of Sound and Vibration, 267, 3, pp.761–772.

Eadie, D.T., Santoro, M. and Kalousek, J., 2005. “Railway noise and the effect of top of rail liquid friction modifiers: Changes in sound and vibration spectral distributions in curves”. Wear, 258, 7-8, pp.1148–1155.

Eadie, D.T. Elvidge, D., Oldknow, K., Stock, R., Pointner, P., Kalousek, J. and Klauser, P., 2008. “The effects of top of rail friction modifier on wear and rolling contact fatigue: Full-scale rail-wheel test rig evaluation, analysis and modelling”. Wear, 265, 9-10, pp.1222–1230

Eadie, D.T., Lu, X., Santoro, M. and Oldknow, K., “Wayside lubrication: How much do we really understand?” Proceedings of the International Heavy Haul Association Conference 2011, Calgary Canada, 19-22 June 2011.

Egana, J., Vinolas, J. and Gil-Negrete, N., 2005, “Effect of liquid high positive friction (hpf) modifier on wheel-rail contact and rail corrugation,” Tribology International, 38, 8, pp. 769 – 774

Fletcher, D.I., Beynon, J.H., 2000a, “Development of a machine for closely controlled rolling contact fatigue and wear testing”, Journal of Testing and Evaluation, 28, 267-275

Fletcher, D.I. and Beynon, J.H., 2000b. “The effect of contact load reduction

on the fatigue life of pearlitic rail steel in lubricated rolling – sliding contact." Fatigue & Fracture of Engineering Materials & Structures, 23, pp.639–650

Fletcher, D.I. and Beynon, J.H., 2000c. "The effect of intermittent lubrication on the fatigue life of pearlitic rail steel in rolling-sliding contact." Proceedings of the Institution of Mechanical Engineers, Part F: Journal of Rail and Rapid Transit, 214(3), pp.145–158

Fletcher, D.I. and Lewis, S.R., 2013. "Creep curve measurement to support wear and adhesion modelling, using a continuously variable creep twin disc machine." Wear, 298-299(1), pp. 57–65.

Fulford, C. and Tunna, J., 2010, Chapter 4 in "Wheel-Rail Best Practice Handbook", Birmingham: University of Birmingham Press. Print.

Godet, M., 1984, "The 3rd body approach: a mechanical view of wear". Wear, 100, 437–452

Godfrey, D., 1999. Iron oxides and rust (hydrated iron oxides) in tribology. Tribology & Lubrication Technology, 55, 2, pp. 33

Hardwick, C., Lewis, R., Eadie, D.T. and Rovira, A., 2011, "Rail wear – Understanding the effect of third body materials", Proceedings of the IoM3 Conference on 20th Century Rail, York United Kingdom, 1-3 November 2011

Hardwick, C., Lewis, R. and Olofsson, U., 2012. "Low adhesion due to oxide formation in the presence of NaCl."" Proceedings of 9th international conference on contact mechanics and wear of rail/wheel system, pp.27–30

Hardwick, C., Lewis, R. and Eadie, D.T., 2013a. "Wheel and rail wear-Understanding the effects of water and grease." Wear, vol. 314(1-2), pp.198–204

Hardwick, C., Lewis, S.R. and Lewis, R., 2013b. "The effect of friction modifiers on wheel/rail isolation at low axle loads." Wear, pp.1–16

Harrison, H., McCanney, T. and Cotter, J., 2002. "Recent developments in coefficient of friction measurements at the rail/wheel interface." Wear, 253(1-2), pp.114–123

Harrison, H., 2008. "The development of a low creep regime, hand-operated tribometer." Wear, 265(9-10), pp.1526–1531

Ishida, M., Ban, T. and Moto, T., 1998, "The development of two-disc rolling contact test machine and some experimental results of checking its performance." Japan Rail Technology Joint Symposium, 1998, pp. 301–302.

Ishida, M., Aoki, F., Sone, Y., Ban, T. and Shirouzu, K., 2005, "Rail corrugations caused by low coefficient of friction in submarine railway tunnel" World Tribology Congress III, Volume 1, Washington, D.C., USA, pp. 931-932

Jendel, T., 2000, "Prediction of wheel profile wear—methodology and verification, Licentiate thesis", Royal Institute of Technology, Sweden, TRITA-FKT, 2000, p. 49

Kalousek, J., Magel, E., Strasser, J., Caldwell, W.N., Kanevsky, G. and Blevins, B., 1996, "Tribological interrelationship of seasonal fluctuations of freight car wheel wear, contact fatigue shelling and composition brakeshoe consumption", Wear, vol. 191, pp. 210–218

Kalousek, J. and Magel, E., 1997, “Optimising the Wheel/Rail System, Railway and Track Structure”, January vol.93(1), p.3

Kapoor, A. and Johnson, K.L., 1994, “Plastic ratchetting as a mechanism of metallic wear”, Proceedings of the Royal Society, London. vol. 445, pp. 367-381

Lewis, R., Dwyer-Joyce, R.S. and Lewis, J., 2003. “Disc machine study of contact isolation during railway track sanding”, Proceedings of the Institution of Mechanical Engineers, Part F: Journal of Rail and Rapid Transit, 217, 1, pp.11–24

Lewis, R. and Dwyer-Joyce, R.S., 2004a, “Wear mechanisms and transitions in railway wheel steels”, 218, pp. 467–478, 2004

Lewis, R. and Olofsson, U., 2004b “Mapping rail wear regimes and transitions” Wear, 257, 7–8, pp. 721–729, 2004

Lewis, R. and Dwyer-Joyce, R.S., 2006a, “’Industrial Lubrication Practice: Wheel/rail Tribology’ in *STLE* Handbook *of* Lubrication”, Second Edition

Lewis, R. and Dwyer-Joyce, R.S., 2006b. “Wear at the wheel/rail interface when sanding is used to increase adhesion.” Proceedings of the Institution of Mechanical Engineers Part F-Journal of Rail and Rapid Transit, 220, 1, pp.29–41

Lewis, R., Gallardo-Hernandez, E.A., Hilton, T. and Armitage, T., 2009. “Effect of oil and water mixtures on adhesion in the wheel/rail contact.” Proceedings of the Institution of Mechanical Engineers, Part F: Journal of Rail and Rapid Transit, 223, 3, pp.275–283

Lewis, R., Dwyer-Joyce, R.S., Olofsson, U., and Hallam, R.I., 2010a, “Mapping railway wheel material wear mechanisms and transitions”

Lewis, R., Dwyer-Joyce, R.S., Olofsson, U., Pombo, J., Ambrósio, J., Pereira, M., Ariaudo, C. and Kuka, N., 2010b, “Mapping railway wheel material wear mechanisms and transitions”, Proceedings of the Institution of Mechanical Engineers, Part F: Journal of Rail and Rapid Transit, 224: pp. 125

Lewis, R. Gallardo-Hernandez, E.A., Cotter, J., Eadie, D.T., 2011a. “The effect of friction modifiers on wheel/rail isolation.”, Wear, 271(1-2), pp.71–77.

Lewis, S.R., Lewis, R. and Olofsson, U., 2011b. “An alternative method for the assessment of rail head traction”, Wear, 271, 1-2,, pp.62–70

Lewis, R., Dwyer-Joyce, R.S., Lewis, S.R., Hardwick, C. and Gallardo-Hernandez, E.A., 2012a, “Tribology of the Wheel-Rail Contact: The Effect of Third Body Materials”, *Int. J. Railw. Technol.*, vol. 1, no. 1, pp. 167–194,

Lewis, S.R. Lewis, R., Olofsson, U., Eadie, D.T., Cotter, J. and Lu, X., 2012b. “Effect of humidity, temperature and rail head contamination on the performance of friction modifiers: Pin-on-disk study”. Proceedings of the Institution of Mechanical Engineers, Part F: Journal of Rail and Rapid Transit, 227(2), pp.115–127.

Lewis, R., Lewis, S.R., Zhu, Y., Abassi, S. and Olofsson, U., 2012c. “The modification of a slip resistance meter for measurement of rail head adhesion.” Proceedings of the Institution of Mechanical Engineers, Part F:

Journal of Rail and Rapid Transit, 227(2), pp.196–200.

Lyu, Y., Zhu, Y. and Olofsson, U., 2015. Wear between wheel and rail: A pin-on-disc study of environmental conditions and iron oxides. Wear, 328, pp.277-285.

Li, Z. Arias-Cuevas, O., Lewis, R., Gallardo-Hernandez, E A., 2009. “Rolling–Sliding Laboratory Tests of Friction Modifiers in Leaf Contaminated Wheel–Rail Contacts.” Tribology Letters, 33(2), pp.97–109

Lu, X., Cotter, J. and Eadie, D.T., 2005. “Laboratory study of the tribological properties of friction modifier thin films for friction control at the wheel/rail interface”. Wear, 259(7-12), pp.1262–1269.

Lu, X., Makowsky, T.W., Eadie, D.T., Oldknow, K., Xue, J., Jia, J., Li, G., Meng, X., Xu, Y., and Zhou, Y., 2012. “Friction management on a Chinese heavy haul coal line”. Proceedings of the Institution of Mechanical Engineers, Part F: Journal of Rail and Rapid Transit, 226(6), pp.630–640.

Marshall, M.B., Lewis, R., Dwyer-Joyce, R.S., Olofsson, U. and Björklund, S., 2006, “Experimental characterization of wheel-rail contact patch evolution.”, Journal of Tribology, 128(July), pp.493–504

Mota, V. and Ferreira, L.A., 2009, “Influence of grease composition on rolling contact wear: Experimental study.”, Tribology International, 42(4), pp.569–574.

Nakahara, T., Baek, K.S., Chen, H. and Ishida, M., 2011. Relationship between surface oxide layer and transient traction characteristics for two steel rollers under unlubricated and water lubricated conditions. Wear, 271(1-2), pp.25–31

Network Rail, 2011, “Network Route Utilisation Stratergy Passenger Rolling Stock”, September, pp. 1–88

Niccolini, E. and Berthier, Y., 2005, “Wheel-rail adhesion: Laboratory study of “natural” third body role on locomotives wheels and rails.”, Wear, 258(7-8), pp.1172–1178

Ohyama, T., 1991, “Tribological studies on adhesion phenomena and rail at high speeds.”,144, pp.263–275

Oldknow, K., Eadie, D.T. and Stock, R., 2012. “The influence of precipitation and friction control agents on forces at the wheel/rail interface in heavy haul railways.” Proceedings of the Institution of Mechanical Engineers, Part F: Journal of Rail and Rapid Transit, 227(1), pp.86–93.

Olofsson, U. and Telliskivi, T., 2003, “Wear, plastic deformation and friction of two rail steels - A full-scale test and a laboratory study”, Wear, vol. 254, no. 1–2, pp. 80–93

Olofsson, U. and Sundvall, K., 2004. Influence of leaf, humidity and applied lubrication on friction in the wheel-rail contact: pin-on-disc experiments. Journal of Rail and Rapid Transit Proceedings of IMechE Part F, 218, 3, pp.235–242

Olofsson, U. and Lewis, R., 2006, “Tibology of the wheel-rail contact”, Handbook of Railway Vehicle Dynamics, pp. 121–138

Olofsson, U. Zhu, Y., Abbasi, S., Lewis, R., Lewis, S.R., 2013, “Tribology of the wheel–rail contact – aspects of wear, particle emission and adhesion.” Vehicle System Dynamics, 51, 7, pp.1091–1120

Pearce, T., Watkins, D., and British Rail, 1987, “Adhesion and leaves - A review of the problem and potential solutions”, Internal document TRIB263-374-017

Rail Accident Investigation Branch (RAIB), 2007, “Autumn Adhesion Investigation Part 1: Signals WK338 and WK336 Passed at Danger at Esher, 25 November 2005”, Rail Accident Report, Report 25 (Part 1)/2006

Rail Accident Investigation Branch (RAIB), 2011. “Station overrun at Stonegate, East Sussex 8 November 2010” Rail Accident Report, Report 18/2011

Schmid, F. et al., 2010, “Best Practice in Wheel-Rail Interface Management for Mixed Traffic Railways”, Birmingham: University of Birmingham Press, Print.

Rail Safety & Standard Board (RSSB), 2014, ‘Investigation into the effect of moisture on rail adhesion (T1042)”

Sinclair, J., 2004, Friction Modifiers in Vehicle Track Interaction: Identifying and Implementing Solutions, IMechE Seminar, February 17th.

Sone, Y. Suzumura, J., Ban, T., Aoki, F. and Ishida, M., 2008. “Possibility of in-situ spectroscopic analysis for iron rust on the running band of rail.” Wear, 265(9-10), pp.1396–1401.

Sundh, J. and Olofsson, U., 2011, “Relating contact temperature and wear transitions in a wheel-rail contact.” Wear, 271, 1-2, pp.78–85

Stock, R., Eadie, D.T., Elvidge, D. and Oldknow, K., 2009, “Influencing rolling contact fatigue through top of rail friction modifier application a full scale wheelrail test rig study,” Wear, 271, 12, pp. 134 – 142,

Stock, R., Stanlake, L., Hardwick, C., Yu, M.,Eadie, D.T. and Lewis, R., 2016. “Material concepts for top of rail friction management – Classification , characterisation and application” Wear, 366-367, pp.225-232.

Telliskivi, T. and Olofsson, U., 2001, Contact mechanics analysis of measured wheel – rail profiles using the finite element method Journal of Rail and Rapid Transit Proceedings of IMechE Part F, 215, 65–73

Tournay, H., 2001, “Supporting Technologies Vehicle Track Interaction in ‘Guidelines to Best Practice for Heavy Haul Railway Operations: Wheel and Rail Interface Issues’”, Virginia, USA

Vasic, G., Franklin, F., Kapoor, A. and Lucanin, V., 2008, “Laboratory simulation of low-adhesion leaf film on rail steel”, International Journal of Surface Science and Engineering, 2, 1-2, 84–97

Wilson, L.J., 2006. Performance measurements of rail curve lubricants” PhD Thesis, Queensland University of Technology

Zhang, W., Chen, J., Wu, X. and Jin, X.S., 2002, “Wheel/rail adhesion and analysis by using full scale roller rig”, Wear, 253, 1–2, pp. 82–88

Zhu, Y., Olofsson, U. and Persson, K., 2012. “Investigation of factors

influencing wheel-rail adhesion using a mini-traction machine.” Wear, 292-293, pp.218–231

Zhu, Y., Olofsson, U. and Chen, H., 2013, “Friction between wheel and rail: A pin-on-disc study of environmental conditions and iron oxides,” Tribolology Letters, 52, 2, pp. 327–339.

Zhu, Y., Olofsson, U. & Nilsson, R., 2014, “A field test study of leaf contamination on rail head surfaces.” Proceedings of the Institution of Mechanical Engineers, Part F: Journal of Rail and Rapid Transit, 228, 1, pp.71–84

Zhu, Y., Lyu, Y. and Olofsson, U., 2015. “Mapping the friction between railway wheels and rails focusing on environmental conditions”, Wear, 324-325, pp.122–128

3. Assessment of railway curve lubricant performance using a twin-disc tester

S.R. Lewis [1], R. Lewis [1], G. Evans [2], L.E. Buckley-Johnstone[1]

[1] Department of Mechanical Engineering, The University of Sheffield, UK
[2] Network Rail, UK

Poster Presentation at *9th International Conference on Contact Mechanics and Wear of Rail/Wheel Systems, Chengdu, 2012*

Published in *Wear, Volume 314, Issues 1–2, 2014, Pages 205–212*

Abstract

Tests have been carried out to assess the performance of ten different grease types used as curve lubricants. All greases tested have been designed for wayside flange lubrication and some are currently used on the UK's rail network. Each grease's performance was assessed in terms traction coefficient, retentivity (how long a fixed amount of grease provided lubrication), and wear. Two series of tests were carried out: one running the test until the traction level reached that of a dry contact, referred to as a "lubricant starvation test", and the other running the test up to the point where the traction started to rise i.e. when there was still grease on the disc, referred to as a "fully lubricated test". In initial starvation tests slip was varied along with amount of grease applied. In both series repeat tests were carried out on the same disc pairs to monitor the effect of changes in surface roughness on grease performance.

Grease retentivity was found to be greater with lower roughness and with more grease applied. Repeat tests with discs used for starvation tests led to very high wear rates. This was thought to arise as cracks initiated as the first run reached dry conditions were pressurised by grease reapplied in the subsequent tests causing crack growth and intersection and associated pitting and spalling. Clear differences were seen between the greases in terms of their retentivity performance although there was considerable scatter. Coefficients of traction (COT) in the early stages of the starvation tests and during the fully lubricated tests were below 0.1 and very consistent. Again differences could be found between greases under the test conditions used.

3.1. Introduction

Grease is widely used to lubricate the rail gauge corner/wheel flange contact as a locomotive passes through a curve. The conditions of the gauge corner/flange contact are very severe with high contact pressure and slip in comparison to the wheel tread/rail head contact. Grease therefore helps protect the wheel and rail from excessive wear and can help suppress noise. Grease is usually automatically applied to the rail gauge at the beginning of a curve by a wayside applicator. A varying amount of grease will be applied according to the number of axles of the approaching train. The grease passes through ports on the applicator, as shown in Figure 1.

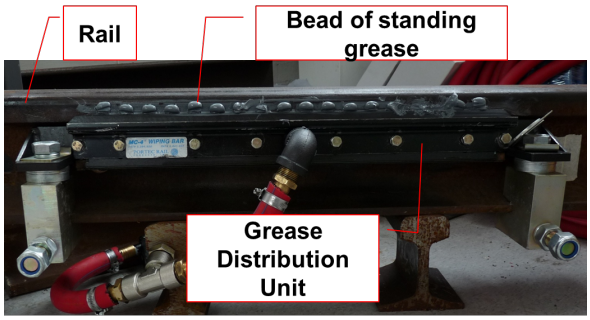

Figure 1: **Rail with attached Grease Distribution Unit (GDU) showing grease adhered to rail gauge.**

The standing grease is picked up by the passing wheel flanges of the train that will then lubricate the length of the curve. There are many brands of grease designed for use on rail curves. Ten such greases are tested in this research. Part of the work carried out in this paper was to design a standard test for new greases which are intended for use on the UK's rail network. This initial laboratory test would be used as part of the certification of a particular grease for track use. The second aspect the work was to assess the performance of each grease using the established tests. Similar experiments have been carried out previously by Eadie (2011) using an Amsler (twin-disc) rig and Clayton (1989). This study was to go further by understanding the spread of results by repeating and by studying the effects of surface roughness.

It is important for infrastructure owners to have a set of tests for any products being applied to the rail head as part of an approval process that verifies their performance before they are bought and used. Some of these may be standard, but others, such as friction, retentivity and pumpability need to resolve bespoke tests. The full set of tests now required by Network Rail are detailed in their specification NR/L3/TRK/3530/A01 (2012).

3.2. Test methodology

This study was carried out using the University of Sheffield Rolling Sliding (SUROS) rig (Fletcher, 2000). Figure 2a shows a schematic of the SUROS rig. The discs typically used are shown in Figure 2b.

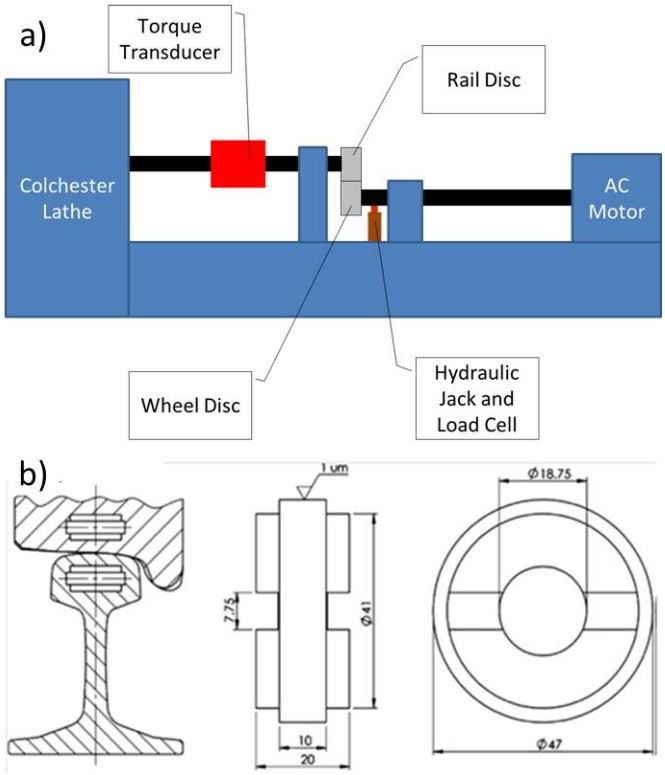

Figure 2: **a) Schematic of SUROS rig; b) Extraction and dimensions of SUROS specimens.**

Before each test the discs were cleaned (in an ultrasonic bath of acetone), weighed and a fixed mass of grease was applied to the (circumference of the) rail disc. After trial tests were carried out the main (body of) tests were run in two series: 1) Lubrication Starvation (LS) tests; where the test was run until all of the grease had gone from the disc contact and a dry coefficient of traction was yielded from the test, 2) Fully Lubricated (FL) tests; where the test was run up until the point where the traction had started to rise from its steady state/lubricated level i.e. the grease had reached its useful life. Repeat tests were performed on each set of discs to subject each grease to varying surface roughness conditions.

3.2.1. Trial tests

A series of trial tests were performed so that test parameters such as slip and amount of grease could be determined. Two slip levels were used in the trials, namely 7.5 and 10%, both typical of a rail gauge/wheel flange contact. In a SUROS test at 400rpm, sliding speeds in the contact would be 0.075m/s and 0.1m/s at these slip values, so at the mild end of possible conditions, as shown in Figure 3. A Hertzian contact pressure of 1500 MPa was used for the tests, which is a typical of a rail gauge/wheel flange contact as shown in Figure 3. Nominal amounts of grease of 0.05g and 0.1g were used, scaled down from amounts applied in the field through a Grease Distribution Unit (GDU), such as that shown in Figure 1.

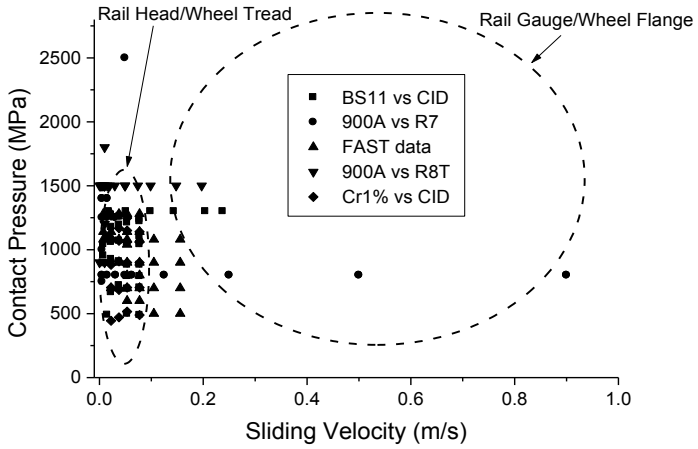

Figure 3: Rail steel wear data plotted over typical wheel/rail contact conditions (Lewis, 2004).

Figure 4 shows traction curves from the trials. This shows how traction curves were affected by slip, amount of grease added and surface roughness (higher roughness tests were achieved by repeating tests with the same discs). It shows that the amount of time the grease remained in the contact, retentivity was longest for the test at 7.5% slip. Testing at 10% gave values that would probably not allow differences in greases to be resolved. The greatest influence on retentivity was the roughening of the surface of the test samples. When running the tests for the first time on new discs the roughness went from 1µm Ra to 10µm Ra (more detail on roughness is given in a later section). Repeat tests then started at 10µm. Figure 4 also shows that there was a large amount of scatter in the cycles taken to reach dry conditions which means that ideally in assessing grease many repeats should be carried out.

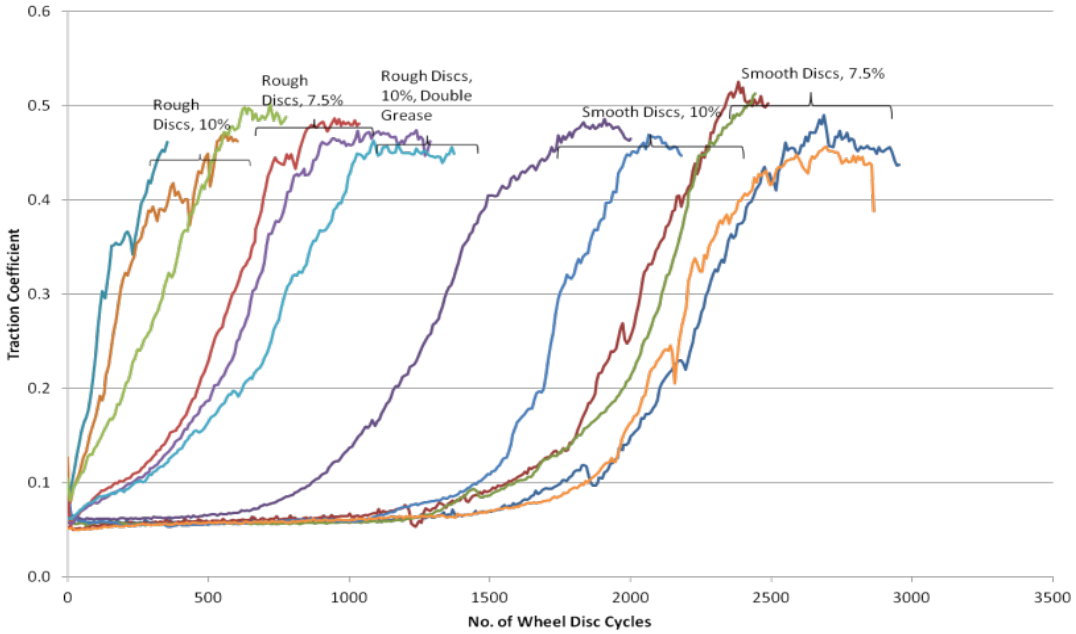

Figure 4: Traction curves for grease trials using grease D.

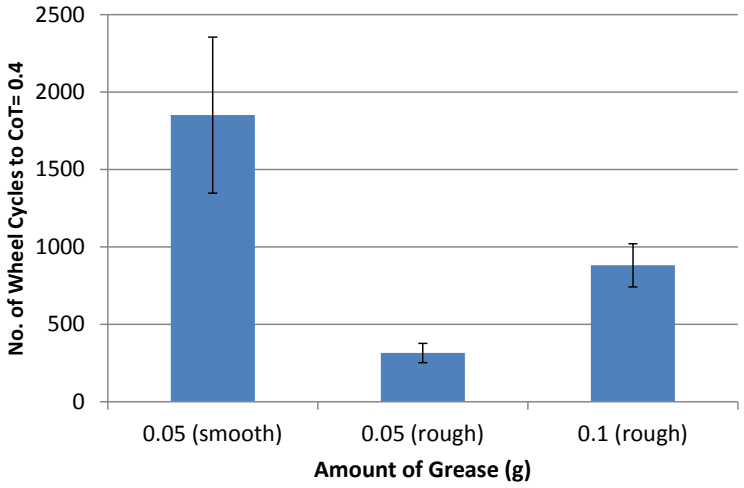

Figure 5: Retentivity with amount of grease used generated using grease D.

Figure 5 shows the retentivity in cycles for the smooth and rough discs which were tested at 10% slip with 0.05g and 0.1g of grease added to them, error bars show standard deviation. It can be seen that 0.1g gives a greater retentivity with a rougher set of discs.

Therefore in order to be able to resolve the performance differences between greases on repeat tests, grease application amount and slip value of 0.1g and 7.5% were used in subsequent tests.

3.3. Results

3.3.1. Lubrication starvation tests

The lubrication starvation tests were designed to simulate the transition from fully lubricated to dry rail gauge/wheel flange contact. Four greases were tested in the starvation tests namely: D, E, H and J. To take into account the effects of surface roughness each experiment was repeated on the same set of discs four times. Friction results can be seen in Figures 6 to 9. These figures illustrate how grease D shows lower dependability on surface roughness, but has much lower retentivity in the first test compared to the other three.

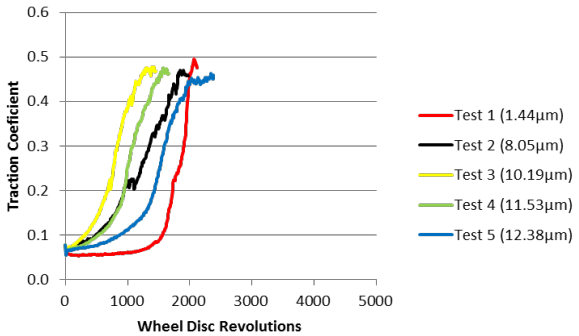

Figure 6: Traction coefficient curves for starvation tests with grease D. Starting combined Ra value of discs for each test shown in brackets.

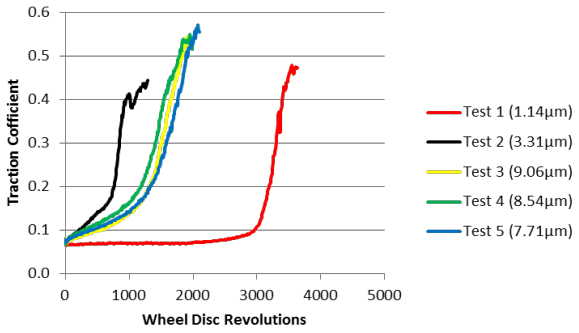

Figure 7: **Traction coefficient curves for starvation tests with grease E. Starting combined Ra value of discs for each test shown in brackets.**

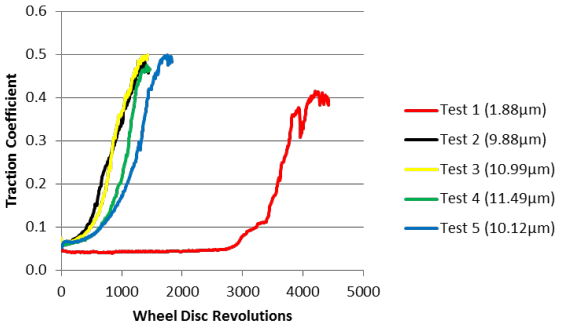

Figure 8: **Traction coefficient curves for starvation tests with grease H. Starting combined Ra value of discs for each test shown in brackets.**

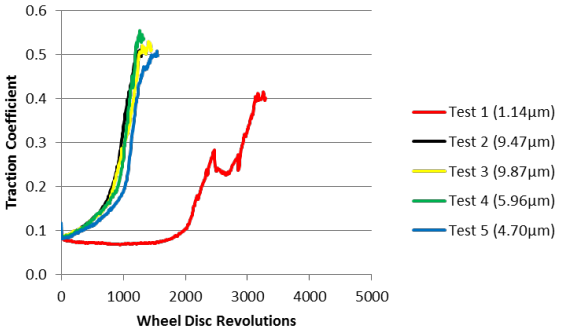

Figure 9: **Traction coefficient curves for starvation tests with grease J. Starting combined Ra value of discs for each test shown in brackets.**

Figures 10 to 13 show wear data from the lubricant starvation series of tests including the specimen's respective combined roughness for each test. The combined surface roughness is a way of representing the individual surface roughness' of each disc using one number. It is calculated using equation 1.

$$Rc = \sqrt{{R_1}^2 + {R_2}^2} \quad (1)$$

Where: Rc is the combined surface roughness; R_1 is the roughness (Ra) of disc 1 and R_2 is the roughness (Ra) of disc 2

Each test was repeated on the same set of discs. Typical wear data for un-lubricated discs under the same conditions has been included in Figures 10 to 13 (from (6)).

As can be seen in Figures 10 to 13 the wear rapidly increases from Test 1 onwards and a strong correlation is shown between the increased wear rate and large increase in surface roughness between Tests 1 and 2. However, with all greases there is a drop off in wear rate between Tests 2 and 5, but this is not always the case with the surface roughness which sometimes keeps on increasing as in Figure 10. What is also striking is that the wear for the lubricated tests (Test 1 to 5) are much greater in most cases than that of an un-lubricated one (Dry Typical).

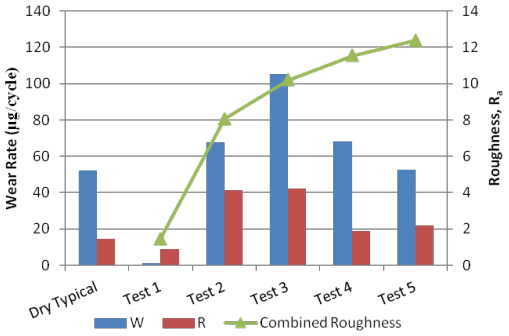

Figure 10: **Wear data for grease D from the lubricant starvation tests.**

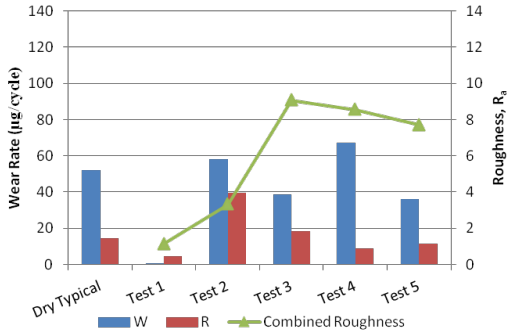

Figure 11: **Wear data for grease E from the lubricant starvation tests.**

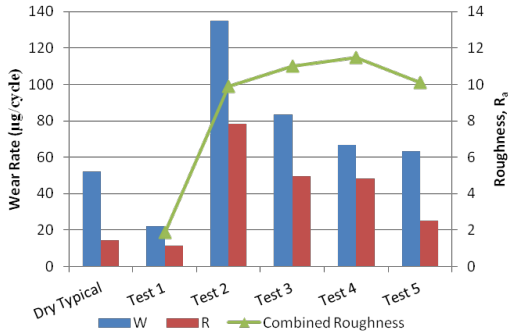

Figure 12: **Wear data for grease H from the lubricant starvation tests.**

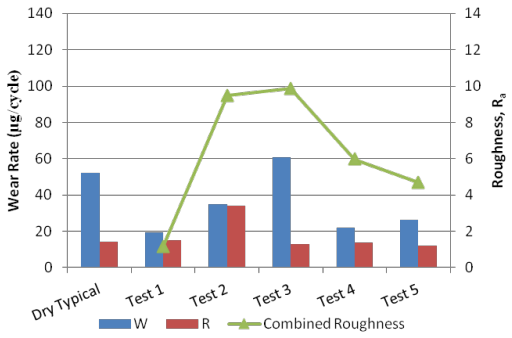

Figure 13: Wear data for grease J from the lubricant starvation tests.

Figure 14 shows the effect of surface roughness on the retentivity of the grease during the lubrication starvation tests and there is a general trend of decreasing retentivity of the grease with increasing surface roughness. Note how for greases E, H and J there is a dramatic decrease in retentivity when surface roughness increases beyond 2µm Ra. The relative independence between retentivity and surface roughness for grease D can also be seen in Figure 6.

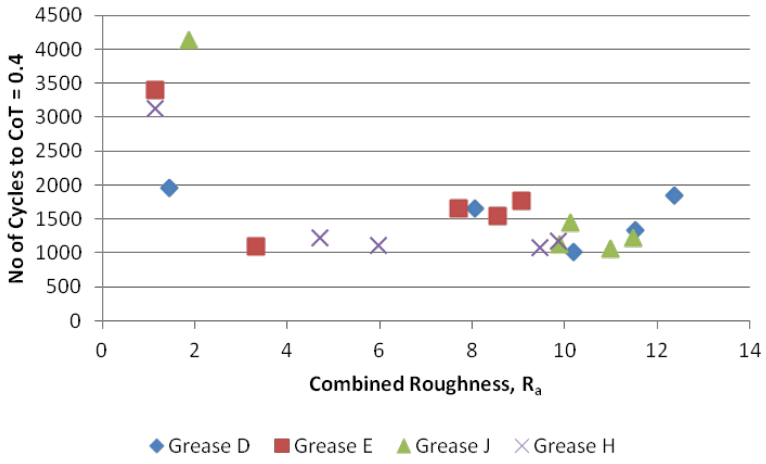

Figure 14: Relationship between retentivity and surface roughness. In this case retentivity was defined as the number of cycles taken for the traction coefficient to reach 0.4.

3.4. Fully lubricated tests

The fully lubricated (FL) tests were designed to investigate the wear inhibiting performance of each grease while it was still active in the contact. In these tests 0.1g of grease was placed onto the rail disc before each test as in the starvation tests. The FL tests were, however, stopped when the traction coefficient had risen 0.03 from its steady state baseline value. Four tests in total were done during the FL series of tests. Test for each grease were run on 2 new surfaces and 2 used surfaces. The used discs were the same discs as had been used for the initial (new disc) tests. Figure 15 shows the traction curves for initial fully lubricated tests. (Greases D, E, H and J are the same as used in the starvation tests).

Figure 16 shows both the initial and repeat baseline friction level for each grease in the FL test. Figures 16 to 19 have one column to represent the mean of the two initial test and one column representing the mean of the two repeat tests. Grease J had only one initial and one repeat test and hence has no error bars. Error bars indicate standard deviation.

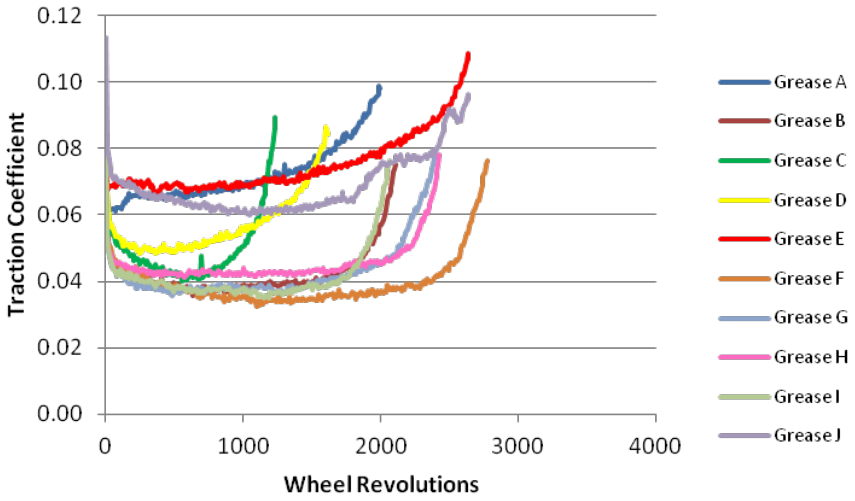

Figure 15: **Chart showing traction coefficient curves for fully lubricated initial tests.**

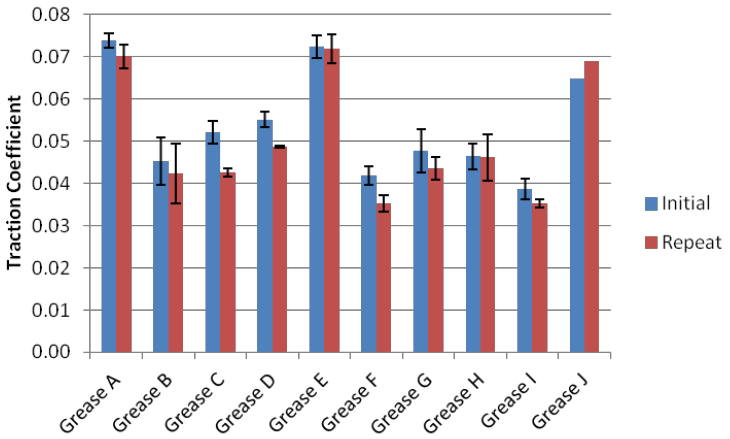

Figure 16: **Traction coefficient curves for fully lubricated initial and repeat tests.**

Figure 17 shows the retentivity of each of the greases tested. For the fully lubricated test this is defined as the number of test cycles when the traction coefficient rises 0.03 above its steady state/baseline value.

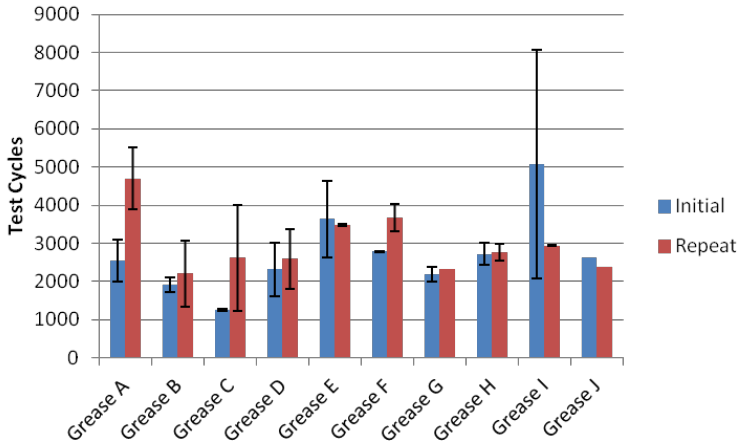

Figure 17: Retentivity for greases during fully lubricated friction coefficient for each of the greases.

In Figure 16, greases A to I show a drop in mean traction coefficient in the repeat test compared to the initial test. Grease J, however, displays the opposite behaviour. Figure 17 shows how much scatter there is in the retentivity of the greases.

Figures 18 and 19 show wear rates during the fully lubricated tests for the wheel and rail discs respectively.

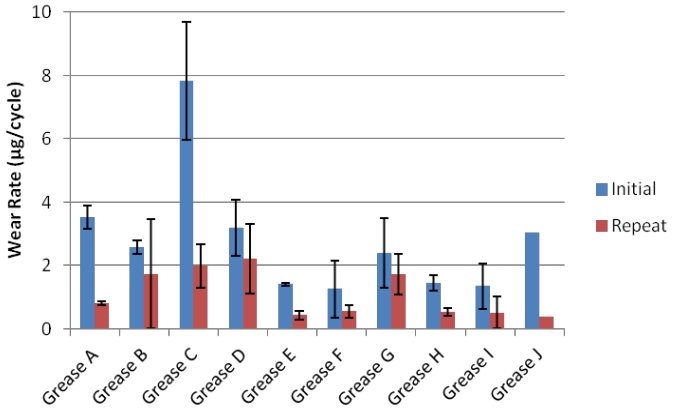

Figure 18: Wear rate in µg/cycle, for wheel discs for initial and repeat tests.

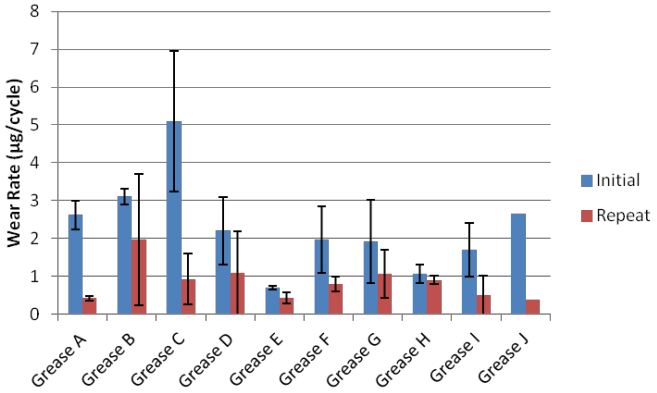

Figure 19: Wear rate in µg/cycle, for rail discs for initial and repeat tests.

3.5. Discussion

Lubricated traction from both the FL and LS test was below the 0.1 level which is what would be expected of a grease. Figure 20 shows that good agreement in traction levels was shown between the four greases that were tested in both the FL and LS tests.

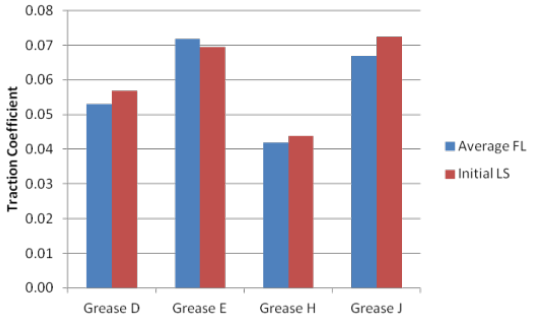

Figure 20: **Comparison of traction coefficients of four greases which were tested in both the FL and LS tests.**

There was a strong correlation between traction coefficient and surface roughness with higher surface roughness giving higher traction. The correlation was most strong between the rail disc surface roughness and traction. Correlation was also shown between surface roughness and retentivity with increasing roughness leading to a decrease in retentivity. This correlation was strongest between rail surface roughness and retentivity. A stronger correlation was seen between retentivity and wear rate. Figure 21 shows a scatter graph of retentivity and wear rate for the wheel and rail discs used with all ten greases in the initial FL tests.

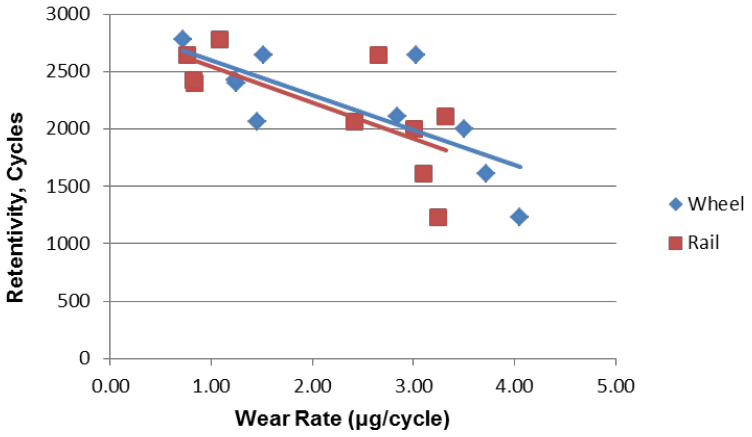

Figure 21: **Correlation between wear rate, in µg/cycle, and retentivity for wheel and rail discs under the fully lubricated regime.**

This is quite interesting as the calculated wear rate does not represent any physical property of the discs which would be thought to correlate with the retentivity of the grease, such as surface roughness. It may be then that the wear rate is an indication of some other surface property which is affecting the greases retentivity which is not being measured by the 2-dimensional measure of surface roughness.

The wear rates seen under the FL regime are much lower than those seen under the lubrication starvation, LS, regime. This seems to suggest that most of the wear seen in the LS tests occurred during the part of the test where the grease was no longer effective and friction was starting to rise. In most cases the wear of the wheel and rail is much lower in the repeat tests than in the initial tests. Figures 22 and 23 show a comparison of the averaged wear rates from the FL tests and wear rates seen in the LS tests with greases D, E, H and J for the wheel and rail respectively. Comparisons are made using the average initial test and the average repeat test for the FL regime and the lowest and highest wear rates seen during the LS tests. They are also shown with a typical un-lubricated/dry wear rate for identical contact conditions.

As can be seen from Figures 22 and 23 the wear rates seen in the majority of the starvation tests were vastly higher than those of the FL tests. It was seen with the wheel discs that the lowest wear rate of the LS test was lower than both the FL tests for greases D and E only; typically between 30 and 59% of the FL wear rates. Obviously this would not be expected as the LS tests were subject to the grease removal phase in which increased wear rates were thought to occur. In all other cases (wheel or rail) the lowest wear rate of the LS tests was mainly (between 4.1 and 51) times greater than the wear of the FL tests.

For both wheel and rail the first and second FL wear rates and all but one of the lowest LS wear rates (grease J rail) were between 1 – 79%, of the associated un-lubricated value. The lowest LS wear rate for the rail disc with grease J was 104% of the un-lubricated rail wear. For the rail, all of the highest LS wear rates ranged between 2.4 – 5.5 times the un-lubricated rail wear rate. For the wheel the highest LS wear rate was between 0.67 – 2.6 times the un-lubricated wheel wear rate. Lubricated wear rates would be expected to be a fraction of un-lubricated wear rates regardless of whether full or partial lubrication was achieved throughout the test.

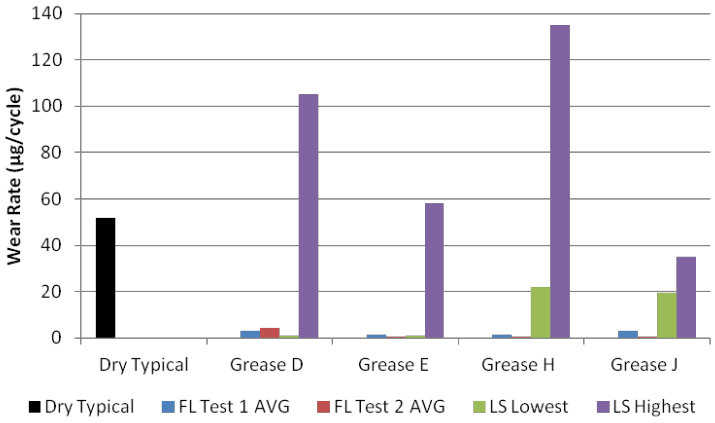

Figure 22: Comparison of wear rate in µg/cycle, for wheel discs under FL and LS regimes.

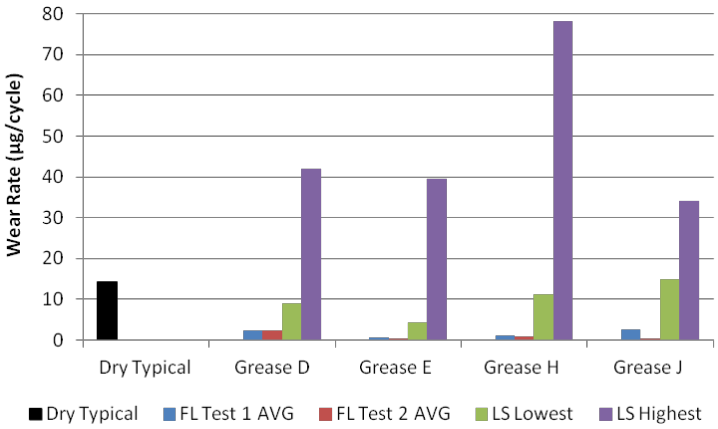

Figure 23: Comparison of wear rate in µg/cycle, for rail discs under Fully Lubricated and Lubrication Starvation regimes.

It was observed during these tests that the dark layer of grease would wear from the surface of the discs in bands leaving sections of the disc un-lubricated. Figure 24 shows an image of the grease as it was wearing from the rail disc surface.

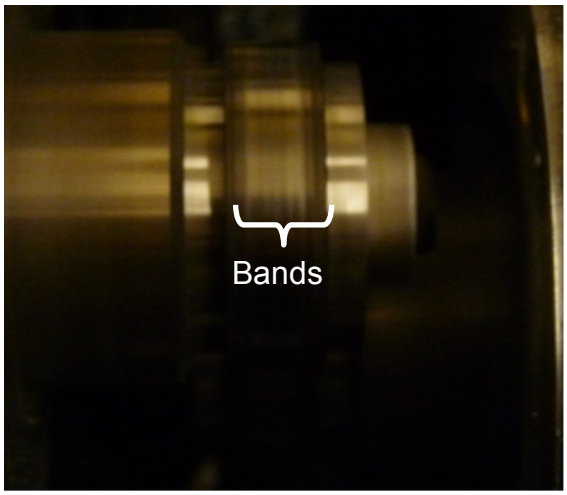

Figure 24: Image of grease wearing from disc in bands.

It was also observed after the fully lubricated tests that a dry soap-like substance was adhered to the surface of the discs which could be rubbed off by hand, but bonded strongly enough to the surface that it could not be removed by the ultrasonic cleaner. It is proposed that this substance may be a mixture of the particular grease's additives with most of the oil extracted. Additives are added to greases and oils to improve their properties. Agents are added such as: anti-wear, anti-foaming, fire retardant, extreme pressure, high temperature, etc. For commercial reasons, the specific chemical constituents of these additives are not known. However, most of these additives will be designed to work within the base oil. What is not known is the tribological effect of these additives when present without the base oil which is what may be the case in these tests. This could help explain the very high wear rates seen in the starvation tests. It is proposed that during the starvation tests the oil in the grease is burnt off as the traction curve turns upward. It seems that this soap-like layer is removed from the contact at some

point between where the traction curve starts to turn upward and the traction coefficient reaches a dry level. This is because it was not witnessed on the discs at the end of the LS tests, but was witnessed on the disc surfaces after the FL test where the tests were stopped before the traction reached dry levels. The slow rise of the traction coefficient during this stage of the LS test is also evidence of this substance being removed from the contact.

Figure 25 shows an image of the test specimens used with grease B after a FL test, but before the discs have been cleaned. It shows how the grease has been removed from the surface of the disc in bands as also shown in Figure 24. Other greases showed different patterns of the soap-like substance on their surface.

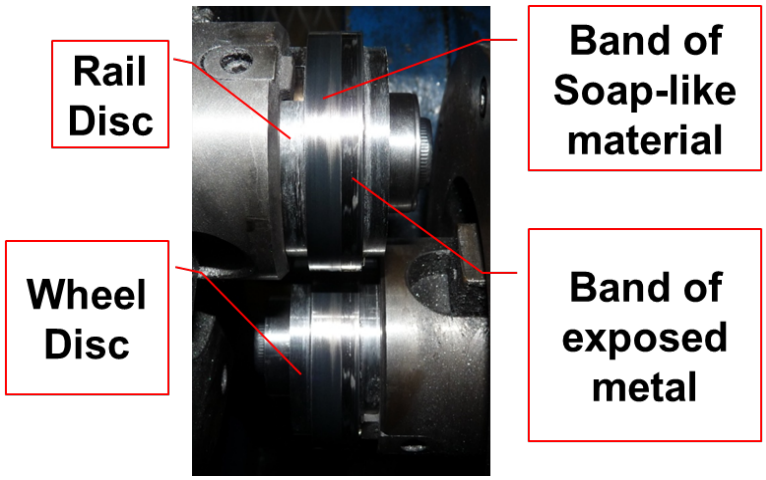

Figure 25: **Image of soap-like material left on the disc surface after a FL test with grease B.**

Figure 26 shows the same discs as in Figure 25 after the substance has been removed from their surface. Damage can be observed on the portion of the disc which was un-coated as seen in Figure 24.

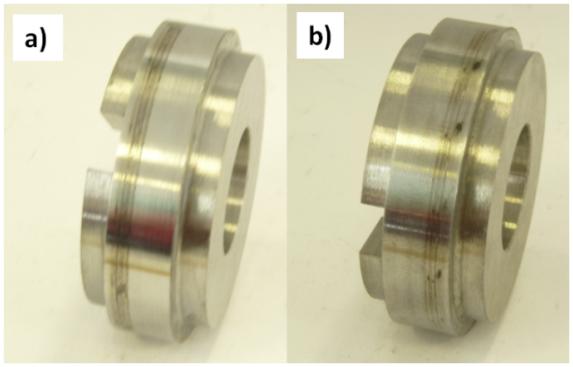

Figure 26: **Image of the cleaned discs after FL test with grease B a) rail disc b) wheel disc.**

Removal of the grease from the disc surface in bands could also provide a clue as to the high wear rates which were seen during the LS tests. Most of the discs tested in both the FL and LS tests showed localised surface damage as shown in Figure 26. These areas of damage coincided with bands of grease which had been removed from the surface. It is hypothesised that wear and crack initiation will occur in these damaged sections. During

subsequent tests these cracks can then become pressurised by the reapplication of grease, leading to spalling. To observe any cracks the discs were sectioned. Firstly an eddy current probe was used to locate a section of disc containing a crack. The cracked section was then extracted from the SUROS sample using an abradable cutting wheel. The extracted section was then mounted in Bakelite and polished so that any cracks would be clear under an optical microscope. Images of discs run using greases D and H in LS and FL tests are shown in Figure 27. Cracks, while not present for FL tests where the discs have not run dry at all, are evident in discs run dry several times in LS tests. This confirms the damage model proposed above.

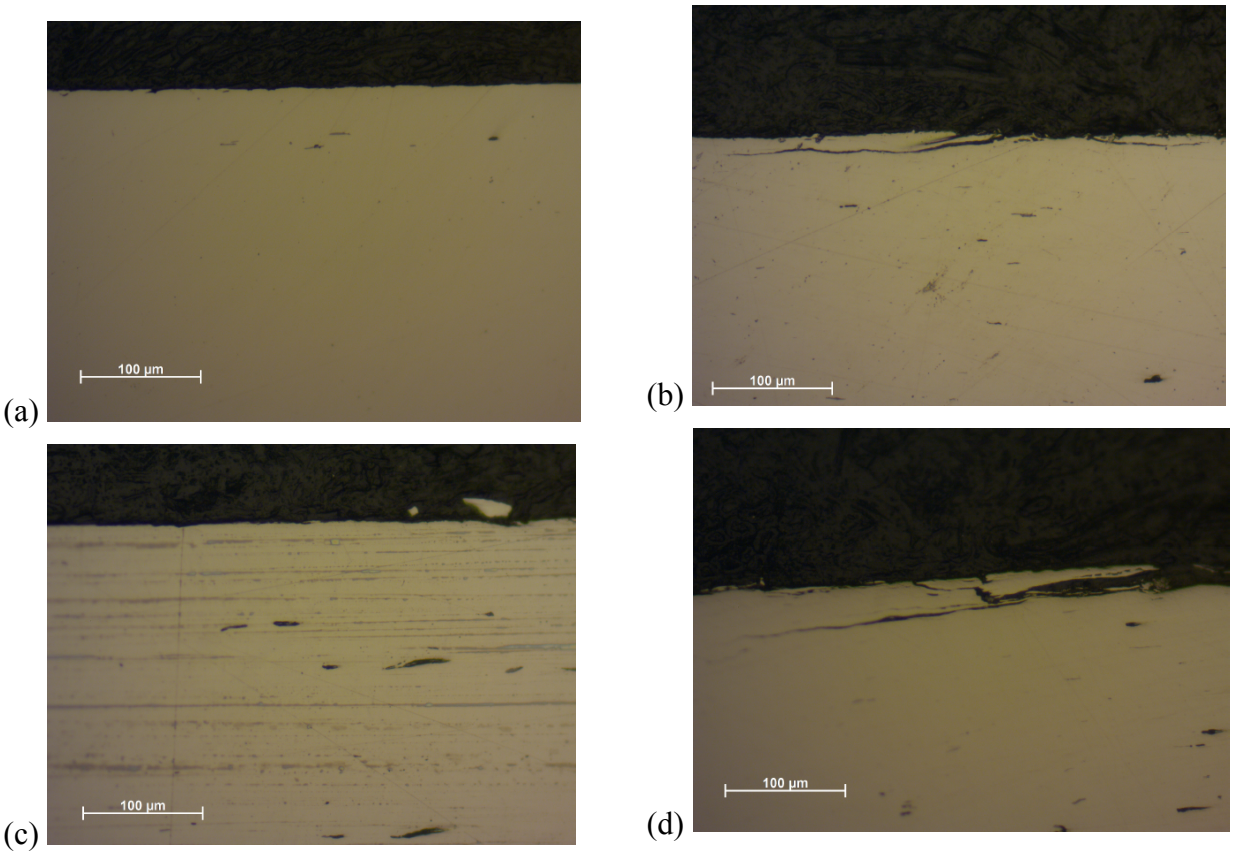

Figure 27: **Images of sectioned discs from (a) FL test with Grease D; (b) LS test with Grease D; (c) FL test with Grease H and (d) LS test with Grease H**

3.6. Conclusions

Two series of test have been performed to assess the performance of different types of flange lubricator grease and the effects of surface roughness upon this performance.

- Lubricated friction levels are what would be expected with a grease, i.e. C.O.T < 0.1
- High wear rates are being observed under the lubrication starvation tests due to the grease wearing off in bands leading to localised damage of un-lubricated sections of the disc. This in turn is leading to excessive wear of the discs in subsequent tests.
- There is a distinct inverse relationship between surface roughness and grease retentivity.

- There is also an inverse relationship between retentivity and disc wear rate.
- Some scatter was seen in these tests but has also been seen in similar tests with grease in previous studies.
- The test method described in this work clearly highlights the performance differences between different greases and is therefore considered suitable as a method of certification for new greases before they are introduced onto the rail network.
- Tests should be repeated on new disc surfaces each time to mitigate the effects of changes in surface roughness on the grease performance.

3.7. References

Clayton, P., Danks, D., Steele, R.K., 1989, “Laboratory assessment of lubricants for wheel/rail applications” Lubrication Engineering, 45, pp. 501-506

Eadie, D.T., Lu, X., Santoro, M., Oldknow, K., 2011, “Wayside gauge face lubrication: How much do we really understand?” Proceedings of the International Heavy Haul Association Conference 2011, Calgary Canada, 19-22 June

Fletcher, D.I., Beynon, J.H., 2000, “Development of a machine for closely controlled rolling contact fatigue and wear testing”, Journal of Testing and Evaluation, 28, 267-275.

Hardwick, C., Lewis, R., Eadie, D.T., Rovira, A., 2011, “Rail wear – Understanding the effect of third body materials”, Proceedings of the IoM3 Conference on 20th Century Rail, York United Kingdom, 1-3 November

Lewis, R., Olofsson, U., 2004, “Mapping Rail Wear Regimes and Transitions.” Wear, 275 721-729.

Network Rail, 2012, “Curve Lubricants”, Network Rail Test Specification NR/L3/TRK/3530/A01

4. Field trials of a new method for the assessment of gauge face condition using a modified pendulum test rig

L.E. Buckley-Johnstone[1], R. Lewis [1]

[1] Department of Mechanical Engineering, The University of Sheffield, UK

To be submitted to Journal of Rail and Rapid Transit Proceedings of IMechE Part F

Abstract

There is currently no friction measurements taken when making an assessment of grease carry down in the field. This paper presents two field studies to assess the use of a modified pendulum tester as a means to measure the presence of a rail curve lubricant on the gauge face of a rail. The first study assess grease carry down along a curve on a heritage railway line by taking successive measurements at set distances away from a fixed location lubricator. The second study looks at the effect of successive axle passes and the adhesion condition development to assess whether the modified pendulum tester is capable to measure the presence of lubricant when visual inspection would indicate otherwise. Both studies showed that the modified pendulum tester is suitable for field measurements to assess the presence of lubricant on a rail curve.

4.1. Introduction

The carry down of grease along the entire rail curve is important for the effective lubrication of the wheel flange/rail gauge face. This has become more important in recent years where Grease Distribution Units (GDUs) have been used to treat multiple back-to-back curves to reduce maintenance time (reducing the time teams have to travel between lubricators). The carry down of rail grease is necessary for full lubricating this severe contact and if not consistent can have detrimental affects on wear and rolling contact fatigue (Fletcher, 2000).

Currently visual assessment of the rail gauge is used to determine whether grease has been carried down and deposited around the curve. In the UK a service engineer can wipe the rail gauge clean to expose the rail surface (an example of this is shown in Figure 1) and judge whether there is lubricant present.

Figure 1: **Example of the wipe test to evaluate grease carry-down.**

This visual assessment is obviously a crude method of assessing whether grease has been carried down and does not assess whether substance wiped from the surface is in fact a lubricant.

The nature of the railway network means that some sites are not easily accessible which makes bringing large test equipment impractical. Traditional portable railway tribometers are limited in assessing the top of rail friction (Harrison, 2002). Another disadvantage of a traditional tribometer is the adhesion measurement is an average over the distance measured; localised areas cannot be measured.

Recently Lewis et al. (2011) have shown that a pendulum tester that is traditionally used to measure adhesion of a road (BS EN 13036-4:2003) and different floor surfaces (AS/NZS 4586:2004) can accurately produce adhesion measurement of the rail head friction. The advantage of the pendulum tester is that it is highly portable, has a short set-up time making it suitable for in-service measurements and can be used with minimal training.

The foot of a pendulum tester allows the user to change the material in contact depending on what slider pad is attached. A simple modification to the connector and the slider pad can allow the slider to contact the gauge far of the rail head. This can then be used to measure whether there is any lubricant present on the gauge face.

In this work two small-scale field trails have been conducted using a modified pendulum with an adapted foot designed to contact the rail gauge face to assess the presence and carry-down of lubricants.

4.2. Apparatus

The pendulum used was a Munro-Stanley pendulum, a schematic of which is given in Figure 2, which has been calibrated according to the British Standard (BS 7976-3:2002). The pad material used for both top of rail (TOR) and gauge measurements is the Slider 96 rubber (formerly Four-S), which is a hard rubber akin to that found on the sole of a shoe. The pendulum rig measures the energy loss from the slider moving over a finite distance as the slip resistance value (SRV). A simple relationship between the SRV and the equivalent coefficient of friction has been established using historical test data that can be used for TOR measurements (Lewis, 2011).

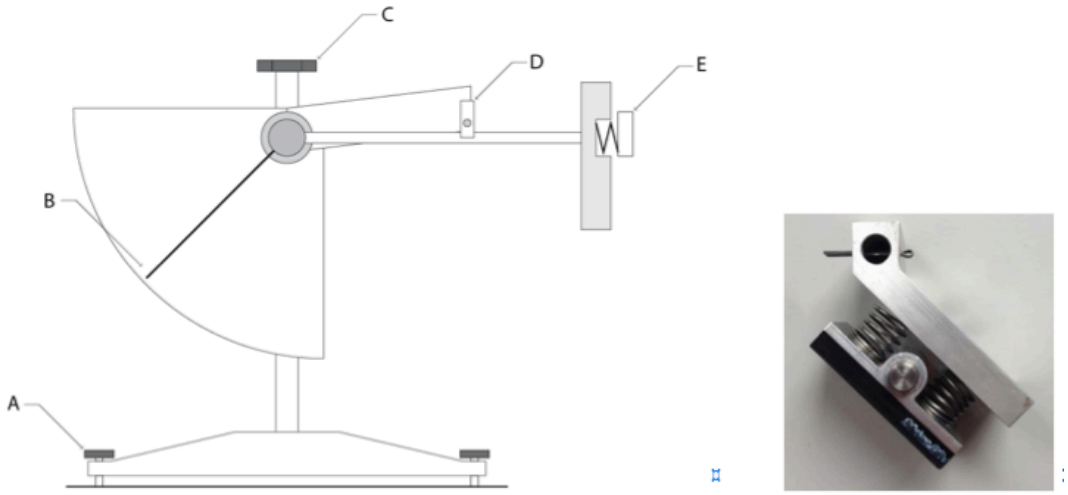

Figure 2: **From left) Pendulum test rig schematic [A) Adjustable feet; B) Pointer; C) Height adjuster; D) Release catch; E) Slider pad]; modified pendulum foot attachment**

The modified foot allows contact with the gauge face of the rail, allowing measurement of the adhesion (SRV) at the gauge to be taken. The angled pendulum foot attachment is shown in Figure 2. It has been designed to contact the rail gauge at a 45^{o} angle in the mid part of the pad – note the pad's width has been reduced from 76 mm to 50 mm as only the centre is in contact. The foot will slip both vertically and horizontally during the initial and final phase of contact due to the geometry of the rail gauge corner. Because of the different profiles and states of wear found on rails, the contact will vary slightly from measurement to measurement, especially if severe gauge face wear has taken place.

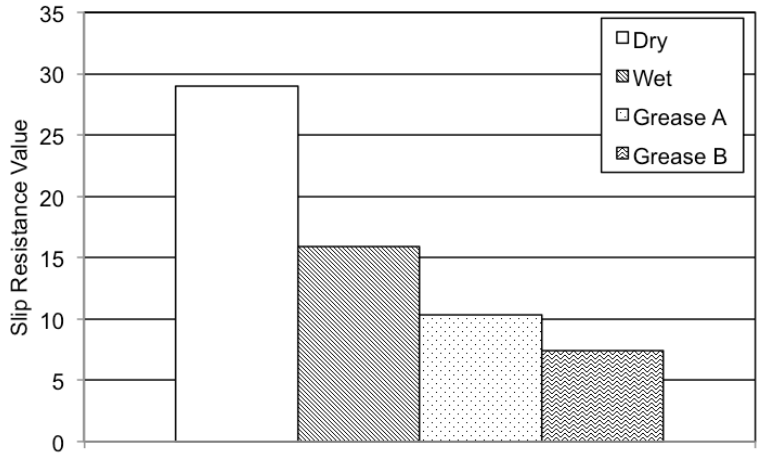

Figure 3: **Pre-field laboratory tests using a modified pendulum foot to measure gauge face adhesion in dry, wet and lubricated conditions.**

Pre-trial laboratory tests compared SRVs taken using the modified foot in dry, wet and 2 different grease conditions (Figure 3). These laboratory tests showed a clear difference between a dry, wet and grease, which indicated the suitability of this modified foot as a lubricant detection method. The pretrial

tests also highlighted the care required in setting up the pendulum. Small lateral shifts can cause large variations in the energy loss during contact.

4.2.1. Methodology

A setsquare, or right-angled guide should be used to measure the distance from the field side of the rail (face that is not being measured), to the edge of the pendulum foot (a convenient reference point). Once this distance is established for a measurement, the rig should be placed in this position for each subsequent measurement. It was found in laboratory testing that any movement +/- 5 mm from this position can cause large variations in the SRV measured. Measurements of this distance at both the toe and heal of the pendulum foot also ensure the pendulum is parallel to the rail head.

Figure 4: Pendulum set up for left) Gauge corner measurement; right) TOR measurement.

The method of operation for the TOR measurements has been previously detailed by Lewis (2011). The method of operation when using the angled pendulum foot is the same as when taking a TOR measurement with additional measurements required to achieve reliable and repeatable results. The procedure to follow is given here:

- Align the centre of the pendulum foot with the centre of the gauge corner of the rail (Figure 4).
- Measure the distance from the field side of the rail to the edge of the pendulum foot using the right angle guide.
- Adjust the height of the pendulum to give a contact length of 127 mm. Contact length is defined as the length from first contact between the pad and the rail to the final contact between the pad and the rail. The initial contact will be very minimal. The load on the pendulum foot will increase as the pendulum reaches a minimum.
- Place the pendulum in the initial position so that it is held at 90^{o} to the rail (see Figure 2).
- Ensure that the pointer is level with the pendulum foot. Press the release button and catch the foot on its return after making contact.
- Record the SRV, as indicated by the pointer rest position.
- Repeat for until 6 measurements have been taken.

In Study A, pendulum measurements were taken as stated above whilst moving away from the lubricator site whilst no trains passed through the section of the line.

In Study B, which was conducted on a curve in a maintenance yard, pendulum measurements were taken at a single location whilst a vehicle completed passes at regular intervals.

4.3. Study A: Field-testing on the Severn Valley Railway using a pendulum tester with a modified foot

4.3.1. Site information

The pendulum tribometer with a modified foot attachment has been field tested on the Severn Valley Railway (SVR) heritage line.

The friction levels found on a single bi-directional curve, serviced by two LBFoster MC4 grease distribution units (GDUs) using the traditional pendulum set-up and the gauge face using the new angled foot to assess the rail head adhesion and carry down of grease, respectively.

A curve on the SVR was chosen to perform the initial study as it allowed measurements to be taken on an active line (see Figure 5). Three measurement locations were chosen around the curve, as shown in Figure 6 and detailed in Table 1. The SVR is a heritage line and is a single bi-directional track that carries a mixture of vintage steam and diesel locomotives of variable sizes. The frequency of trains is between 1 and 2 trains per hour.

Measurements were taken on a dry, partially cloudy day in mid-June 2014. The grease in use on the line was Claretech Supreme rail curve grease.

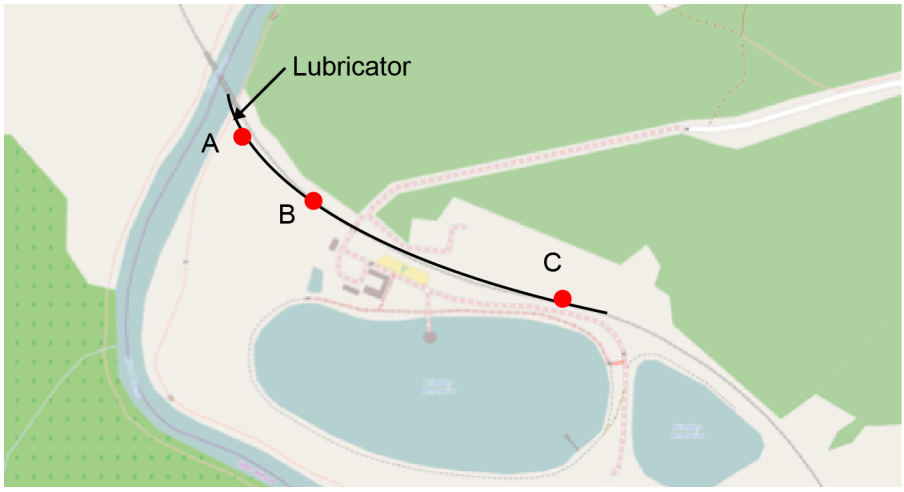

Figure 5: **Map of test site detailing locations of measurements.**

Figure 6: **Images of site, clockwise from top left: General curve image; Location 1 showing GDU; Location 3; Location 2.**

Table 1: Location details of test sites

Location	Direction of traffic	Lubricator type	Distance from lubricator (m)	Description
A	Single track - Bi-directional	2 x Portec MC4 GDU	0	Lubricator site. Victoria bridge.
B			150	Midpoint of curve
C			400	End of curve. Beginning of transition to next curve

4.4. Study B: Field-testing of angled pendulum in Stockholm, Sweden.

4.4.1. Site information

Study B was conducted in a maintenance yard in Stockholm, Sweden. Measurements were taken on the high rail of a single low radius curve at a set location, as shown in Figures 7 and 8. The vehicle used comprised of 4 carriages with a total of 8 wheelsets. Each pass of a curve would therefore complete 8 wheel passes over the defined measurement point.

The first measurements were made after cleaning the rail and prior to any train passes (zero wheel passes). This initial condition is considered steady state and represents a clean, dry and lubricated surface. A vehicle was then run bi-directionally around the curve in an un-lubricated condition. Three further sets of dry measurements were taken after 96, 192 and 272 wheel passes.

After 272 wheel passes the high rail was manually lubricated with oil (see Figure 8). A set of measurements in a lubricated condition was then taken. An additional 48 wheel passes were then completed and a final set of measurements were taken.

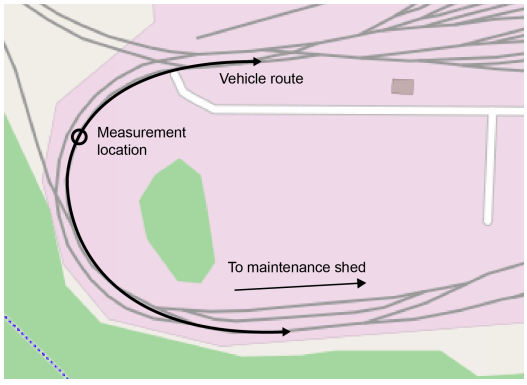

Figure 7: Test curve for fixed location gauge face measurements in Stockholm, Sweden.

Figure 8: **Stockholm test site images clockwise from top left: SL vehicle completing a trip; manual lubricant application to high rail and pendulum test set-up in-situ.**

4.5. Results

4.5.1. Results – Study A

Figure 9 shows a bar chart of the average SRV for both TOR and gauge measurements. The adhesion measurements of the gauge face show increasing friction as the distance from the lubricator is increased.

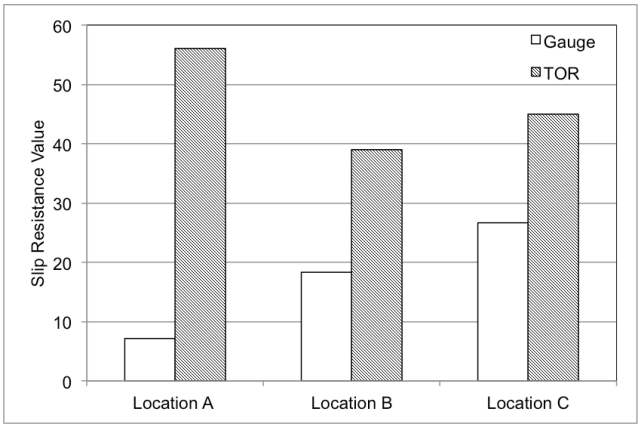

Figure 9: **Bar chart of Pendulum test results from Severn Valley Railway carry down field trial.**

4.5.2. Results – Study B

The results from Study B are shown in Figure 10. In dry conditions the average over the 4 sets of measurements was 48. The standard deviation of all dry measurements was 2. A minimum reading of 44 and a maximum of 52 were recorded.

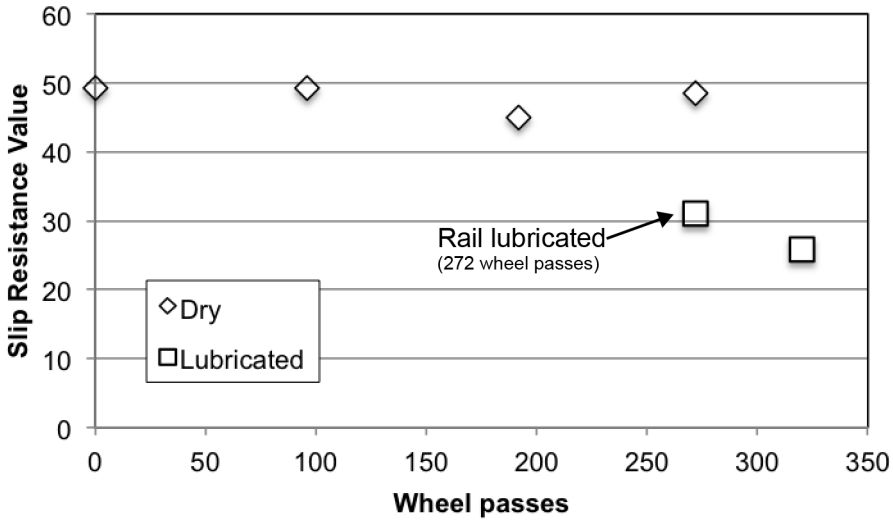

Figure 10: **Results from field tests in Stockholm showing average SRV measurements of the gauge face in dry and lubricated conditions.**

4.6. Discussion

4.6.1. Study A

The measurements of gauge face friction showed increasing SRV as the distance from the lubricator site was increased from location A to C.

At location A there was an extremely low average slip resistance value measured indicating a very well lubricated gauge face. Location A was next to the GDU and was heavily greased. This is shown in the extremely low SRV that was measured.

Profiles of the rail section were taken at each location. The profiles were taken prior to pendulum measurements with a non-contact profilometer. This ensured that the profiles represented the state of the rail gauge face that measurements characterise. At location A there is a clear build up of grease (see Figure 11), whereas there is no evidence of grease in locations B and C. These profiles also show the little to no variation in profile between location indicating that minimal gauge face wear has happened.

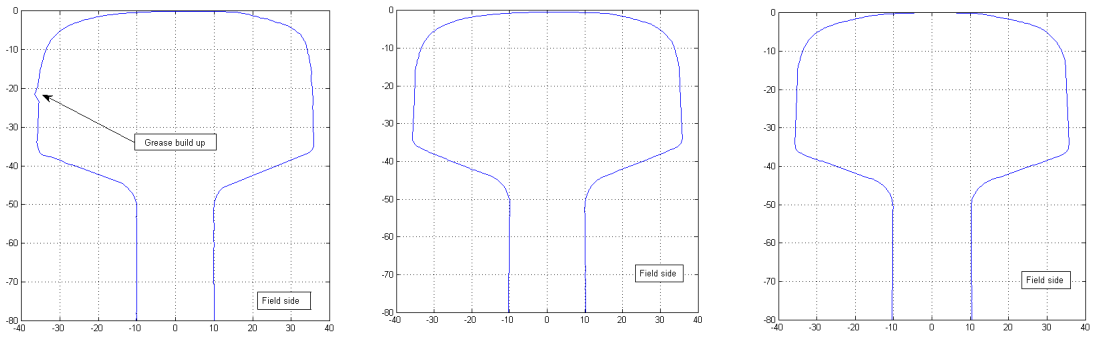

Figure 11: Rail profiles from SVR study, as measured by the NextSense Calipri CW40, from the left: Location A; Location B; Location C

Samples of the gauge face contamination were also taken using adhesive backed plastic and are shown in Figure 12. These samples were taken from the rail outside of the pendulum measurement area to avoid removing any lubricant, but can be considered to give a good representation of the state of the gauge face. Top of the images show TOR condition and point of gauge measurement is highlighted.

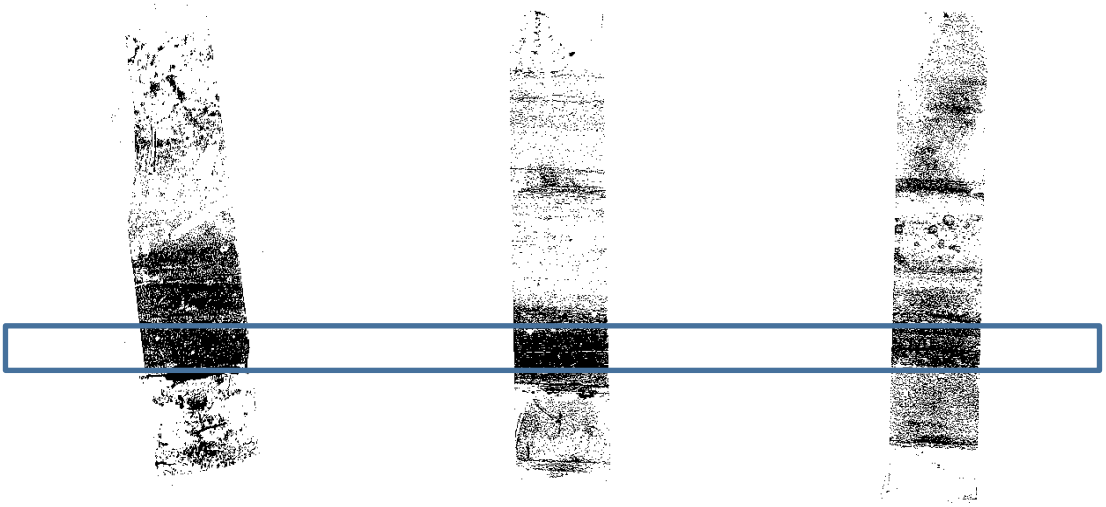

Figure 12: Grease samples from SVR study, from left: Location A; Location B; Location

4.6.2. Study B

Adhesion measurements were taken of the gauge face only. Adhesion is reduced from dry conditions to lubricated conditions. The adhesion levels measured were much higher than those measured in the laboratory in both dry and lubricated conditions (see Figures 3 and 10).

Dry adhesion levels were equivalent to those expected for TOR measurements (SRV of 50). The adhesion was reduced by less than half under lubricated conditions (SRV of 30).

It is possible that the rail profile caused a wider contact on the angled pad that previously due to significant wear. From inspecting the foot of the rail metal

wear particles were found confirming large amounts of contact between the flange and gauge face (see Figure 13).

Figure 13: Wear debris at the rail foot from Stockholm study.

The measurements in Stockholm were conducted (under supervision) by an individual who had never previously used the angled pendulum. The judgment of when contact is made between the rail and pad may have lead to a slightly increased contact length. This increased length would increase the amount of energy absorbed and could explain the different in measured values. However, the difference between SRV measured in the laboratory and field dry is the same (SRV difference of 20).

4.7. Conclusions

Two field tests using a pendulum tribometer with the tradition setup as well as a new modified angled pendulum foot adaptor have been conducted in the UK and Sweden.

- Results from Study A showed that the pendulum tester with an adapted foot attachment can be used to more accurately detect whether a lubricant (grease) is present on the rail gauge face. There is a clear difference in the measured energy loss (SRV) at the gauge corner as the distance from the lubricator is increased. This method allows lubricator site inspection with adhesion measurements for the assessment the carry down of grease along a curve - although repeatability on different days is questionable.
- Top of rail adhesion measurements were again shown to be comparable to previous laboratory and field-testing using a pendulum tribometer to measure rail head traction (Lewis, 2011).
- Results from Study B showed the difference between dry and oil lubricated gauge face. The dry measurements showed little variation in SRV, showing that consistent readings can taken.
- The adhesion measurements between the two trials showed a large variation between the SRV measured in a lubricated condition
- Unlike the pendulum measurement on the TOR, the gauge corner measurement will give an indication of whether there is a reduction in

adhesion (dry versus lubricated) rather than giving a value of the coefficient of friction

4.8. References

AS/NZS 4586:2004, Slip Resistance Classification of New Pedestrian Surface Materials

BS EN 13036-4:2003, Road and Airfield Surface Characteristics. Test Methods. Method for Measurement of Slip/Skid Resistance of a Surface. The Pendulum Test.

BS 7976-2:2002 7976-2002 +A1:2013., Pendulum testers — Part 2: Method of operation.

BS 7976-3:2002 +A1:2013. Pendulum testers — Part 3 : Method of calibration

Fletcher, D.I. and Beynon, J.H., 2000. “The effect of intermittent lubrication on the fatigue life of pearlitic rail steel in rolling-sliding contact.” Journal of Rail and Rapid Transit Proceedings of the Institution of Mechanical Engineers Part F, 214, 3, pp.145–158

Harrison, H., McCanney, T. and Cotter, J., 2002. “Recent developments in coefficient of friction measurements at the rail/wheel interface.” Wear, 253, 1-2, pp.114–123

Lewis, S.R., Lewis, R. and Olofsson, U., 2011. “An alternative method for the assessment of rail head traction”, Wear, 271, 1-2, pp.62–70

5. Assessment of friction modifiers performance using two different laboratory test-rigs

L.E. Buckley-Johnstone[1], M. Harmon[2], R. Lewis[2], C. Hardwick[3] and R. Stock[4]

[1]Department of Mechanical Engineering, The University of Sheffield, UK
[2]Centre for Doctoral Training in Integrated Tribology, University of Sheffield, UK
[3]L.B. Foster Rail Technologies Ltd, Sheffield, UK
[4]L.B. Foster Rail Technologies Ltd, Burnaby, Canada

Study B formed part of work presented at *40th Leeds-Lyon Symposium on Tribology*

Published in '*Proceedings of the Third International Conference on Railway Technology: Research, Development and Maintenance'*

Abstract

This paper describes two methods for assessing friction modifier performance carried out on two different testing scales. Study A used wear data from a full scale rig test at Voestalpine Schienen GmbH (Stock, 2011) and compared it with wear data from twin disc tests using the SUROS machine at The University of Sheffield. Study B compared 'retentivity' data from a full scale rig at The University of Sheffield and the SUROS tests. Study A concluded a good correlation between the two scales although assumptions made in the full scale contact calculation introduce a large spread into the results. There was a greater correlation between the two data sets at more severe contact conditions. Study B showed a different baseline coefficient of traction between the two scales and a longer test length is required to fully evaluate the 'retention' of the friction modifier on the full-scale rig.

5.1. Introduction

The ability to perform controlled testing of wheel-rail interaction phenomena is vital to improve the understanding of the wheel-rail interface. Under most circumstances it is uneconomical to perform testing under fully representative conditions. Access to track and instrumented rolling stock is limited, that encompassed with limited control leads to the need for the use of representative laboratory test methodologies.

Friction modifiers (FM) are used to provide an intermediate coefficient of friction (usually between 0.3-0.4) thereby improving energy efficiency of the railways by ensuring friction is not too high. The intermediate friction level will also ensure safe train operations by not compromising traction and braking of the train. Friction modifiers also eliminate the negative gradient on creep curves over an extended creepage range. A negative gradient in the creep curve will allow two creep levels for a certain given traction/adhesion level. This can create an oscillation between the two creep levels which can lead to increased damage and squealing (Eadie, 2002).

There are many different scales and styles of test facility with different operating principles that exist to allow for representative contact conditions

within controllable environments. Twin-disc rolling contact simulation and full scale wheel-rail test frames are two types that are used within the work outlined in this paper. Tests have been carried out to compare the performance of a water based Friction Modifier (FM) when subjected to two different scales of laboratory experiments: 1) twin disc; 2) full-scale linear test rig. Two separate, but comparable, test regimes have looked at the performance of the FM with respect to coefficient of traction levels and wear amounts. Study A compared wear and Tγ/A data between twin disc tests in dry and FM conditions against wear data from a full-scale rig equipped with a typical vehicle based FM applicator that replenished the product as well as dry conditions. Study B compared coefficients of traction in terms of evolution, retention and baseline levels between twin disc and full scale tests where a single application of FM was applied initially. Both studies used the SUROS test rig (Fletcher, 2000) for the twin disc tests, a schematic of the rig is shown in Figure 1. The discs are machined from real rail and wheel steel with the dimensions shown in Figure 2; Study A used data from tests run on the full-scale rolling rig at Voestalpine Schienen GmbH (Stock, 2011) and Study B the full-scale wheel-rail rig at the University of Sheffield shown in Figure 3.

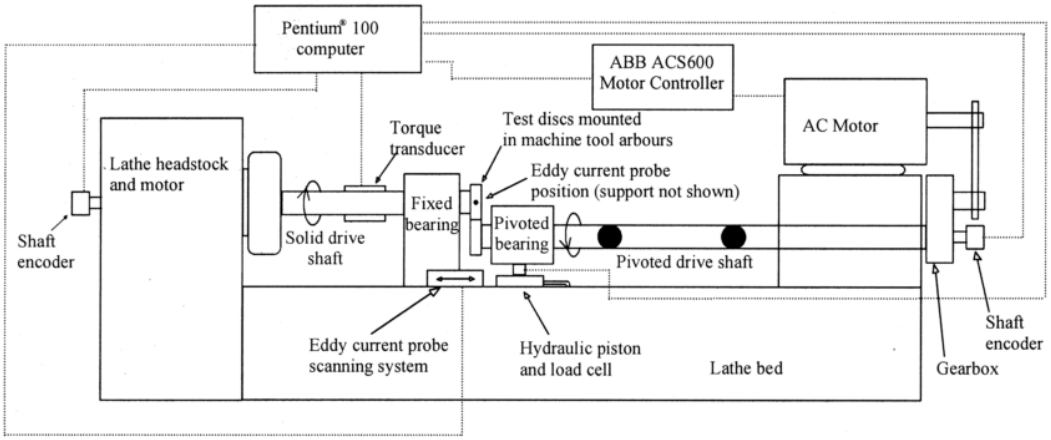

Figure 1: **Schematic of the SUROS twin disc tester (Fletcher, 2000)**

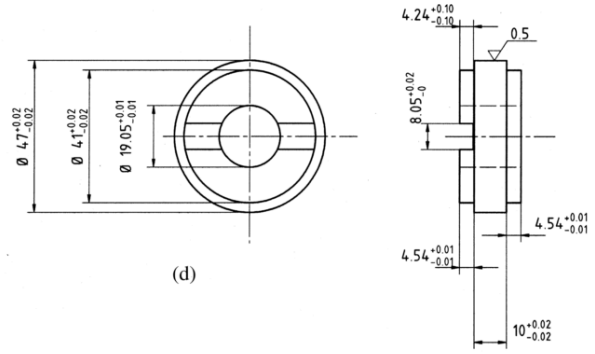

Figure 2: **Dimensions of SUROS test specimen 2 (Fletcher, 2000)**

Figure 3: **Full scale test rigs at: left) Voestalpine Schienen GmbH (Stock, 2011), right) University of Sheffield.**

5.2. Literature review

Top of rail FMs are nowadays a widely used concept in the North American heavy haul environment as well as in passenger / transit systems all over the world. There are a number of different material concepts with regards to materials for TOR application which has led to confusion. However, a paper has recently been published (Stock, 2015) which has provided and clearly defined FMs according to their “drying behaviour” and how to differentiate them from TOR lubricant type materials. Drying materials are particles suspended in water which quickly evaporates in the wheel-rail contact, leaving behind the solid particles to mix with the existing third body layer between wheel and rail to provide the optimised friction level (Friction Modifier). Non-drying materials provide the optimised friction through the mixed lubrication mechanism (TOR lubricants and sub-classes). Besides, solid stick FM’s are also available which are applied to the wheel and provide intermediate friction levels though similar mechanisms.

The benefits of friction modifiers are well documented. They reduce rolling contact fatigue (RCF) and wear by reducing lateral forces in curves (Fletcher, 2000; Stock, 2015), which also leads to a reduction in noise (Oldknow, 2012; Eadie, 2006; Eadie, 2005; Grassie, 2005; Tomeoka, 2002). There are also reductions in low frequency vibrations (Eadie, 2008a) (which leads to reduced corrugations and improved ride comfort) and reduced fuel consumption (Chiddick, 2014) (via reduced rolling and curve resistance). Additionally there is no impact of FM’s on track isolation circuits (Lewis, 2011) and braking capabilities (Stock, 2014), which are important safety aspects of any product to be applied to the rail.

A recent field test using a TOR Lubricant (hybrid material containing water and oil) (Lundberg, 2015) showed that the friction coefficient was highly

dependent on the amount of TOR lubricant applied and if too much is applied then the friction coefficient is too low for safe operation of the train. Additionally if the amount of TOR lubricant applied is too little then the friction coefficient is above the desired intermediate levels. This supports the statement that TOR lubricants work in the mixed mode lubrication regime and that a very close control of application rates is necessary to obtain a desired friction level (Stock, 2015).

Recent research has focussed on the optimisation of the application of FM's, i.e. how much to apply and when, how far down the track does the effect last and how does it interact with oxides on the rail (Eadie, 2008a; Lu, 2005; Eadie, 2008b). Most of the current research has been either field studies or full scale rig studies, both of which are costly in terms of time and money. Therefore, if twin disc test results are shown to provide scalable results, then research can be carried out at a faster rate and cost less. This is because small scale twin disc rigs can be used to carry out large test programs quickly, meaning many variables can be tested in a relatively short timeframe, with a small number of the most promising results tested on full scale rigs and field trials to verify the small scale results.

5.3. Test methodology

5.3.1. Study A

Voestalpine full-scale tests used vertical and lateral loads of 23 tonnes and 4 tonnes, respectively. Full details of the rigs operation have been previously outlined (Eadie, 2002). Dry tests were run as well as tests with FM sprayed on to the rail head every 250 wheel passes for a duration of 100000 wheel passes. Wheel and rail profile measurements were performed both pre and post testing using a Greenwood Engineering mini prof allowing for the calculation of wear. Change in area was converted into μg/cycle. Creep and traction were not able to be controlled or measured. As such, Vampire simulations and field tribometer measurements were used when calculating Tγ/A values, with allowances for extremities of conditions, hence the large error bars presented in the results section. The following assumptions have been made to calculate the wear rate for the full scale data:

- The contact patch has been modelled using VAMPIRE Rail Vehicle Dynamics Software (Eadie, 2008b) to generate contact patch dimensions.
- The test rail length for each pass is 0.5m as 0.2m is covered whilst rig is accelerating and 0.2m is also covered when the rig is decelerating
- The creep is estimated to be 0.5%. This value is obtained from evaluating a creepage distribution vector plot.
- Coefficient of friction is assumed to be 0.5-0.6 for dry tests and 0.28-0.35 for FM tests

Twin disc tests were performed at 900 MPa maximum Hertzian contact pressure with creep values ranging from 0-5 % in dry conditions and with FM. A nominal rail disc speed was set at 400 rpm which gives a surface speed of 1 m/s. These values were chosen to be representative of wheel tread/rail head contact. FM was reapplied every 250 cycles. Tests were run for 25000

cycles. Wear was calculated using mass loss and calculated per cycle of the rail disc.

5.3.2. Study B

The Sheffield full-scale rig comprises of a section of rail on a slide bed, which can be brought into contact with a fixed-axle-location wheel (nominal diameter 900mm), which is free to rotate in bearing housings. Three hydraulic actuators are used to control the normal load, rail velocity and slip of the contact. The normal actuator is set vertically above the wheel, and a pancake load cell is used to measure the applied load. The rail velocity is controlled through a horizontal actuator which moves the slide bed with the mounted rail - velocity is measured using a linear variable differential transformer (LVDT). The final actuator is mounted on the slide bed, and is linked, via a chain, to the rim of the wheel. This actuator moves at a set velocity relative to the slide bed actuator to produce a slippage at the wheel-rail contact. The force required to produce this relative movement is equal to the frictional force within the contact and is measured by a load cell.

FM was applied evenly to a section of the rail head using a brush. A normal load application of 86kN was applied, which equates to a maximum contact pressure of 1000 MPa. Due to limited actuator pressure the rail velocity was restricted to 40 mm/s. The low velocity is one of the main limitations of this test rig when comparing its operation to field operation. Retention tests were run for 800 cycles with a fixed creep of 2 %.

In the twin disc tests a comparable contact stress was used, 1500 MPa maximum Hertzian contact pressure, and tests were run at 2% slip. Tests were run at a nominal rail disc speed of 400 rpm, with a driven wheel disc a higher speed to generate the slippage. Before testing 0.1 g of the FM product was evenly applied to the rail disc only. The traction coefficient was measured over 5000 cycles of testing for measurement of a creep curve, and ran with a slippage of 2 % until the traction coefficient reached 0.5 (that of a typical dry test).

5.4. Results

Figure 4 shows the traction curve from a twin disc test at 1% slip with FM reapplied every 250 passes. It is clear that traction levels sharply drop when FM is reapplied. This could be due to the nature of the product which is applied wet, after which the contact dries out/is worn away leading to an increase in traction, although the traction coefficient never reaches the level where it is designed to operate in (0.3- 0.4). Another interesting observation is that during the first few applications of FM the maximum traction coefficient decreases. Both of these observations seen in this twin disc test have been observed previously in other twin disc research (Matsumoto, 2006). This type of test is useful in analysing what happens when the FM is first applied but it is difficult to draw other conclusions due to it not representing field conditions closely enough.

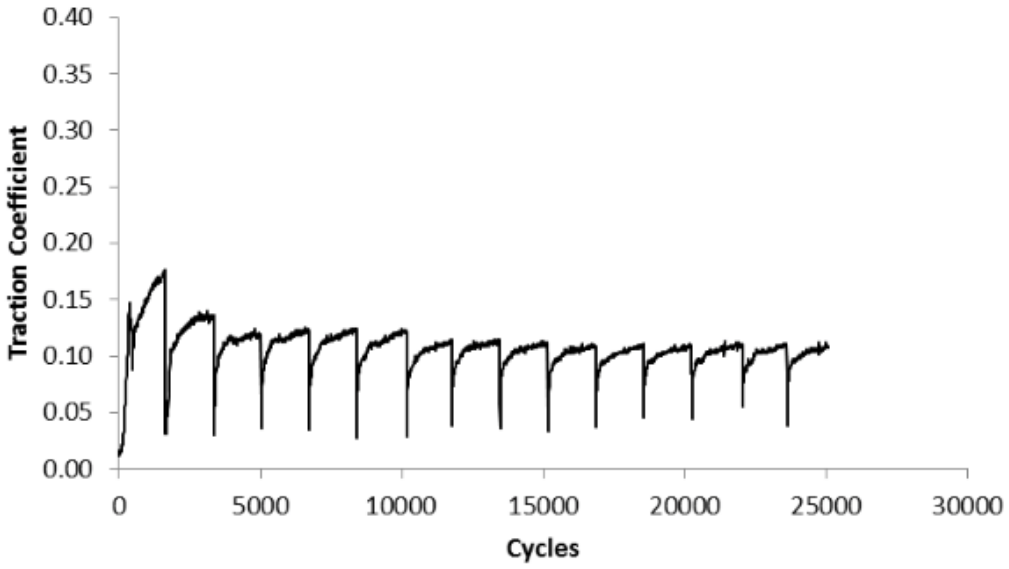

Figure 4: Traction coefficient curve for twin disc test with FM at 1% slip at 900MPa contact pressure

Figure 5 displays wear rate data from previous twin disc tests for wet and grease conditions (Hardwick, 2013) with the results from the twin disc FM tests overlaid. It shows that the FM has a significantly lower wear rate at all slip values tested when compared to other conditions.

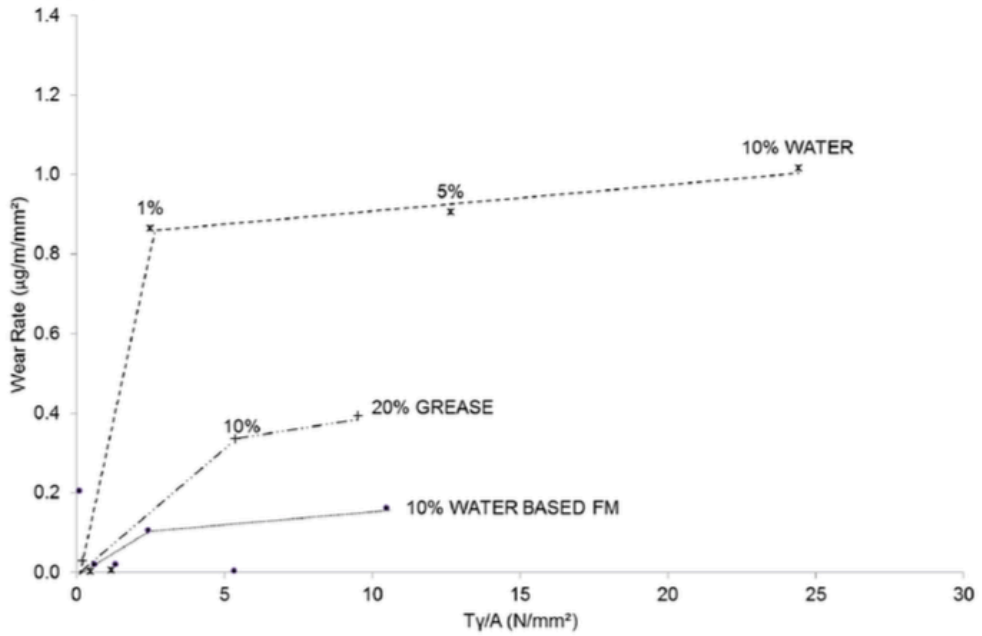

Figure 5: Tγ/A wear rate data for twin disc tests with different contaminants.

Tγ/A versus wear rate for both twin disc and full scale in both lubrication conditions is shown in Figure 6. Error bars show the range of values when variation in full scale contact data is accounted for, as discussed in the test methodology section above.

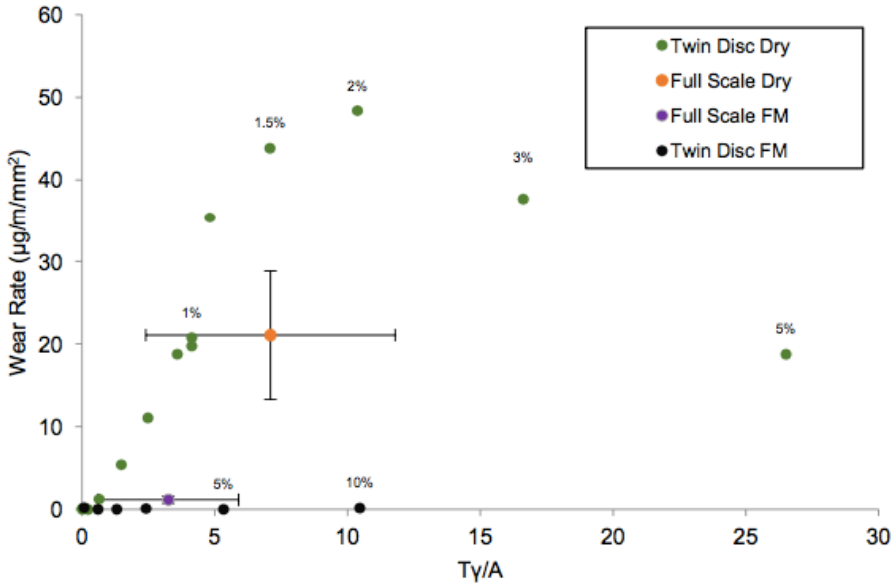

Figure 6: **Tγ/A Wear Rate Data Twin-Disc / Full-Scale Comparison for Dry and Applied Friction Modifier Conditions**

Retention curves for FM for both types of testing are shown in Figure 7 and Figure 8 for twin disc and full-scale tests respectively. Figure 7 shows a much lower baseline coefficient of traction than that of the full-scale tests. Whilst Figure 8 shows a rapid evolution to a stable traction coefficient (0.3-0.35) that is more in-line with the level required to ensure optimum traction. However, the full-scale tests were not run for long enough to see a return to dry levels of traction therefore the test should in future be extended until a dry level traction coefficient is reached.

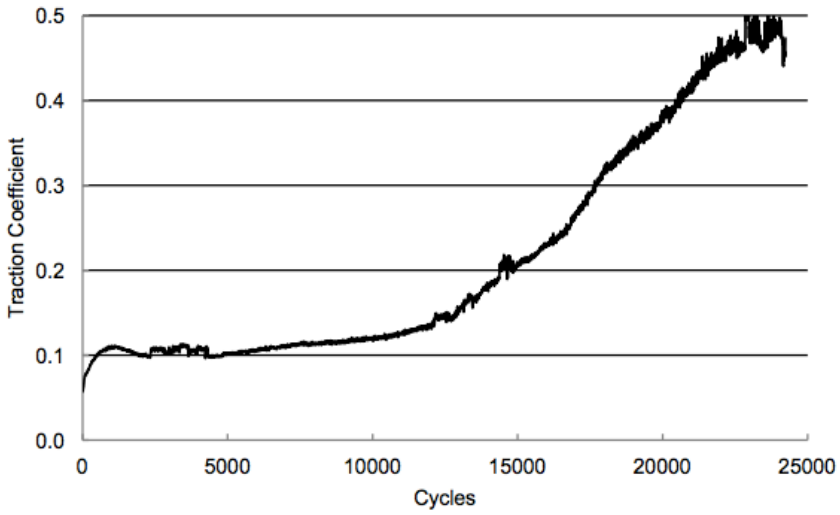

Figure 7: **Retention curve for FM at 2 % slip and 1500 MPa in a twin disc test**

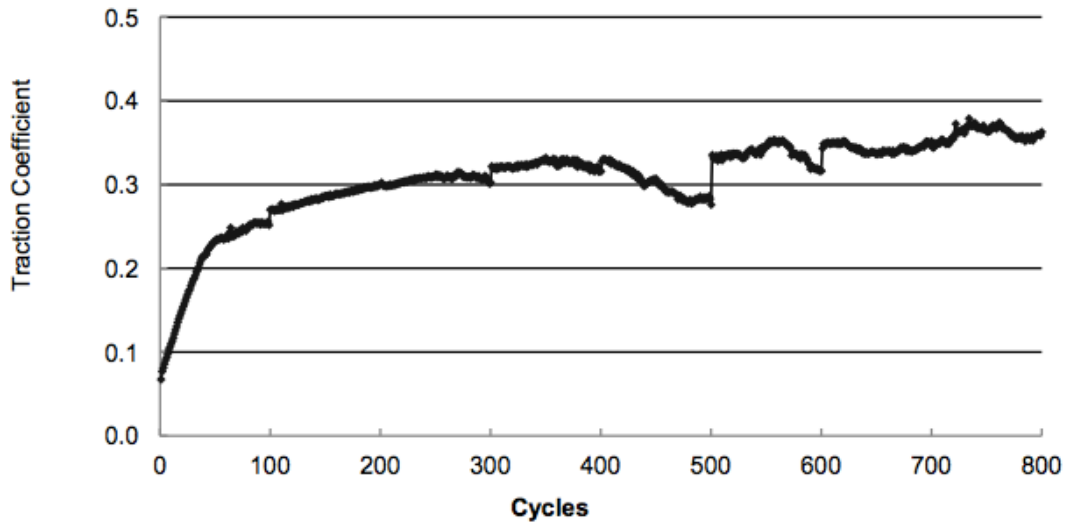

Figure 8: Retention curve for FM at 2 % slip and 86 kN in full-scale rig test

The initial evolution of traction and longevity of FM retained in the contact is similar in both cases. The lower baseline traction coefficient shown in Figure 7 is believed to be caused by too much product present in the contact. This is because even though the amount of product used was scaled down to be appropriate for the size of the discs; all of the product on the disc ends up in to contact whereas on the full scale rig (FSR) not all the product applied ends up in the contact.

Neither test is completely representative of the field. The twin disc test is on a much smaller scale and is a line contact. Also, whereas in the field where a wheel travels down a long section of track, the 'wheel' in the twin disc case is always in contact with the same small section of 'rail'. The FSR whilst being more representative of the field, in terms of contact geometry, does have some limitations. As with the twin disc, the same wheel passes over the same rail all the time. The contact point and load is always the same, whereas in the field different profiled wheels in a variety of worn conditions with different axle loads run on the same track. Despite this however, the 'retentivity' measured in these tests, could give an indication of product "carry down" and how durable it is, i.e., how many wheel passes occur before the effects of the product are no longer seen. Further work is required to prove these links. Unlike lubricants (Lewis, 2014) there are no 'certification' tests to define the performance of a friction modifier. Therefore if the 'retentivity' is shown to be linked to performance then these tests could form the basis of an approval process.

5.5. Conclusions

5.5.1. Study A

- Taking account of the assumptions made with respect to the full-scale data (contact patch size, traction coefficient, creepage) it can be said that reasonable correlation exists between small-scale and full-scale tests.

- For dry contact conditions it can be seen that the full-scale data sits within the bounds of the twin disc data (see Figure 6).
- Far greater correlation exists when comparing applied friction modifier conditions with the full-scale data displaying a marginally higher wear rate.

5.5.2. Study B

- Absolute/baseline friction coefficients differ from twin disc (0.11) and full scale (0.31) tests.
- Evolution of friction modifier traction coefficient shows similarities between the two test methods used.
- Further testing is needed to full evaluate the retention in a full-scale contact. This would be done by increasing the number of cycles until the traction coefficient reaches 0.5
- The tests described in this paper could be used as a basis to define approval tests for FM's, there are currently no standards for approval for these type of products.

5.6. References

Chiddick, K., Kerchof, B. and Conn, K., 2014, "Considerations in Choosing a top-of- rail (TOR) Material," in AREMA Annual Conference and Exposition, pp. 1–2.

Eadie, D.T., Kalousek, J. and Chiddick, K.C., 2002, "The role of high positive friction (HPF) modifier in the control of short pitch corrugations and related phenomena," Wear, 253, 1–2, pp. 185–192

Eadie, D.T., Santoro, M. and Kalousek, J., 2005, "Railway noise and the effect of top of rail liquid friction modifiers: Changes in sound and vibration spectral distributions in curves," Wear, 258, pp. 1148–1155

Eadie, D.T. and Santoro, M., 2006, "Top-of-rail friction control for curve noise mitigation and corrugation rate reduction," Journal of Sound Vibration, 293, pp. 747– 757

Eadie, D.T., Santoro, M., Oldknow, K., and Oka, Y., 2008a, "Field studies of the effect of friction modifiers on short pitch corrugation generation in curves" Wear, 265, 9–10, pp. 1212–1221

Eadie, D.T., Elvidge, D., Oldknow, K., Stock, R., Pointner, P., Kalousek, J. and Klauser, P., 2008b, "The effects of top of rail friction modifier on wear and rolling contact fatigue: Full-scale rail-wheel test rig evaluation, analysis and modelling" Wear, 265, pp. 1222–1230

Fletcher, D. and Beynon, J., 2000, "Development of a Machine for Closely Controlled Rolling Contact Fatigue and Wear Testing," Journal of Testing and Evaluation, 28, 4, p. 267

Grassie, S.L., 2005, "Rail corrugation: advances in measurement, understanding and treatment" Wear, 258, 7–8, pp. 1224–1234

Hardwick, C., Lewis, R. and Eadie, D.T., 2013, "Wheel and rail wear-Understanding the effects of water and grease" Wear, 314, 1–2, pp. 198–204

Lewis, R., Gallardo, E.A., Cotter, J. and Eadie, D.T., 2011, “The effect of friction modifiers on wheel/rail isolation,” Wear, 271, 1–2, pp. 71–77

Lewis, S.R., Lewis, R., Evans, G. and Buckley-Johnstone, L.E., 2014 “Assessment of railway curve lubricant performance using a twin-disc tester,” Wear, 314, 1–2, pp. 205–212

Lu, X., Cotter, J. and Eadie, D.T., 2005, “Laboratory study of the tribological properties of friction modifier thin films for friction control at the wheel/rail interface,” Wear, 259, pp. 1262–1269

Lundberg, J., Rantatalo, M., Wanhainen, C. and Casselgren, J., 2015, “Measurements of friction coefficients between rails lubricated with a friction modifier and the wheels of an IORE locomotive during real working conditions,” Wear, 324–325, pp. 109–117

Matsumoto, A., Sato, Y., Ono, H., Wang, Y., Yamamoto, M., Tanimoto, M. and Y. Oka, 2002, “Creep force characteristics between rail and wheel on scaled model,” Wear, 253, 1–2, pp. 199–203

Matsumoto, K., Suda, Y., Fujii, T., Komine, H., Tomeoka, M., Satoh, Y., Nakai, T., Tanimoto, M. and Kishimoto, Y., 2006, “The optimum design of an onboard friction control system between wheel and rail in a railway system for improved curving negotiation,” Vehicle System. Dynamics, 44, 1, pp. 531–540

Oldknow, K., Eadie, D.T. and Stock, R., 2012, “The influence of precipitation and friction control agents on forces at the wheel/rail interface in heavy haul railways,” Journal of Rail and Rapid Transit Proceedings of the IMechE Part F, 227, 1, pp. 86–93

Stock, R., Eadie, D.T., Elvidge, D. and Oldknow, K., 2011, “Influencing rolling contact fatigue through top of rail friction modifier application - A full scale wheel-rail test rig study,” Wear, 271, 1–2, pp. 134–142

Stock, R., Stanlake, L., Hardwick, C., Eadie, D. and Lewis, R., 2015, “Material concepts for top of rail friction management – classification, characterization and application, Proceedings of 10th international conference on contact mechanics and Wear of Rail/Wheel Systems

Tomeoka, M., Kabe, N., Tanimoto, M., Miyauchi, E. and Nakata, M., 2002 “Friction control between wheel and rail by means of on-board lubrication,” Wear, 253, pp. 124–129

6. Assessing the impact of small amounts of water and iron oxides on adhesion in the wheel/rail interface using High Pressure Torsion testing

L.E. Buckley-Johnstone[1], G. Trummer[2], P. Voltr[3], A. Meierhofer[2], K. Six[2], D.I. Fletcher[1], R. Lewis[1*]

[1]The University of Sheffield, UK
[2]Virtual Vehicle Research Center, Graz, Austria
[3]The University of Pardubice, Czech Republic

To be submitted to Journal of Engineering Tribology Proceedings of the *IMechE Part J*

Abstract

A new High Pressure Torsion (HPT) set-up has been developed for assessing the effect of third body materials in the wheel/rail interface in a controlled way. In this study the technique has been used to investigate the effect of small amounts of water and iron oxides mixtures when subjected to different contact pressures. HPT tests showed reduction in adhesion when testing with reduced amounts of water, however sustained low adhesion ($\mu<0.05$) was not produced. An 'adhesion model' has been developed to understand the difficulties encountered when testing water and iron oxide mixtures. The model related the shear properties of water and oxide mixtures (with increasing solid content) to a predicted friction coefficient. The model showed the narrow window of water to oxide fraction that is required for reduced adhesion, particularly on rough surfaces that are generated in a HPT test.

6.1. Introduction

Low adhesion has been a problem on railways since they were first invented. It can cause a safety problem in braking and delays in traction. With train speeds increasing, and time between trains reducing to get the optimum network utilization, either can be very costly.

It is well known that leaves cause a large problem, particularly in the Autumn season. Analysis of the incidents occurring during this period resulting from low adhesion events such as Signals Passed at Danger (SPADs) and station overruns (White et al., 2016), has shown that at least 50% do not however, involve leaves, but arise due to "wet-rail" syndrome, where low adhesion results from a small amount of water present on the rail head. This was confirmed by analysis of the incident time which revealed that most non-leaf incidents occurred in the morning or evening around the dew point where a thin film of water would form on the rail head. There is no information available to indicate exactly what level of moisture is critical. This is probably due to the fact that these conditions are highly transitory and investigations of

low adhesion incidents ends up occurring well after the environmental conditions that may have caused recede.

Some experimental testing has shown that friction levels reduce when a wet-contact is dried (Beagley & Pritchard, 1975; Lewis et al., 2009). One example is illustrated in Figure 1, where water was applied to a twin disc contact and then stopped and the contact allowed to dry out. It is thought in both cases that the small amount of water combined with solid material, such as oxides generated in the contact, were responsible for the drop in adhesion. In neither case, however, was ultra-low (<0.05) adhesion achieved, that would lead to the train incidents described above.

It is clearly very difficult to reproduce the ultra-low adhesion conditions in the laboratory, but it is evident why. Another issue with the testing carried out is that it involves continually cycling over the same specimen surface and is therefore not representative of the field operation. A new test that has emerged recently, based on high Pressure Torsion Testing (HPT) could help get around this problem as it allows a creep curve to be generated in less than one rotation of the contacting specimens (Evans et al., 2015) and as the specimens are flat it means that application of a third body material is easier.

The aims of this work were therefore: initially to quantify the levels of water present on a rail head at dew point environmental conditions; to then use an HPT test to assess the impact on adhesion of these water levels along with applied and pre-generated oxides and then to develop a physical model on the interface to understand the key parameters involved in the low adhesion mechanism.

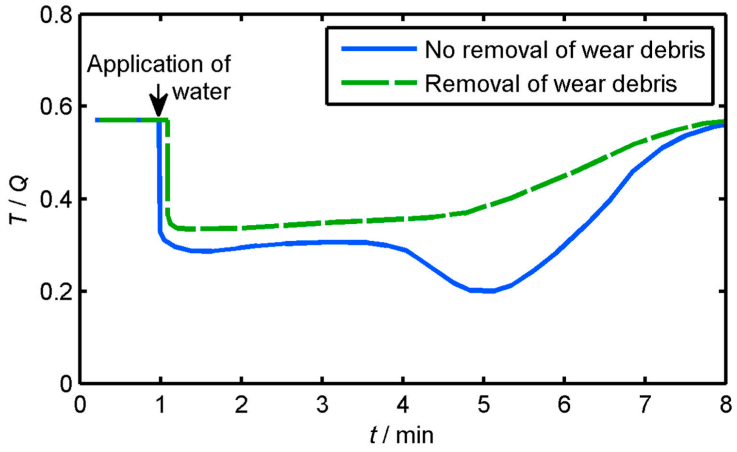

Figure 1: **Schematic of results from Amsler twin disc experiments (Beagley & Pritchard, 1975) showing that wear debris (iron oxides) are necessary to significantly reduce the adhesion level**

The HPT tests were used to investigate the effects of water amounts at different contact pressures, velocities and in combination with iron oxide particles.

From the literature review, there was no information regarding the amount of water formed on the rail surface through water condensing from the surrounding air. There is often anecdotal evidence of low adhesion at the on-set of rain, particularly fine rain or drizzle. A starting point of a suitable estimation of expected water amounts present at low adhesion conditions can

be made from using the classification of drizzle rainfall rates. The amount of water present on the surface of the rail through atmospheric water vapour was investigated using controlled testing in an environment chamber. This was then compared to the amounts of water as a consequence of drizzle falling on a flat surface of equivalent area. It thought that the amounts from drizzle would be comparable to those measured at dew point.

6.2. Water quantification

To give a basis for amounts of water that are expected to form on the rail head at dew point a small scale test was conducted. As these results have been used to inform the HPT tests an overview of the water quantification testing is presented below.

6.2.1. Apparatus

The water quantification test set-up is shown in Figure 2. The set-up comprises a rail placed in an environment chamber (Espec ET34) capable of controlling the temperature and relative humidity (RH) within a metre cube cell. Humidity is monitored using a wet bulb and dry bulb thermometers. Dry and wet air is pumped in as necessary to achieve the set RH.

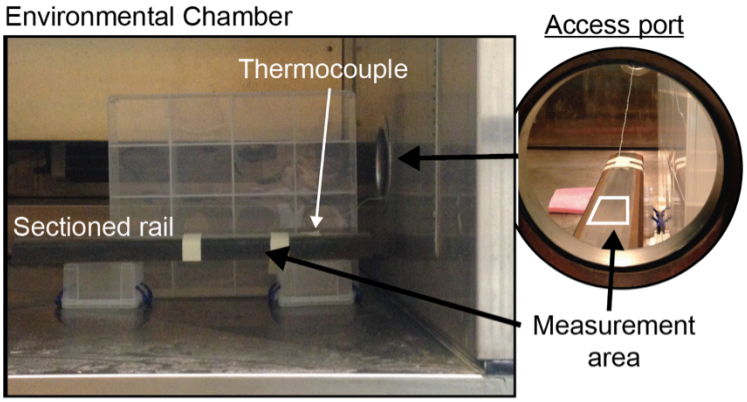

Figure 2: Water quantification test set-up.

A section of rail with a flat top was selected to accurately measure the surface area of interest. An area was then marked out measuring 100 × 50 mm for the sample to be taken from. A digital scale with a measurement accuracy of ±5 µg was used to measure the mass gain of blotting paper after wiping the rail head.

6.2.2. Methodology

The rail head was wiped dry with a clean cloth and samples of the water condensing onto the rail head were taken after 5, 30, 60, 90 and 120 seconds. Each measurement was taken a total of 3 times and an average mass gain was taken. Rail temperature was initially 3°C, but would rise throughout testing, in some cases rising above the dew point temperature.

Results have been plotted as volume of water per 100 mm^2 (chosen as an average rail-wheel contact patch size) and are shown in Figure 3. Mass

measurements were converted to volumes with an assumed standard density of water (ρ = 1000 kg/m^3).

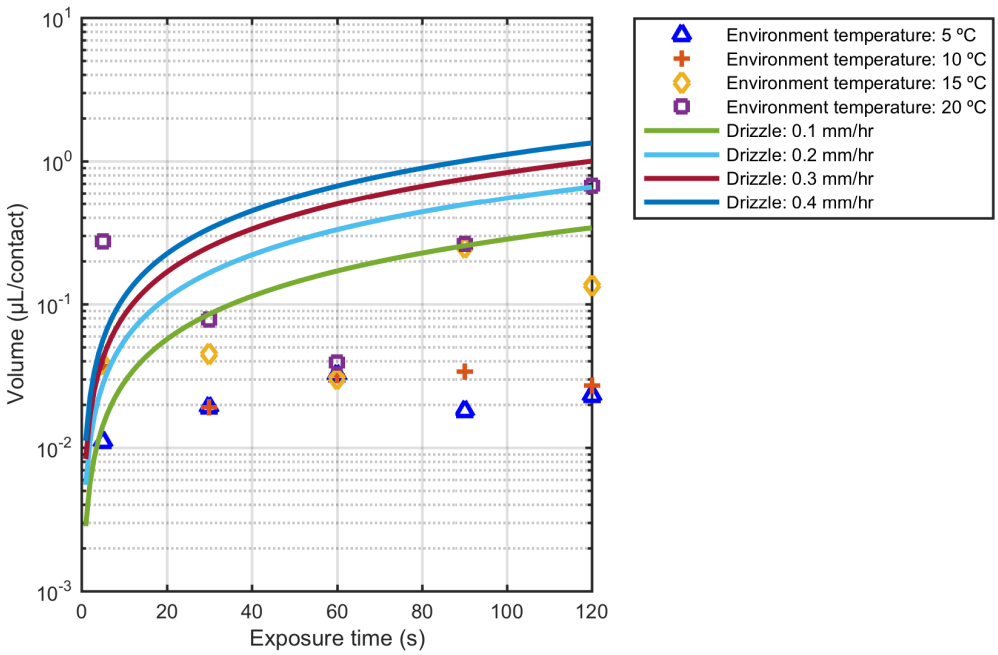

Figure 3: Volume of measured water at set environment temperatures over different exposure lengths. Average drizzle data has been plotted to show range of water amounts.

The experiment had limitations, including uncontrolled rail temperature (rising throughout), poor humidity control and sampling that was not restricted to measuring the water only. However, even with these limitations, the measured amounts fell within the range of average amounts of drizzle. The range of average water volume from these measurements is 0.01 – 0.68 µL per 100 mm^2.

These amounts under set conditions are not absolute, as temperature effects from convection and radiation are not accounted for and will have dramatic effects on amount of water present on the rail head. For example, the difference between a section of rail in direct sunlight versus a section in the shade.

Using these values of water amounts generated environmentally, in conjunction with drizzle data information, a range of water coverage can be defined. Considering equipment limitations the range of water for investigating was set as 0.5 µL / 100 mm^2 to 12 µL / 100 mm^2.

6.3. High Pressure Torsion testing

6.3.1. Apparatus

The HPT rig (shown in Figure 4) is an adapted hydraulic test rig that applies a constant normal load between two specimens whilst rotating one specimen relative to the other at a fixed speed. A tension-compression-torsion load cell

measures the normal and torque force whilst a Rotary Variable Differential Transformer (RDVT) measures the rotational speed.

Upon the initiation of the (slow) rotation, there is a period of sharply increasing friction, followed by a gradual transition towards a peak friction as the contact is brought into sliding (see Figure 5). Upon sliding the friction value tends to remain around the peak level, as evidenced by only a small variation of friction with increasing displacement. Initial work on this as a test method for assessing wheel/rail contact issues is described in Evans et al. (2015).

Any materials of interest can be applied to the specimen surface prior to bringing the surfaces into contact. The effect of third body materials have on the torque required to rotate the surfaces against one another can be investigated. The friction effects of the third body layer can then be better understood.

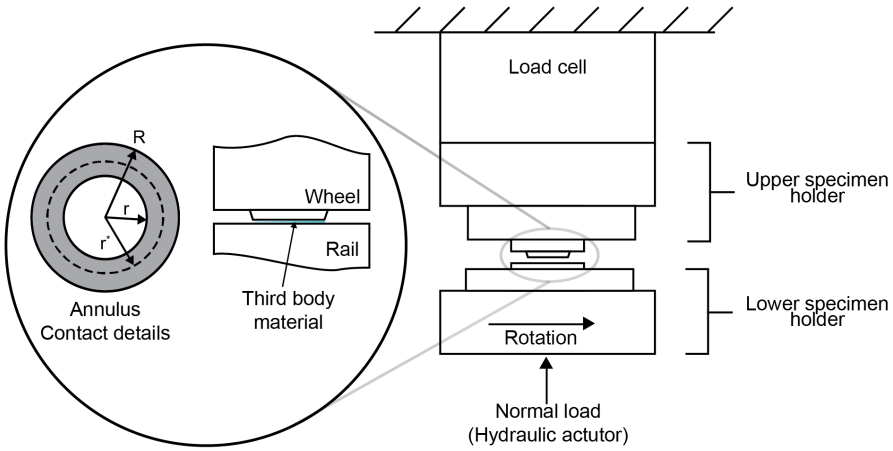

Figure 4: High Pressure Torsion rig schematic diagram showing contact patch area.

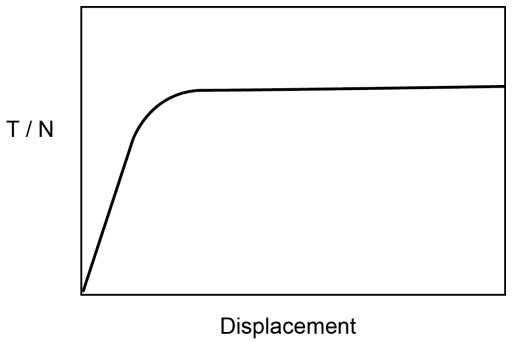

Figure 5: An example of the output of a HPT test.

Wheel and rail specimens were manufactured from R8T wheel steel and 260 grade rail steel respectively. The wheel specimen has an annulus that is in contact with the flat surface of the rail specimen. This creates a contact patch, as seen in Figure 6, with a standard contact area of 167.9 mm^2. The average initial roughness (R_a) of both specimens is 0.5 µm.

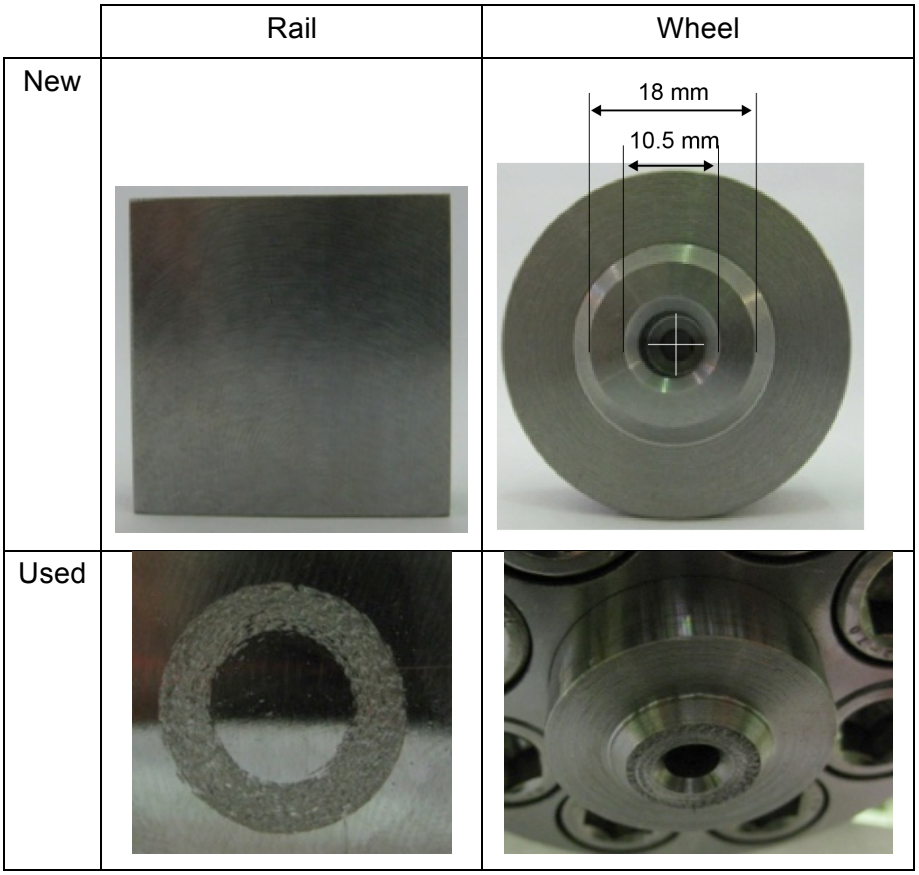

Figure 6: New and used HPT specimens contact surfaces. Clockwise from top left: new rail specimen; new wheel specimen; used wheel specimen (in-situ); used rail specimen.

The normal force is related to the average pressure and the radii of the outer and inner circles by:

$$Pressure = \frac{Force}{Area} = \frac{Applied\ load}{\pi(R^2 - r^2)} \quad (1)$$

6.3.2. Methodology

The process to generate a displacement curve using the HPT rig was the same for both dry and contaminated tests. Roughness measurements are taken prior to testing to ensure the initial surface roughness of each set of specimens was similar. The specimens were then cleaned with acetone before being mounted into the test rig.

A typical HPT test procedure was then followed and can be described as a set of discrete stages:

1. Check contact patch dimension with pressure sensitive film to ensure load is applied evenly across contact patch and accurate dimensions of contact area can be inputted (adjust if necessary)
2. Clean test specimens surfaces with acetone
3. Apply third body material to rail specimen if required
4. Load specimens into contact and apply required normal load.

5. Rotate bottom specimen, whilst top specimen remains in a fixed position (fixed via a keyway), through 0.4 mm at a constant rate.
6. Unload applied torque prior to separating specimens.
7. Remove normal load and separate specimens.
8. Rotate bottom specimen to new start point and repeat steps 3-6 (include 2a if required).

Figure 7 shows steps 4 though 6 and the corresponding measured values of normal load and torque. Note that the normal load is negative due to the sign convention used in the test rig (negative in compression).

In step 7 there is rotation to a new start point that ensures that the initial contact points between specimens is not the same for consecutive tests. The minimum rotation between consecutive tests is 10 degrees. It has been previously found that this will generate a curve with a secondary plateau (Evans, 2015).

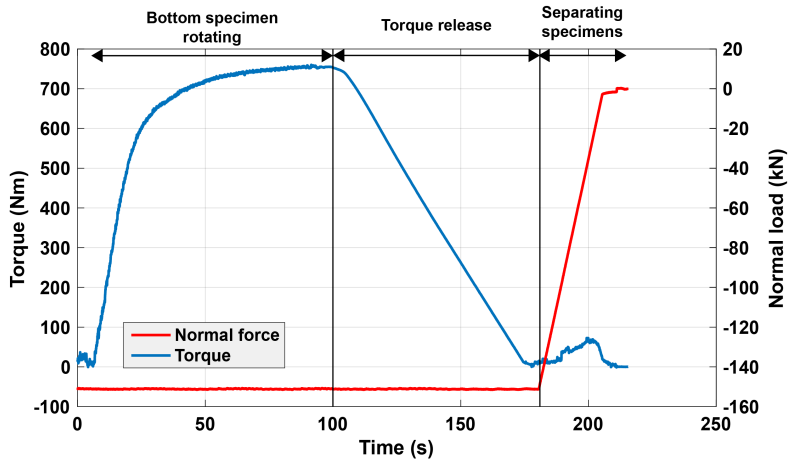

Figure 7: An example of the raw data taken from the HPT test results showing phases 4 through 6.

The torque data is then processed to produce the average shear force at each measured point. It is assumed that the average shear force can be calculated as the measured torque divided by the effective radius:

$$Shear\ force = \frac{measured\ torque}{effective\ radius} = \frac{measured\ torque}{\frac{2}{3}\left(\frac{R^3 - r^3}{R^2 - r^2}\right)} \quad (2)$$

This shear force can then be converted to a creep stress in the contact. Again, it is assumed that the creep stress is uniform across the contact:

$$Creep\ stress = \frac{shear\ force}{measured\ contact\ area} \quad (3)$$

For comparison between tests the coefficient of friction (T/N) has been calculated (shear force divided by normal load) and plots of displacement against friction for each condition are produced.

Displacement is calculated as the length of arc travelled using the effective radius. An angle of 3.2 degrees will produce a 0.4 mm arc at an effective radius of 7.289 mm. The exact angle for a given test will vary depending on the measured radii, whilst the displacement stays constant.

Measurements of surface roughness were made using a stylus profilometer (Mitutoyo Surftest SJ-400) before and after each set of tests. Roughness measurements required the removal of specimens; consequently these measurements were restricted to measuring the final roughness of a test specimen after they had been subjected several loading cycles.

Measurements of environmental temperature and air humidity of the laboratory were recorded, but were not a controlled variable.

6.3.3. Test conditions

The investigation variables of interest were:

- Load, surface condition
- Variable amounts of water + iron oxide mixtures (including water alone)

An initial investigation to produce baseline creep curves and assess the effects of repeated use of specimens was completed. These focused on the run-in procedure effect on adhesion, the effect on multiple tests on a single set of specimens, the application frequency of water (and contaminants) between test and repeats. The standard test conditions are shown in Table 1.

Table 1: Standard HPT test conditions

Speed (deg/s)	Distance (mm)	Area* (mm^2)	Effective radius (mm)	Temperature	Humidity
0.04 – 0.2	0.4	167.9	7.289	Room	Room

The normal pressure range tested was between 200 – 1000 MPa. This range is based on the HPT torque application limit. A standard pressure of 600 MPa was selected to investigate in contaminated conditions.

The iron oxides that were used in this study were haematite (Fe_2O_3) and magnetite (Fe_3O_4), both known to be found in the wheel/rail contact (Lewis, 2012). Tests using water and iron oxides mixtures at different mass ratios were performed. Oxide component masses relative to the measured amounts of water present on the rail head were investigated from 50% to 90% by oxide mass. The amount of iron oxide is calculated from a fixed water component mass in all cases. In this way the volume of water could be kept constant.

All contaminants are applied to the rail specimen immediately prior to testing.

6.4. Results

A selection of results is presented in Figures 8–11. Presented data shows the effects that load, run-in and contaminant (water, iron oxide and water + iron oxide) have on the friction coefficient with increased displacement. Further

results showing the effect of velocity and oxide particle size can be found in Appendix A.

The displacement/friction (T/N) graphs have two distinct sections; the initial steady gradient and transitions as the specimens begin to rotate (0-0.1 mm); and a section of a steady adhesion that can be stable, marginally increasing and rarely marginally falling (0.1-0.4 mm).

In the first section, as the annulus rotates against the flat surface the outer edge will dominate the contribution of friction force as it begins to slide whilst the inner edge remains static. As rotation is increased, the whole surface is brought into sliding and the adhesion is brought a maximum plateaued value.

For the purpose of the work carried out here the mean, maximum and/or minimum adhesion measured after full sliding has occurred is most critical. The initial gradient is marginally affected by the steel properties and the presence of a third body contaminant (for example extending the displacement by providing an alternative shearing medium), but is less important to low adhesion mechanisms.

Figure 8 shows the effect of normal load in dry conditions. There is a similar trend evident for all dry curves showing a slight reduction of the peak friction coefficient with increasing normal load. The peak adhesion is above 0.5 for all loads (max(T/N) > 0.5). These measurements were made on a single set of specimens and have been run until a steady curve is present. Running in the surface significantly increases the roughness and changes the curves generated.

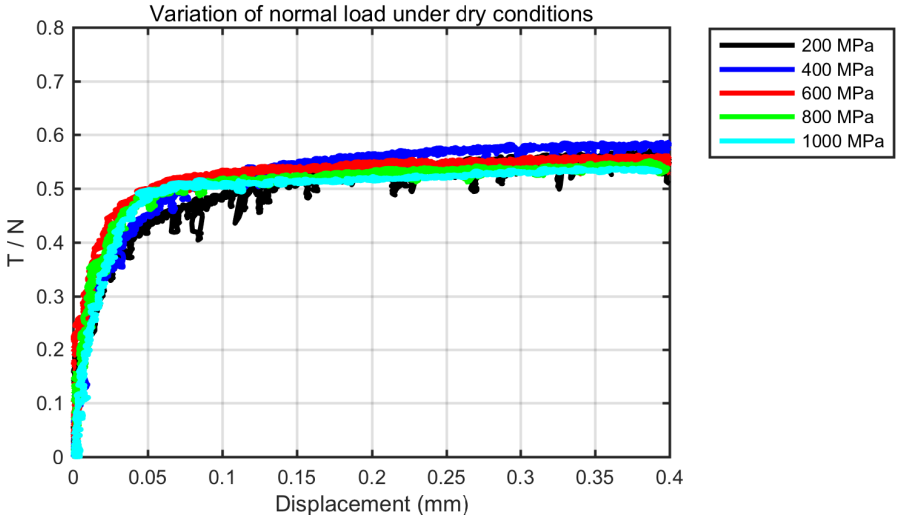

Figure 8: Dry data at different normal pressures showing the coefficient of friction as a function of displacement. Curves shown have been produced using run-in specimens.

The effect of the run-in can be seen in Figure 9, which presents the results from iron oxide tests with zero water. These tests were completed on fresh specimens, and have been plotted against a dry curve that was also performed on unused specimens. The peak coefficient of friction on unused specimens (max(T/N) > 0.7) is reduced upon further working of the surface until to a steady peak value is reached (max(T/N) ≈ 0.55). The results show that oxides alone do not reduce the maximum friction but have an influence

on the curve characteristics. No difference was evident between the two types of oxide.

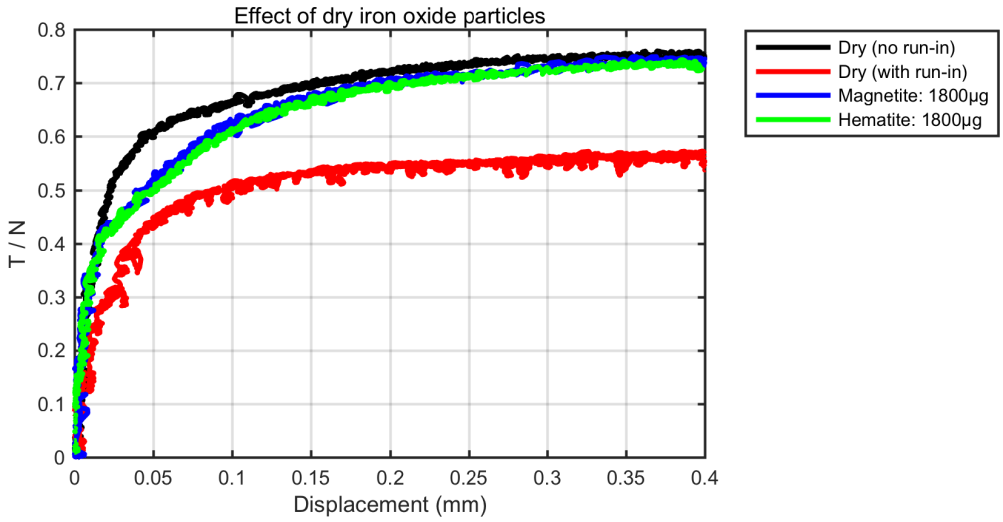

Figure 9: Effect of oxide only as a third body layer when compared to dry conditions with no run-in and dry conditions with a worked surface. Normal pressure: 600 MPa.

Figure 10 shows a clear reduction in adhesion under reduced water conditions. In 'flooded' conditions a large amount of water was placed between the contact. When the amount of water is reduced the adhesion conditions cause stick-slip of the interface to occur. This can be seen as sudden drops on the plots of 10 µL and 20 µL curves. It is not clear if this is a result of dynamic effects in the rig or interface conditions. Further dynamic modelling is under way to investigate this phenomena.

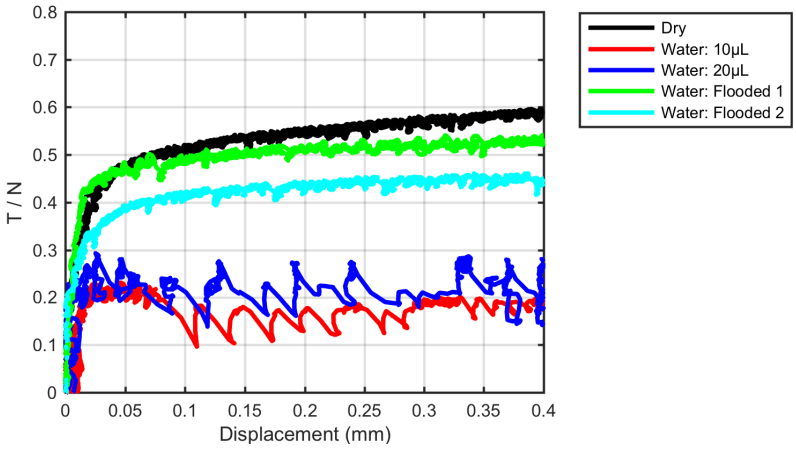

Figure 10: Effect of a range of amounts of water on a HPT test. Dry data has been plotted for comparison. Normal pressure: 600 MPa

Figure 11 shows a sample of the iron oxide + water results. Reduced friction is apparent and the stick-slip behaviour occurred again. However, the ultralow levels of adhesion were not sustained.

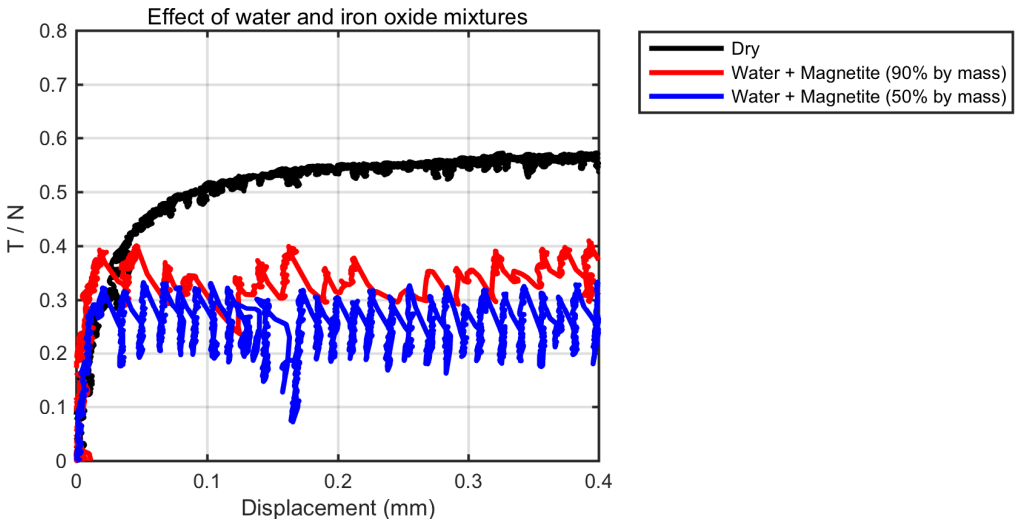

Figure 11: Effect of a range of water + iron oxide (magnetite) on a HPT test. Dry data has been plotted for comparison. Normal pressure: 600 MPa.

6.5. Low Adhesion Model

During experimentation it was found that sustained generation of low adhesion was not currently possible (see Figures 10 and 11).

To investigate the possible reasons for these results a model, termed the 'Adhesion Model', was developed to relate amounts of water and iron oxide to the adhesion level. The adhesion value is a function of the following key parameters:

- Flow properties (yield stress) of the iron oxide/water mixture
- Amount of iron oxide/water mixture in the contact
- Surface roughness
- Friction value in the solid-solid contact (boundary lubrication of the asperity contacts)
- Asperity contact stiffness

The idea of the model is based on the assumption that the overall normal load is partially carried by asperity contacts (solid-solid contact) and partially carried by the iron oxide/water mixture. In the model the surface roughness is approximated by a zigzag contour (height $2R_a$) as shown in Figure 12. The area of asperity contacts is geometrically approximated by the intersection of the zigzag contour with a plane.

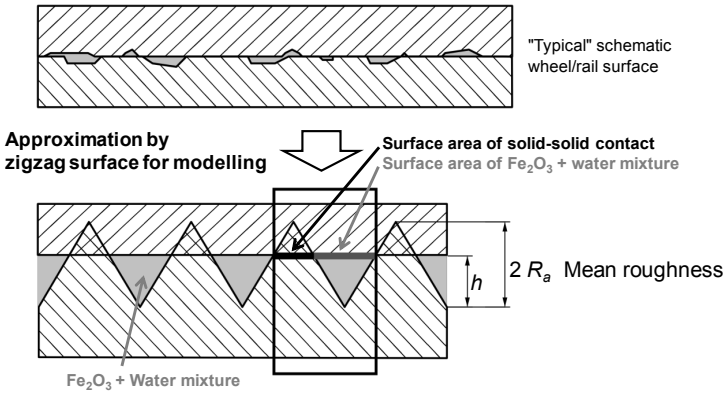

Figure 12: Schematics of a contact between rough surfaces with an additional layer of iron oxides and water (top); Approximation of the contact situation by a zigzag contour for modelling (bottom).

In this model the yield strength τ of the iron oxide/water mixture plays a key role because it determines the separation of the surfaces and thus the extent of solid-solid (asperity) contact. To determine the separation of the surfaces as a function of the yield stress of the iron oxide/water mixtures, the squeeze flow theory has been applied. It is shown in (Covey, 1981) that the static separation h of circular plates in a parallel-plate plastometer (see Figure 13) is a function of the yield stress τ, the radius of the plates *a* and the applied normal load N:

$$h = \frac{2\pi a^3 \tau}{3N} \tag{4}$$

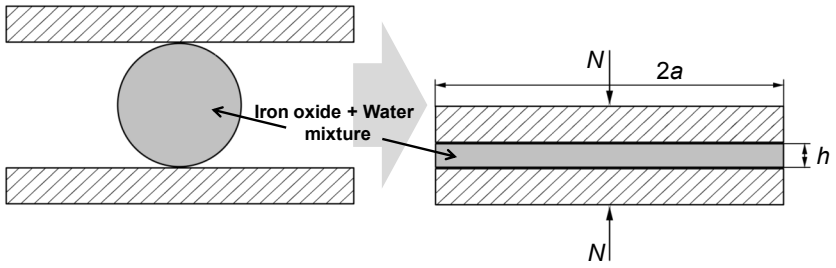

Figure 13: Investigation of the flow properties of pastes by parallel-plate plastometry.

Using the squeeze flow theory requires the assumption that the size of the iron oxide particles is considerably smaller than separation of the surfaces *h* so that the material between the plates can be regarded as homogeneous. Application of squeeze flow theory is not restricted to iron oxide/water mixtures, however substances other than iron oxide and water have not been investigated in this project.

Investigations on the yield stress τ of iron oxide/water mixtures based on this theory were carried out by Beagley (1976). A significant shear yield stress of the iron oxide/water mixture was only observed for high iron oxide fraction in these experiments (see Figure 14).

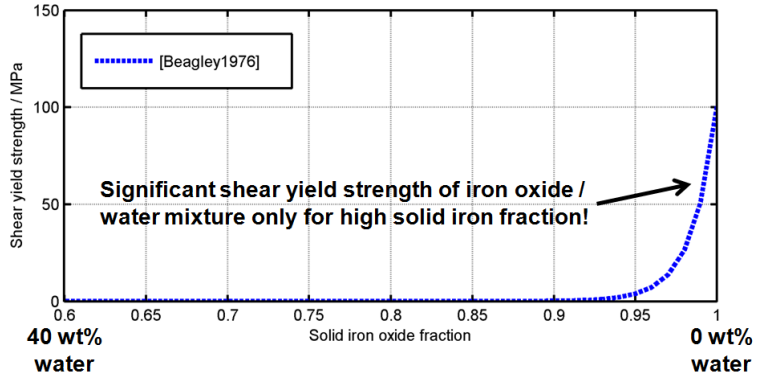

Figure 14: Shear yield stress a function of iron oxide fraction, from (Beagley, 1976).

Figure 15 and Figure 16 show typical results of the Adhesion Model for rough and smooth surfaces respectively. In both cases the boundary conditions were chosen according to the performed HPT tests.

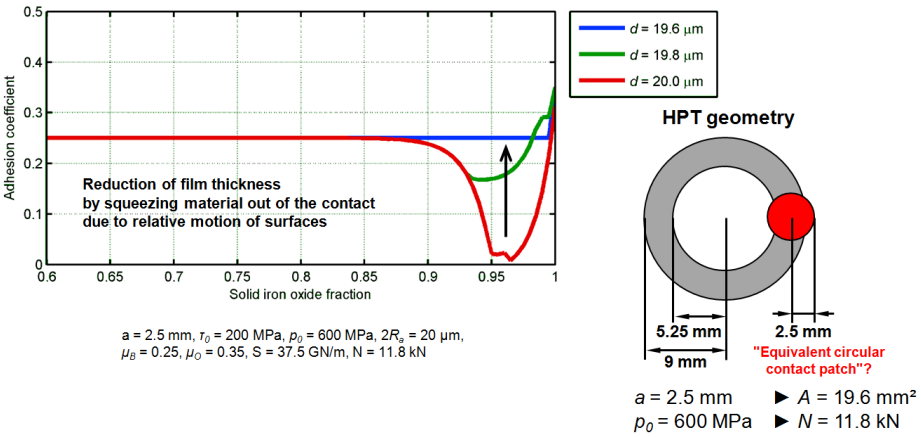

a = 2.5 mm, τ_0 = 200 MPa, p_0 = 600 MPa, $2R_a$ = 20 µm,
μ_B = 0.25, μ_O = 0.35, S = 37.5 GN/m, N = 11.8 kN

Figure 15: Typical Adhesion Model results for rough surfaces; Variation of layer thickness *d*; Boundary conditions according to HPT testing.

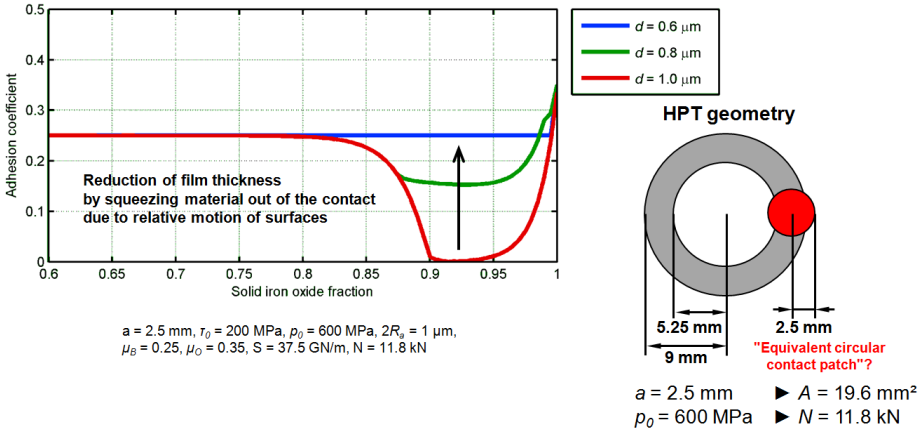

a = 2.5 mm, τ_0 = 200 MPa, p_0 = 600 MPa, $2R_a$ = 1 µm,
μ_B = 0.25, μ_O = 0.35, S = 37.5 GN/m, N = 11.8 kN

Figure 16: Typical Adhesion Model results for smooth surfaces; Variation of layer thickness *d*; Boundary conditions according to HPT testing.

Although the model is quite simple and the model parameters need further calibration and validation, the qualitative behaviour of the model demonstrates a feasible mechanism for real world behaviour. According to the model, there is only a narrow range of conditions causing low adhesion. Low adhesion is observed when the iron oxide/water mixture is able to separate the contact surfaces, but is unable to transmit significant tangential stresses. It has to be mentioned, that the model does not take the reduction of layer thickness due to relative motion of the surfaces in to account. Relative motion of the surface (due to creep) is thought to squeeze material out of the contact so that the extent of solid-solid (asperity) contact increases, which should increase the adhesion level.

6.6. Discussion

HPT tests have been shown to useful in assessing the effect of third body materials in the wheel/rail interface when testing in a laboratory. Tests under low amounts of water showed a reduction in adhesion over fully flooded interface. Addition of oxide/water mixtures also led to a reduction in friction.

Dry friction levels were as would be expected of steel-on-steel contact and are inline with those previously measured using alternative tribometers (Gallardo-Hernandez, 2008). Under dry conditions there is a reduction in the maximum coefficient of friction for a run-in specimen pair. This reduction is evident as a large shift down when compared to a fresh specimen creep curve in similar conditions and will be related to material work hardening and surface roughening.

The run-in of the surfaces in contact also has the effect of increasing the average roughness of surfaces from initial value (Ra = 0.5 μm) in some cases by up to a factor of 20. Where contaminants were included the increase in the roughness was reduced overall, but there were also localised areas of roughening. This roughness increase is a draw back to promoting BL between the specimens.

Several issues arose during tests including finding an effective method of application of water and iron oxide. Difficulties arose in the even distribution of the applied third body layer on the rail sample. It was difficult to effectively mix the oxide at water when using high mass percentages. The increase in oxide fraction leads to a rapid increase in the viscosity of mixture that is formed. At low mass percentages the mixture is a fluid, whilst at high mass percentages the mixture produces a clay-like substance.

Stick-slip behaviour is heavily present through a number of tests. Counter measures were trialed to promote a smooth and consistent rotation of the bottom specimen, but have not proved effective. Therefore, it is thought that overriding influence on stick slip is the contact conditions themselves. It is thought that the stick-slip that is prevalent in tests with contamination is possibly a function of an uneven third body layer. The uneven layer produces areas of metal-to-metal contact between specimens that dominates the adhesion levels seen (see Figure 17).

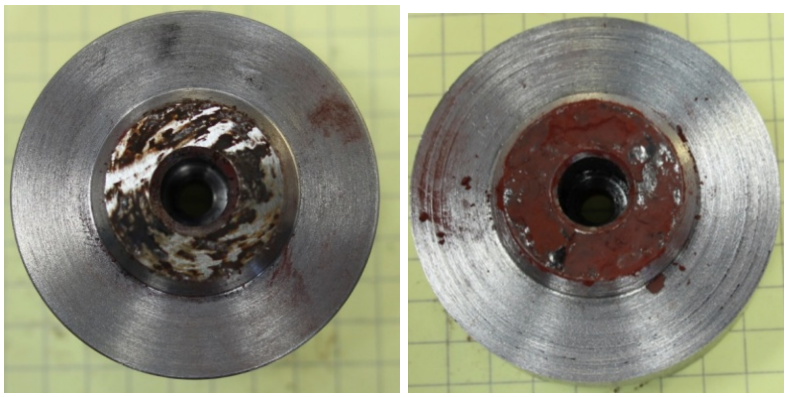

Figure 17: Example of the exposed metal seen post test.

The developed “Adhesion Model” is able to relate the flow properties of iron oxide/water mixtures and surface roughness to the adhesion level under quasi-static conditions in order to study the interplay of iron oxide, water and surface roughness in a qualitative way. There is only a small envelope of conditions that leads to low adhesion: a certain amount of oxides depending on the surface roughness, together with the correct low amount of water needs to be present on wheel/rail surfaces. The model results suggest that with a limited amount of iron oxide/water mixture on the surface an increase in surface roughness can effectively prevent the development of low adhesion conditions. The results of the “Adhesion Model” with respect to the influence of water are qualitatively in accordance with results from High Pressure Torsion experiments where minimum adhesion was found for low amounts of water under quasi-static conditions.

Differences in the absolute values might be explained by the difference in contact conditions between HPT testing and a wheel/rail contact. In HPT testing the surface is cleaned prior to testing, whilst a wheel/rail contact will never have a fully clean and dry contact. The surface stress distribution between a wheel/rail rolling contact (elliptic pressure distribution) cannot be simulated fully by a HPT test (constant pressure distribution). It is these differences in the stress conditions that might contribute to the observed differences in adhesion. However, HPT tests are extremely useful to investigate the behaviour of different third body layers, the influence of different surface conditions, as well as the reduction of the initial gradient of the creep curve. (Ultra) low adhesion conditions have not yet been found in HPT testing, however, the absolute value of maximum adhesion under dry conditions is higher in HPT testing than those measured on the tram wheel rig (Voltr, 2014).

6.7. Conclusions

The main outcome of the investigations was that significant reduction of friction (over dry conditions) was observed when applying low amounts of water. This reduction is much higher compared to flooded conditions. An adhesion model was developed to get a better understanding of the interplay between iron oxides/wear debris, water and surface roughness under quasi-static conditions.

Ultra-low friction was not achieved in HPT tests, however. This was a result of the difficulties in applying and distributing third body layers and their inevitable evolution during a test.

An Adhesion Model has been developed that can estimate adhesion levels in the presence of different water and iron oxide mixtures The model is in accordance with the experience that low adhesion is predominately observed with low amounts of water and explains the difficulties with accurately testing these mixtures (As seen in the HPT test results).

Tribological testing guided the identification of parameters key to the low adhesion mechanisms such as roughness and amount of water. Furthermore, the general characteristic of the adhesion level as a function of the amount of water predicted by the Adhesion Model was confirmed under rolling contact

conditions by the experiments on a full-scale test rig where it has been used to support the specification of these tests (Buckley-Johnstone, 2016).

Despite the simplifications and the limitations of the model, conclusions with regard to the interplay of the amount of water, the amount of iron oxide and the surface roughness with respect to adhesion conditions may be drawn for the design of future HPT experiments and wheel/rail contact conditions in the praxis. According to the results a reduction of adhesion due to the presence of iron oxide and low amounts of water in the contact is feasible in quasi-static conditions, however this reduction of adhesion is limited to a narrow range of conditions

6.8. Acknowledgements

This work was funded by the Rail Safety and Standards Board (RSSB) and Network Rail within the project T1077.

6.9. References.

Beagley, T.M., Pritchard, C., 1975, “Wheel/Rail Adhesion - The Overriding Influence of Water”, Wear, Vol. 35, No. 2, pp299–313.

Buckley-Johnstone, L.E., Trummer, G., Voltr, P., Six, K., Lewis, R., 2016, “Full-scale testing of low adhesion effects with small amounts of water in the wheel/rail interface”, to be submitted to Journal of Rail and Rapid Transit, Proceedings of the IMechE Part F.

Covey, G.H. and Stanmore, R.R., 1981, “Use of the Parallel-plate Plastometer for the Characterisation of Viscous Fluids with a Yield Stress”, Journal of Non-Newtonian Fluid Mechanics, 8, 249-260.

Engmann, J.,. Servais, C. and Burbidge, A.S., 2005, “Squeeze flow theory and applications to rheometry: A review”, Journal of Non-Newtonian Fluid Mechanics, 132, 1-27.

Evans, M.D., Lewis, R., Hardwick, C., Meierhofer, A., Six, K., 2015, “High Pressure Torsion testing of the Wheel/Rail Interface”, Proceedings of CM2015, 10th International Conference on Contact Mechanics and Wear of Rail/Wheel Systems, Colorado, USA, 30 August-3 September 2015.

Gallardo-Hernandez, E. A., and Lewis, R., 2008, Twin disc assessment of wheel/rail adhesion,*Wear*, vol. 265, no. 9–10, pp. 1309–1316

Lewis, R., Gallardo-Hernandez, E.A., Hilton, T., Armitage, T., 2009, “Effect of Oil and Water Mixtures on Adhesion in the Wheel/Rail Contact”, Journal of Rail and Rapid Transit, Proceedings of the IMechE Part F, Vol. 223, pp275-283.

Polycarpou, A.A. and Etsion, I., 1999, “Analytical approximations in modeling contacting rough surfaces”, Journal of Tribology, 1999, 121, 234-239.

Voltr, P. and Lata, M., 2014, “Transient wheel–rail adhesion characteristics under the cleaning effect of sliding”, Vehicle System Dynamics, 53, 605-618

White, B.T., Fisk, J., Evans, M.D., Arnall, A.D., Armitage, T., Fletcher, D.I., Lewis, R., Nilsson, R., Olofsson, O., 2016, “A Study into the Effect of the

Presence of Moisture at the Wheel/Rail Interface during Dew and Damp Conditions”, submitted to Journal of Rail and Rapid Transit, Proceedings of the IMechE Part F.

7. Full-scale testing of low adhesion effects with small amounts of water in the wheel/rail interface

L.E. Buckley-Johnstone[1], G. Trummer[2], P. Voltr[3], K. Six[2], R. Lewis[1],

[1]Department of Mechanical Engineering, The University of Sheffield, Sheffield, UK
[2]Virtual Vehicle Research Center, Graz, Austria
[3]Jan Perner Transport Faculty, University of Pardubice, Pardubice, Czech Republic

To be submitted to Journal of Rail and Rapid Transit Proceedings of the IMechE Part F

Abstract

It is hypothesized and shown in some small scale experiments that low adhesion between the wheel/rail contact can be caused by a small amount of water combining with iron oxides. This small amount of water can be found on the rail head in drizzle conditions or at the dew point temperature. This paper presents test results from a full-scale tram rig with small applications of water into the contact. Test procedures were run in conditions that represent amounts of water equivalent to low rainfall (drizzle) through to a fully flooded contact (heavy rain). Tests were run with constant water application, as well as with bulk water application at the start and the running until dry for comparison. Tests showed sustained reduced adhesion when only water is applied to the wheel/rail contact. The sustained low adhesion was achieved during tests of constant water application. No low adhesion was measured with tests in the bulk water application tests. From observing the contact band the it is clear that for low adhesion to occur the water must be combined with wear debris and iron oxides from the contact.

7.1. Introduction

Low adhesion is a serious problem for railway networks. In braking it causes safety problems as it can lead to Signals Passed at Danger (SPADs) and station overruns as brakes fail to stop trains. In the worst case these can lead to collisions. In traction it poses a different problem, as failure to accelerate as required can cause delays to a train. Both these can be very costly.

Work carried out to analyse the frequency of the braking related incidents described above during the Autumn period has shown that the cause is split 50:50 between leaves and ‘wet-rail’ syndrome (White et al., 2016). Wet-rail syndrome relates to low adhesion caused by the presence of small amounts of water along with some solid material, such as oxides generated in the wheel/rail interface. Looking at the timing of the incidents revealed that most occurred during the morning and evening dew point, where a thin film of water would have been present on the rail head. Measurements on a rail head in an environment chamber have revealed that this amount was approximately 0.01 – 0.68 µL per 100 mm^2 (Buckley-Johnstone et al., 2016).

Twin disc experimental testing showed that friction decreased in a drying contact where there was a small amount of water mixed with oxides (Beagley & Pritchard, 1975) (see Figure 1). Similar testing using a different type of test (High Pressure Torsion (HPT)) has shown similar effects (Buckley-Johnstone et al., 2016). Here friction clearly dropped as the amount of water applied was reduced. Neither, however, showed a drop to ultra-low adhesion conditions that would lead to braking problems (<0.05). Physical modelling of the HPT testing (see Figure 3) showed that it would be very difficult to achieve the exact conditions required for very low adhesion as only a small range of water/oxide mixture proportions leads to this occurring (Buckley-Johnstone et al., 2016).

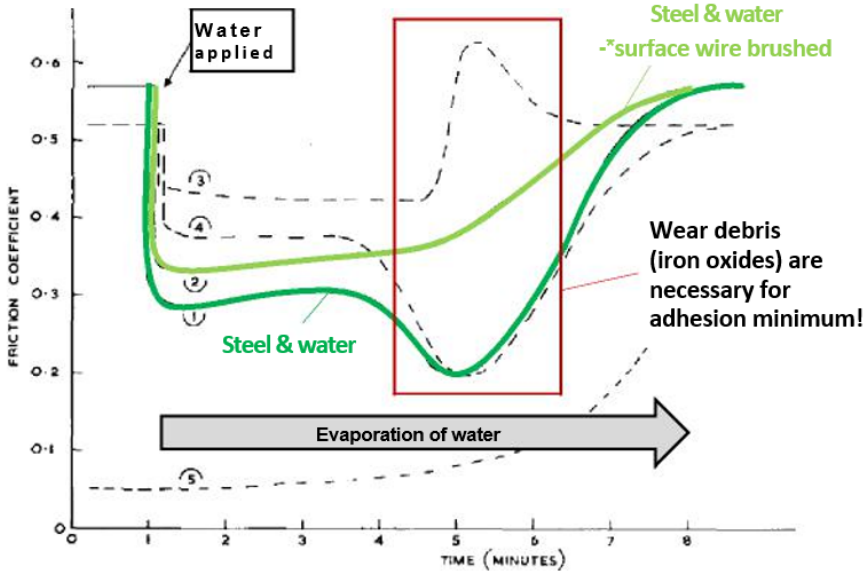

Figure 1: Results from Amsler Twin Disc Experiments (Beagley & Pritchard, 1975) showing that Wear Debris (iron oxides) are necessary to Significantly Reduce the Adhesion Level

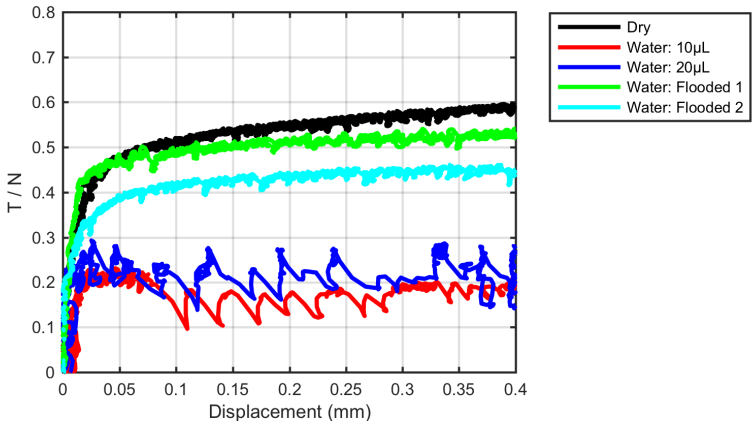

Figure 2: Effect of a range of amounts of water on a HPT test. Dry data has been plotted for comparison. Normal pressure: 600 MPa (Buckley-Johnstone et al., 2016)

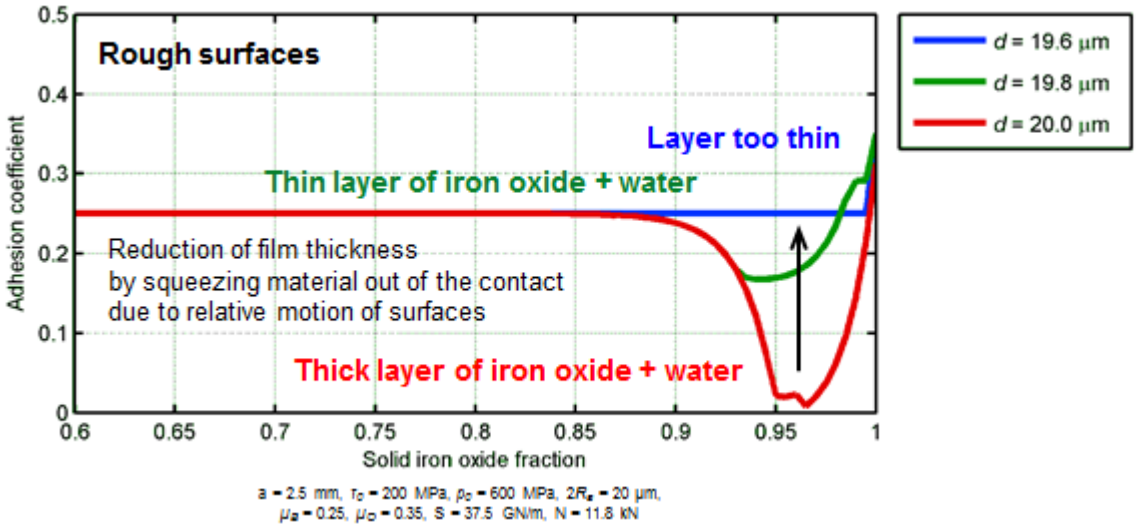

Figure 3: **Physical Modelling of Adhesion against Water/Oxide Mixture Proportion in HPT Test Interface (Buckley-Johnstone et al., 2016)**

It was thought that it might be easier to study the mechanisms using a full-scale test approach. The larger contact would make it easier to achieve the small amounts of water required over that possible in the scaled approaches mentioned above. No full-scale work in the literature has achieved ultra-low adhesion using water and oxide mixtures. The aim of this work was to create low adhesion conditions in a full-scale rig and determine creep force characteristics for a range of different water amounts.

7.2. Experimental details

7.2.1. Test apparatus

Tests have been carried out at the Janer Perner Transport Research Centre at the University of Pardubice. The test rig comprises a full-scale tram wheel (Ø700 mm) mounted onto a fixed frame by a swing arm and a roller 'rotating rail' (Ø916 mm) mounted below. An air spring between the swing arm and main frame is used to apply a normal load between the wheel and rail. The wheel is driven by a permanent magnet synchronous motor with torque control, whilst the roller is driven by an asynchronous motor to maintain constant speed. A torque sensor located on the rail roller axis is used to measure the torque as a result of the wheel-roller contact throughout testing. Further detail on the test rig can be found in previously published literature (Voltr, 2014).

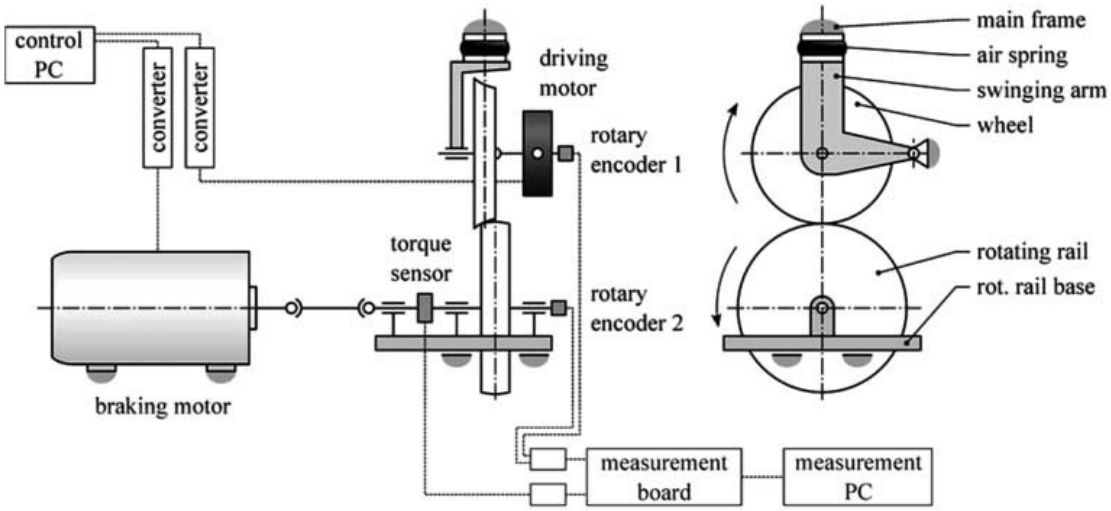

Figure 4: **Schematic of the tram wheel test rig (Voltr, 2014).**

The torque motor is capable of applying up to 850 Nm of torque in braking or traction (equivalent to a 2.4 kN friction force). This limit has a consequence on the creepage range that can be investigated at higher loads. This is due to the longitudinal friction force induced by the maximum motor torque that cannot exceed the creep force at the contact required to get into full sliding under certain conditions. These limits are shown in Table 1.

Table 1: **Maximum permissible friction coefficients for different normal loads in the tram wheel/rail rig to achieve full sliding.**

Normal load (kN)	Investigation friction (T/N) limit
4	0.60
10	0.24
20	0.12
40	0.06

A typical test history plot is shown in Figure 5. This shows how a test progresses over time: A normal load (N) is applied to the two discs using the air spring. The discs are then accelerated to the test speed of interest. The longitudinal force (T) in the contact is measured by a torque sensor.

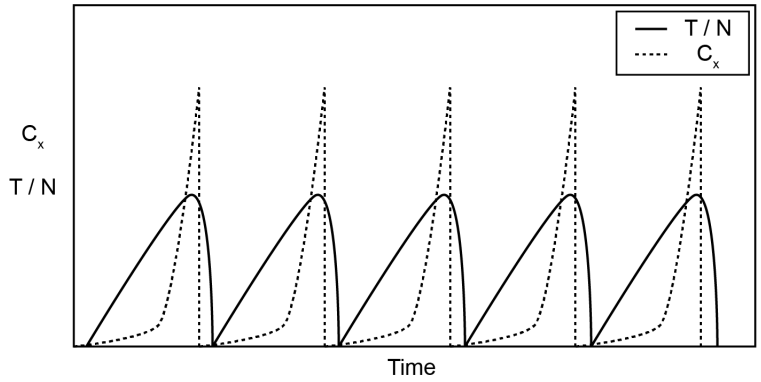

Figure 5: Creepage and coefficient of adhesion data from the tram wheel rig. Plot shows 5 instances of testing where torque is increased until slip occurs.

Creep is generated by applying a controlled torque on the wheel roller until the adhesion limit is exceeded and slippage between wheel and roller occurs.

Instantaneous velocities of the wheel and roller are measured using rotary encoders on each shaft. This allows calculation of longitudinal creep c_x over the duration of a test run, with corresponding measured torque.

$$c_x = \frac{v_{rail} - v_{wheel}}{v_{rail}} \quad (1)$$

If slippage occurs, the prescribed torque is returned to zero and rolling resumes. The control software has recently been updated and is programmable to detect a slip and automatically reduce the applied torque. The threshold for detecting slip was set at a level dependent on test conditions. Multiple creep curves are then generated by increasing the applied torque from zero again until slippage occurs. This can be repeated several times in a single test run (see Figure 5).

Two different application methods to supply water to the contact were used. The first employed a voltage micropump (M100S-180 TCS Micropumps) with options to divert water back into the reservoir for reducing flow rates. This test set up included a nozzle to supply compressed air to clean the contact band post contact. The minimum delivery rate in this set-up was 350 µL/s over an area larger than the contact width. The test schematic is shown in Figure 6

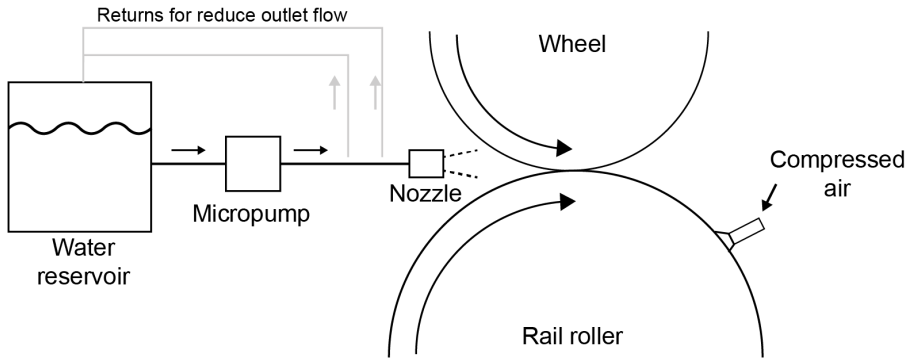

Figure 6: Constant water application test set-up schematic.

Constant water and bulk water application tests were performed using the micropump water application system. The compressed air was only used during the constant water application tests.

Application amounts when using the micropump application exceeded ‘low’ amounts. Therefore, tests with constant water applied using controlled application of water drops were performed. The system was a gravity fed water supply through pipe with the outlet directed at the contact band. The average droplet amount was measured at 60 µL/drop Water drop rate was controlled by adjusting a valve, as shown in Figure 7. No additional contaminants were applied during the water droplet test.

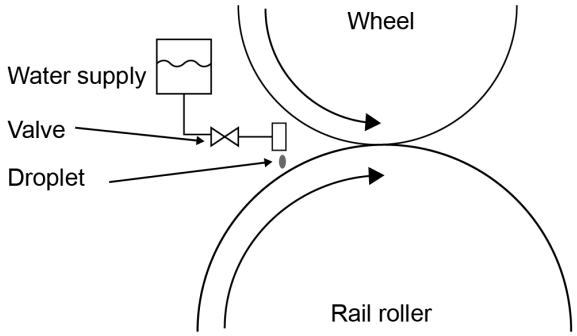

Figure 7: Schematic diagram of the water droplet application system. Droplets applied to rail roller as close as possible to contact.

It was intended that roughness measurements of the surface would be taken intermittently throughout the test series using a portable stylus profiler. However, it was not possible during this test series due to space limitations reducing access to the top of either the wheel or rail surface.

7.2.2. Methodology

A standard test produces 5 creep curves. However, the test procedure varied depending on the exact conditions under investigation. This variation in procedure arises as testing with contaminants necessitates possible variations in test length and number of cycles. For example, allowing enough time to complete the drying out of water whilst completing creep curves at regular intervals.

In dry conditions it was sufficient to generate 5 creep curves sequentially. The standard procedure for all dry tests was as follows:

1. Apply normal load
2. Accelerate to steady rolling velocity
3. Increase torque until wheel slide initiates, or motor torque limited is reached
4. Torque returned to zero and free rolling resumes

5. Repeat steps 3 and 4 until sufficient amount of creep curves are generated.

When contaminants are investigated, there are additional steps that have been described below.

The set of 'water + drying with compressed air' tests used the micropump applicator in conjunction with the compressed air feed. Water was supplied to the running band before entering the contact, and then any water that remained on the running band area was removed by the compressed air. The application of water was started and stopped before and after each cycle (see Figure 8).

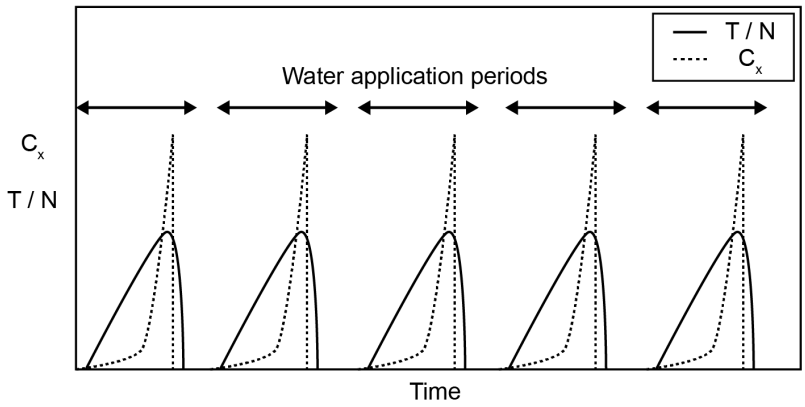

Figure 8: Schematic test timeline for constant water application using micropump + compressed air set-up.

The set of bulk water tests used the micropump applicator alone. Cycles were run to check the level of adhesion before any water was applied to the surface. Water was then applied to the roller at 6 ml/s over a period of 10 seconds under free rolling conditions. Steps 3 – 5 were then repeated until the contact band was observed to be dry and the adhesion level had returned to dry values. Figure 9 shows a schematic test time line for bulk water tests.

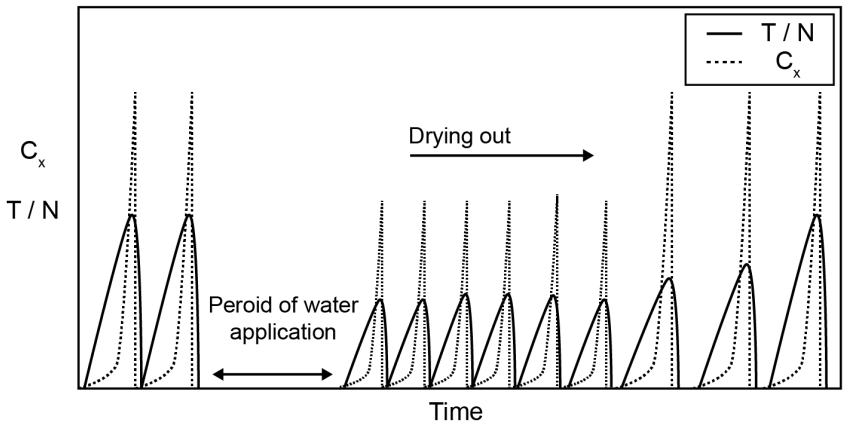

Figure 9: Schematic test timeline for bulk water application tests.

The tests for water droplets included two initial curves generated under clean conditions prior to water application followed by constant water application during torque increase and decrease, as shown in Figure 10. In these test conditions water was applied to the contact for 15 cycles then stopped and cycles were then run until dry values were returned to.

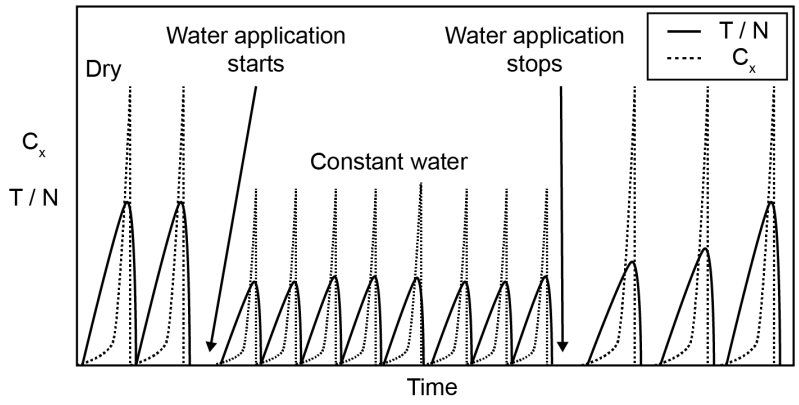

Figure 10: Constant water application using water droplet set-up test timeline schematic. Number of curves shown for illustrative purposes only.

7.2.3. Test conditions

The investigation looked at the following wheel/rail third body conditions:

- Dry 'clean' contact
- Water + drying with compressed air
- Bulk water application
- Constant low water application (droplets)

Table 2 shows the tests that have been carried out on the tram wheel rig. Tests sequences as shown for test numbers 1 -12 are subdivided by load, as the load can only be significantly changed when the test rig is not running. Tests sequences for 13-15 were run as a single continuous test. Number of cycles shown and the number of cycles conducted can vary depending on the test. For example, additional cycles may be included if a steady state had not been reached under constant conditions.

To map these water volumes to real world situations the equivalent amounts of rainfall has been calculated and plotted in Figure 39. The rainfall (mm/hr) is based on the assumption that the water is evenly distributed between the roller and wheel contact bands. The water volume is assumed to deposited over the measured deposit width of 11 mm to give a combined area of 0.0558 m^2. This should only be treated as an estimation of the equivalent rainfall.

Table 2: Table of tests on the full-scale tram wheel rig.

No.	Speed	Load sequence	Contact conditions
	[m/s]	Normal force [kN] (Cycles)	
1	1	4(5)_10(5)_20(5)_40(5)[3]	Dry (baseline)
2	5	4(5)_10(5)_20(5)_40(5)	Dry (baseline)
3	10	4(5)_10(5)_20(5)_40(5)	Dry (baseline)
4	16	4(5)_10(5)_20(5)_40(5)	Dry (baseline)
5	1	4(5)_10(5)_20(5)_40(5)	Water + drying with compressed air
6	5	4(5)_10(5)_20(5)_40(5)	Water + drying with compressed air
7	10	4(5)_10(5)_20(5)_40(5)	Water + drying with compressed air
8	16	4(5)_10(5)_20(5)_40(5)	Water + drying with compressed air
9	1	4(A)_10(A)_20(A)_40(A)	Bulk water application (60mL)
10	5	4(A)_10(A)_20(A)_40(A)	Bulk water application (60mL)
11	10	4(A)_10(A)_20(A)_40(A)	Bulk water application (60mL)
12	16	4(A)_10(A)_20(A)_40(A)	Bulk water application (60mL)
13	5	4(2dry)_4(15)_4(A)	Water droplet (25µL/s)
14	5	4(2dry)_4(15)_4(A)	Water droplet (35µL/s)
15	5	4(10)	Water pump (350µL/s)
A = run cycles until dry values of adhesion are measured.			

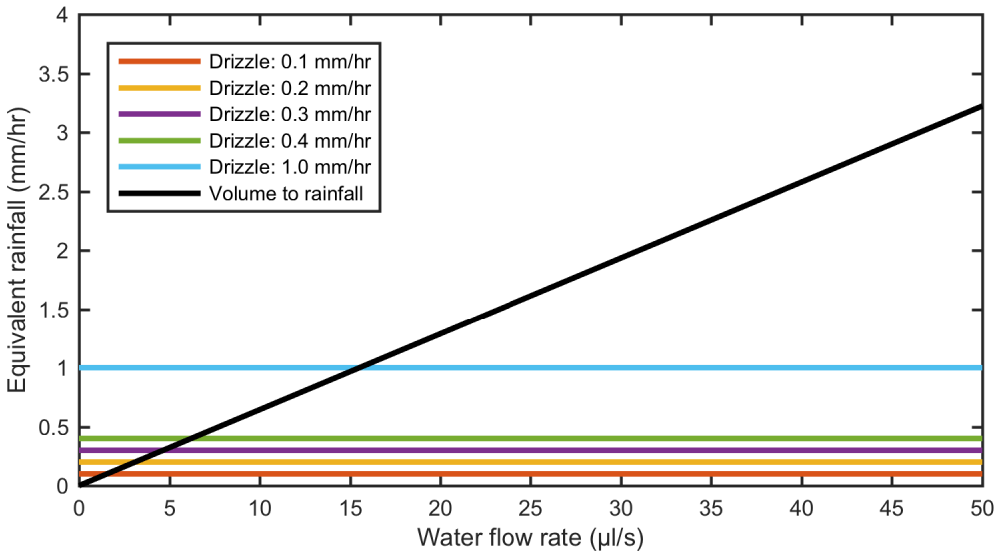

Figure 11: Estimation of the equivalent rainfall per hour against deposited water volume in full-scale tests. Solid black line shows the conversion of droplet application water flow rate into an equivalent rainfall in mm/hr. Horizontal lines do not relate to abscissa.

[3] Clarification of load sequence. The sequence 4(5)_10(5)_20(5)_40(5) is 4 separate tests as follows; 4 kN for 5 cycles, 10 kN for 5 cycles, 20 kN for 5 cycles, 40 kN for 5 cycles.

7.3. Results

Tests were performed under all conditions in dry, bulk water application and constant water + drying with compressed air. However, due to the torque limitation, reducing the maximum recordable adhesion under higher normal loads, sliding was not initiated in all cases and curves are limited to the initial gradient. Therefore, results presentation is exclusively limited to tests performed under a 4 kN normal load at 5 m/s. All results shown in Figure 9 to Figure 12 have been plotted against dimensionless longitudinal creep c_x. Note that the creep range for Figures 12 to 14 is up to 10 % (0.1) whilst Figure 15 is plotted to 100 % (1.0). Full test results are given in Appendix A.

Figure 12 shows the results under dry conditions. In dry conditions the peak adhesion is at a friction coefficient of 0.4. This level of adhesion is as expected for a dry rolling contact.

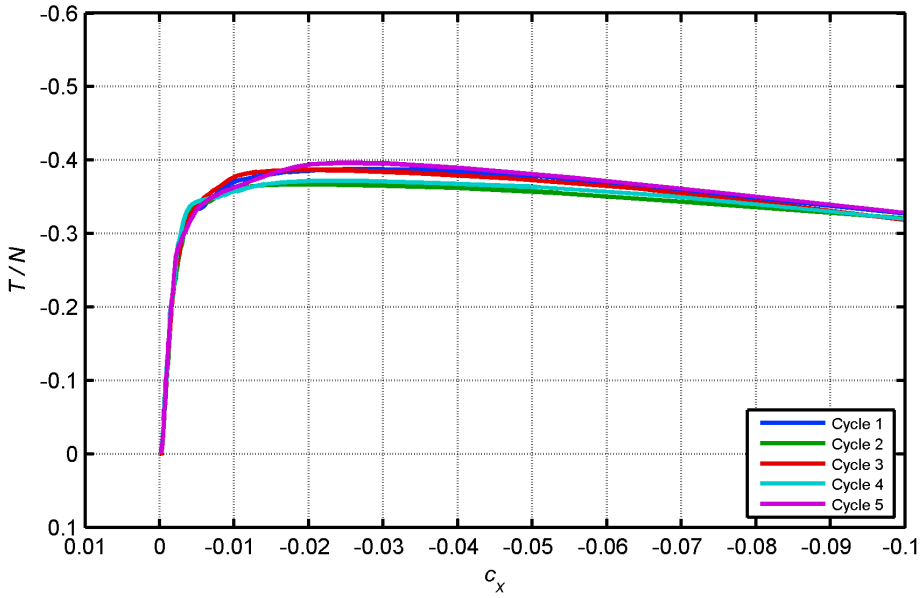

Figure 12: Creep curves from dry tests performed under 4 kN normal load and 5 m/s rolling velocity.

Figure 13 shows the results from constant water plus drying experiments. Water reduces the adhesion from dry levels as would be expected. Upon sliding the adhesion level stays steady at the creepage range shown.

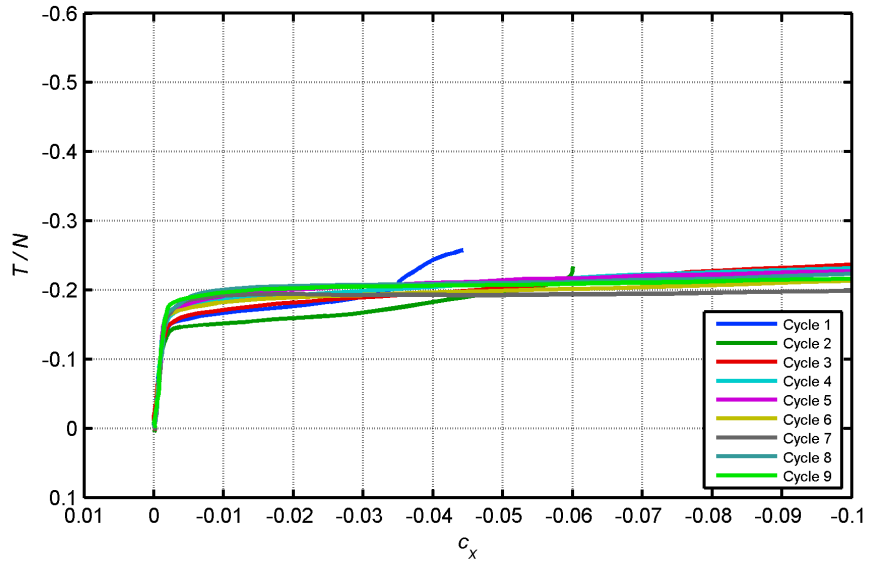

Figure 13: Creep curves from constant water (350 µL/s) + drying with compressed air tests performed under 4 kN normal load and 5 m/s rolling velocity.

Figure 14 shows the bulk water application creep curves generated under a 4 kN load. The initial curves (blue and dark green) were generated under dry conditions. After water application was stopped there is a sustained level of reduced adhesion that can be seen in cycles 3 to 7, when water is still present on the roller. Once there is no longer any water in the contact dry levels of adhesion are again seen (cycles 8 and 9).

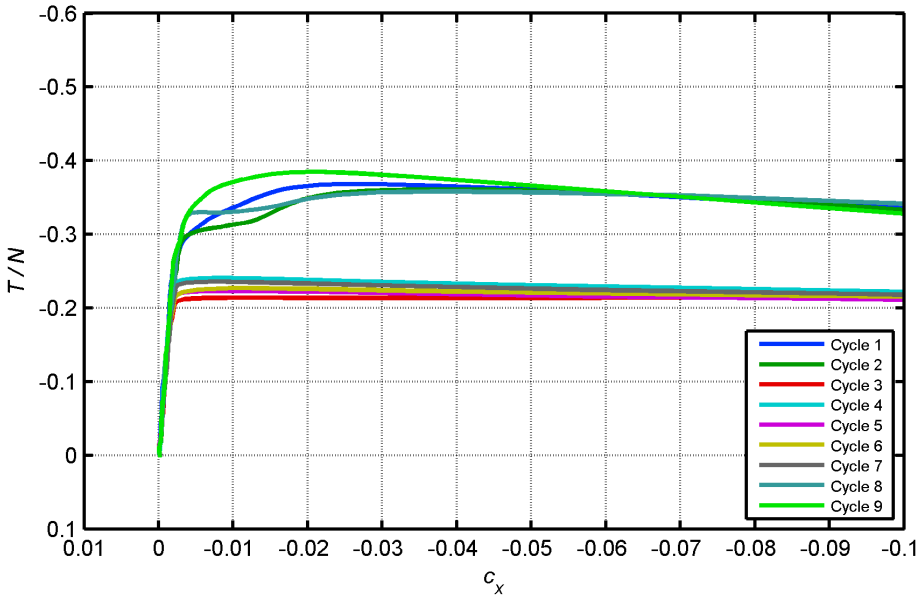

Figure 14: Creep curves from bulk water application (60 ml) tests performed under 4 kN normal load and 5 m/s rolling velocity.

Figure 15 shows a sample of the curves generated using the water droplet application system at a rolling speed of 5 m/s. As water droplet rate is increased from 25 µl/s to 35 µl/s there is a clear change in adhesion behaviour. At the low water deposit rate there was a rapid decrease in adhesion upon sliding. The traction control system on the rig was unable to effectively return to pure rolling once sliding was initiated and high creepage rates were seen. Levels of adhesion were reduced to below 0.1 (T/N). The

high water rate (350 µl/s) produced similar curves to those from bulk water application tests (see full wet curves from Figure 13).

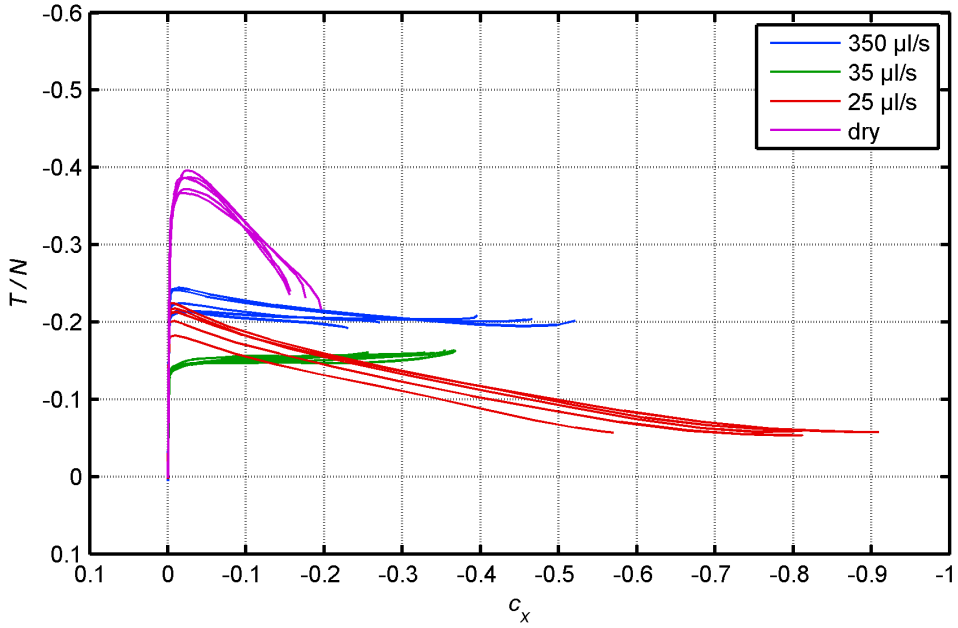

Figure 15: Creep curves from water droplet tests showing variation of water rate at fixed load and speed. Plot shows adhesion improvements as water rate is increased from a low value.

7.4. Discussion

From observing the contact patch during testing the third body in the contact is clearly seen to change over the course of a test. Under water droplet tests with water sufficient to keep the surface wetted, a layer is clearly seen on the running band of both the wheel and roller. This layer is formed of oxides and wear debris generated from the contact and the added water.

As the amount of water is increased from zero to fully wet conditions the solid fraction (from oxides and wear debris) will decrease from 100 % (dry) to below the levels shown to reduce adhesion. This transition will have an effect on how the mixture is entrained into the contact with lower solid fractions (higher water) being cleared more readily whilst the higher solid fractions are able to sustain the low adhesion.

To investigate the drying process under water droplet application, a recording was made of a test where the water application was stopped and a set of curves ran until the contact patch was again dry. After stopping the supply of water to the contact, the third body layer begins to undergo a transition as it begins to dry out. This drying out process can be seen in the Figure 16 from (a) to (c), where the final image shows a clear running band, with wet debris still evident at the sides of the band.

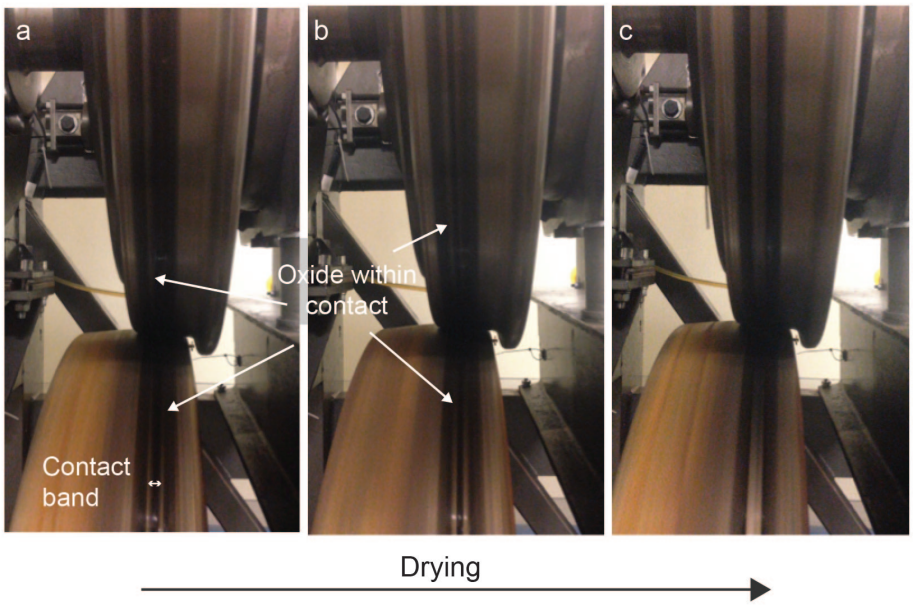

Figure 16: Appearance of contact patch during water droplet tests

The final removal of oxide from the contact happened over a very short period, perhaps only a few rotations of the rollers. It is likely that this is when the water/oxide mixtures are suitable for causing low adhesion. This period is too short to generate a full creep curve, unless the water supply is kept at the correct level to sustain the water/oxide mix. It is for this reason that the bulk water tests did not produce low adhesion even as the water amounts were steadily decreased.

The depth of the water film on the surface has been estimated from the volume of water deposited over the combined surface area of the roller and wheel surfaces. For simplicity it has been assumed that the water is not accumulated on the surface and the surfaces is perfectly smooth. The expected average surface roughness of the roller and wheel is 1 μm. As can be seen in Figure 17 the depth of water never exceeds the surface roughness in the range shown (up to 50 μL), which indicates that the amount water in the contact varies over this range.

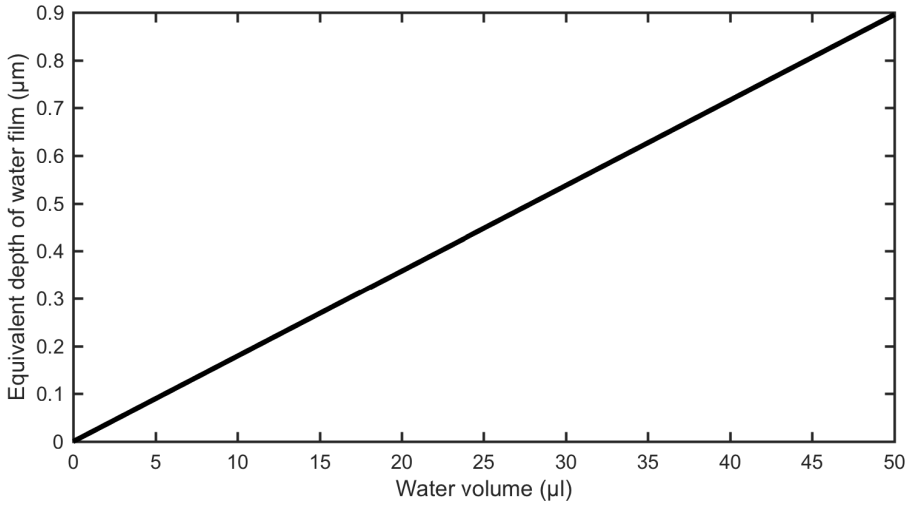

Figure 17: Estimation of the equivalent water depth formed on a flat surface for specific water volume. Estimated surface roughness in tram wheel rig 1µm.

In the field, the wheel would be a fresh supply of contaminant sufficient to sustain low adhesion. When the water rate is increased from this low amount there is a transition phase up to fully wet curves.

7.5. Conclusions

Tests on the full-scale rig have shown that when the right set of wet conditions are sustained once sliding is initiated adhesion levels are rapidly reduced to low levels (min(T/N) = 0.052). The low adhesion conditions are formed and sustained during sliding. This level of adhesion is on the boundary of low and exceptionally low adhesion as defined by Vasic et al. (2008).

Visual inspection of the contact band during tests indicated that the third body layer formed changes during tests when water is allowed to evaporate. The mixture is comprised of water, oxides and wear debris generated from the contacting bodies. It was observed that this oxide/water is fully removed during a few rotations of the rollers as the water evaporates. The short time span indicates there is a high chance of missing this transition point during a test unless water application is constant (and at the right level to produce a viscous oxide water mixture). This is perhaps why others have not been able to generate such low adhesion conditions during testing.

Creep curves have been generated that can now be used in modeling to link water amount to wheel/rail interface friction levels and for informing braking models.

7.6. Acknowledgements

This work was funded by the Rail Safety and Standards Board (RSSB) and Network Rail within the project T1077.

7.7. References

Beagley, T.M., Pritchard, C., 1975, “Wheel/Rail Adhesion - The Overriding Influence of Water”, Wear, Vol. 35, No. 2, pp299–313.

Buckley-Johnstone, L.E., Trummer, G., Voltr, P., Meierhofer, A., Six, K., Fletcher, D.I., Lewis, R., 2016, “Assessing the Impact of Small Amounts of Water and Iron Oxides on Adhesion in the Wheel/Rail Interface using High Pressure Torsion Testing”, to be submitted to IMechE Part J.

Trummer, G. Buckley-Johnstone, L.E., Voltr, P., Meierhofer, A., Lewis, R., Six, K., 2017, “Wheel-rail creep force model for predicting water induced low adhesion phenomena” Tribology International, 109, pp. 409-415

Vasic, G., Franklin, F., Kapoor, A. and Lucanin, V., 2008, “Laboratory simulation of low-adhesion leaf film on rail steel”, Int. J. Surface Science and Engineering, 2(1/2), pp. 84–97

Voltr, P. and Lata, M., 2014, “Transient wheel–rail adhesion characteristics under the cleaning effect of sliding”, Vehicle System Dynamics, 53, 605-618

White, B.T., Fisk, J., Evans, M.D., Arnall, A.D., Armitage, T., Fletcher, D.I., Lewis, R., Nilsson, R., Olofsson, O., 2016, “A Study into the Effect of the Presence of Moisture at the Wheel/Rail Interface during Dew and Damp Conditions”, submitted to *Journal of Rail and Rapid Transit*, *Proceedings of the IMechE Part F*.

8. Wheel-Rail creep force model for predicting water induced low adhesion phenomena

G. Trummer[1], L. Buckley-Johnstone[2], P. Voltr[3], A. Meierhofer[1], R. Lewis[2], K. Six[1]

[1]Virtual Vehicle Research Center, Graz, Austria
[2]Department of Mechanical Engineering, The University of Sheffield, Sheffield, UK
[3]Jan Perner Transport Faculty, University of Pardubice, Pardubice, Czech Republic

Pubished: *Trummer, G. Buckley-Johnstone, L.E., Voltr, P., Meierhofer, A., Lewis, R., Six, K., 2017, "Wheel-rail creep force model for predicting water induced low adhesion phenomena" Tribology International, 109, pp. 409-415*

Abstract

A computationally efficient engineering model to predict creep forces respectively adhesion in rolling contact in the presence of water is presented. This model has been developed in a project funded by the Rail Safety and Standards Board (RSSB) and Network Rail. It is referred to as the water-induced low adhesion creep force (WILAC) model. The model covers the calculation of creep forces in a wide range of conditions from dry over damp to wet. Special emphasis has been put on low amounts of water in the contact – conditions that may be encountered at the onset of rain for example. The model has been parameterised based on experimental results from a tram wheel test rig. These results show that adhesion changes with the water flow rate in a complex way. Adhesion values as low as 0.06 have been observed in the experiment at high creep with only wear debris and little amounts of water present in the contact. The model results also agree with experimental data from locomotive tests (recorded at high normal contact force) in dry and wet conditions. The model may be implemented in multibody software or in braking models to study train performance and braking strategies, especially in damp conditions.

8.1. Introduction

In Great Britain during the autumn period (from October to November) numerous incidents, such as "station overruns" and signals passed at danger (SPADS) occur every year which are related to low adhesion conditions (RSSB, 2014). For about half of the incidents an autumn leaf contamination has been reported that are known to cause low adhesion (Cann, 2006; Olofsson, 2004; Arias-Cuevas et al., 2010; Li, 2009; Gallardo-Hernandez et al., 2008). A proportion of the other half were related to small amounts of water on the rail head caused by prevailing environmental conditions. Detailed analysis shows a peak in incidents, for example, around dew point conditions in the morning and evening (White et al., 2016). There is also experimental evidence that low amounts of water in combination with iron oxides on the surface reduce adhesion in rolling contacts without the presence of other contaminants (Beagley, 1975).

The objective of this work was to develop a computationally efficient creep force model which is able to predict adhesion depending on the “wetness” of the surface. The focus is on low amounts of water causing low adhesion conditions. Model development is accompanied by experiments on a tram wheel test rig which provided data for the model parameterisation. The model may be used in multibody dynamics (MBD) simulations to study the effect of low adhesion on train performance, or it may be implemented in braking models to study possible braking strategies.

8.2. Literature review

For braking of railway vehicles a minimum adhesion of approximately 0.15 is usually required between wheels and rails for safe operation (UIC 544). Adhesion values $T/N < 0.15$ may be referred to as “low adhesion” (Vasic 2008).

8.2.1. Influence of water on adhesion

Two mechanisms govern the adhesion in rolling contact in the presence of interfacial fluids: Boundary lubrication (BL) and hydrodynamic lubrication (HL). The transition region where both mechanisms govern adhesion is referred to as mixed lubrication (ML). Which mechanism dominates depends on the relative velocity between the surfaces, the fluid viscosity and the normal force (Stachowiak, 2006). In addition the size and the shape of the contact patch and the surface roughness play a role (Tomberger, 2011).

Creep curves (adhesion as a function of creep) in dry conditions differ from creep curves in wet conditions with respect to the adhesion level, the shape of the curve and the initial slope (Polach, 2005). Wetting the surface with water reduces the adhesion level, shifts the adhesion maximum to higher creep values and reduces the decrease of adhesion with increasing creep (Polach, 2005).

Beagley and Pritchard (Beagley, 1975) investigated the change of adhesion over time in an Amsler experiment, where two steel discs roll on each other with a fixed (longitudinal) creep of 0.033 at a circumferential velocity of about 0.3 m/s (see Figure 1). When water is applied to the contact the adhesion drops from around 0.6 to around 0.3. When the wet surfaces are allowed to dry a viscous paste of wear debris and water forms on the surface which reduces the adhesion to a minimum value of 0.2 before the dry adhesion value is observed again. If the generated wear debris in the rolling contact is continuously removed from the surface by a wire brush, no adhesion minimum is observed (Beagley, 1975). These experiments demonstrate that wear debris in combination with little amounts of water reduce adhesion to values well below the adhesion value when large amounts of water are present on the surface (Beagley, 1975). However, the observed minimum adhesion values cannot be considered “low adhesion”.

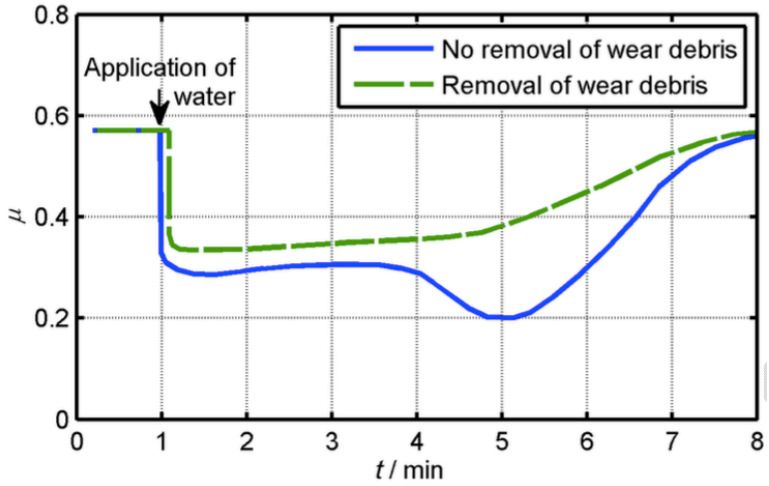

Figure 1: **Schematic change of adhesion in an Amsler experiment when the surface dries up after an initial application of water; Solid line: Adhesion minimum without continuous removal of wear debris; Dashed line: Continuous removal of wear debris by wire-brushing the surface; data reproduced from (Beagley 1975).**

8.2.2. Existing creep force models taking the effect of water into account

Kalker's half-space model CONTACT (Kalker, 1967) considers BL only. The influence of water on adhesion is usually included by adjusting the values of the static and dynamic coefficient of friction. Recent extensions of CONTACT (Vollebregt, 2014) include the implementation of a falling friction law and the implementation of an elastic interfacial layer.

Likewise, in the simplified theory of rolling contact, which is implemented in the algorithm FASTSIM (Kalker, 1982), the influence of water can be considered by adjusting the coefficient of friction in terms of BL. Spiryagin (2013) extended the FASTSIM algorithm by a variable contact flexibility and a slip dependent friction law to allow a better reproduction of measured creep curves.

The Polach model (Polach, 1999; Polach, 2005) is a computationally fast alternative to the FASTSIM algorithm, built on the theory of BL as well. The model can be tuned to experimental results under wet conditions by adjusting the initial slope of the adhesion curve and the decrease of adhesion with increasing slip velocity. The amount of water is not explicitly taken into account.

Beagley (1976) estimated adhesion in the wheel/rail contact based on HL theory assuming full sliding. Key input parameters are the viscosity of the iron oxide/water mixture and the film thickness on the rail. This model is not a full creep force model, so that adhesion at low creep cannot be calculated.

The Chen model (Chen, 2002; Chen, 2005) uses both BL theory and HL theory. Adhesion under wet conditions for rough surfaces is predicted by distributing the load between contact asperities experiencing BL and the hydrodynamic water film based on statistical methods.

Key input parameters are the surface roughness and the fluid viscosity. The Popovici model (Popovici, 2010) uses BL theory for the contact between surface asperities and HL theory to describe the behaviour of the fluid layer. The model takes rough surfaces, frictional heating in the elastohydrodynamic component and starved contact conditions (limited supply of liquid to the contact) into account.

The Tomberger model (Tomberger, 2011) combines the FASTSIM algorithm with an interfacial fluid model, a temperature model and a micro-contact model. Fluid related input parameters are the viscosity and the amount of liquid on the rail surface.

The Extended Creep Force (ECF) model (Meierhofer, 2015: Six, 2014) extends the Tomberger model by a temperature- and normal stress-dependent elasto-plastic third-body layer model. Adhesion is governed by the solid interfacial layer whose properties are changed by interfacial fluids.

For the objective of this work computational efficiency, a fully published model structure and the ability of the model to describe complex adhesion characteristics are crucial points. With respect to applicability in the practice of railway operation a simple approximate model with a minimum of input parameters is preferred over a detailed and sophisticated model. In railway operation little amounts of wear debris in combination with water are expected at the rail surface so that mainly boundary lubrication with some influence of hydrodynamic lubrication (creating a mixed lubrication condition) may be assumed.

Considering all these points the Polach model (based on BL theory) seems to suit these needs best, thus the Polach model has been chosen as the basis for the development of the WILAC model, which is described in section 5

8.3. Tram experiments wheel test rig

Experiments investigating the influence of water on adhesion in rolling contacts have been performed at the tram wheel test rig at the University of Pardubice. The tram wheel test rig comprises of a full-size tram wheel (diameter 0.696 m) and a rail roller (diameter 0.905 m). The effective radius in lateral direction of the contact was estimated to be 0.660 m based on imprints of the contact patch on carbon paper. The normal load is applied to the wheel by an air spring. The rail roller with the torque transducer is kept at constant rotational speed during the experiment.

To record adhesion as a function of creep the circumferential velocities of the wheel and the rail roller are brought to the desired value. Then a slowly increasing torque is applied to the wheel, while the rail roller is kept at the pre-set constant circumferential velocity. When large sliding of the wheel is detected, the torque applied to the wheel is reduced to zero and free rolling resumes. During an experiment the torque is increased and decreased multiple times. From the measured torque at the rail roller and the rotational speed of the wheel and the rail roller (measured by rotary encoders) adhesion curves can be deduced. Usually traction is applied to the wheel to prevent damage to the surface caused by a blocking wheel. Further details about the test rig can be found in (Voltr, 2015).

Adhesion curves have been recorded for a normal contact force of 4.2 kN at a rolling speed of 5 m/s. Temperature and relative humidity were uncontrolled at the test rig. During the experiments the temperature ranged from 20°C to 25°C, and the relative humidity was between 54 %RH and 70 %RH. To realize low amounts of water in the wheel/rail contact, water has been applied drop-wise to the rotating rail roller at a constant rate by a gravity fed application system (see Figure 2). Water drop rate was controlled by a valve. The end of the pipe where the droplets formed was brought as close as possible to the contact. With this setup average water flow rates of 25 µl/s, 35 µl/s, and 60 µl/s were realized. The measured average water volume of one drop is about 60 µl. The water rate of 350 µl/s was realized by using a micro-pump.

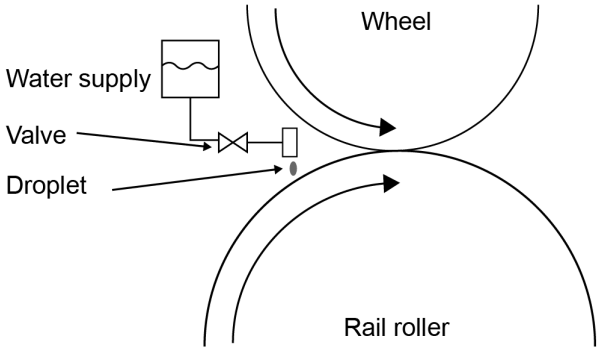

Figure 2: **Drop-wise application of low amounts of water by a gravity fed water application system.**

Multiple adhesion curves have been recorded in dry condition and for different water flow rates. The results are shown in Figure 3.

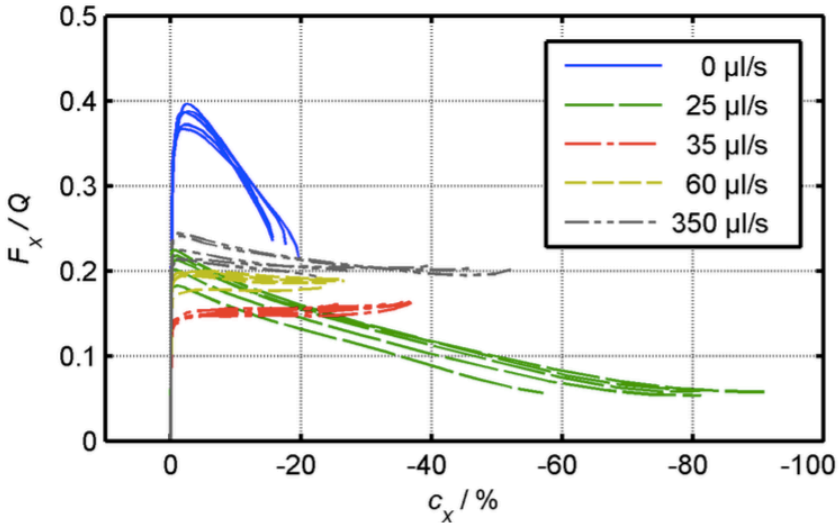

Figure 3: **Measured adhesion in the tram wheel test rig experiments as a function of the water rate at 4.2 kN normal force and 5 m/s rolling speed.**

The experimental data show two types of adhesion characteristics: The “dry” type (observed at water flow rates 0 µl/s and 25 µl/s) shows a high peak adhesion at low creep in combination with a steep decrease of adhesion with increasing creep.

Typical for the “wet” type (observed at water flow rates 35 µl/s, 60 µl/s and 350 µl/s) is an almost constant adhesion value with increasing creep.

The adhesion curve at a water flow rate of 25 µl/s is particularly interesting, because the peak adhesion value at low creep is comparable to the peak adhesion values observed at higher water flow rates. But in contrast to other wet curves, a strong reduction of the adhesion value with increasing creep is observed in this case. Adhesion values of 0.06 have been measured in the creep range from -60% to -90%.

8.4. WILAC model

The WILAC model (acronym for Water-Induced Low Adhesion Creep Force Model) describes the wheel/rail adhesion in dry, moist and wet conditions with special emphasis on moist conditions. In the model the wetness of the contact surface is quantified in terms of a water flow rate w to the surface.

The structure of the WILAC model is shown in Figure 4. It consists of linear regression models, a Polach creep force model and a function for blending in between conditions. These parts of the WILAC model are described in the following sections.

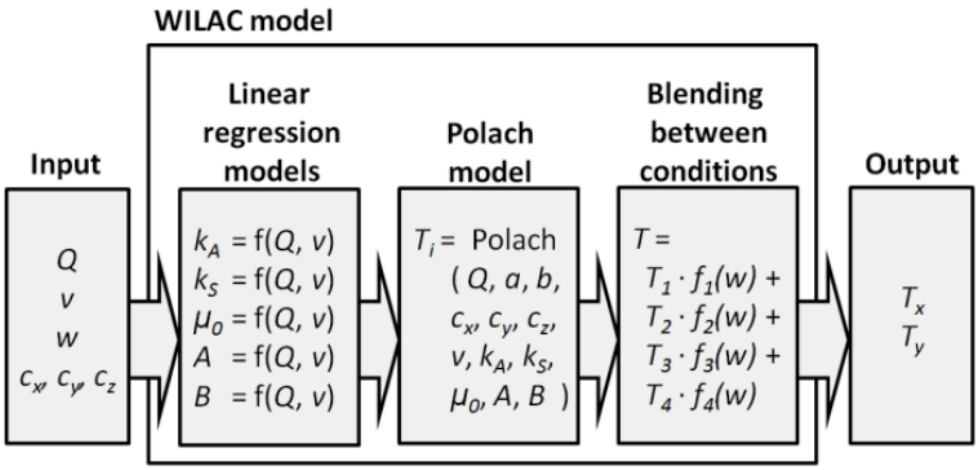

Figure 4: **General structure of the WILAC model for calculating creep forces in dry, moist and wet conditions.**

8.4.1. Creep force calculation

The WILAC model for estimating the wheel/rail adhesion is built around the Polach model (Polach, 1999). The Polach model is a state-of-the-art creep force model which is extensively used in multibody simulations of railway vehicles. It calculates the longitudinal and lateral creep forces T_x and T_y as a function of the contact normal force Q, the dimensions of the Hertzian contact ellipse a and b, and the relative motion between the surfaces in terms of longitudinal creep c_x, in lateral creep c_y, and spin creep c_z.

The original model has been extended to consider the decrease in adhesion with increasing relative velocity between the contact surfaces and to consider the experimentally observed reduction of the initial gradient of the creep curve

(Polach, 2005). These features are described by five Polach model parameters: k_A and k_S, which are related to the gradient of the adhesion curve at low creep; and A, B, and μ_0 which are related to the decrease of adhesion at high creep values.

8.4.2. Linear regression models

Linear regression models have been implemented for the (internal) calculation of the Polach parameters in the WILAC model because the observed change of the adhesion characteristic as a function of vehicle speed and normal force does not agree well with available experimental data from locomotive tests (Six 2015) when fixed values are used for the Polach parameters in the calculation.

Experimental data from the tram wheel test rig were not available for the whole range of operating conditions with respect to normal force and rolling speed for the WILAC model development. Thus, extrapolation of data to a wider range of normal forces and rolling speeds was necessary, which was done with the Extended Creep Force (ECF) model (Meierhofer, 2015; Six, 2015).

The ECF model explicitly considers third-body layers and the effects of plastic deformation, material hardening, and temperature-related softening of this layer on the adhesion level. Therefore the model behaviour of the ECF model differs from that of the Polach model with respect to normal force and rolling speed.

Adhesion curves calculated with the ECF model can be reproduced with a Polach model by individually adjusting the Polach parameters for each adhesion curve. If the ECF model behaviour needs to be reproduced over a whole range of normal forces and vehicle speeds, the Polach parameters of the Polach model need to be adjusted for each combination of normal force Q and rolling speed v. The necessary adjustment of the Polach parameters is done by five linear regression models in the WILAC model which calculate the (internal) parameters k_A, k_S, A, B and μ_0 as a function of the normal force Q and the vehicle speed v.

For example, a multiple linear regression model relating parameter k_A to the normalized normal contact force Q' and to the normalized rolling speed v' can be chosen as:

$$k_A = a_0 + a_1 Q' + a_2 v' + a_3 Q'^{-1} + a_4 v'^{-1} + a_5 e^{Q'} + a_6 e^{v'} + \cdots + e \qquad (1)$$

Therein, k_A is the dependent variable. Q' and v' are the independent variables, which are normalized to their maximum values in the investigated parameter range. a_i are the regression coefficients and e is an error term. The terms Q', Q'^{-1}, $e^{Q'}$, v', v'^{-1} and $e^{v'}$ up to order 3 including mixed terms are used as independent variables in building the regression model. The regression coefficients a_i are determined by the method of least squares based on i observations of the dependent variable k_A. Only those independent variables, which improve the R^2-value by at least 10^{-4} are included in the regression model.

For each of the Polach parameters k_A, k_s, μ_0, A and B separate multiple linear regression models are set up. The R^2-values of these regression models are typically equal or better than 0.996.

8.4.3. Blending between conditions

The WILAC model has been parameterised based on four representative conditions (Dry, Damp2, Damp1, Wet) associated with different degrees of wetness of the surface. For each condition an independent set of linear regression models for estimating the (internal) Polach parameters has been determined based on the experimental data and the data extrapolation as described in section 5.2.

Because the experimental data have been recorded at fixed water flow rates an interpolation method is needed to be able to change the water flow rate continuously in the WILAC model. Thus, the actual longitudinal adhesion T_x/Q (and the lateral adhesion T_y/Q) as a function of the water flow rate w is determined by interpolating between the four representative conditions according to the following weighted sum:

$$\frac{T_{i=x,y}}{Q} = \frac{1}{Q}\left(f_{Dry} \cdot T_{i,Dry} + f_{Damp1} \cdot T_{i,Damp1} + f_{Damp2} \cdot T_{i,Damp2} + f_{Wet} \cdot T_{i,Wet}\right) \quad (2)$$

The weights f_i as a function of the water flow rate w are shown in Figure 5.

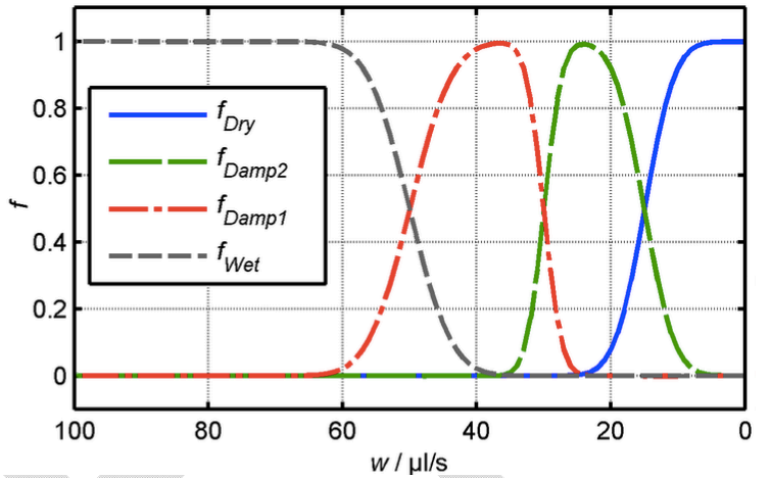

Figure 5: Weights f_i as a function of the water flow rate w, which are used to calculate the actual adhesion T_i/Q

The weights f_i are derived from three functions e_1 to e_3 as:

$$f_{Dry} = 1 - e_1 \quad (3)$$

$$f_{Damp2} = e_1 - e_2 \quad (4)$$

$$f_{Damp2} = e_2 - e_1 \quad (5)$$

$$f_{Wet} = e_3 \quad (6)$$

Functions e_1 to e_3 are related to the transition between the conditions. The functions e_1 to e_3 are calculated as

$$e_i = \frac{1}{2}\left(erf\left(\frac{w - m_i}{s_i}\right) + 1\right) \tag{7}$$

Therein, m defines the position of the transition with respect to the water flow rate w. s specifies the width of the transition. Functions e_1 to e_3 are shown in Figure 6 and the associated parameters m and s are given in Table 1.

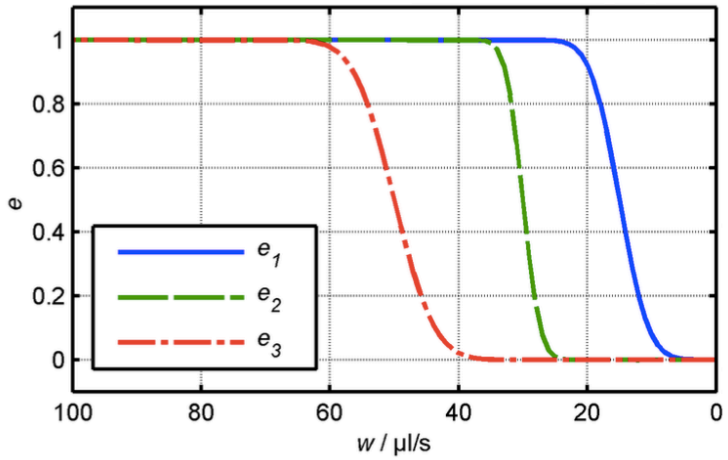

Figure 6: **Functions e_1 to e_3 used to derive the weight functions f_i.**

Table 1: **Parameters m and s for functions e_1 to e_3 used to describe the transitions between different surface conditions.**

Function	Transition	*m* / (µl/s)	*s* / (µl/s)
e_1	Damp2 - Dry	15	5
e_2	Damp1 – Damp2	30	3
e_3	Wet - Damp1	50	7

The described approach for blending between different surface conditions ensures smooth transitions between the different measured adhesion conditions (Dry, Damp2, Damp1, Wet). Moreover, each transition can be individually adjusted according to experimental data.

8.5. Model parameterisation and validation

Four representative experimental datasets from the tram wheel test rig experiments with respect to the water flow rate w have been used for the WILAC model parameterisation. These were the “Dry” data, the damp datasets recorded at water flow rates of 25 µl/s and 35 µl/s (“Damp2”, “Damp1”) and the “Wet” dataset recorded at a water flow rate of 350 µl/s. Each of these experimental data (at fixed water flow rate w) were recorded at a normal force of 4.2 kN and a rolling speed of 5 m/s. These data were extrapolated to a wider range of operating conditions with the ECF model (Meierhofer, 2015; Six, 2015), which was parameterised based on locomotive test data previously. The experimental data and the extrapolated data then served as the basis for the determination of the linear regression models for

the (internal) calculation of the Polach parameters in the WILAC model (see Section 8.4.).

Figure 7 shows the WILAC model results after the final model parameterisation (thick lines) together with the underlying experimental data used for model parameterisation (thin lines).

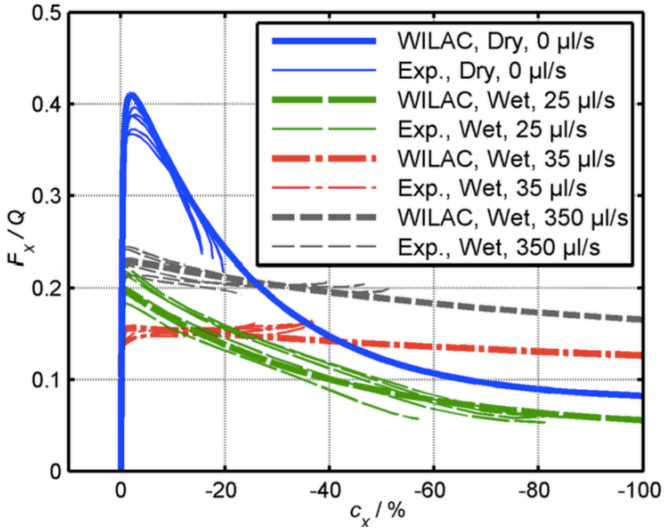

Figure 7: Experimental data (thin lines) used for model parameterisation and associated WILAC model results (thick lines) for different water flow rates w at 4.2 kN normal force and 5 m/s rolling speed.

Figure 8 shows the change of the adhesion for different fixed longitudinal creep values c_x as a function of the water flow rate w calculated with the WILAC model. Depending on the longitudinal creep adhesion minima are obtained for water flow rates in the range from 20 µl/s to 40 µl/s. The shape of the curve at cx = -3% is very similar to the adhesion curve reported by Beagley and Pritchard (1975) without removal of wear debris from the surface (see Figure 1).

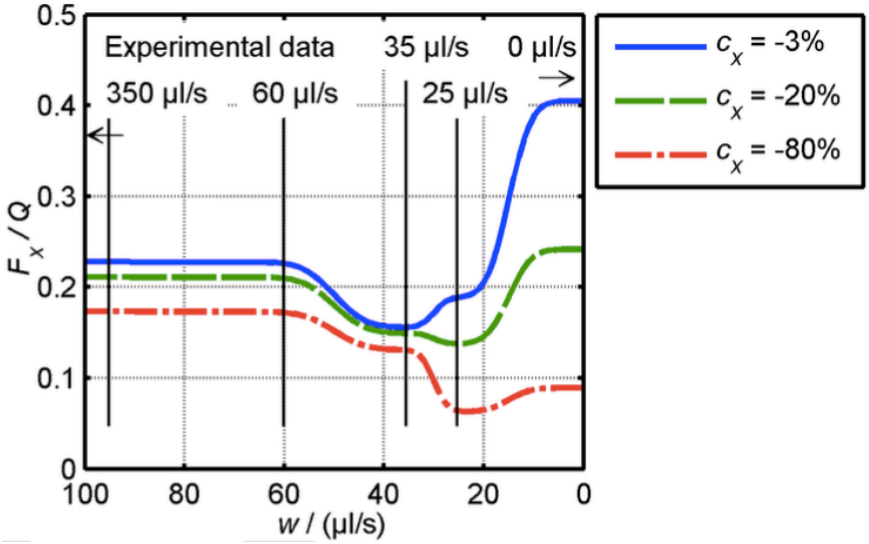

Figure 8: **Change of adhesion F_x/Q as a function of water flow rate w for different fixed values of longitudinal creep c_x. Water flow rates w where experimental data have been recorded are marked by vertical lines.**

Figure 9 compares WILAC model results to experimental adhesion data from full-scale locomotive tests in dry condition for different rolling speeds. Results have also been compared in wet condition (Figure 10), where the track was artificially watered (flooded conditions). These locomotive tests have been recorded at a normal contact force of 110 kN, which is significantly higher than the normal contact force used in the experiments at the tram wheel test rig (see section 4).

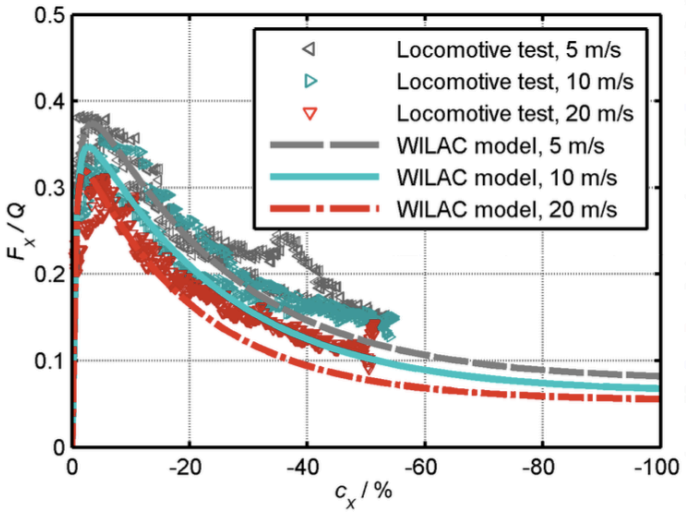

Figure 9: **Comparison of WILAC model results with locomotive test data from literature (Six 2015) in dry surface condition.**

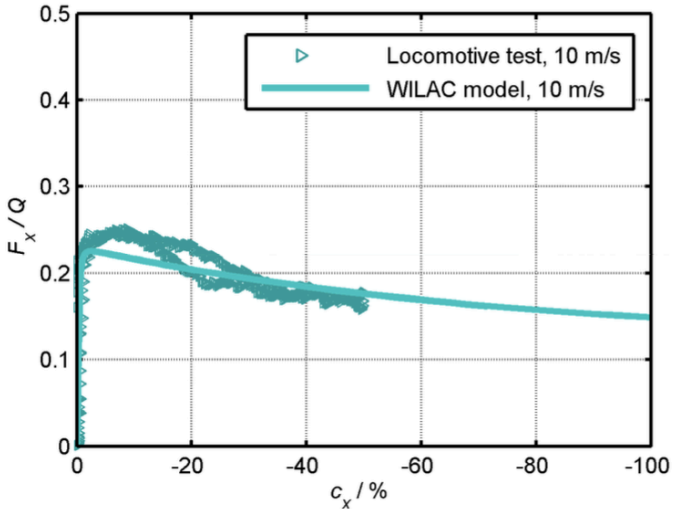

Figure 10: **Comparison of WILAC model results with locomotive test data from literature (Six, 2015) in wet surface condition.**

Figure 11 demonstrates the change of adhesion as a function of rolling speed according to the Polach model in comparison with the adhesion data from locomotive tests in dry surface condition. For this purpose the Polach parameters in the WILAC model for the adhesion curve at 10 m/s in Figure 10

have been taken. These (fixed) Polach parameters have then been used to calculate the adhesion curves at 5 m/s and 20 m/s (with the linear regression models deactivated). The variation of the adhesion curve in Figure 11 reflects thus purely the behaviour of the Polach model. A comparison of the WILAC adhesion curves in Figure 10 (Linear regression models + Polach model) with the adhesion curves in Figure. 11 (Polach model with fixed Polach parameters) show that the change in adhesion with rolling speed in the creep range from approximately -10% to approximately - 50% is too large in the Polach model when compared to locomotive test data. The adjustment of the (internal) Polach parameters by linear regression models in the WILAC model gives a better agreement with locomotive test data, as shown in Figure 9.

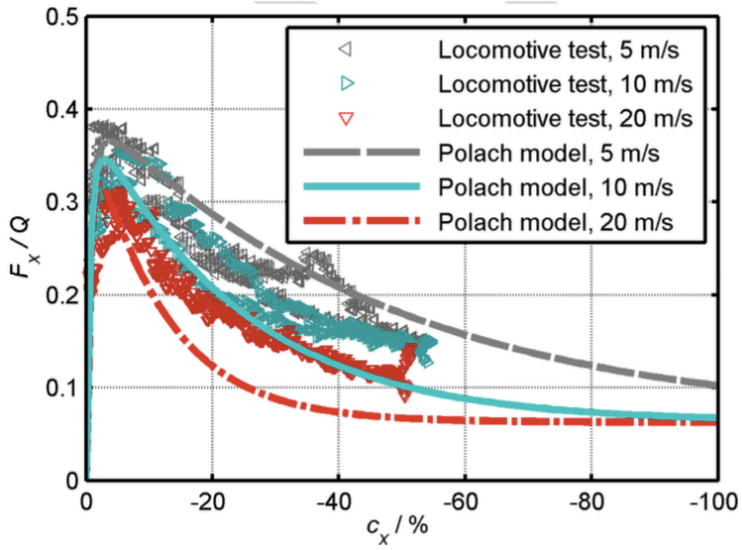

Figure 11: Variation of adhesion calculated with the Polach model and comparison with locomotive test data in dry condition. The Polach parameters from the curve at 10 m/s have been used for calculating the Polach adhesion curves at 5 m/s and 20 m/s (with deactivated linear regression models).

8.6. Discussion

The experimental results from the tram wheel test rig show that the adhesion characteristic changes in a complex way with the water flow rate. The adhesion characteristic in damp condition is not just a linear interpolation between the adhesion curves observed in dry and in wet conditions.

The observed adhesion characteristic at a water flow rate of 25 µl/s proves that low adhesion conditions can occur with only wear debris and little amounts of water present in the contact. Under the right set of conditions the adhesion drops to values of 0.06 at large creep without the presence of grease or oil. Increasing the water flow rate to 35 µl/s changes the adhesion curve to the “wet” type with adhesion values of approximately 0.15. At a water flow rate of 60 µl/s (see Figure 3) the adhesion curve is already very similar to the adhesion curve at a water flow rate 350 µl/s. Thus a water flow rate of 60 µl/s can be regarded as the upper limit of the range in which the water flow rate has a considerable influence on the adhesion characteristic.

With the tram wheel test rig only an accelerating wheel has been studied. However, a similar adhesion characteristic can be expected for a braking wheel if one assumes that the adhesion is independent of the direction of the relative motion between wheel and rail. The above findings may be relevant for railway operation: If both rails are covered with wear debris over a certain distance and if the rail surface is just slightly wet (for example at the onset of rain, or in dew conditions) then the surface conditions may be comparable to the conditions at the tram wheel test rig at a water flow rate of 25 µl/s. If a constant braking torque is applied to the wheel in such a condition then the creep between wheel and rail will increase. If the working point exceeds the maximum adhesion value the creep will further increase and probably reach the low adhesion part of the adhesion curve. When the brakes are released the low adhesion condition may persist for some time because of the slow (re)acceleration of the wheelset to rolling speed due to the small tangential friction forces in the contact.

The water flow rate is the only parameter related to the “wetness” of the surface in the WILAC model. When the model is used in engineering practice the water flow rate to the surface may be estimated from meteorological data such as the precipitation rate, humidity and temperature. Other parameters which certainly play a role in causing low adhesion conditions such as the surface roughness, or the amount and the composition of the interfacial layer on rails and wheels, are probably unknown in practice in most circumstances. Consequently, these are not input parameters for the WILAC model.

Hydrodynamic lubrication theory is not implemented directly in the WILAC model, which is based on boundary lubrication theory, although the WILAC model predicts adhesion in the presence of fluids. However hydrodynamic effects are indirectly considered in terms of the characteristics of the experimentally determined adhesion curves at the various water flow rates. This empirical approach adopted in the development of the WILAC model has the advantage that it results in a simple and computationally efficient engineering model in which the necessary input parameters are reduced to a minimum. Nevertheless the WILAC model is able to predict wheel/rail adhesion under a wide range of conditions ranging from dry to wet conditions including moist conditions.

The WILAC model may be implemented in multibody software to study the effect of low adhesion on train performance or it may be implemented in existing braking models to study braking strategies in moist conditions.

The modelling approach for predicting wheel/rail adhesion adopted for the WILAC model is not restricted to water and oxides in the contact. It can be extended to describe the influence of purposely added substances (such as friction modifier) on adhesion as well if the model development is accompanied by appropriate experiments.

8.7. Conclusions

Low amounts of water considerably influence the adhesion level and the shape of the adhesion curve. The adhesion curve in damp condition is not just a linear interpolation between the adhesion curve observed in dry condition and the adhesion curve observed in wet condition.

Adhesion values as low as 0.06 have been observed in a tram wheel test rig experiment at high creep at a water rate of 25 µl/s solely due to the presence of wear debris and water in the contact.

An engineering tool (WILAC model) has been developed which predicts the effect of water on wheel/rail adhesion in the whole range of conditions from dry over damp to wet. Main emphasis has been put on damp contact conditions.

WILAC model results agree with existing locomotive test data from literature in dry and wet conditions.

8.8. Acknowledgements

This work was funded by the Rail Safety and Standards Board (RSSB) and Network Rail within the project T1077.

8.9. References

Arias-Cuevas, O., Li, Z., Lewis, R. and Gallardo-Hernandez, E.A., 2010, “Laboratory Investigation of some Sanding Parameters to Improve the Adhesion in Leaf Contaminated Wheel-Rail Contacts”, Journal of Rail and Rapid Transit, Proceedings of the IMechE Part F, 224, pp. 139-157

Beagley, T.M. and Pritchard, C., 1975, “Wheel/Rail Adhesion -- The Overriding Influence of Water”, Wear, 35, pp. 299-313

Beagley, T.M., 1976, “The Rheological Properties of Solid Rail Contaminants and their Effect on Wheel/Rail Adhesion”, Proceedings of the Institution of Mechanical Engineers, 190, pp. 419-428

Cann, P.M., 2006 “The ‘leaves on the line’ problem - a study of leaf residue film formation and lubricity under laboratory test conditions”, Tribology Letters, 24, pp. 151-158

Chen, H., Ban, T., Ishida, M. and Nakahara, T., 2002, “Adhesion between rail/wheel under water lubricated contact”, Wear, 253, pp. 75-81

Chen, H., Ishida, M. and Nakahara, T.,2005, “Analysis of adhesion under wet conditions for three-dimensional contact considering surface roughness, Wear, 258, pp. 1209- 1216

Gallardo-Hernandez, E.A. and Lewis, R., 2008, “Twin Disc Assessment of Wheel/Rail Adhesion”, Wear, Vol. 265, pp. 1309- 1316

Li, Z., Arias-Cuevas, O., Lewis, R. and Gallardo-Hernández, E.A., 2009, “Rolling-Sliding Laboratory Tests of Friction Modifiers in Leaf Contaminated Wheel-Rail Contacts”, Tribology Letters, 2009, 33, No. 2, pp. 97-109

Meierhofer, A., 2015, “A new Wheel-Rail Creep Force Model based on Elasto-Plastic Third Body Layers”, PhD Thesis, Graz University of Technology, Austria

Olofsson, U. and Sundvall, K., 2004, “Influence of leaf, humidity and applied lubrication on friction in the wheel-rail contact: pin-on-disc experiments”,

Proceedings of the Institution of Mechanical Engineers, Part F: Journal of Rail and Rapid Transit, 218, pp. 235-242

Polach, O., 1967, “Creep forces in simulations of traction vehicles running on adhesion limit, Wear, Elsevier, 2005, 258, 992- 1000

J. J. Kalker, On the Rolling Contact of Two Elastic Bodies in the Presence of Dry Friction”, Delft University of Technology

Polach, O., 1999, “A fast wheel-rail forces calculation computer code”, Proc. of the 16th IAVSD Symposium, Pretoria, August 1999, Vehicle System Dynamics Supplement, 33, pp. 728-739

Popovici, R., 2010, “Friction in Wheel - Rail Contacts”, University of Twente, Enschede, The Netherlands

Rail Safety and Standards Board (RSSB), 2014, “T1042: Investigation into the effect of moisture on rail adhesion.” Project Report

Six, K., Meierhofer, A., Müller, G. and Dietmaier, P., Physical processes in wheel-rail contact and its implications on vehicle-track interaction, Vehicle System Dynamics: International Journal of Vehicle Mechanics and Mobility, 53, pp. 635–650

Spiryagin, M., Polach, O. and Cole, C., 2013, “Creep force modelling for rail traction vehicles based on the Fastsim algorithm”, Vehicle System Dynamics: International Journal of Vehicle Mechanics and Mobility, 51, pp. 1765-1783

Stachowiak, G.W. and Batchelor, A.W., 2006, “Engineering Tribology”, Butterworth-Heinemann

Tomberger, C., 2009, “Der Rad-Schiene Kraftschluss unter Berücksichtigung von Temperatur, fluiden Zwischenschichten und mikroskopischer Oberflächenrauheit”, Technische Universität Graz

UIC 544-1:2004 Bremse - Bremsleistung, International Union of Railways

Vasic, G., Franklin, F., Kapoor, A. and Lucanin, V., 2008, “Laboratory simulation of low-adhesion leaf film on rail steel”, Int. J. Surface Science and Engineering, 2(1/2), pp. 84–97

Vollebregt, E.A., 1982, “Numerical modeling of measured railway creep versus creep-force curves with CONTACT, Wear, 2014, 314, 87-95 J. J. Kalker, A Fast Algorithm for the Simplified Theory of Rolling Contact”, Vehicle System Dynamics, 11, pp. 1-13

Voltr, P. and Lata, M., 2015, “Transient wheel–rail adhesion characteristics under the cleaning effect of sliding”, Vehicle System Dynamics, 53, 605-618

White, B.T., Fisk, J., Evans, M.D., Arnall, A.D., Armitage, T., Fletcher, D.I., Nilsson, R., Olofsson, U. and Lewis, R., 2006, “A Study into the Effect of the Presence of Moisture at the Wheel/Rail Interface during Dew and Damp Conditions”, submitted to Journal of Rail and Rapid Transit, Proceedings of the IMechE Part F

9. Investigation of the isolation and frictional properties of hydrophobic products on the rail head, when used to combat low adhesion

S.R. Lewis[1], L.E. Buckley-Johnstone[1], P. Richards[2], R. Lewis[1]

[1]Department of Mechanical Engineering, The University of Sheffield, Sheffield, UK
[2]Network Rail, Milton Keynes, UK

Published in *Wear, Volume 314, Issues 1–2, 2014, Pages 213–219.*

Abstract

Low adhesion affects rail networks around the world. A recent unpublished study by Network Rail has shown a strong correlation between low adhesion incidents and the occurrence of the dew point. It is hypothesised that at or below the dew point water vapour from the air condenses onto the rail head forming a fluid film that leads to a loss of traction within the wheel/rail contact. It has been proposed that this formation of dew on the rail could be prevented by treating rails with commercially available hydrophobic products. In this work laboratory based trials of the hydrophobic products were carried out in order to test their suitability for field use. Traction and impedance properties of the products in a twin disc wheel/rail contact simulation were compared with dry and pure water conditions. Tests were also carried out using a pendulum friction measurement device with the products applied to a rail head. At present there is not a convincing case for applying hydrophobic products to help reduce low adhesion incidents, but pendulum tests with a layer of moisture applied to a dried product film indicated that an increase in friction over moisture on a clean rail may be possible.

9.1. Introduction

Low adhesion presents a major concern for many rail operators. Railway vehicles under these circumstances can experience a serious loss of braking capability giving rise to dangerous situations such as platform overruns and signals passed at danger. An unpublished study by Network Rail and a train operator has highlighted that there is a correlation between adhesion loss events (indicated by the activation of a train's wheel slide protection system for long periods of time) and the occurrence of the dew point. The dew point is defined as the temperature at which the air, at a given relative humidity, becomes fully saturated and water vapour will start to condense into liquid water. Beagley (1975a) observed that friction was reduced during laboratory tests when the ambient relative humidity became so high that water would condense onto the test surfaces. It is thus hypothesised that at the dew point water will condense onto the rail and this could contribute towards adhesion loss. Commercially available hydrophobic products can form a water repulsive layer on some surfaces. Hydrophobic products are often based on lipophilic substances (oils and greases) to act as the water repellant. However, other

produces use silicone and fluorocarbons to act to repel the polar water molecules that may be more suitable in this context (RSSB, 2013). The products tested in this work are used to build a hydrophobic layer on car windscreens. Thus treatment of rail with these hydrophobic products may prevent the formation of dew on the rail head. The frictional and isolation properties of two commercially available hydrophobic products were assessed in this work. The two aims of this research were to determine, through laboratory testing, that safe levels of traction/friction are maintained and acceptable levels of impedance for track circuit shunting occurs when these products are introduced between the wheel and rail. Further to the twin disc testing, a comprehensive study has been taken using a pendulum tester to assess the effects the hydrophobic fluids have on the rail head adhesion and water settlement. The pendulum tester has been previously used as an alternative to a traditional push tribometer (Lewis, 2011; Lewis, 2013). The tester allows rapid, repeatable and easily controllable testing so various conditions can be investigated.

9.2. Test methodology

9.2.1. Twin disc test

This study was carried out using the University of Sheffield Rolling Sliding (SUROS) rig (Fletcher, 2000). Figure 1 shows a schematic of the SUROS rig and the discs typically used. For these tests a nominal speed of 400 rpm was used with 3% creep in the contact and a maximum contact pressure of 1200 MPa. Typical dry running slip in normal conditions can be anywhere up to 1%, thus a 3% slip for testing was thought to be representative of a wheel approaching low adhesion conditions (see previous work on the rig in which creep curves were determined for various types of third body material (Gallardo-Hernandez, 2008)).

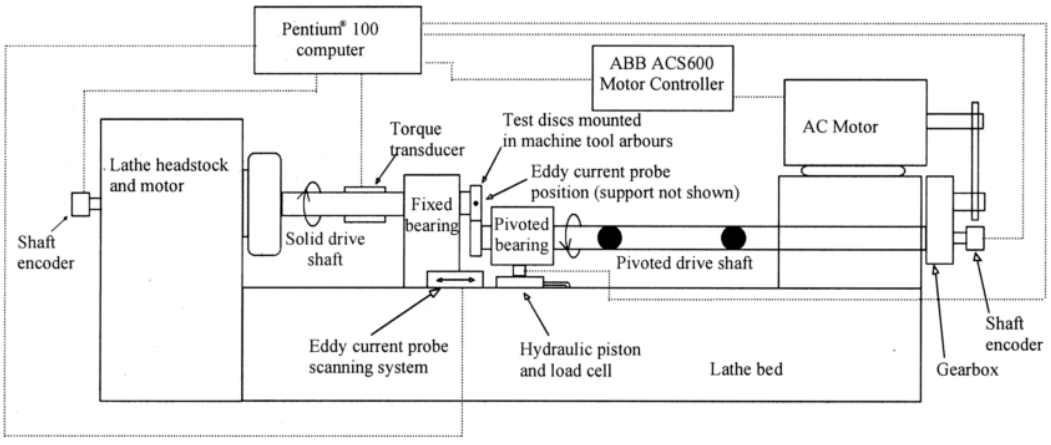

Figure 1: Schematic representation of the SUROS rig

A representation of the TI21 track circuit was used to measure impedance changes caused by the product. The circuit passed a current of 1 Amp through the twin-disc contact at 2 kHz and 50 Hz; representative of two circuit frequencies used on the UK rail network. This circuit has been used in previous work (Lewis, 2003; Lewis, 2006; Lewis, 2011). The two hydrophobic

products were diluted in de-ionised water and dripped onto the discs at a rate of 1 drip per second, which was enough to keep the contact flooded. A baseline purewater test was also run. The tests were split into two parts:

- (1) The test was started and a dry coefficient of traction was reached. At this point the diluted product was dripped into the contact for 2000 cycles to allow a hydrophobic layer to build on the discs. After 2000 cycles the profiles of the discs were measured.
- (2) The test was then re-started with dripping of diluted product for 500 cycles. At this point the dripping of the product was stopped and the test was run until a dry traction level had been reached.

Initially the discs were run dry to condition them and ensure that the product was placed onto a similar surface every time. Dripping of the product was then started to simulate the product being applied to the rail and rolled over by a train. A period of 2000 cycles was considered long enough for a layer of hydro- phobic product to build on the surface. The test was then stopped so that the surface of the discs could be examined by measuring their surface roughness. The test was then re-started under the dripping of the diluted product for 500 cycles so that the disc surfaces could return to the condition that they would have had before the test was stopped. After 500 cycles the dripping of the product was stopped. This part of the test was designed to see how the product was removed from the contact.

The products were tested at three different concentrations: each at their manufacturers' recommended dilutions, which were 4 and 5% for product A and B respectively, and both at 2 and 3%.

9.2.2. Pendulum test

The pendulum test rig, shown in Figure 2, has been traditionally used to assess slip resistance levels on different flooring and in cases of accidents. However, more recently it has been applied to the assessment of friction levels found on the rail head (Lewis, 2011; Lewis, 2011). The rig is designed to measure the loss in energy resulting from a finite sliding contact between a pad (part E in Figure 2) and a horizontal contact surface placed at the mid-point of the pendulum's swing (bottom middle of Figure 2). This loss of energy is read from a scale and is subsequently converted to a level of friction in the contact (more details can be found in BS 7976-1:2002).

The pendulum was used to test the two hydrophobic solutions in 4 different conditions at two different dilutions. The conditions shown in Table 1 were chosen. The pendulum test rig was set to contact over the marked out area on the rail head. A new rubber Slider 96 pad was used (previously known as the Four S; properties and characteristics remain the same). A set contact length of 127mm was used. There are in total 19 different rail head conditions, each condition was tested a total of 10 times to give an average slip resistance value (SRV) and subsequent coefficient of friction.

A common garden spray bottle containing the liquid was used to spray the made up fluid onto a marked out area on the rail surface. The number of complete sprays was kept the same to ensure the same amounts of fluid were being sprayed.

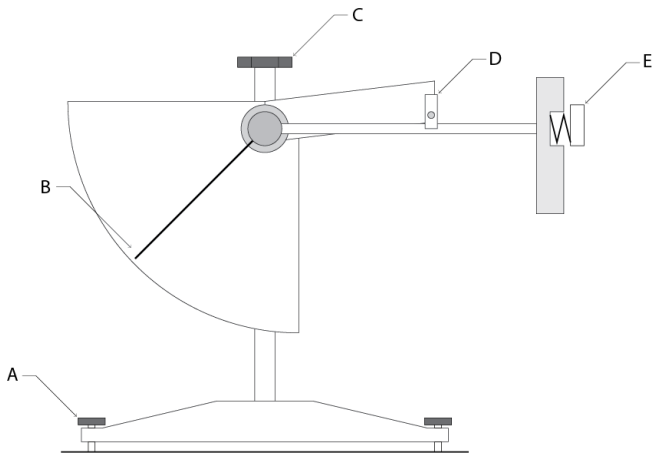

Figure 2: Pendulum test rig schematic. A) Adjustable feet; B) Pointer; C) Height adjuster; D) Release catch; E) Slider pad

Conversion of the SRV, read from the point reached by the pendulum post contact, into a coefficient of friction value is achieved through the use of Equation 1. Full details of the derivation of this equation can be found in BS 7976-1:2002.

$$\mu = \left(\frac{110}{SRV} - \frac{1}{3}\right)^{-1} \quad (1)$$

where, μ is the coefficient of friction, and SRV is the slip resistance value as measured from the scale on the pendulum.

A simple test procedure was followed for all sets of rail treatments, with the application of water from a second spray bottle being to simulate rainfall post application of hydrophobic liquids. An ultrasonic humidifier was used to treat the rail head to generate a “moist” condition – that which represents the dew point of fog conditions.

The rail was mounted onto a bench at room temperature and humidity with the pendulum rig set up over it. Masking tape was used to mark out the area for analysis (the area was set to that of the test area needed for the pendulum tester). The following steps were then taken:

1. Dilution to be tested was made up and put into the spray bottle (400 ml total)
2. Rail head cleaned with acetone.
3. Area on rail was sprayed from a set distance
4. Image was taken using camera at a set cure time
5. Pendulum was released and energy loss was measured.
6. Pendulum foot was wiped down and experiment reset.

Three different tests were carried out on the rail untreated, and four carried out for each dilution of the two products. Two dilutions were chosen to be tested; 2% and 4%. The four test conditions were: **Wet** - the product sprayed onto the rail head; **Dry** - the product sprayed onto the rail head and dried out with a heater; **Re-wet** - the product sprayed onto the rail head, dried out with a heater and then water applied; and **Moist** - the product sprayed onto the rail head, dried out with a heater and water directed at the rail head via a hose from a ultrasonic humidifier for 10 seconds. For the clean rail the wet tests

were with water from the humidifier only. All applications of the dilutions were from a set distance of 30 cm from the rail head.

9.3. Results

9.3.1. Twin disc results

Friction results from the water baseline test can be seen in Figure 3. The key for this and the following charts is as follows:

- a = Dripping of diluted product or pure water for 2000 cycles
- b = Test re-started under wet conditions with water/diluted product dripped for 500 cycles
- c = Dripping stopped and allowed to reach dry friction.

What is striking here is the amount of time taken (1500 cycles) between stopping the water (at the end of section b/start of section c) and the traction reaching a dry level. It was witnessed during this particular period of the tests with pure water that a black liquid was clinging to the edges of the disc. This is similar to what was seen by Beagley during laboratory tests (Beagley, 1975b), however, friction coefficients as low as 0.05 were reported in their experiments.

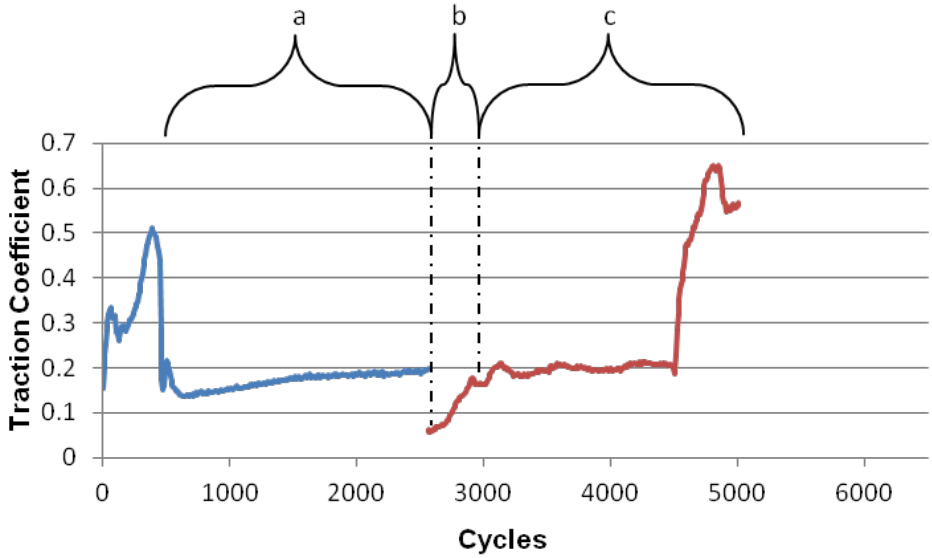

Figure 3: **Pure water baseline traction curves.**

Figures 4 to 7 show the traction curves for products A and B at their maximum and minimum tested concentrations.

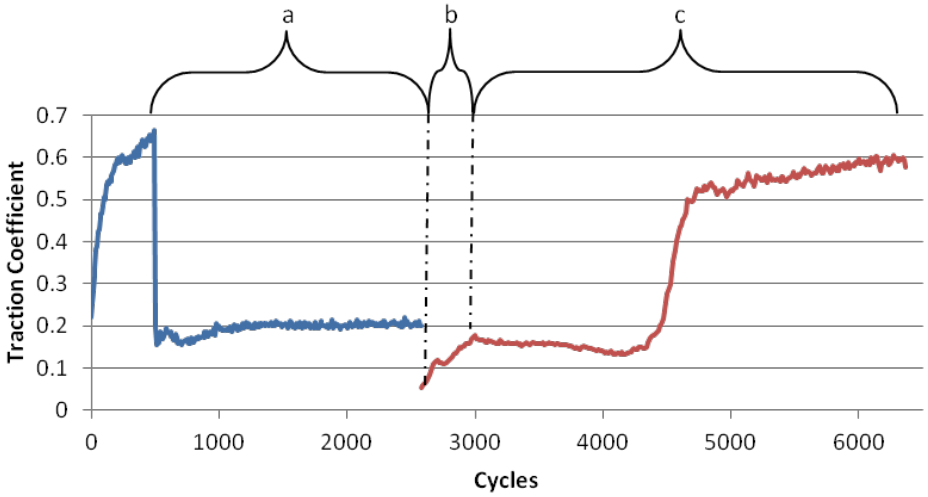

Figure 4: **Product A, at 4% concentration traction curves.**

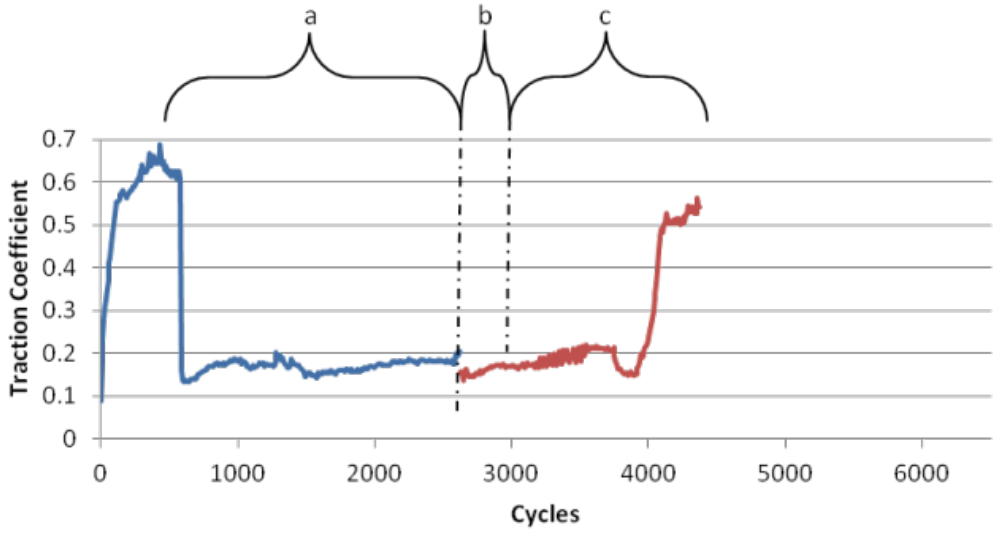

Figure 5: **Product A at 2% concentration traction curves.**

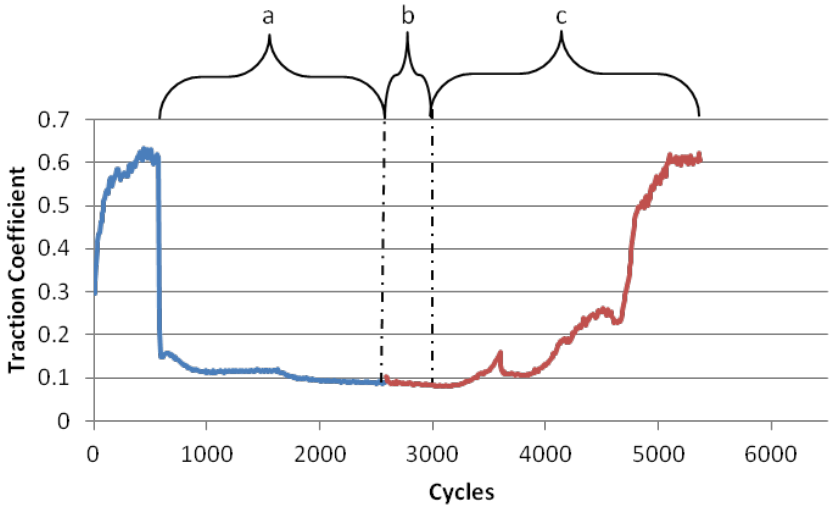

Figure 6: **Product B at 5% concentration traction curves.**

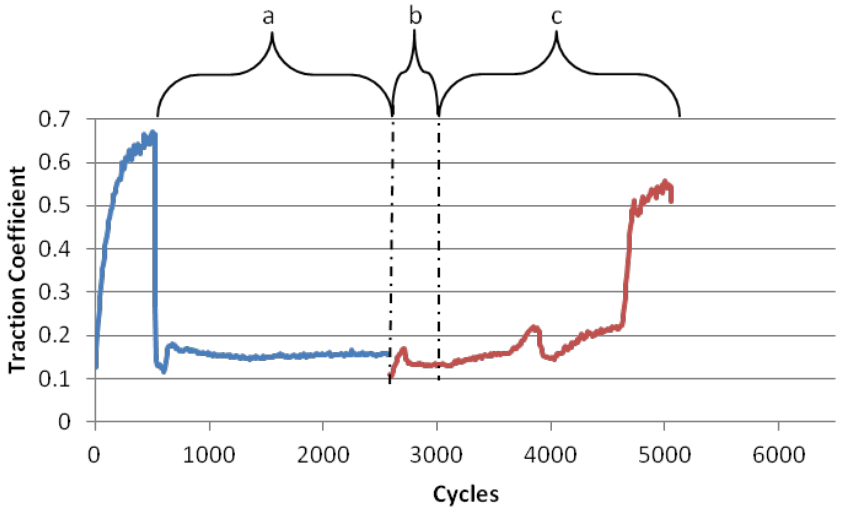

Figure 7: **Product B at 2% concentration traction curves.**

Note how the test with diluted hydrophobic products show the same tendency for the traction to stay low long after the dripping of the product was stopped (start of section c) as was seen with pure water. The sharp upturn in traction is not as sudden when the diluted products are used as it is with pure water. It also seems that the higher the concentration of hydrophobic product used the more gradual the friction rise during section c. Figure 8 shows average traction coefficients yielded from the tests.

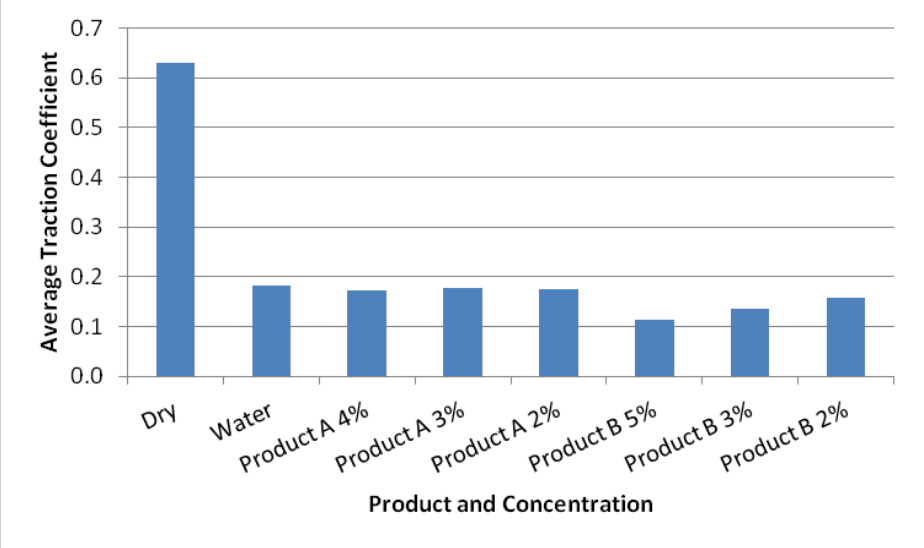

Figure 8: **Average traction levels yielded from the tests.**

Product A seems to yield a traction coefficient close to that of pure water which shows little dependency on concentration. The traction coefficient seen with Product B is lower than that of water alone, but seems to be dependent on concentration.

Figure 9 shows impedance data for all of the tests showing the average dry, wet and hydrophobic products at circuit frequencies of 50Hz and 2kHz. These impedance levels are below the Network Rail threshold of 5Ω above which track circuit isolation becomes an issue.

As can be seen from Figure 9 the strongest relationship between circuit frequency and impedance was shown with product B with higher impedance levels at the lower circuit frequency, however, no correlation was seen between product concentration and impedance at this circuit frequency. Product B also showed an inverse relationship at the higher circuit frequency between product concentration and impedance level. Almost the reverse was seen with product A as it showed little dependence between product concentration and impedance at the highest frequency and a strong positive correlation between impedance and product concentration at the lower frequency. It would be expected that the dilute products would show different impedance levels at different circuit frequencies, because the products are introducing electrolytes to the contact that will have the effect of creating a capacitive reactance in the AC track signal circuit. The test with product A at 2% concentration was the only test with product to show lower impedance at the lower frequency. The difference in impedance for this test is small, however, at only 0.023 Ω. Little correlation of impedance with circuit frequency was shown for dry or pure water conditions.

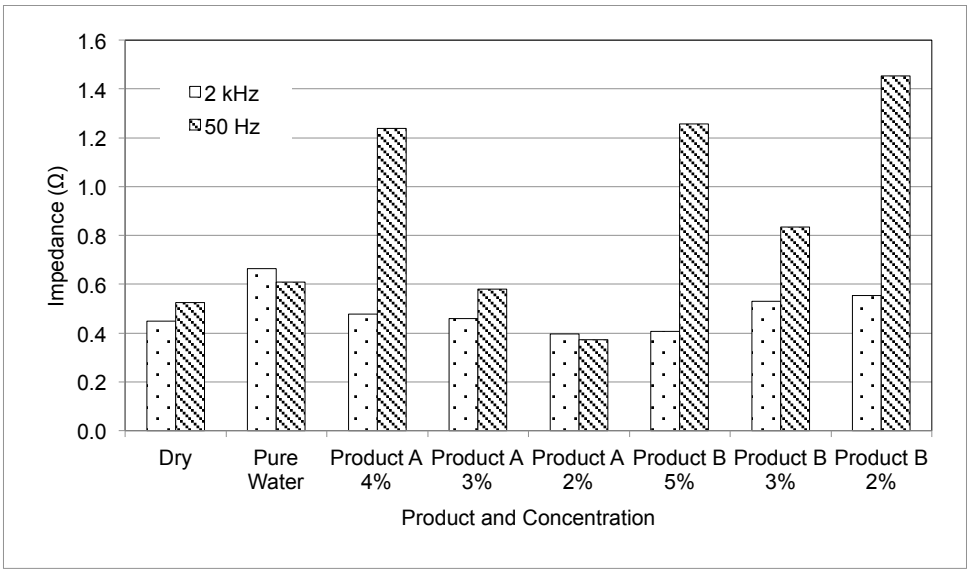

Figure 9: Impedance data from SUROS tests.

9.3.2. Pendulum results

Average values of the coefficients of friction and SRVs are given in Table 1, and are graphically given in a bar chart in Figure 10. Standard deviation error bars are shown.

Table 2: Average SRV and Coefficient of Friction values taken in pendulum testing.

Condition	Measurement	Clean	2%		4%	
			Product A	Product B	Product A	Product B
Wet	SRV	16	11.5	14.2	9.5	13.5
	COF	0.15	0.11	0.13	0.09	0.13
Dry	SRV	57	71.2	65.4	82	68.5
	COF	0.63	0.83	0.74	0.99	0.79
Rewet	SRV	n/a	10.1	12.1	9.6	13.5
	COF	n/a	0.09	0.11	0.09	0.13
Moist	SRV	13.4	16.5	32.6	23	23.6
	COF	0.13	0.16	0.35	0.23	0.24

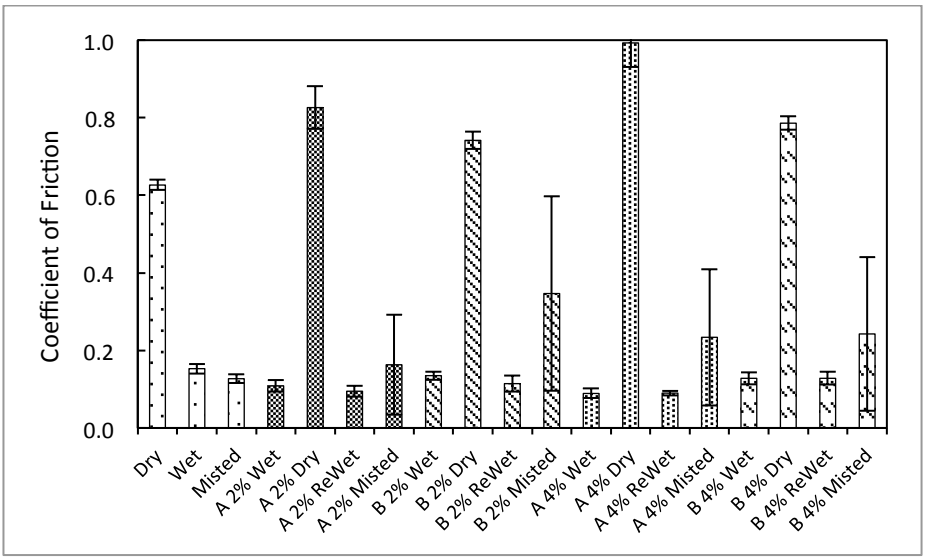

Figure 10: **Average coefficients of friction data from pendulum testing, with standard deviation error bars.**

Untreated tests

Dry tests were run to establish a baseline figure that should be met on each day of testing to ensure consistency in results. The initial dry control value was 0.63, which varied by +/-0.05 over the days of testing. The wet result showed variation of the coefficient of friction between 0.17 and 0.13, with an average of 0.15, which showed good overall consistency. For the wet result, two full pumps of a spray bottle were used. As the results showed good consistency it was decided that the amount of water being deposited on the rail was consistent for experimentation purposes.

Hydrophobic products - wet

For these tests the dilutions of products were made up and placed into the spray bottle. The number of sprays of the water bottle was kept the same as those used to cover the rail in the product. The experiment was carried out immediately after the water had settled onto the rail head. Figure 11, comparison of the different dilutions of hydrophobic products tested in wet conditions, shows that both products have an effect on the adhesion level, with the more concentrated in each case lowering the friction levels more than just wet levels. This was particularly the case for product A at 4% where an average coefficient of friction of 0.09 was found.

Attempts were made to assess “hydrophobicity” of the products by characterising the dispersion of water on dried layers on the rail head, but this proved difficult. It was noted that the water would tend to settle in various and sporadic ways throughout the repeats of any particular test with the different dilutions and no clear trend could be observed.

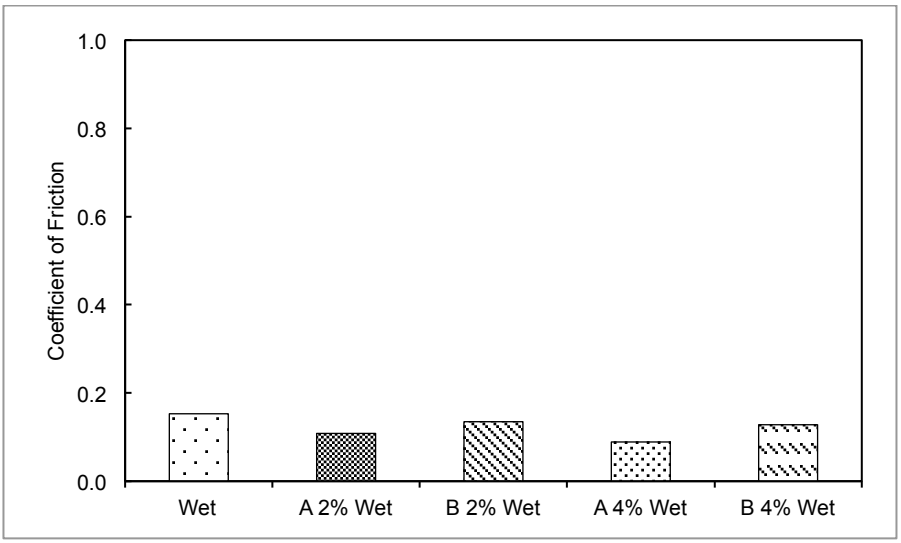

Figure 11: **Average coefficients of friction data from pendulum testing, comparing each product in "wet" conditions.**

Hydrophobic products – dry

The diluted product mixtures were then sprayed onto the cleaned rail surface and dried out using a heat lamp. This was to bring the variance in drying times down, as the variation in the natural light conditions had a marked effect on drying time, which altered the visible oxidation on the rail head. Once the mixture was dried on the rail head, the experiment was run. It was found that the products left some patchy residue on the surface of the rail and this would increase the level of adhesion between the rubber pad and steel.

The adhesion level was particularly increased with the increase in concentration of product/water mixture, as seen in Figure 12. Product A showed higher coefficients on both dilutions, than that of product B, with product A at 4% increasing the adhesion to an average level of 0.99, which is much higher than that of the clean rail.

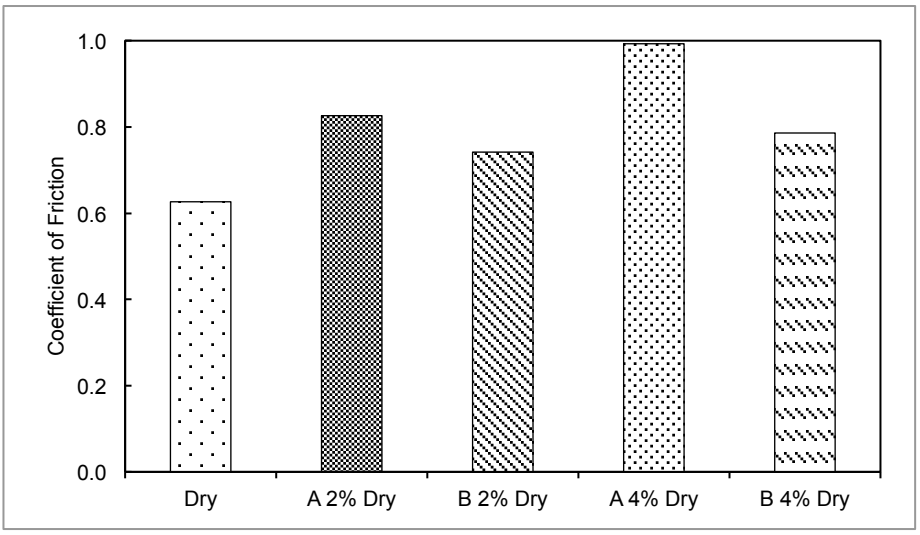

Figure 12: **Average coefficients of friction data from pendulum testing, comparing each product in "dry" conditions.**

Hydrophobic products – rewet

The rewet test was much like the dry test, only water was applied to the rail head to look at whether the products were aiding in dispersing a water film. The volume of water sprayed was the same as the sprayed volume of the hydrophobic mixture prior to drying.

From Figure 13 it can be seen that the reapplication of water onto the rail head with dried out hydrophobic solution reduces the adhesion at the rail head. Coefficient of friction values similar to those from a wet product were seen. It is possible that the applied water was dissolving the layer creating a mixture like that used in the wet tests.

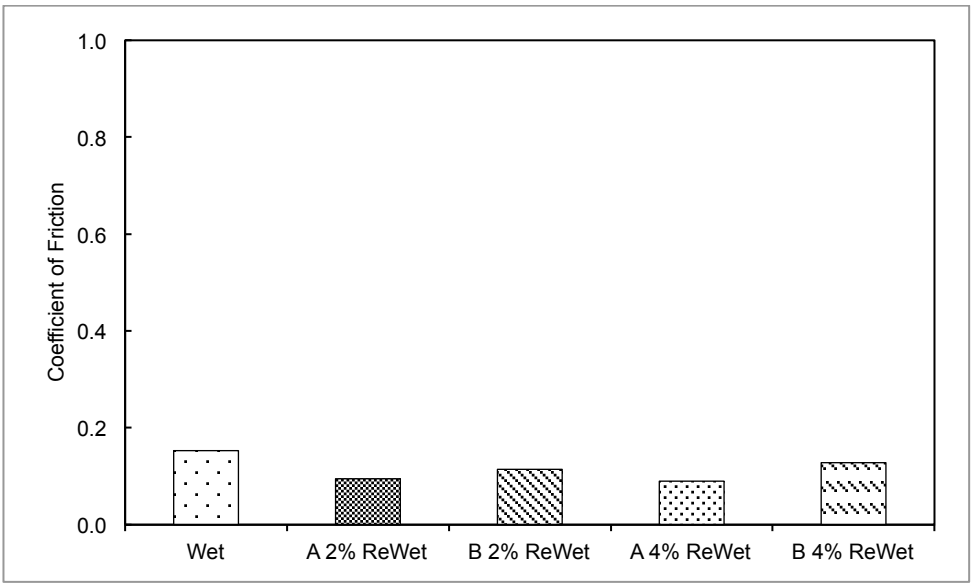

Figure 13: **Average coefficients of friction data from pendulum testing, comparing each product in "rewet" conditions.**

Hydrophobic products – moist

For the moist experiments an ultrasonic humidifier was used to deposit small amounts of water mist onto the rail head post application of each hydrophobic product which had dried. A pipe ran from the humidifier and was directed at the rail head for 10 seconds immediately prior to running the experiment.

From Figure 10, the friction value for the misted clean rail was slightly below that of the wet rail. This condition, with only a small amount of water deposited on the rail is the closest representation to that of the dew point condition. It produced friction values as low as 0.11.

Moist tests on the dried product films shown in Figure 14 include minimum and maximum values of friction. For product A, both dilutions produced values as low as 0.09. Data though shows that the product layer may have a positive effect and increase friction over a clean moist rail head surface. However, there is a large spread in results. It is possible that this may have been due to some residual warmth in the rail from the drying process. The effect of temperature needs further examination.

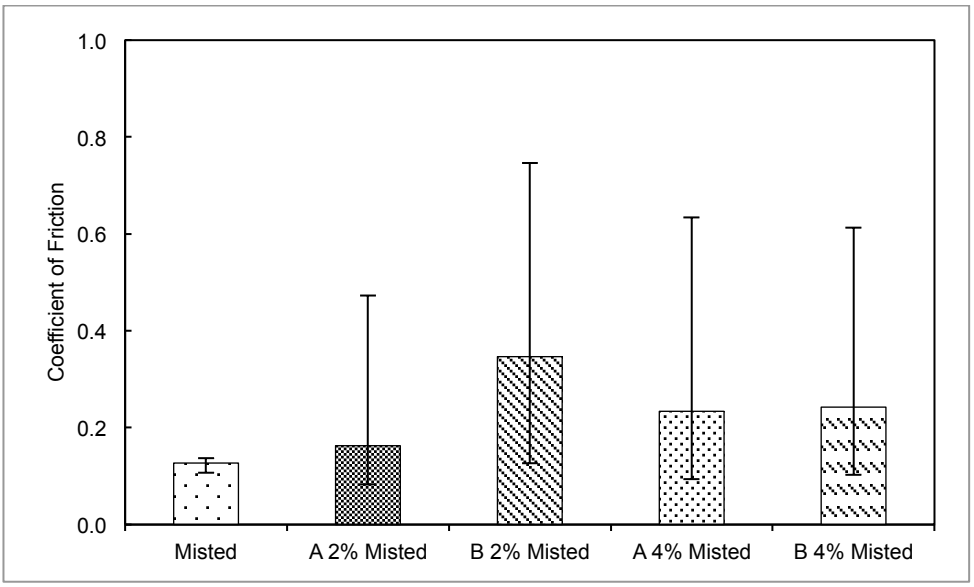

Figure 14: **Average coefficients of friction data from pendulum testing, comparing each product in "misted" conditions.**

9.4. Discussion

Laboratory tests with diluted commercially available hydrophobic products were performed in order to assess the traction and impedance performance of these products when used in the wheel/rail contact.

9.4.1. Twin disc testing

Traction levels obtained using product A were in line with that of pure water and showed little dependency on dilution. The traction coefficient measured for pure water was 0.18 and the coefficient measured for product A ranged between 0.17 – 0.18. Trains can function adequately on a wet track without any traction issues hence product A is thought to be fine for use in the field based on these measured traction properties. Traction levels obtained with product B showed an inverse relationship between traction coefficient and dilution. At the maximum concentration (manufacturer's recommended) it showed a traction coefficient of 0.11 and at its lowest concentration yielded a coefficient of 0.16. It seems that product B is introducing some traction reducing properties to the wheel/rail contact which lowers the traction below that of pure water. This effect is not seen as strongly with product A.

Dry and pure water tests showed little dependence between circuit frequency and impedance. This was not the case for the majority of tests with the diluted products. Product B displays a relationship of increasing impedance with decreasing solution at the higher frequency of 2kHz suggesting that as more of it is introduced into the contact it reduces resistance between the wheel and rail at 2kHz. At this higher frequency product A seems to show the opposite in that the more of it there was in the contact (i.e. higher concentration) the higher impedance. At the higher frequency the dilution of both products in water reduced the impedance compared to water alone. This was not true for product B at the lower frequency which showed an increase

in impedance compared to pure water. Product A on the other hand only showed an increase in impedance at 50Hz at a concentration of 4%.

The highest impedance shown by product A was 1.2 Ω at a frequency of 50Hz. This was at the manufacturer's recommended dilution of 4%. At the same concentration and a circuit frequency of 2kHz product A showed an impedance of 0.48 Ω. The highest impedance shown by product B was 1.45 Ω at 50Hz and 0.55 Ω at 2kHz. These were shown at product B's lowest concentration of 2%. Even though these impedance levels are below the Network Rail track circuit shunting level of 5Ω it is important to note that these laboratory based measurements cannot be translated directly into the field. This is because of the relative scale of the contact patch in either case. It is therefore more important that these measured values be used as a comparison between products.

The traction coefficients measured in these tests (0.19 while the black liquid was seen) and by Beagley & Pritchard (1975b) (between 0.15 and 0.3 while the viscous paste was witnessed), are not considered low enough to impede braking. However, as previously stated results from the lab cannot be directly translated into the field and therefore friction coefficients in the field could fall to unsafe levels. Also note from Figure 3 at the beginning of section 3 the traction coefficient is very low at 0.06, it does, however, rise to 0.2 within 500 cycles just as the water dripping is stopped. A coefficient of friction of 0.05 was reported by Beagley (1975b) when water mixed with Fe_2O_3 was added to the contact. It may be that in the field this low level of friction is maintained for longer because of the difference between the laboratory based twin-disc methods and the real life wheel/rail contact. In a twin-disc test the same area is being slid over in quick succession whereas in the real wheel/rail contact, on the leading axle at least, fresh rail comes into contact with the wheel. These differences must also be taken into account when comparing what is seen in the laboratory and the field.

9.4.2. Pendulum Testing

It was found that both products had an effect on the adhesion levels between the rubber pad and the rail head under all conditions tested. From Figure 10 it can be seen that both products at both concentrations when applied to the rail head would reduce friction levels below that of pure water to coefficient of frictions levels around 0.10. This level is low, but as it is a rubber on steel contact it can only be said that this product would reduce adhesion, not that the product would reduce adhesion to this exact level in the actual wheel-rail contact. Having said this, the matchup between the friction values found in the twin disc testing and the pendulum testing is rather good, with the same trends being found; water alone giving highest level of friction, product A giving higher levels of friction than product B, and product B at the highest concentration giving the lowest levels of friction for the comparative tests.

The hydrophobic products used in the tests have been specifically designed for use on windscreens, with a solvent to cut through and remove any contamination that can be found on these, such as bug residue. From purely visual inspection, there was little noticeable difference in the hydrophobicity of the steel before and after treatment. Product A when sprayed onto the rail head often produced a film, rather than water droplets, whilst steel that was

sprayed with just water would have water droplets forming. It is therefore difficult to attribute the change in levels of adhesion to the change in hydrophobicity at the rail head due to the treatment with either of these products, rather than just the products themselves being friction modifiers. With a moist layer applied to a dry film of product, an increase was seen in friction levels, but there was a high level of scatter.

9.5. Conclusions

This paper summarises an assessment of the suitability of two commercially available hydrophobic products for use in addressing low adhesion levels which occur in water-contaminated wheel-rail contacts. The test program also provided some insights into the mechanics of this low adhesion phenomenon.

- Traction levels obtained with product A seem to be in a safe operating range under all dilutions.
- At the manufacturer's recommended dilution product B showed a low traction coefficient sometimes below the safe limit for braking and traction, which is considered to be 0.1.
- A black liquid was witnessed during the second part of the pure water test after the water supply was stopped. This liquid kept the traction at approximately 0.2 (see Figure 3). This liquid seemed to disappear from the disc surface very rapidly and as this happened the friction almost instantaneously started to rise toward dry levels. It is thought that the liquid may be mixed with an oxide which acts as a solid lubricant as the contact initially dries, before being removed.
- Impedance levels seen with the hydrophobic products were below the Network Rail threshold.
- Pendulum friction values from testing on an actual rail head were in agreement with the twin disc values. With a layer of moisture (that perhaps best represents the dew point condition) a dried film of product did increase friction over a moist clean rail head. This, however, needs further investigation as there was considerable scatter in the data, likely due to temperature sensitivities.
- In some cases the hydrophobic solutions degraded the adhesion conditions compared to a purely wet or untreated surface. At higher concentrations in the SUROS tests of product B, the adhesion is almost half that of the equivalent went test in the initial phased (0.1 from 0.2). Although this value is not in the ultra-low adhesion range it should still be considered that this product may actual caused low adhesion when applied – exactly the problem it is intended to treat.
- At present there is not a convincing case for applying hydrophobic products to help reduce low adhesion incidents, but the moist layer effects need further investigation. Another aspect that needs consideration is the role the hydrophobic liquids may play in suppressing oxide formation. Water alone is probably not enough to cause low adhesion problems. As noted by Beagley (1976), solid material is required, which at the dew point could be the oxide that the water film on the rail head creates.

9.6. References

Beagley, T.M. and McEwen, I.J. and Pritchard, C., 1975a, “Wheel/rail adhesion-boundary lubrication by oily fluids”, Wear, 31, pp. 77-88.

Beagley, T.M., Pritchard, C., 1975b, “Wheel/rail adhesion – The overriding influence of water”, Wear, 35, pp. 299 -313.

Beagley, T.M., 1976, “The rheological properties of solid rail contaminants and their effect on wheel/rail adhesion”, Proccedings of the Institute of Mechanical Engineers, 190, pp. 419-428

BS 7976-1:2002, Pendulum Testers: Part 1 – Specification.

Fletcher, D.I. and Beynon, J.H., 2000, “Development of a machine for closely controlled rolling contact fatigue and wear testing”, Journal of Testing and Evaluation, 28, pp. 267-275.

Gallardo-Hernandez, E.A. and Lewis, R., 2008, “Twin Disc Assessment of Wheel/Rail Adhesion”, Wear, 265, pp. 1309-1316.

Lewis, R., Dwyer-Joyce, R.S. and Lewis, J., 2003, “Disc machine study of contact isolation during railway track sanding”, Journal of Rail and Rapid Transit Proceedings of the IMechE Part F, 217, pp. 11-24.

Lewis, R. and Masing, J., 2006, “Static Wheel/Rail Contact Isolation due to Track Contamination.” Journal of Rail and Rapid Transit Proceedings of the IMechE Part F, 220, pp. 43-53.

Lewis, S.R., Lewis, R. and Olofsson, U., 2011a, “An alternative method for the assessment of rail head traction, Wear 271, pp. 62-70.

Lewis, R., Gallardo, E.A., Cotter, J. and Eadie, D.T., 2011b, “The effect of friction modifiers on wheel/rail isolation”, Wear, 271, pp. 71-77.

Lewis, R., Lewis, S.R., Zhu, Y. and Olofsson, U., 2013, “The modification of a slip resistance meter for measurement of rail head adhesion”, Journal of Rail and Rapid Transit, Proceedings of the IMechE Part F. 227, pp. 196-200.

Rail Safety and Standards Board (RSSB), 2013, “Hydrophobic additives for rail sand (S136)” Project report.

10. Discussion

10.1. Adhesion measurements with third body materials

Throughout this thesis the main theme connecting all 7 papers is wheel/rail contact testing of third body layers with a particular focus on the measurement of adhesion. The driving and steering forces are produced through the steel-on-steel contact. As both contacting bodies are in an open system, the point of contact is rarely, if ever, an uncontaminated. Measurement of adhesion using laboratory testing, especially in the presence of third body materials, improves the understanding of vehicle-track interaction to better characterise and represent conditions in the field.

As with all laboratory testing there are limits when conducting scaled testing and selection of appropriate test methods becomes critical. There is a trade-off between control and realistic representation. For example, a field test is fully representative of the contact, but both measurement and control of the third bodies within the contact becomes drastically more difficult - if not impossible - than laboratory based tests. Even in laboratory based testing, the degree of control can vary between test method used.

Each test method has different limitations that need to be considered when designing an experiment. Paper 2 compares the difference in adhesion measurement from a full-scale test to that of a twin disc test. Both tests exhibited the similar development characteristics, but the length of time (number of cycles) differed considerably. The test scales have gone fully representative of an actual wheel/rail contact in terms of geometry and contact pressures/stresses, to pendulum test using a line contact with a harden rubber pad. These two are at the extreme ends of testing scales, with the other test methods using in this thesis falling between these.

The degree of scaling required is highly dependent on the intentions and requirements from a test. The degree of scaling will impact how representative of a wheel/rail contact the test is terms of shape or contact pressure and realistic entrainment or velocities. A Stribeck curve, which shows the fluid effects on friction in terms of load n, velocity V and contact length l is useful in highlighting the influence of scaling when testing with third bodies. This influence the lubrication regime the third body is subjected to is dependent on the ratio of (nV/l).

The entrainment of the third body layer into contact has an effect on the adhesion. The rolling/sliding nature of the wheel/rail contact has an important role in third body materials entering the contact. In small scales of testing, where there is zero roll motion, there is a limit when testing with some third body materials that require replenishment within the contact. For example, in the Paper 4 HPT testing the third body layer was sheared exposing steel, which increased adhesion, without being replaced. In the case of a rolling contact, at the leading edge a fresh supply of water/oxide mixture will be entrained into the wheel/rail contact.

The velocity capabilities of laboratory tests rig used in this thesis do not cover the range of velocities as found on the UK network (0-120 mph). However, the rigs have been sufficient for the current studies. A comparison between WILAC model, which uses experimental inputs, and field tests showing extrapolation from 5 m/s tests up to 20 m/s with good correlation.

The type of data required from testing is important when deciding on a test method. In many cases a small scale test will be more suitable than a full-scale test, as a single contact attribute can be focus on. A relative adhesion measurement comparing similar types of stable third body (e.g. grease) can be conducted using a pendulum tester (Paper 2). But, if you require measurement of wear the pendulum test would not be suitable and the testing scale would need to move to a twin-disc type set-up (see Paper 1). The twin disc test set-up also has an advantage over a full-scale test when conducting wear testing as isolating the cause of wear is less susceptible to errors.

This above discussion excludes the costs and timescales of each type of test method, which generally increases as the contact more accurately represents the real wheel/rail conditions. It is important to understand the information you require from a test, the number of measurements required, the length of per measurements and the budget for specimens when selecting a test method.

10.2. Benchmarking of applied products

10.2.1. Grease

Grease that is used on the UK network as a rail curve lubricant has been evaluated in papers 1 and 2. As discussed in section 10.1 above, the differences between testing in a laboratory and field requires careful consideration when interpreting laboratory results to the real world situation.

In twin-disc testing the entrainment of grease into contact is achieved due to the rolling/sliding contact, meaning grease is being constantly supplied to the contact until it has been exhausted. The twin disc tests began with a single fixed supply of grease to the rail disc surface, which is the transferred to the wheel disc as seen in Figure 1 below.

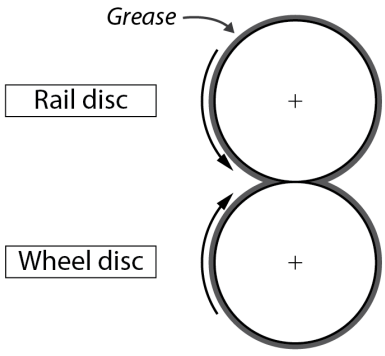

Figure 1: **Twin disc test schematic showing grease transfer between wheel and rail discs.**

In the field the constant grease supply would be the case for a rail gauge near the lubricator, with grease being transferred to the wheel and then deposited down track. Where grease has been previously transferred to the gauge

surface in large enough quantities (enough to be visible) and both contacting bodies have grease on, a twin disc test sufficiently represented this. However, further from the lubricator, where the amount of grease on the rail gauge is little to nothing, only one body would be contaminated with grease.

This difference between field and lab will have an effect on both and retentivity and carry-down length. As the supply of grease is from both bodies, rather than 1, the consumption of grease through the contact will be different to that found in the field. However, as all greases are evaluated in the same manner these twin disc tests give an excellent indication of a greases performance in terms of rententivity and carry down.

The spread of results in the twin disc testing can be partially attributed to removal of grease due to rotation and upon loading contact, both factors that will be present in the field when using a wayside GDU. When testing, every effort was made to ensure even distribution of grease to the disc surface to minimise this. There was no quantification of grease removal due to rotation and squeeze, but it can be assumed that a measurement of a shorter number of cycles indicates more grease has been removed from rotation and squeeze. This is backed up from tests in Paper 1 with different initial grease amounts, where 0.1 g of grease gave more than double the retentivity of the 0.05 g test.

The results indicate that a lot of grease is wasted as only a small percentage actually ever makes it into the wheel/rail contact. There are other forms of lubrication used by railway networks around the world, for example on board oil lubricators, which may have advantages in terms of wasted lubricant.

Assessment of grease carry-down using the pendulum tester has some promise, and will be a useful tool when confirming any carry-down claims a grease manufacturer make. The pendulum tester can also inform interpretation of results from twin disc testing.

10.2.2. Friction modifiers

The friction modifier paper has shown the effectiveness of these products to deal with important friction management issues in the railway industry. Unlike greases, these friction modifiers are not designed to give minimum adhesion, but an intermediate adhesion as well as protecting against wear, noise, corrugation and RCF. Although both types of product are assessed in terms of rententivity and carry-down, the requirements of each vary and must be considered.

The comparison between two scales of testing has highlighted important decisions that need to be made when selecting an appropriate test method.

Similarly to grease, the friction modifiers tested in this thesis are transported by the transfer of friction modifier from the rail to the wheel and back again.

The friction modifiers are designed to be ‘worked’ into the rail head surface to generate a working third body layer. The twin disc test set-up means there is a complex transfer between rail and wheel disc that would not take place in the field. The reduced contact size, along with this double mixing, means there is likely an over application of this particular friction modifier. This

perhaps contributes to the reduced maximum adhesion found between the twin disc results and the full-scale rig results.

These tests results from two scales, using nominally similar contact loads and application amounts, again highlights the need to properly select a test method and accurately interpret the results generated.

10.3. Low adhesion

Papers 4-6 comprise a single package of work to develop the WILAC model and will be discussed separately from Paper 7, the low adhesion mitigation.

In generating the WILAC model, two scales of adhesion tests were used. The small scale laboratory test allowed testing of a third body layer under contact conditions with similar size and pressure on a completely flat surface. The HPT test rig was developed at The University of Sheffield and has shown to be useful in determining test conditions to carry forward into a full-scale test. The HPT test has the advantage over the traditional wheel/rail contact tests as it allowed for far greater control of what was being applied to the contact. This allowed small and tightly controlled variations of a single variable to be achieved in rapid succession. This would not be possible on many types of wheel/rail test rig where timescales, consumables or control of application do not make it possible.

Not all application problems are solved when using a HPT test. It is still difficult to precisely test oxide+water mixtures in a laboratory setting due to uneven distribution of oxide particles with the suspension. This can result in localised areas within the contact when mixtures subjected to shear, altering the actual layer tested. Higher percentage masses also prove difficult to evenly distribute onto the specimen surface due to ‘clay’ like viscosity of >90% by mass mixtures. In fact, the original rheological measurements were made did not reach these high percentage masses and the authors extrapolated data up to the higher percentages (Beagley, 1976).

Another advantage of the HPT test is that it can be used to investigate initial creep curve gradients. This is achievable as when the rotation angle increases the contact moves from stick to slip as found in the wheel/rail contact.

Even though low adhesion was not achieved in the HPT rig, the possible reason for such a result were investigated and the results guided and helped us understand the contact problem more fully. Furthermore the adhesion model alluded to the problems faced by this change in water + oxide ratio.

Paper 5 presents, to the author’s knowledge, the first time repeatable tests showing wheel/rail adhesion reduced to ultra-low levels when only water was added see Figure 2. These results are similar to a result that was presented by Beagley and Pritchard (1975).

The results from the full-scale test also showed how sensitive the wheel/rail adhesion is to a small change in amount of water added to the contact. The adhesion can alter dramatically over a range of only 30μL of water.

The WILAC model can accurately represent this effect and model the change of creep curve shape when varying water amounts. In reference to Figure 2,

The gradient after peak adhesion is different in all three cases as the water amount is increased from zero. It is interesting to observe the transition of gradient of the creep curves between when increasing water amounts. The gradient is affected by the amount of water in the contact. The volume of water determines the influence of the thermal effects on the wheel/rail materials, and this the adhesion. As water is increased the gradient of the curve becomes more shallow, whilst the peak adhesion drops to a minima and then returns to a peak value expected of a full wet contact.

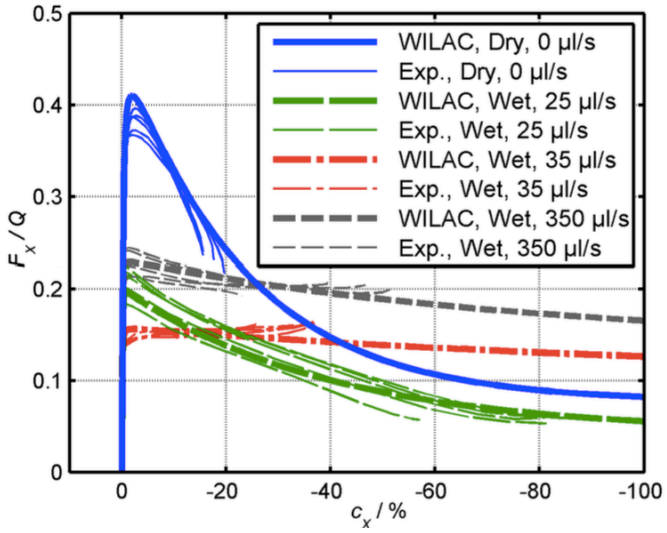

Figure 2: Experimental data (thin lines) used for model parameterisation and associated WILAC model results (thick lines) for different water flow rates w at 4.2 kN normal force and 5 m/s rolling speed

10.4. Hydrophobic products

New strategies in tackling low adhesion on the rail network are vital in improving reliability, efficiency and safety. The use of hydrophobic solutions to directly treat the railhead to improve railhead friction in wet conditions was assessed using both a twin disc and pendulum rig. The current study showed that the solutions tested did not give any traction improvement under wet conditions. In certain cases the adhesion was actually reduced in wet conditions over an untreated railhead.

The hydrophobic solutions work on the principle that the solutions active polar molecules repel water. Lewis *et al.* (2009) showed that oil and water mixtures actually reduced adhesion below that an oil lubricated contact. The solutions tested do not have oil bases, but do contain polar molecules to produce the hydrophobic effect. The reduction in adhesion in wet condition on a treated railhead may be caused by the same effect as found by Lewis.

10.5. References

Beagley, T.M., Pritchard, C., 1975, “Wheel/rail adhesion – The overriding influence of water”, Wear, 35, pp. 299 -313.

Beagley, T.M., 1976, “The rheological properties of solid rail contaminants and their effect on wheel/rail adhesion”, Proccedings of the Institute of Mechanical Engineers, 190, pp. 419-428

Lewis, R., Gallardo-Hernandez, E.A., Hilton, T., and Armitage, T., 2009, “Effect of oil and water mixtures on adhesion in the wheel/rail contact”, Journal of Rail and Rapid Transit Proceedings of the IMechE Part F, 223, pp. 275-283.

11. Conclusions

11.1. Bench marking of applied products

Paper 1: *Assessment of Railway Grease Performance using a Twin-Disc Tester*

Two series of test have been performed to assess the performance of different types of grease and the effects of surface roughness upon this performance. Lubricated friction levels are what would be expected with a gauge face lubricated with grease (i.e., $\mu < 0.1$).

There is a distinct inverse relationship between surface roughness and grease retentivity. There is also an inverse relationship between retentivity and disc wear rate. As such, tests should be repeated on new disc surfaces each time to mitigate the effects of changes in surface roughness on the grease performance.

The test method described in this work clearly highlights the performance differences between different greases and is therefore considered suitable as a method of certification for new greases before they are introduced onto the rail network.

These tests now form part of the Network Rail specification NR/L3/TRK/3530/A01 (Curve Lubricants). When testing grease in a twin disc test rig, 0.1g of grease is applied to the rail disc surface at the start of each test. Tests are repeated until tree additional times, each with a new set of discs.

This work also highlighted the need for consistent lubrication of the rail gauge face. In lubrication starvation tests high wear rates are being observed under the lubrication starvation localised damage of un-lubricated sections of the disc.

Paper 2: Field trials of a *new method for the assessment of gauge face condition using a modified Pendulum test rig*

Two field tests using a pendulum tribometer with the tradition setup as well as a new modified angled pendulum foot adaptor. A clear difference of energy loss at the gauge corner as the distance from the lubricator is increased. Rapid field-testing is possible to assess the carry down of grease along a curve, although repeatability on different days is questionable. Top of rail adhesion measurements were again shown to be comparable to previous laboratory and field-testing using a pendulum tribometer to measure rail head traction.

Paper 3: *A Comparative Study of Twin Disc and Full Scale Experimentation Methods of the Wheel-Rail Contact – Assessment of Friction Modifiers*

Absolute/baseline friction coefficients differ from twin disc (0.11) and full scale (0.31) tests. Evolution of friction modifier traction coefficient shows similarities between the two test methods used. Further testing is needed to fully evaluate the retention in a full-scale contact. The tests described in the paper could be

used as a basis to define approval tests for FMs, there are currently no standards for approval for these type of products.

11.2. Low adhesion

Paper 4: *Assessing the impact of small amounts of water and iron oxides on adhesion in the wheel/rail interface using High Pressure Torsion testing*

The main outcome of the investigations was that significant reduction of friction (over dry conditions) was observed when applying low amounts of water. This reduction is much higher compared to flooded conditions. Ultra-low friction was not achieved in HPT tests, however. This was a result of the difficulties in applying and distributing third body layers and their inevitable evolution during a test.

An “Adhesion Model” has been developed that can estimate adhesion levels in the presence of different water and iron oxide mixtures The model is in accordance with the experience that low adhesion is predominately observed with low amounts of water and explains the difficulties with accurately testing these mixtures (as seen in the HPT test results).

Paper 5: *Full-scale testing small amounts of water in the wheel/rail interface*

The results from the full-scale tram wheel rig have shown water can cause low adhesion when combined with the third body layer that is present (and generated) in the wheel/rail contact. These low water conditions produce a mixture that is sustained in the contact once sliding is initiated adhesion levels are rapidly reduced to low levels (min(T/N) = 0.052). This level of adhesion is on the boundary of low and exceptionally low adhesion as defined by Vasic et al. (2008).

The window for low adhesion as a consequence of water and iron oxide mixtures is small. This was confirmed by the increase adhesion when even marginally decreasing or increasing the amount of water supplied to the contact.

The general characteristic of the adhesion level as a function of the amount of water predicted by the Adhesion Model was confirmed under rolling contact conditions by the experiments on a full-scale test rig.

Visual inspection of the contact band during tests indicated that the third body layer formed changes during tests when water is allowed to evaporate. The mixture is comprised of water, oxides and wear debris generated from the contacting bodies. It was observed in tests with bulk water application that the oxide/water is fully removed during a few rotations of the rollers as the water evaporates. The short time span indicates there is a high chance of missing this transition point during a test unless water application is constant (and at the right level to produce a sufficiently viscous oxide water mixture).

Paper 6: *Wheel/rail adhesion modeling in the presence of water/oxide mixtures*

The outcome from papers 4, 5 and 6 was the WILAC model. This model was developed to predicts the effect of water on wheel/rail adhesion in the whole

range of conditions from dry to damp to wet. WILAC model results agree with existing locomotive test data from literature in dry and wet conditions

Low amounts of water considerably influence the adhesion level and the shape of the adhesion curve. The adhesion curve in damp condition is not just a linear interpolation between the adhesion curve observed in dry condition and the adhesion curve observed in wet condition.

Adhesion values as low as 0.052 have been observed in a tram wheel test rig experiment at high creep at a water rate of 25 µl/s solely due to the presence of wear debris and water in the contact.

11.3. Novel friction management solutions

Paper 7: *Investigation of the isolation and frictional properties of hydrophobic products on the rail head, when used to combat low adhesion*

This paper summarises an assessment of the suitability of two commercially available hydrophobic products for use in addressing low adhesion levels which occur in water-contaminated wheel-rail contacts. The test program also provided some insights into the mechanics of this low adhesion phenomenon..

A black liquid was witnessed during a test with pure water after the water supply was stopped. This liquid kept the traction at approximately 0.2 and was observed to disappear from the disc surface very rapidly. Once this substance was consumed, the friction almost instantaneously started to rise toward dry levels. It is thought that the liquid may be mixed with an oxide that acts as a solid lubricant as the contact initially dries, before being removed.

Pendulum friction values from testing on an actual rail head were in agreement with the twin disc values. With a layer of moisture (that perhaps best represents the dew point condition) a dried film of product did increase friction over a moist clean rail head.

At present there is not a convincing case for applying hydrophobic products to help reduce low adhesion incidents, but the moist layer effects need further investigation. Another aspect that needs consideration is the role the hydrophobic liquids may play in suppressing oxide formation.

11.4. Adhesion measurements

The work presented has generated a bank of wheel/rail friction data at different test scales and contaminant condition. Table 3 shows the general friction measurements in terms of test rig, normal load, velocity and third body material as measured in papers 1-7.

Table 3: Table of general adhesion measurements from papers presented in thesis.

Paper	Test Apparatus	Load/Contact Pressure	Rolling Speed (km/h)	Test Conditions	Stable μ
1	Twin disc (SUROS)	1500 MPa/7.7 kN	3.54	Grease	0.03-0.06
2	Angled Pendulum			Dry	0.25-0.3
				Wet	0.1-0.15
				Grease	0.05-0.09
3	Full scale rig (railway)	87 kN	0.14	TOR-Friction modifier	Life cycle: 0.1-0.3 over 200 cycles.
	Twin disc (SUROS)	1500 MPa/7.7 kN	3.54	TOR-Friction modifier	Life cycle: 0.1-0.3 over 13k cycles.
4	HPT	200 MPa	9.16×10^{-5} (0.4deg/s)	Dry	0.55
		600 MPa			0.54
		1000 MPa			0.53
		600 MPa		Wet (flooded)	Range μ: 0.4-0.5
				Wet (minute water)	Range μ: 0.1 – 0.25
				Oxide (dry)	Range μ: 0.7 – 0.75
				Oxide (wet)	Range μ: 0.3 – 0.4
5	Full scale tram rig	4 kN	18	Dry	0.4
				Wet (350μL)	0.24 μ_{peak}, 0.2 μ_{min}
				Wet (35μL)	0.13 μ_{peak},, 0.15 μ_{min}
				Wet (25μL)	0.2 μ_{peak}, 0.05 μ_{min}
7	Twin disc (SUROS)	1200 MPa	3.54	Wet	0.18
				Hydrophobic (wet solution)	0.11-0.16

12. Future work

Future topics of research are outlined below as possible topics of interest. The streams of this work conducted in this work have brought up aspects of future work throughout the thesis.

12.1. Test methods

1. *Understanding of the shearing of a third body layer in a HPT tes*t
    - The macro stick-slip process seen in the HPT tests are thought to be due to the combination of a changing third body through shearing and partial metal-metal interaction as a result. The control system may also exacerbate this problem as the controller compensates for the sudden gross movement.

12.1.1. Benchmarking of applied products

12.1.2. Grease

2. *Understanding the effects of grease rheology on carry down and retentivity*
    - A better understanding of the rheological aspects of the greases themselves, particularly in respect to dependence on temperature would enable more targeted grease development.
3. *Improvement of grease transfer from a GDU*
    - Adherence and transfer of grease across from wheel to rail is key for the transportation of grease from a wayside lubricator to the wheel/rail contact. Design and manufacture of a reduced scale test rig to measure has been completed at the University of Sheffield. It is recommended that tests be run to assess the effect on environment temperature on grease transfer. Consider the rheology of the greases over the set temperature ranges and compare to pick-up test results.
    - The measurement of tackiness and how the affects grease transfer should also be conducted. This should be done separately from the pick-up rig to increase the control and measurement of mass transfer.
4. *Understanding the affects and sensitivity of the gauge corner measurements with a pendulum tester.*
    - Some sensitivity testing has been completed when using a pendulum testing device, but a more comprehensive study would need to be completed to fully characterise the effects alignment of the pendulum against the gauge corner.

12.1.3. Friction modifiers

5. *Investigate the physical changes of the friction modifier on the railhead under realistic contact pressures*
    - Further work on investigating the physical changes of the FM/natural-third-body-layer mixture over the number of repetitive

cycles in a full-scale test. This can be compare to how the FM layer is formed in the twin-disc type of experiment where constant transfer of product between wheel and rail disc is happening.

6. *Optimisation of friction modifier application amounts*
    - The wayside products are applied using the trackside applicators which are manually set to deliver product to the top of rail at set delivery rates. This can lead to too little product being applied, which can lead to the product not being effective, or too much product being applied, which leads to waste. In terms of friction management neither case is suitable. Application amounts is key to reducing waste and effectively managing friction
7. *Friction modification using onboard application of current friction product*
    - This thesis looked at wayside TOR-FMs products but there are also onboard applicators for treatment over a larger area of the network.
8. *The effect of mixing with other friction management products and track contaminants*
    - The products will mix with other friction management products on the railway network. It is not known to what extent this affects the performance of the friction modifiers. Research should look into the effect of specific products mixing with common on track contaminants and cross product mixing.
9. *Improved friction modifier detection in the field*
    - The friction modification products are applied in such a way that visual inspection is difficult, especially at a distance from the wayside applicator. A new detection method to check whether products are to answer the following questions: Are they being transferred and moved the right place? and how do we monitor this?

12.2. Low adhesion

10. *Velocity dependency of the WILAC model*
    - In the current WILAC model velocity is taken into account using modeling data. The experimental inputs were restricted to 5m/s due to testing limitations. A further study should investigate the effect of speed on the creep curves. Particular focus on water amounts will be required.
11. *Transition of wet creep curves in the WILAC model*
    - Water amounts over the transition period should be investigated to fully analyse the effect on the creep curve transition.
12. *Oxide and water mixture viscosity measurements*.
    - Increased and updated rheological measurements of the oxide-water mixtures, particularly at the higher mass percentages.

12.3. Novel solutions

13. *Hydrophobic coating on rail sand to improve traction enhancement*
    - The efficacy of using hydrophobic solutions to directly treat the railhead is questionable. However, the use hydrophobic solutions

to coat rail sand to improve the effectiveness of entering into the rail contact in sufficient amounts – the rail sand will clump together in the presence of water – could improve current sanding practices. It is recommended that a small scale investigation into the use of hydrophobic sand be conducted.

13. Appendix A

13.1. Additional HTP results

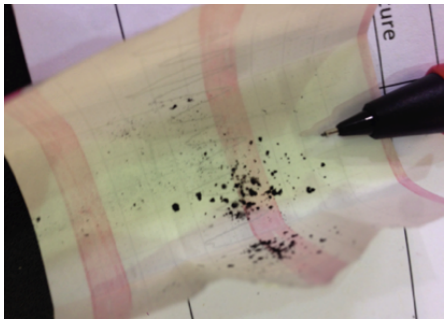

Figure 1: Magnetite iron oxide particles (<5 µm)

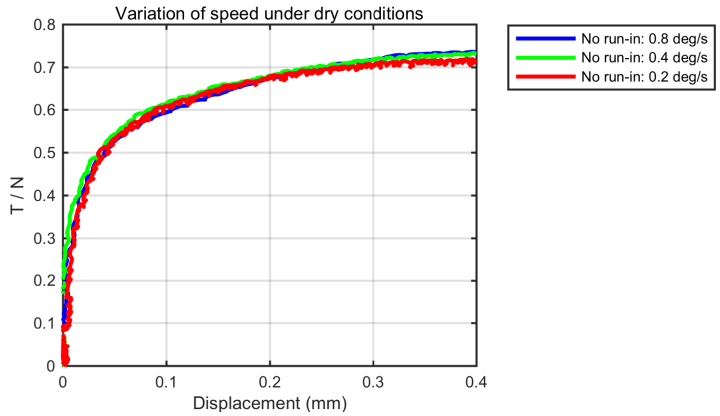

Figure 2: Velocity variation in HPT test under dry conditions

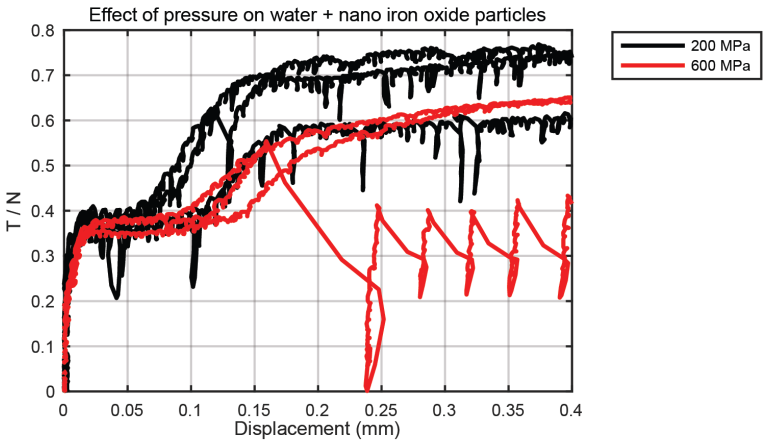

Figure 3: HPT test with water + nano iron oxide particles (<650nm) mixtures applied at 80% when subject to different normal loads

14. Appendix B

14.1. Paper 5: Full-scale tram wheel rig test results

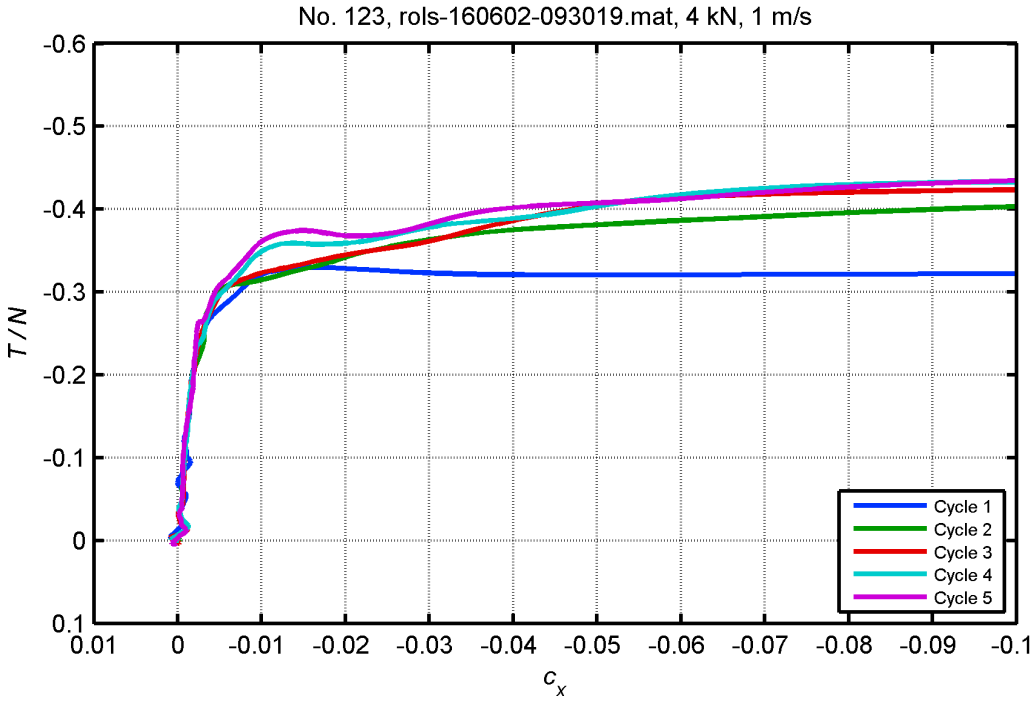

Figure 1: **Creep curves from dry tests performed under 4 kN normal load at 1 m/s.**

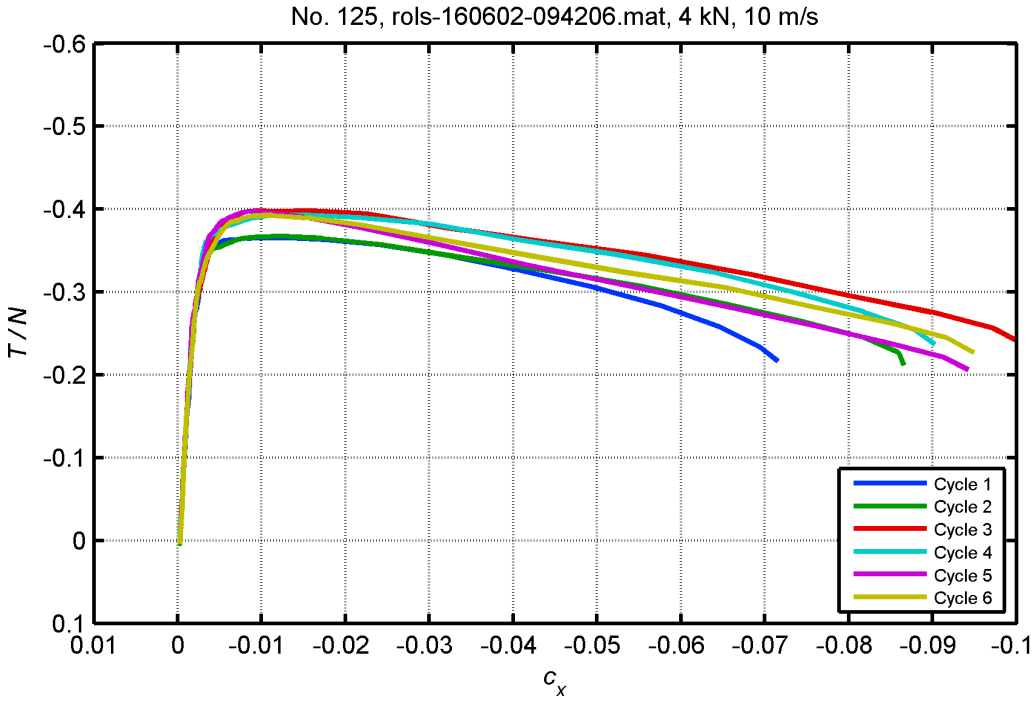

Figure 2: **Creep curves from dry tests performed under 4 kN normal load at 10 m/s.**

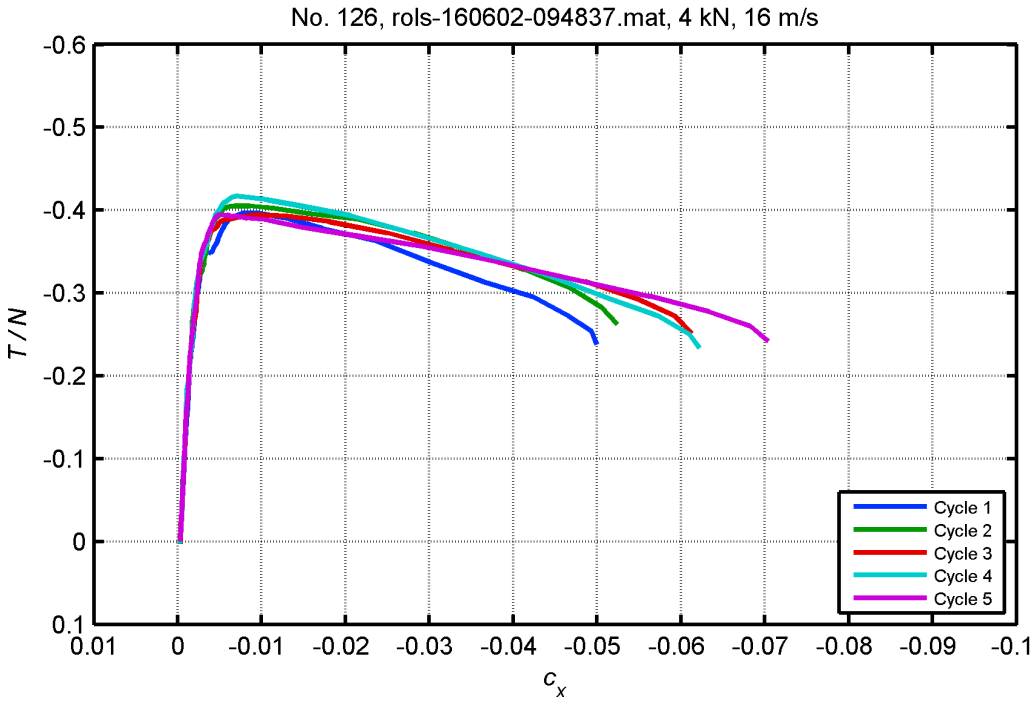

Figure 3: Creep curves from dry tests performed under 4 kN normal load at 16 m/s.

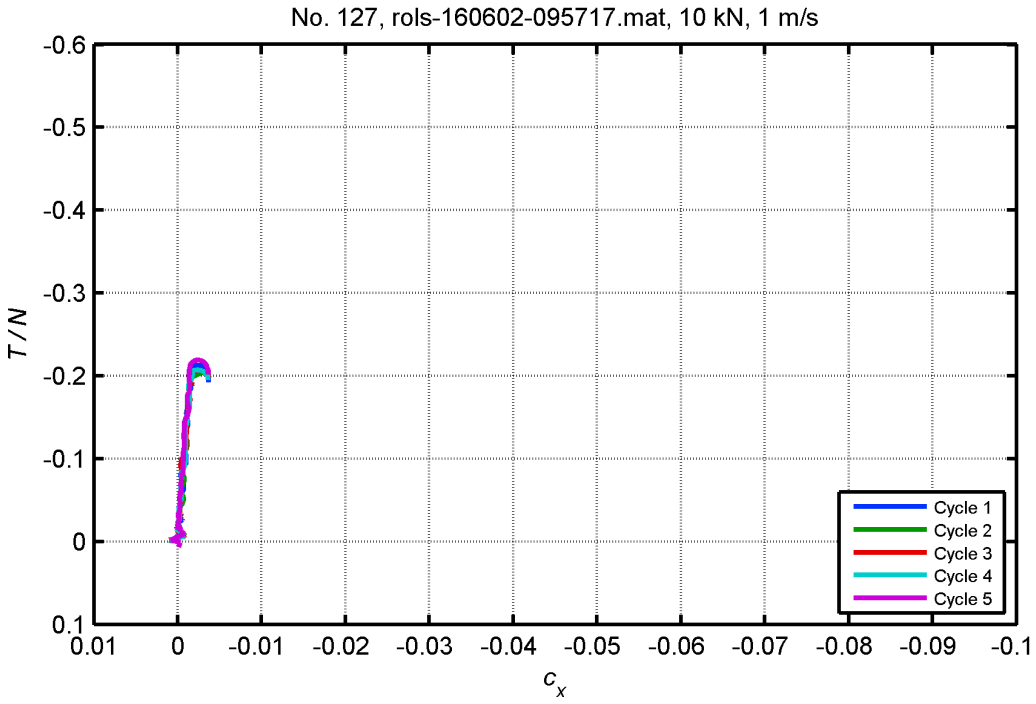

Figure 4: Creep curves from dry tests performed under 10 kN normal load at 1 m/s.

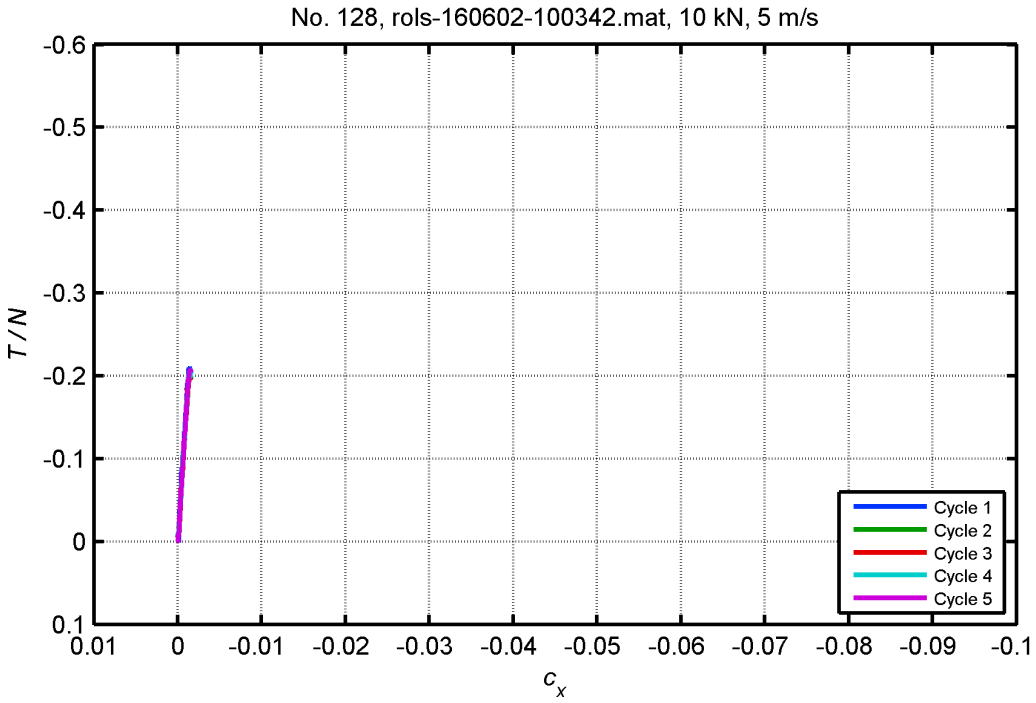

Figure 5: Creep curves from dry tests performed under 10 kN normal load at 5 m/s.

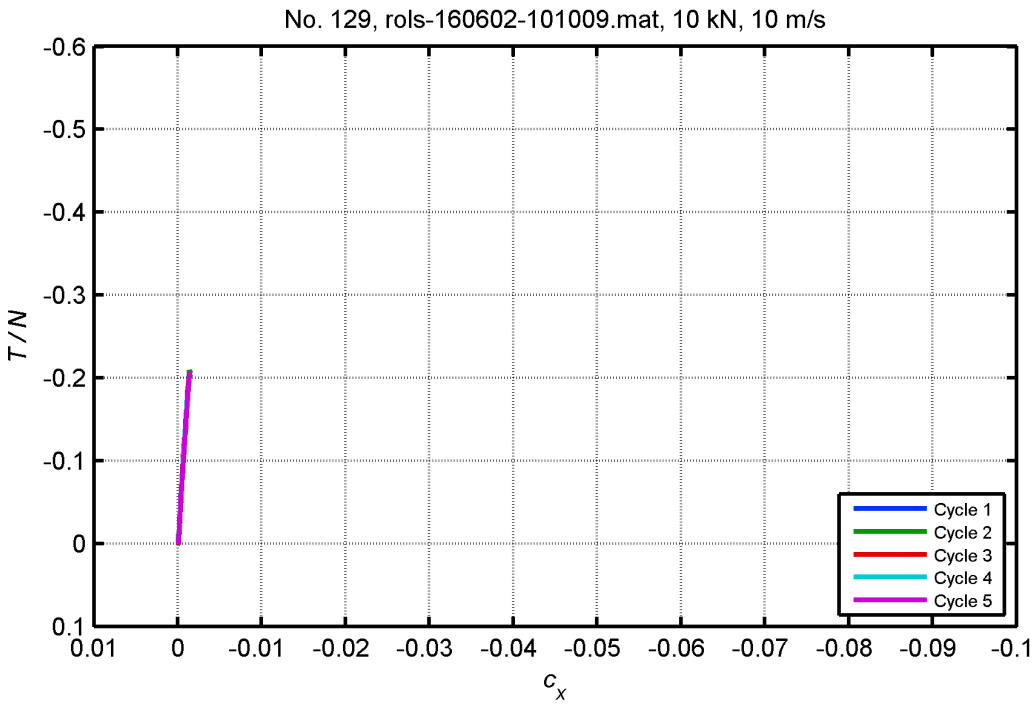

Figure 6: Creep curves from dry tests performed under 10 kN normal load at 10 m/s.

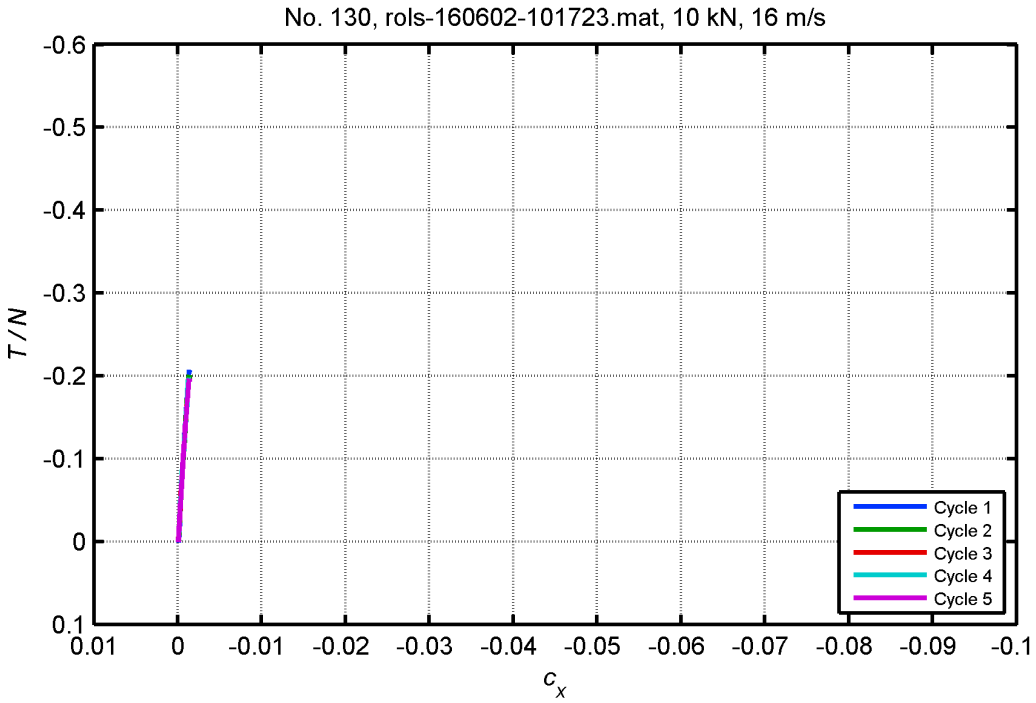

Figure 7: Creep curves from dry tests performed under 10 kN normal load at 16 m/s.

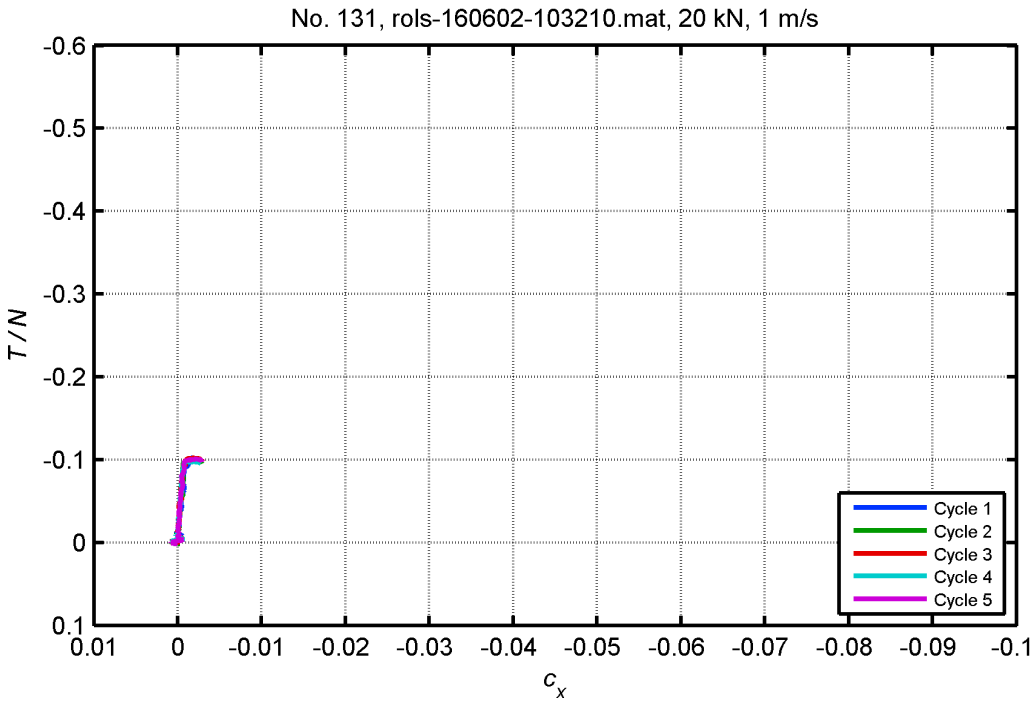

Figure 8: Creep curves from dry tests performed under 20 kN normal load at 1 m/s.

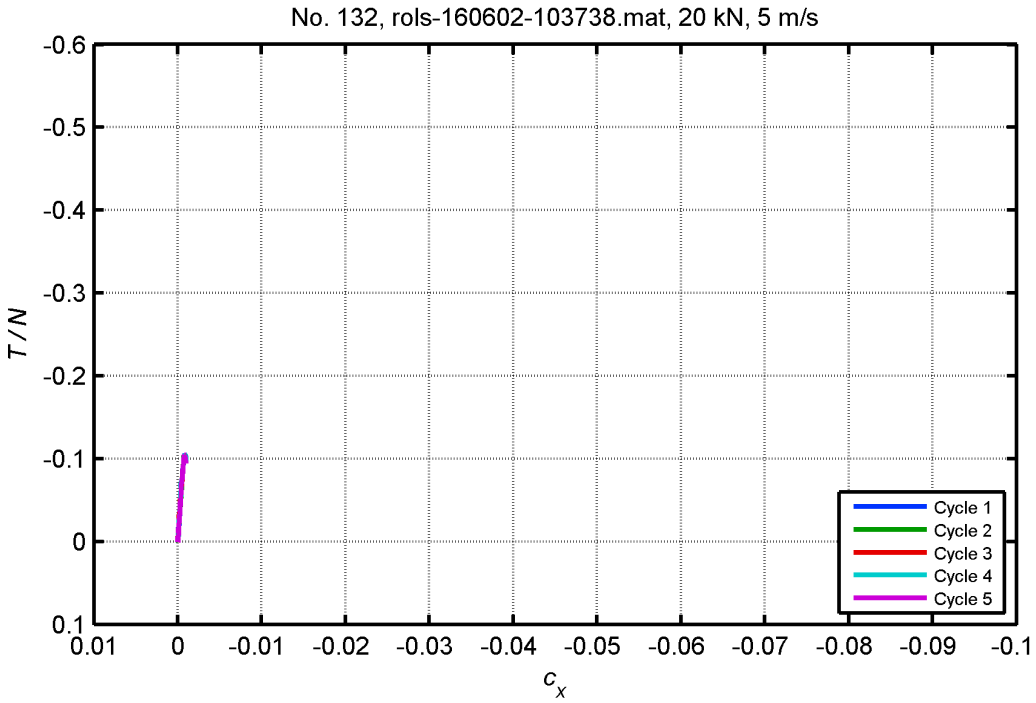

Figure 9: Creep curves from dry tests performed under 20 kN normal load at 5 m/s.

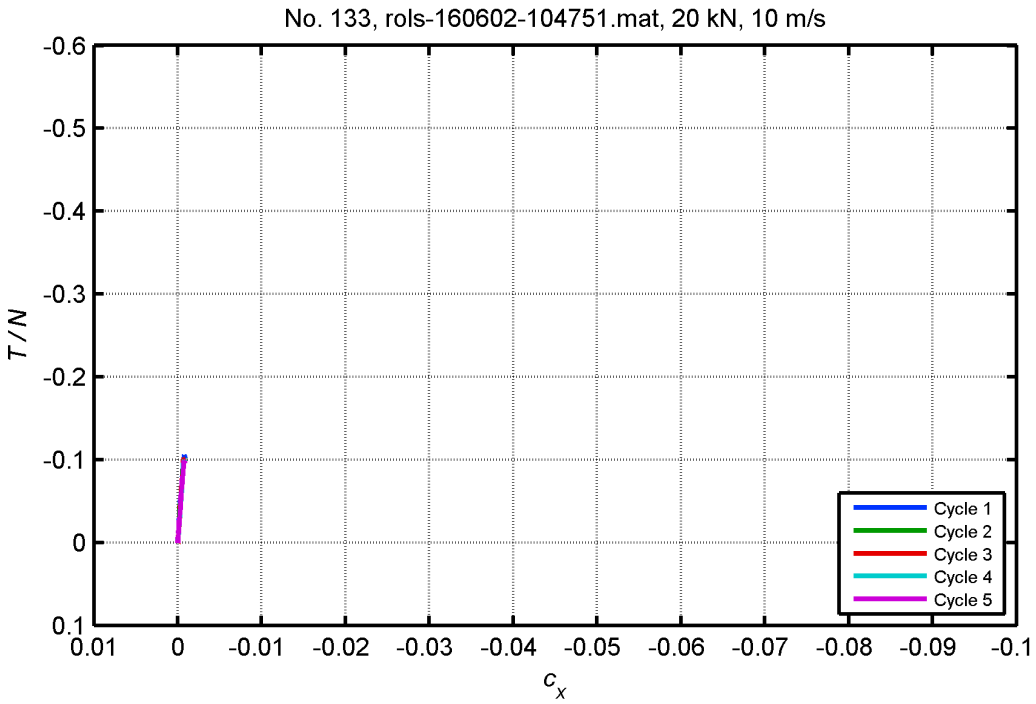

Figure 10: Creep curves from dry tests performed under 20 kN normal load at 10 m/s.

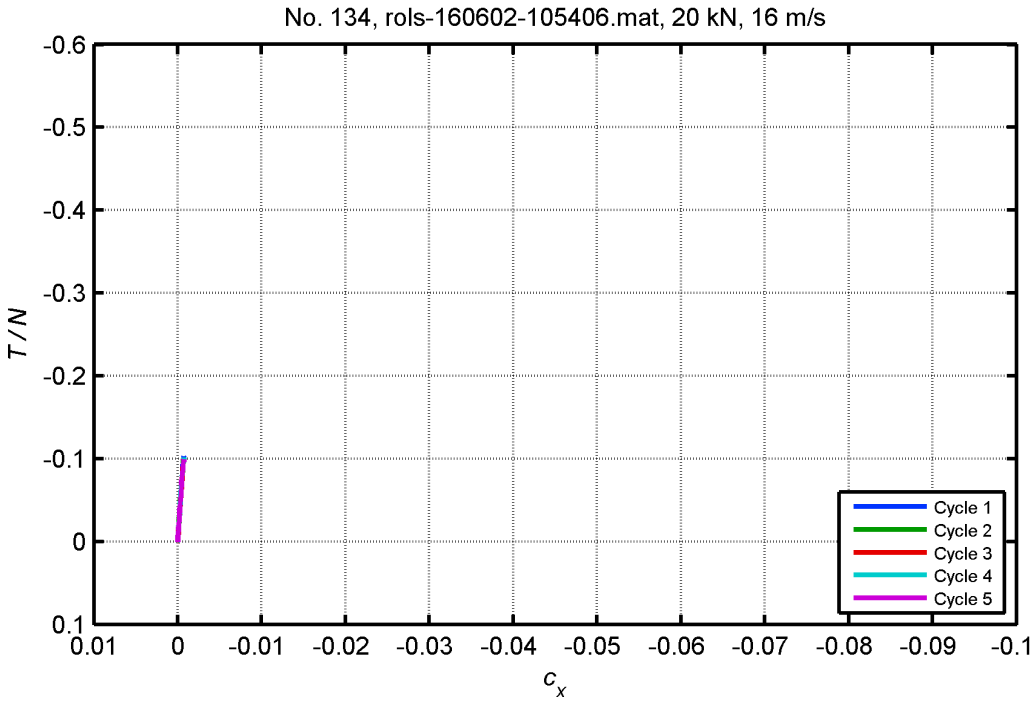

Figure 11: Creep curves from dry tests performed under 20 kN normal load at 16 m/s.

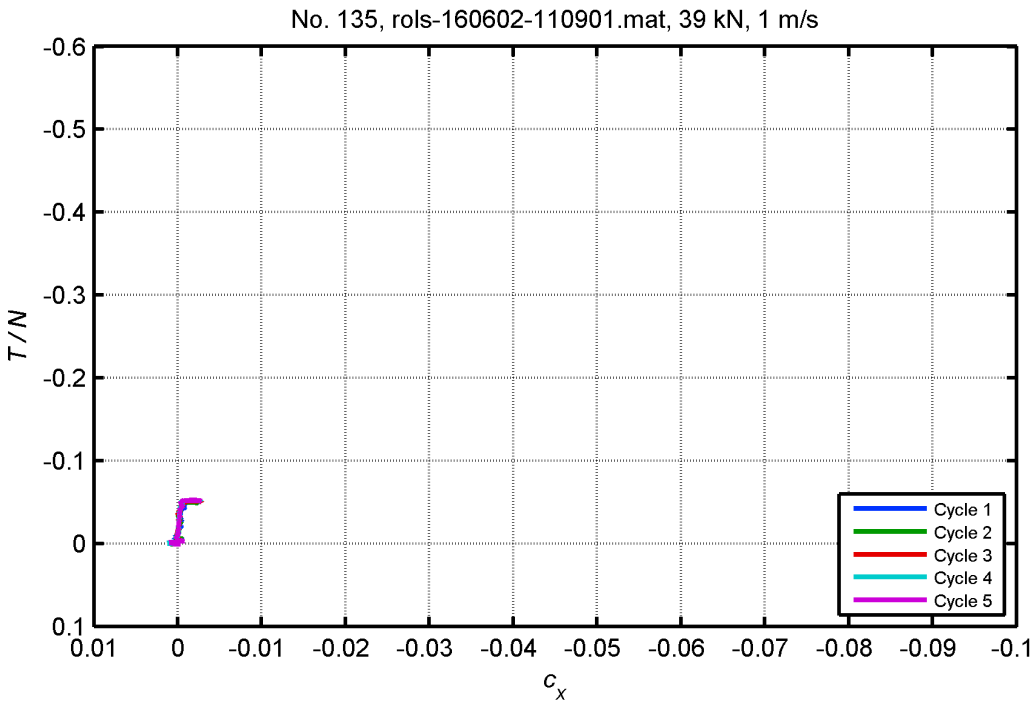

Figure 12: Creep curves from dry tests performed under 40 kN normal load at 1 m/s.

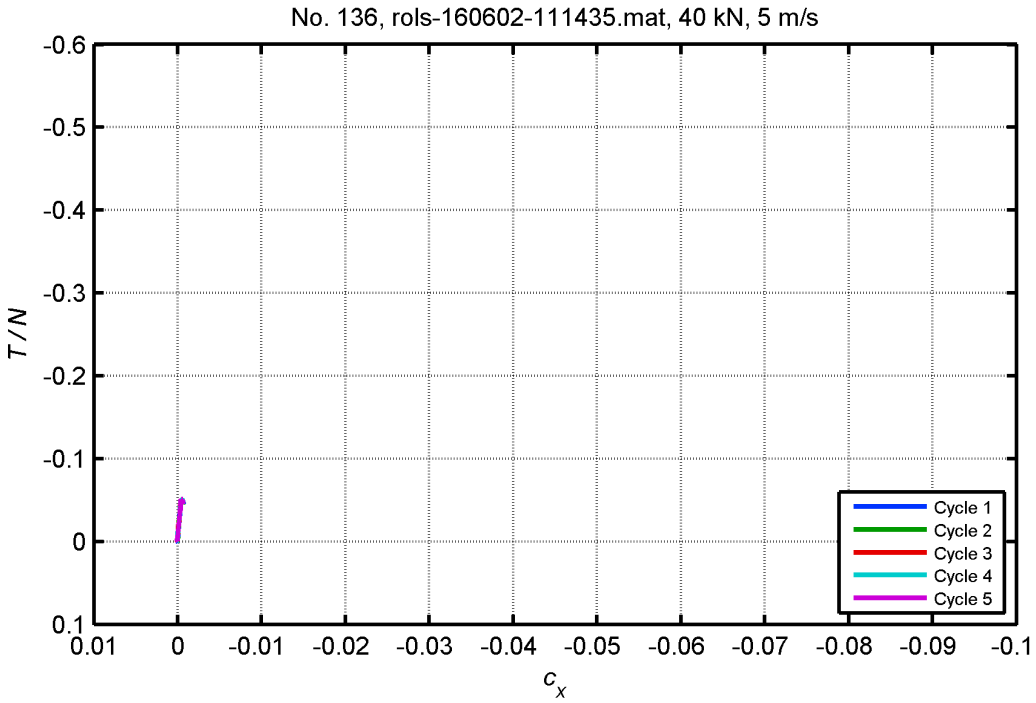

Figure 13: Creep curves from dry tests performed under 40 kN normal load at 5 m/s.

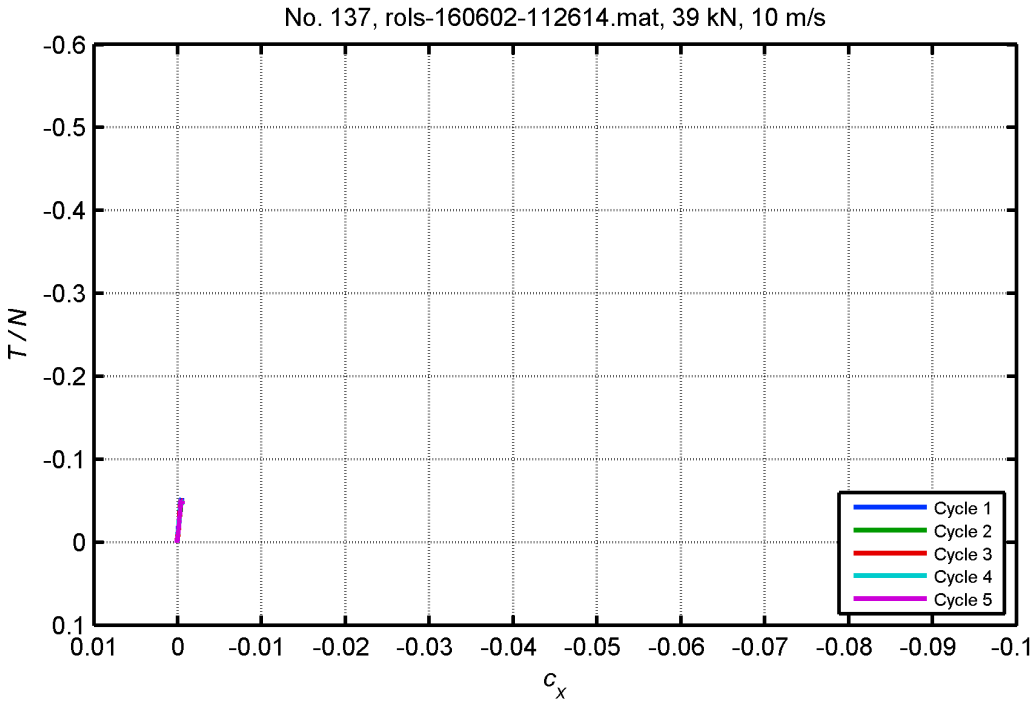

Figure 14: Creep curves from dry tests performed under 40 kN normal load at 10 m/s.

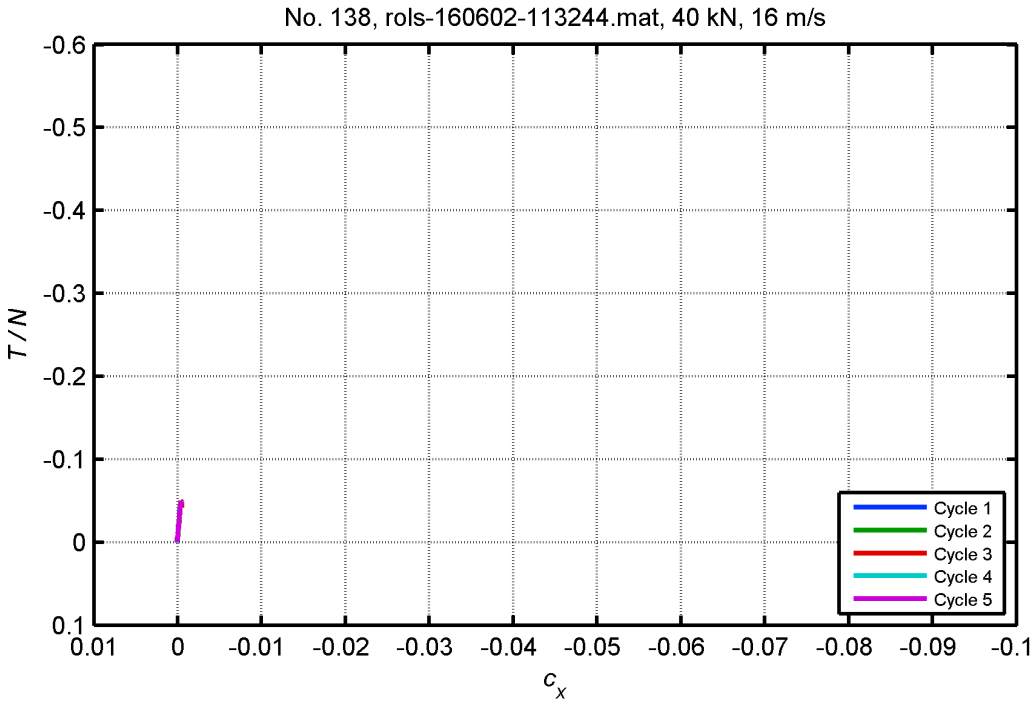

Figure 15: Creep curves from dry tests performed under 40 kN normal load at 16 m/s.

Wet + drying test results

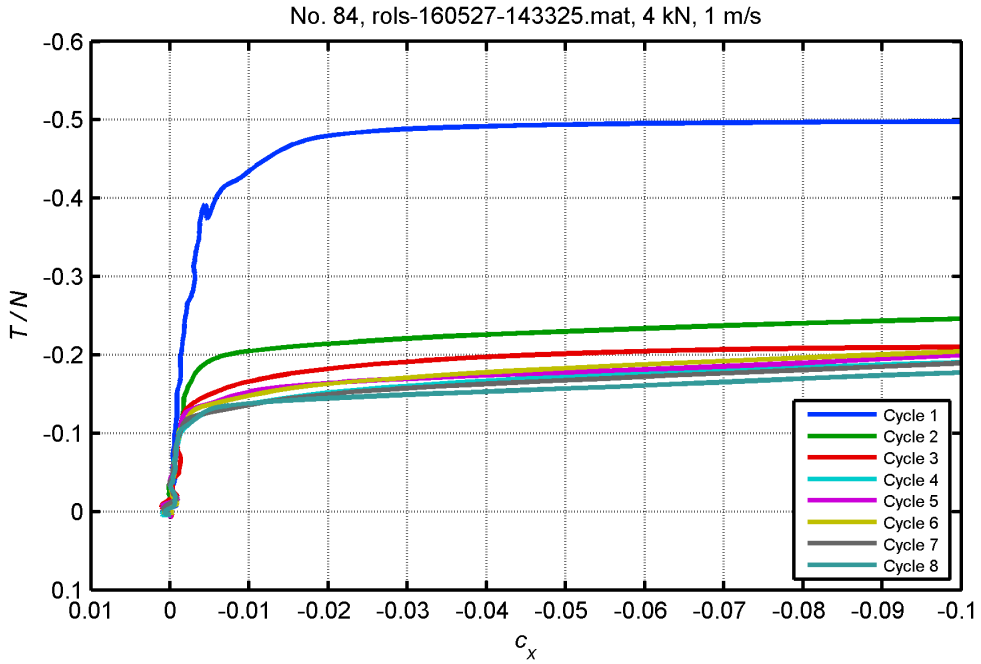

Figure 16: Creep curves from water + drying tests performed under 4 kN normal load at 1 m/s (1st cycle under dry conditions).

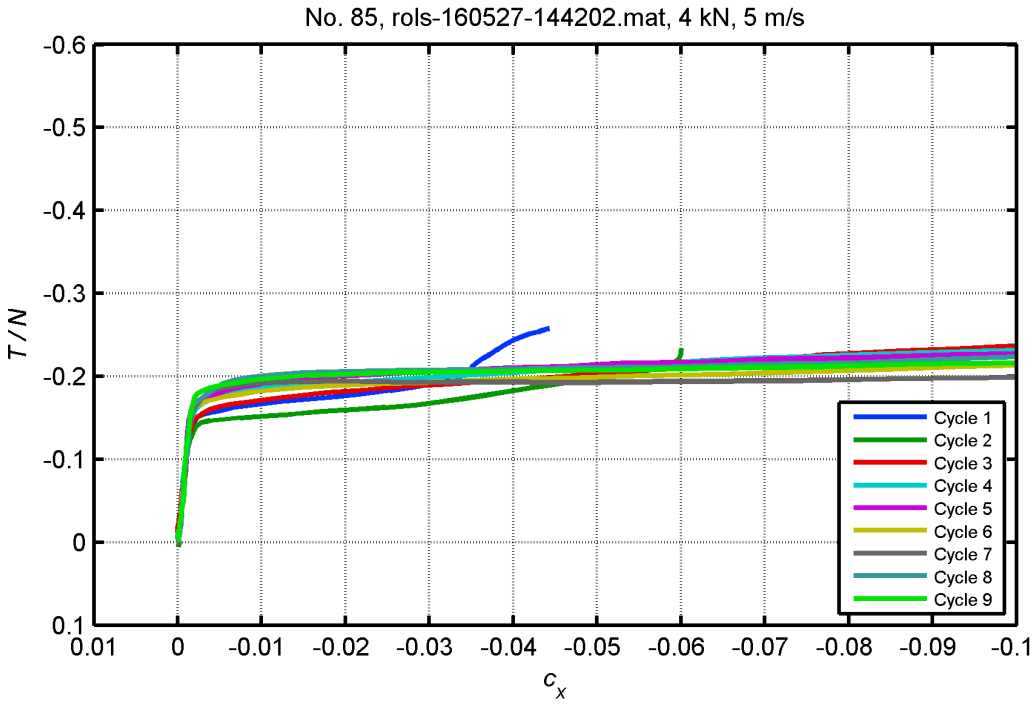

Figure 17: Creep curves from water + drying tests performed under 4 kN normal load at 5 m/s.

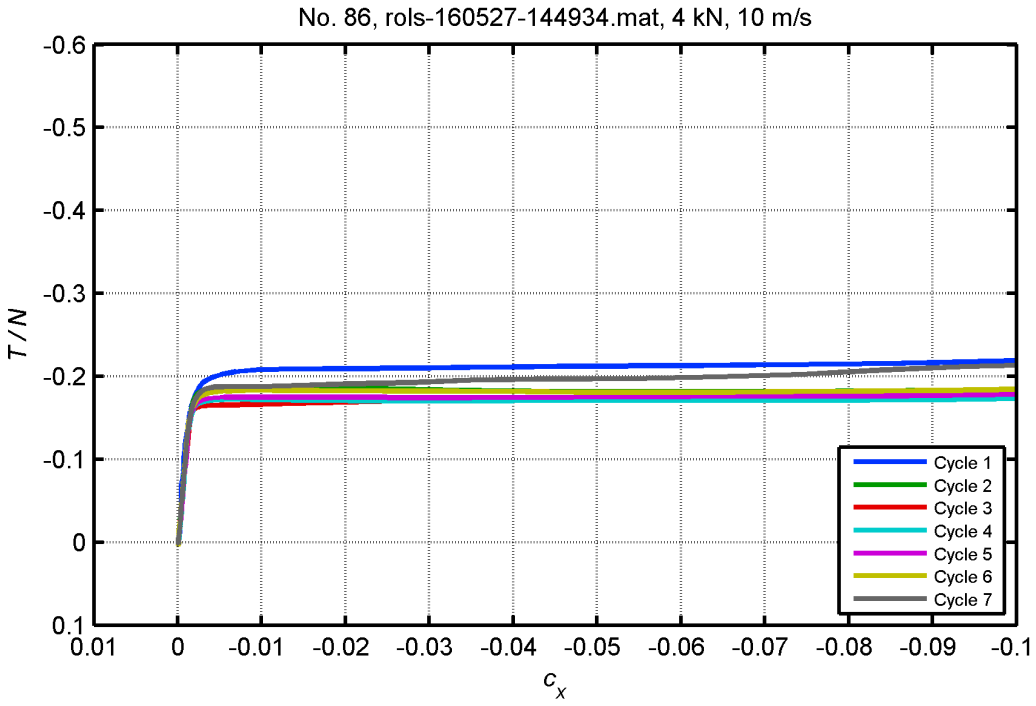

Figure 18: Creep curves from water + drying tests performed under 4 kN normal load at 10 m/s.

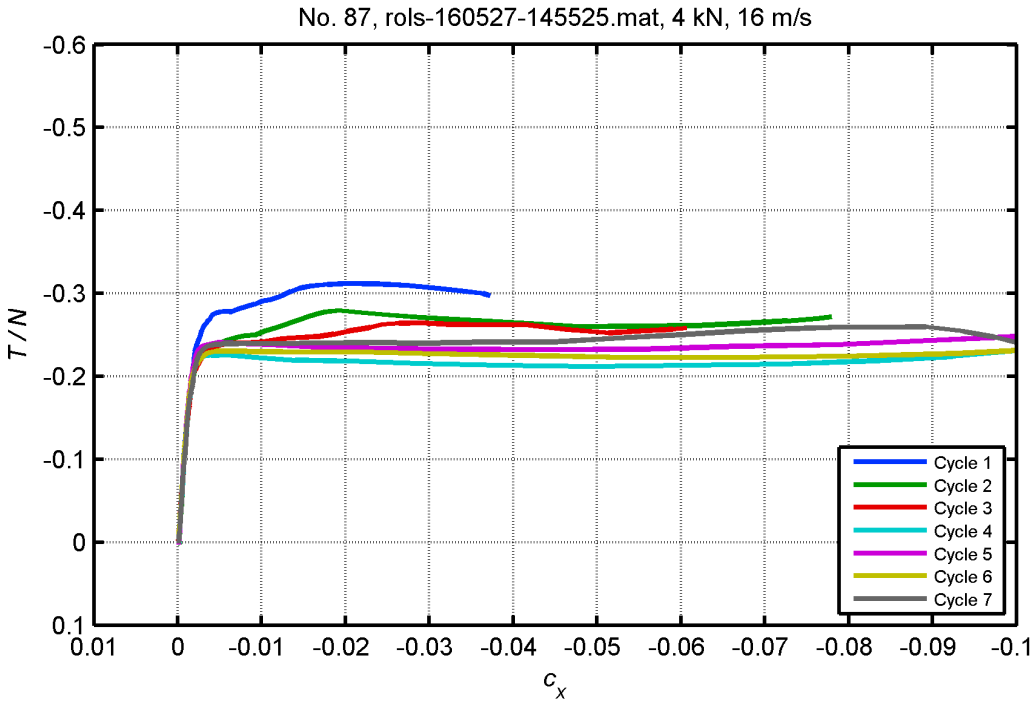

Figure 19: Creep curves from water + drying tests performed under 4 kN normal load at 16 m/s.

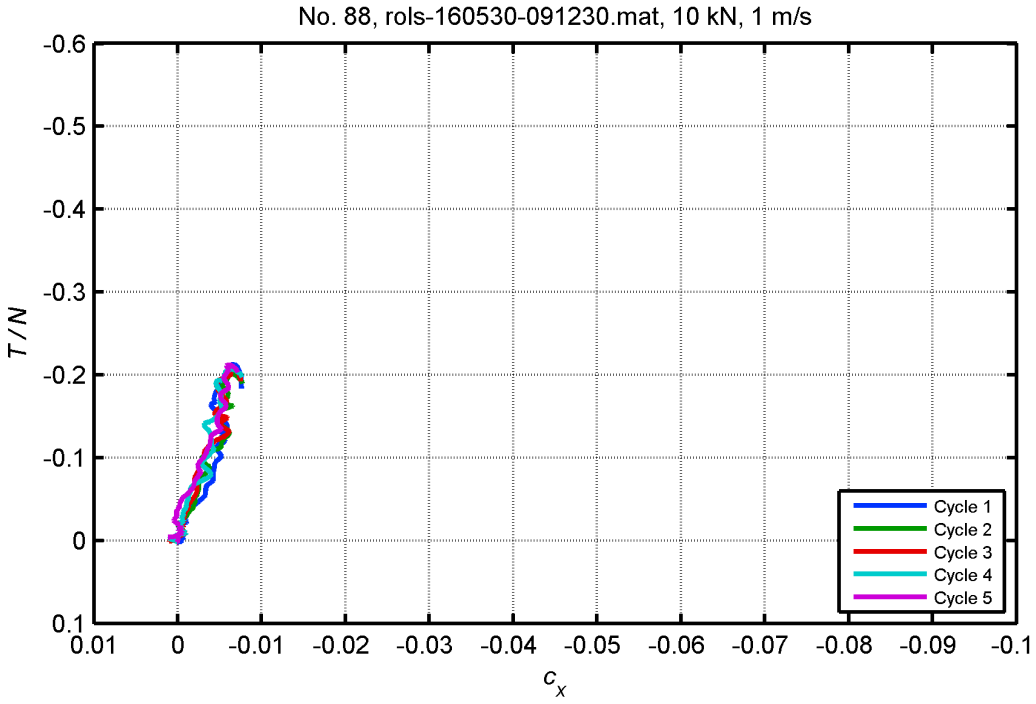

Figure 20: Creep curves from water + drying tests performed under 10 kN normal load at 1 m/s.

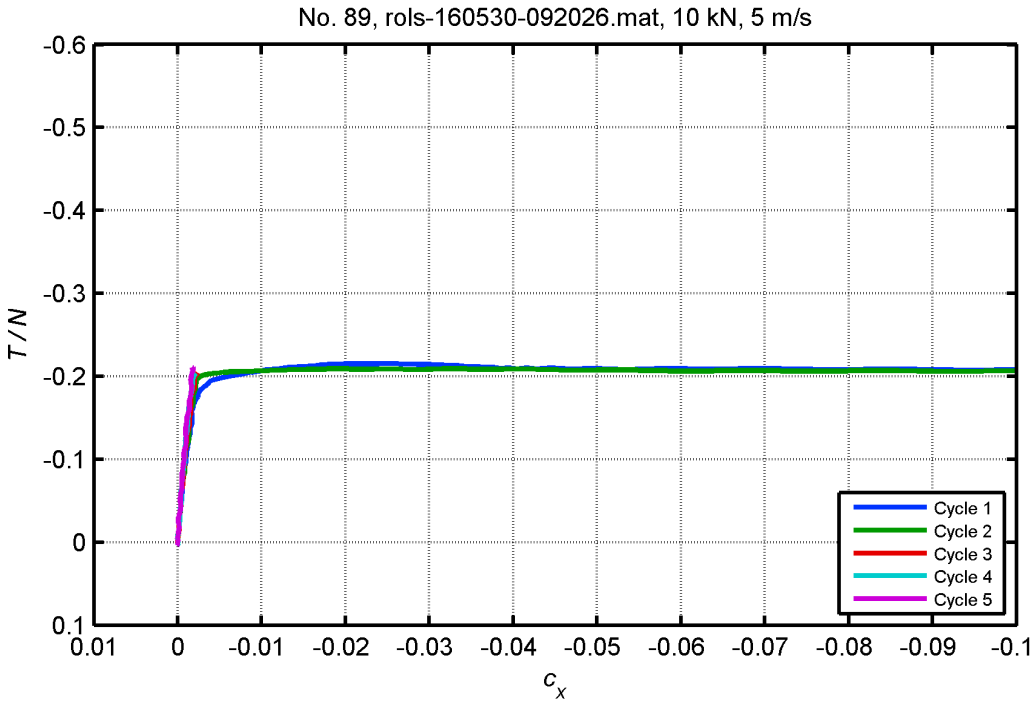

Figure 21: Creep curves from water + drying tests performed under 10 kN normal load at 5 m/s.

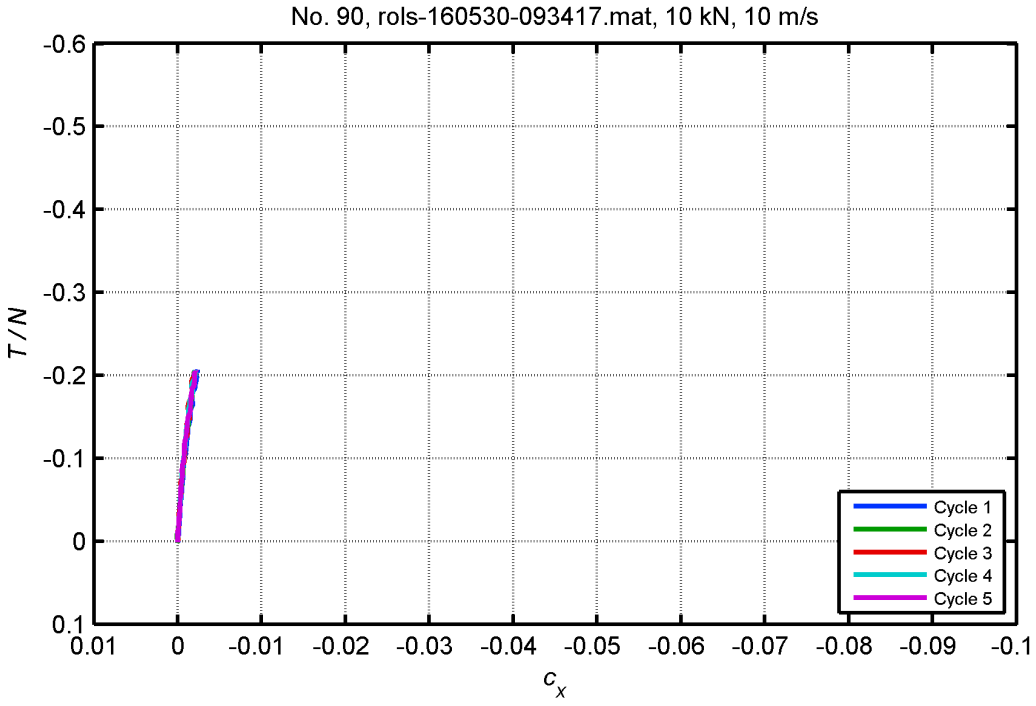

Figure 22: Creep curves from water + drying tests performed under 10 kN normal load at 10 m/s.

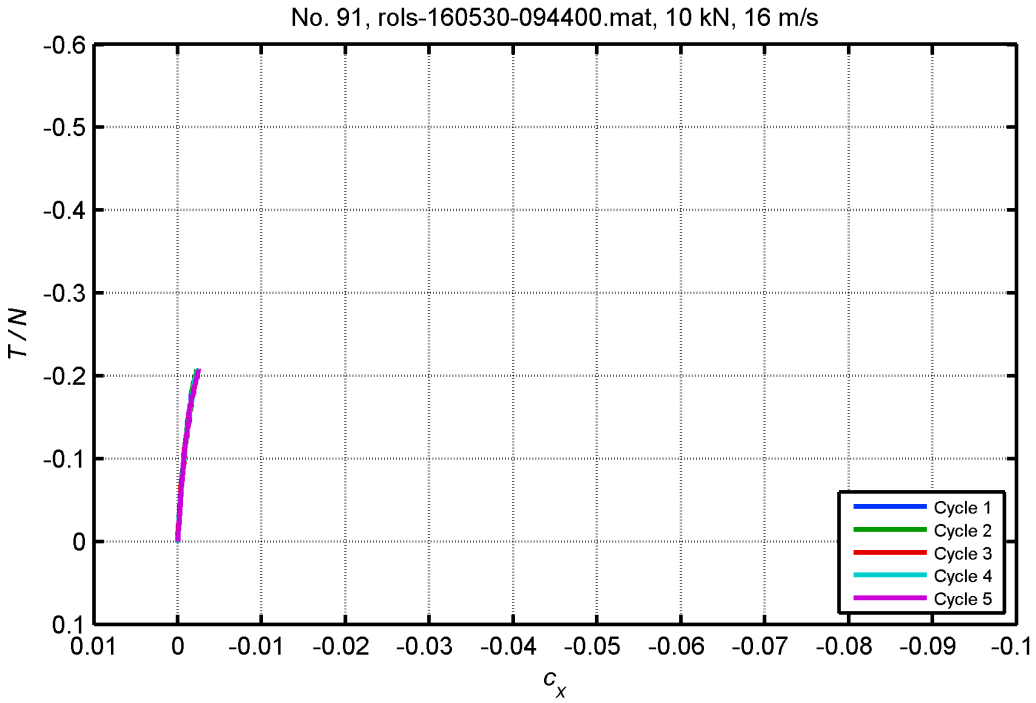

Figure 23: Creep curves from water + drying tests performed under 10 kN normal load at 16 m/s.

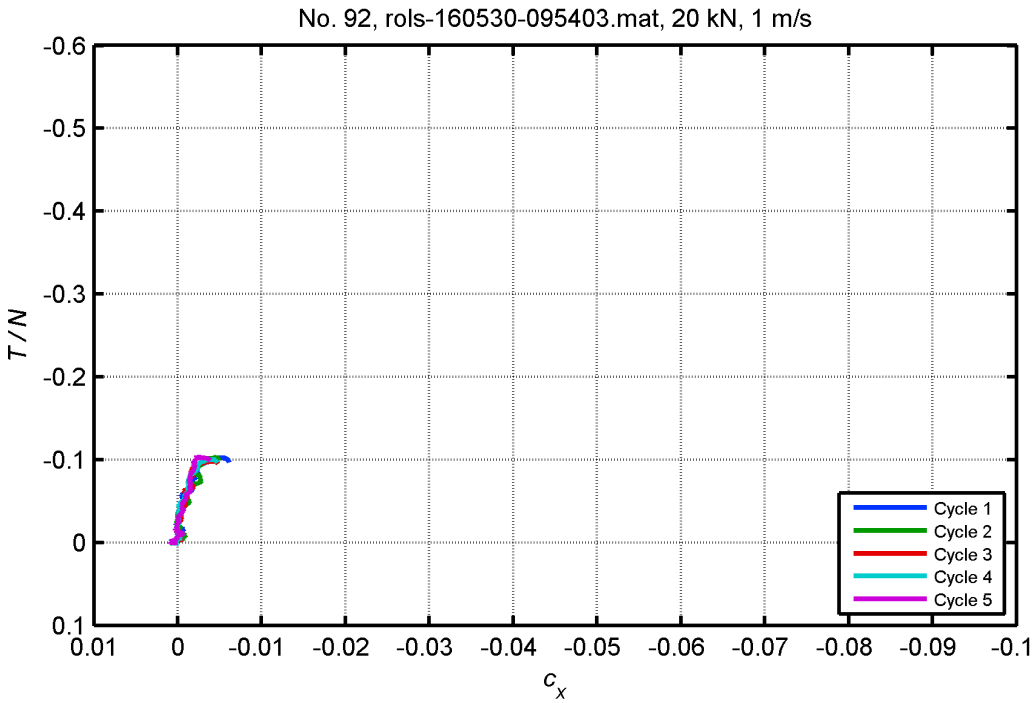

Figure 24: Creep curves from water + drying tests performed under 20 kN normal load at 1 m/s.

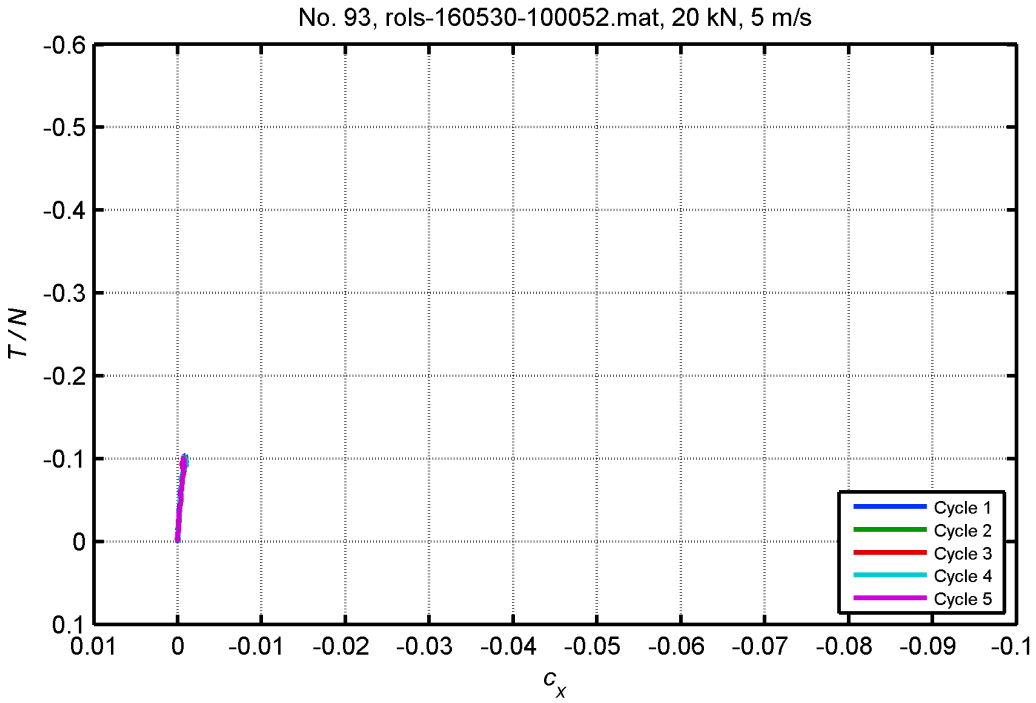

Figure 25: Creep curves from water + drying tests performed under 20 kN normal load at 5 m/s.

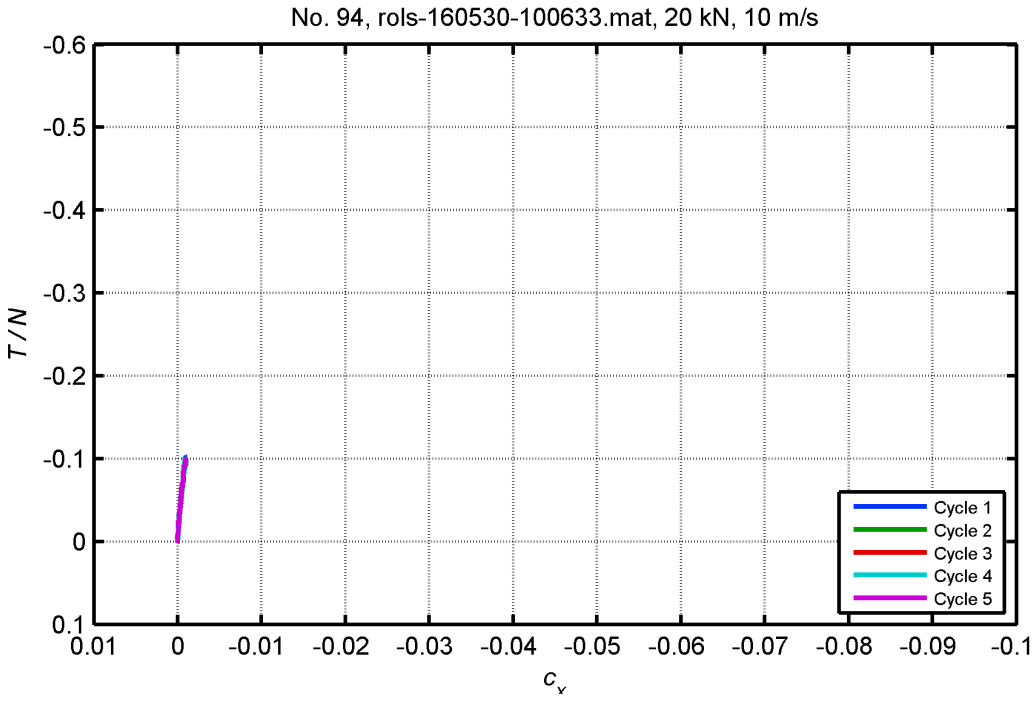

Figure 26: Creep curves from water + drying tests performed under 20 kN normal load at 10 m/s.

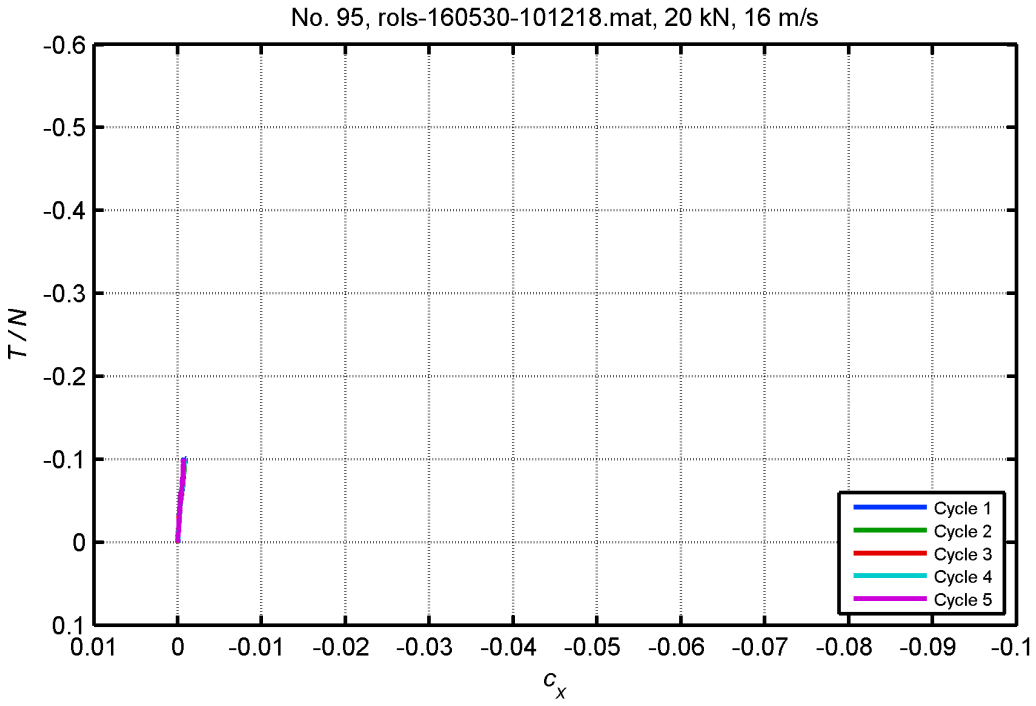

Figure 27: Creep curves from water + drying tests performed under 20 kN normal load at 16 m/s.

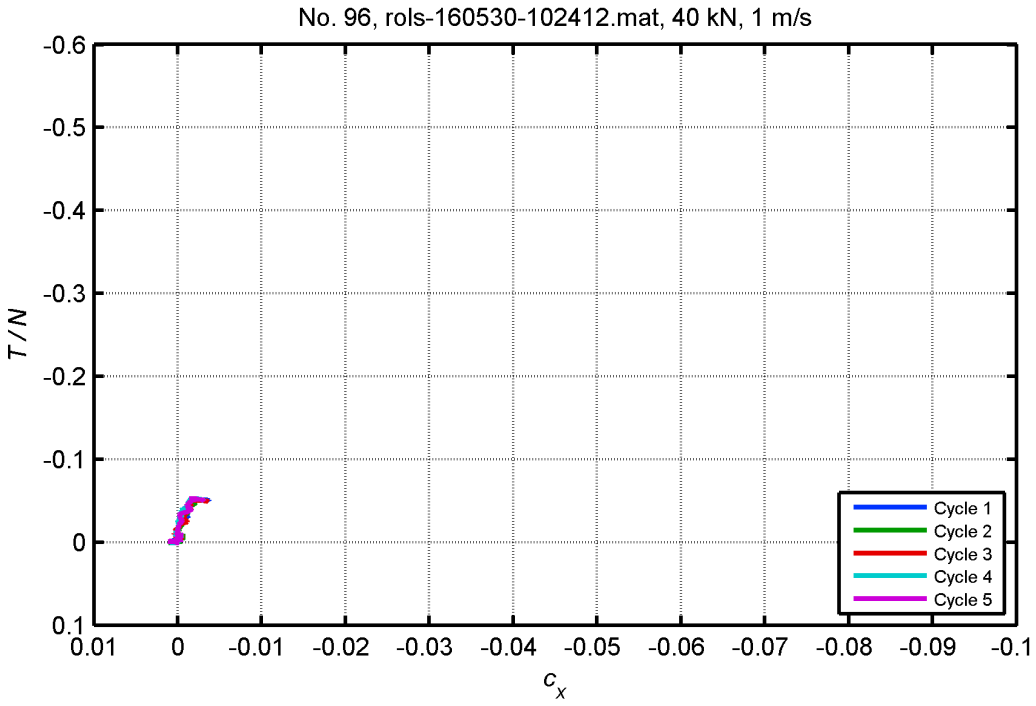

Figure 28: Creep curves from water + drying tests performed under 40 kN normal load at 1 m/s.

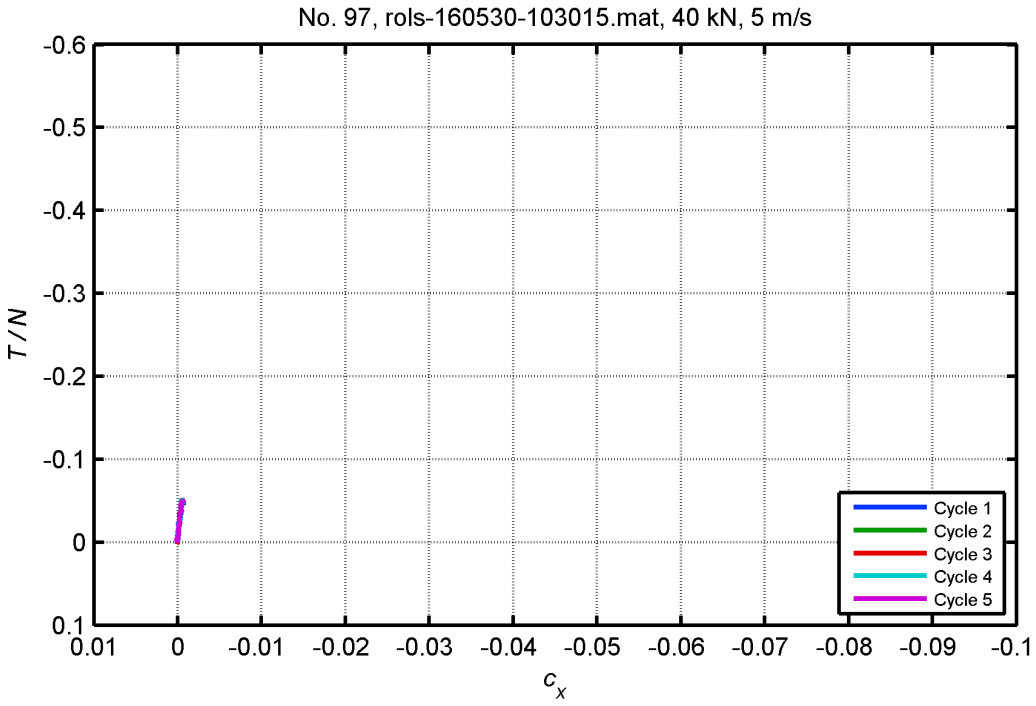

Figure 29: Creep curves from water + drying tests performed under 40 kN normal load at 5 m/s.

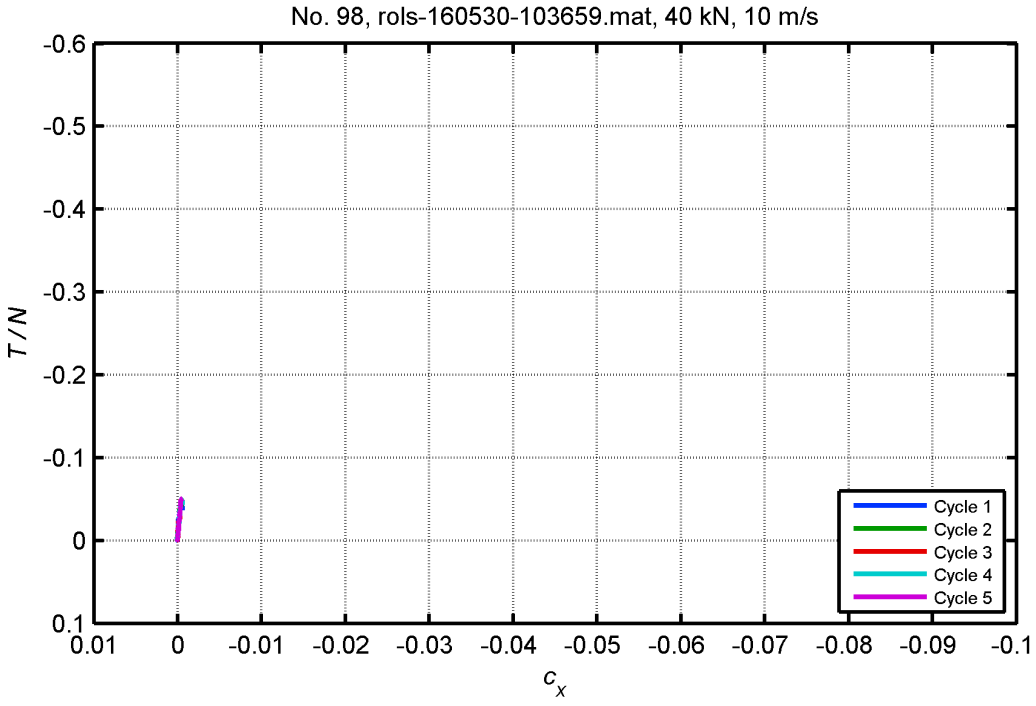

Figure 30: Creep curves from water + drying tests performed under 40 kN normal load at 10 m/s.

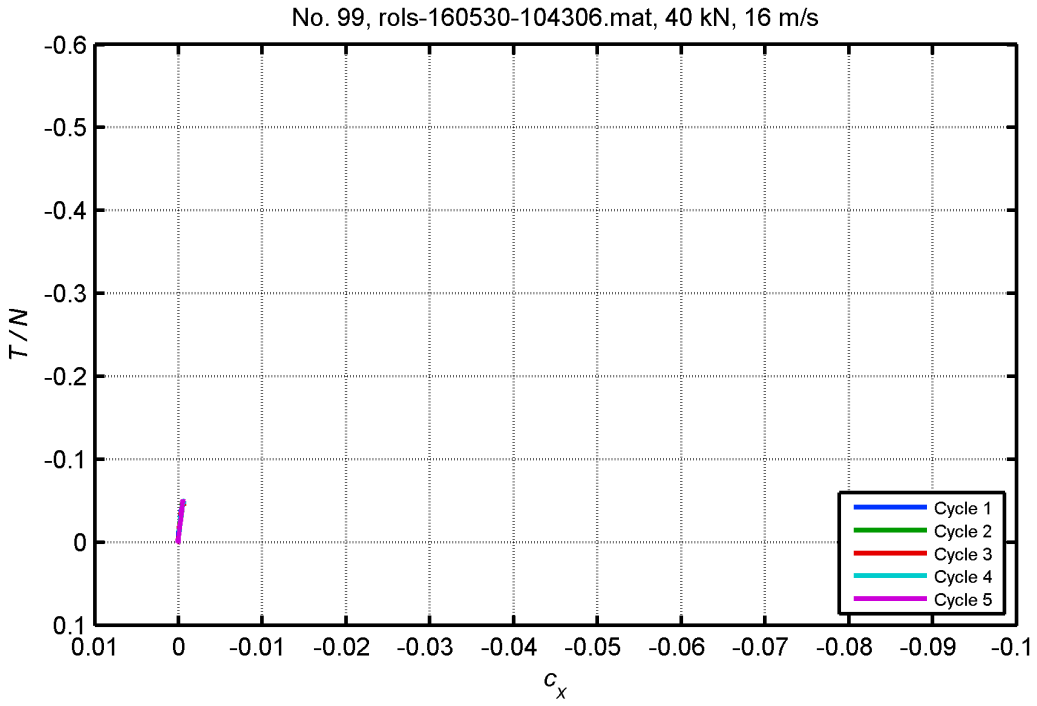

Figure 31: Creep curves from water + drying tests performed under 40 kN normal load at 16 m/s.

Wet (bulk)

Figures 46 – 50 ran as one continuous test.

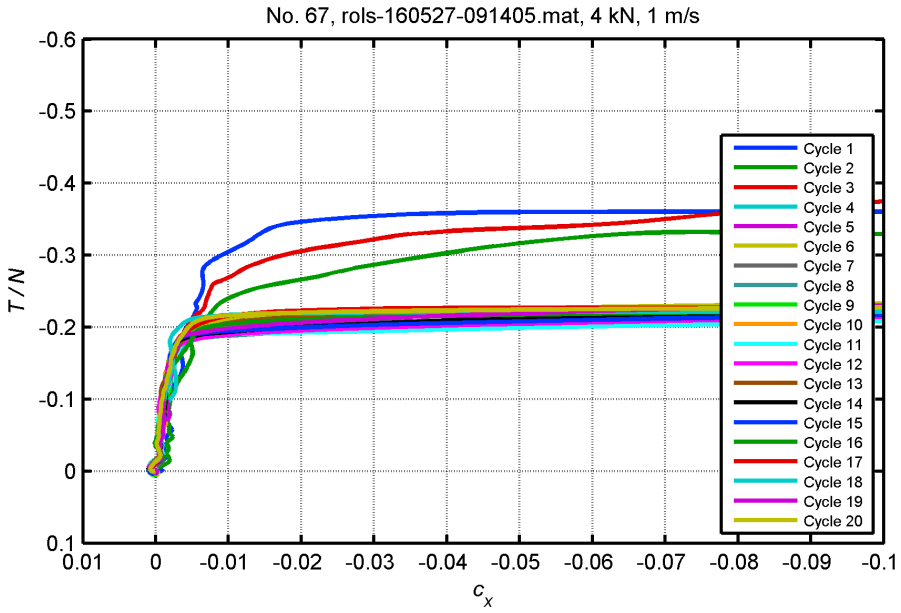

Figure 32: Part 1: Creep curves from bulk water application tests performed under 4 kN normal load at 1 m/s (Cycles 1 – 3 under dry conditions).

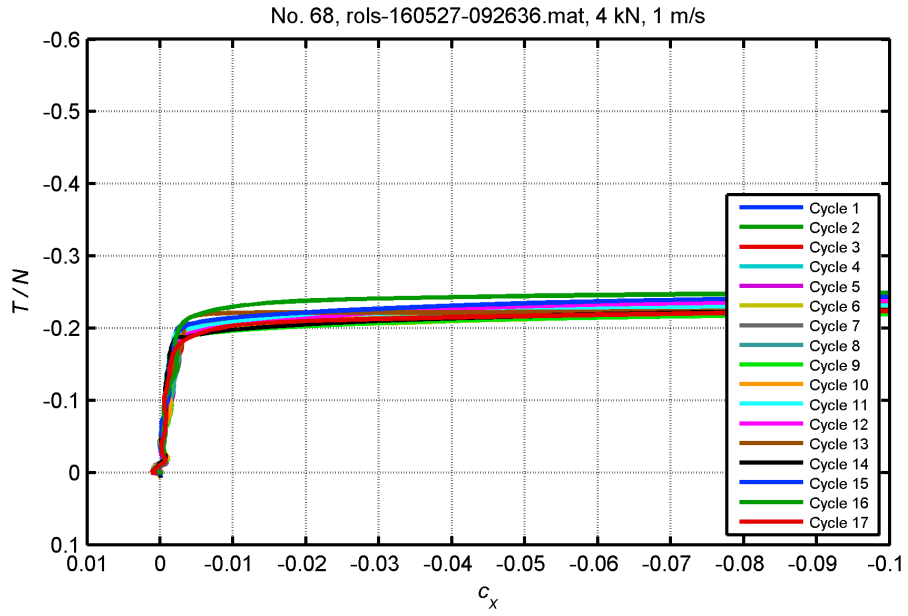

Figure 33: Part 2: Creep curves from bulk water application tests performed under 4 kN normal load at 1 m/s.

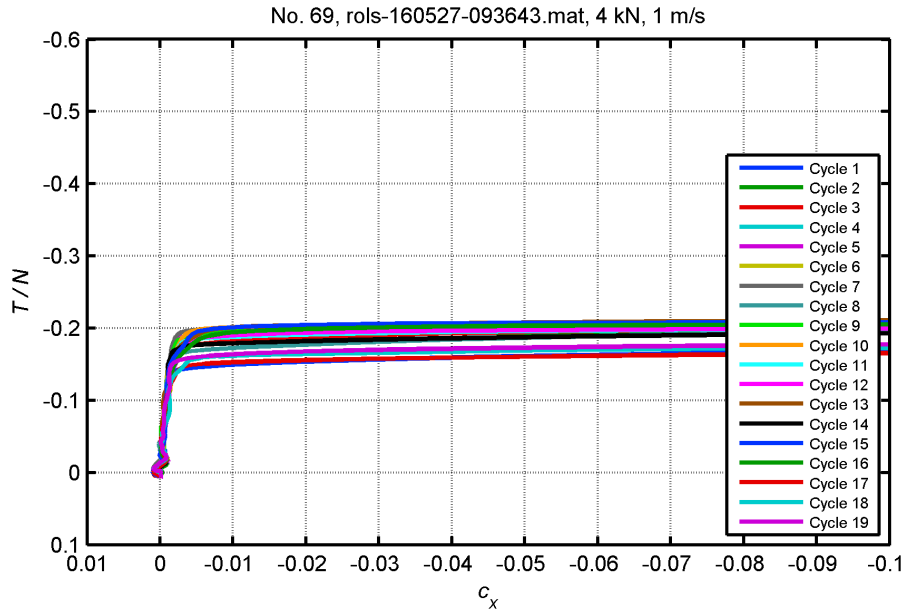

Figure 34: Part 3: Creep curves from bulk water application tests performed under 4 kN normal load at 1 m/s.

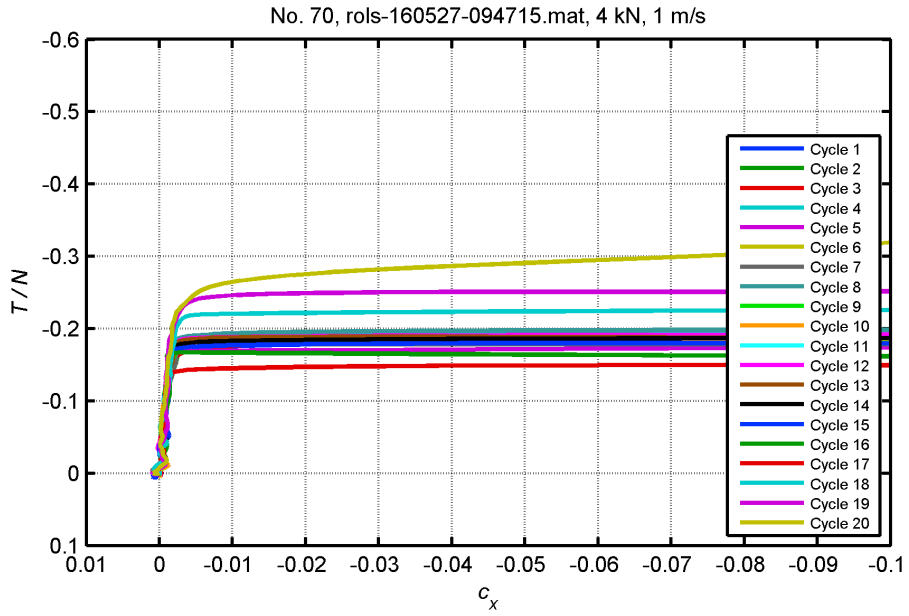

Figure 35: Part 4: Creep curves from bulk water application tests performed under 4 kN normal load at 1 m/s.

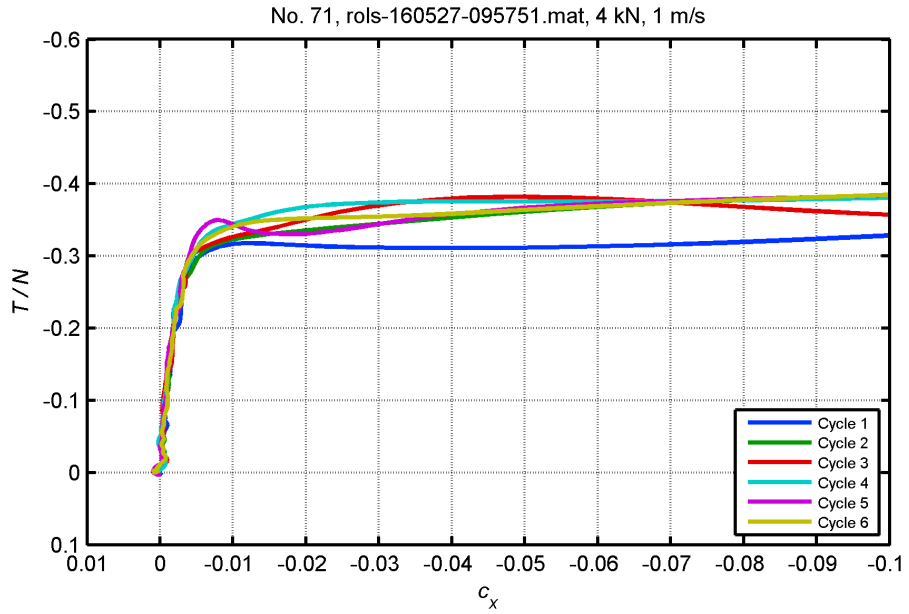

Figure 36: Part 5: Creep curves from bulk water application tests performed under 4 kN normal load at 1 m/s.

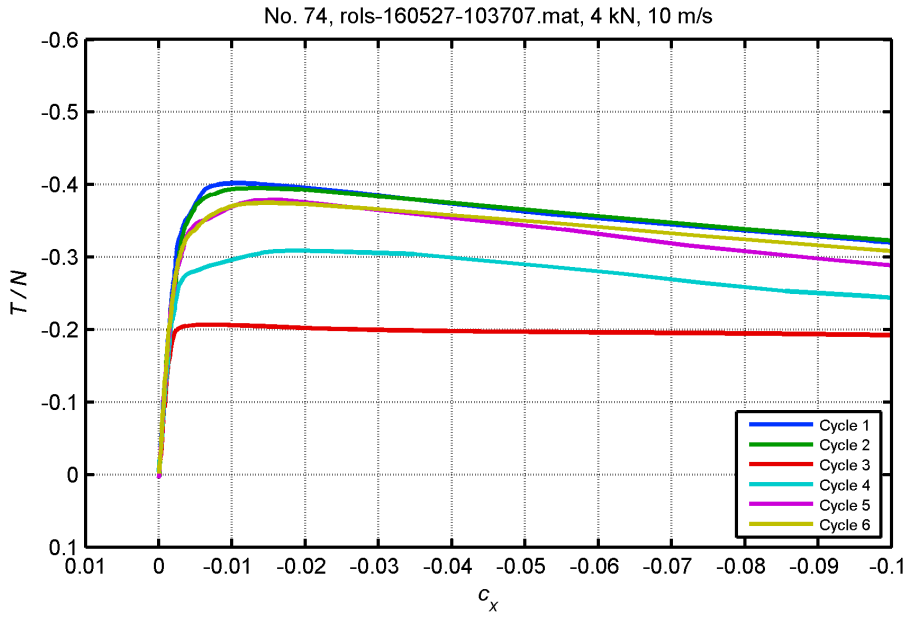

Figure 37: Creep curves from bulk water application tests performed under 4 kN normal load at 10 m/s.

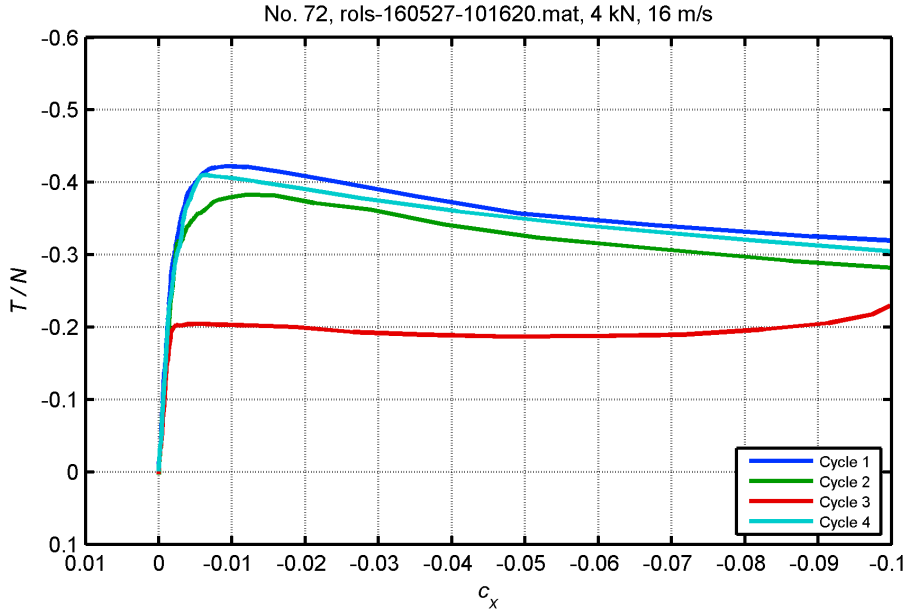

Figure 38: Creep curves from bulk water application tests performed under 4 kN normal load at 16 m/s.

Figures 53 – 56 ran as one continuous test.

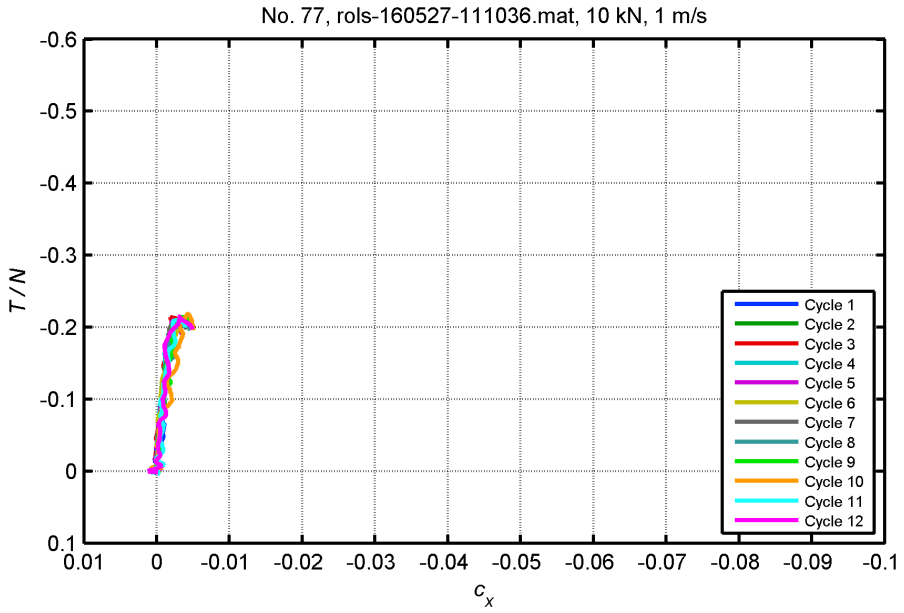

Figure 39: Part 1: Creep curves from bulk water application tests performed under 10 kN normal load at 1 m/s.

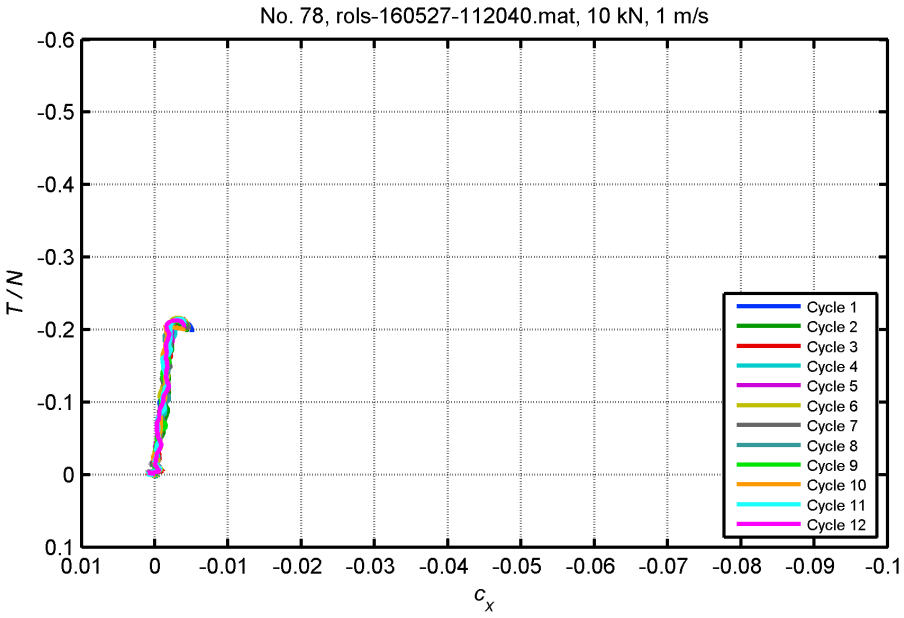

Figure 40: Part 2: Creep curves from bulk water application tests performed under 10 kN normal load at 1 m/s.

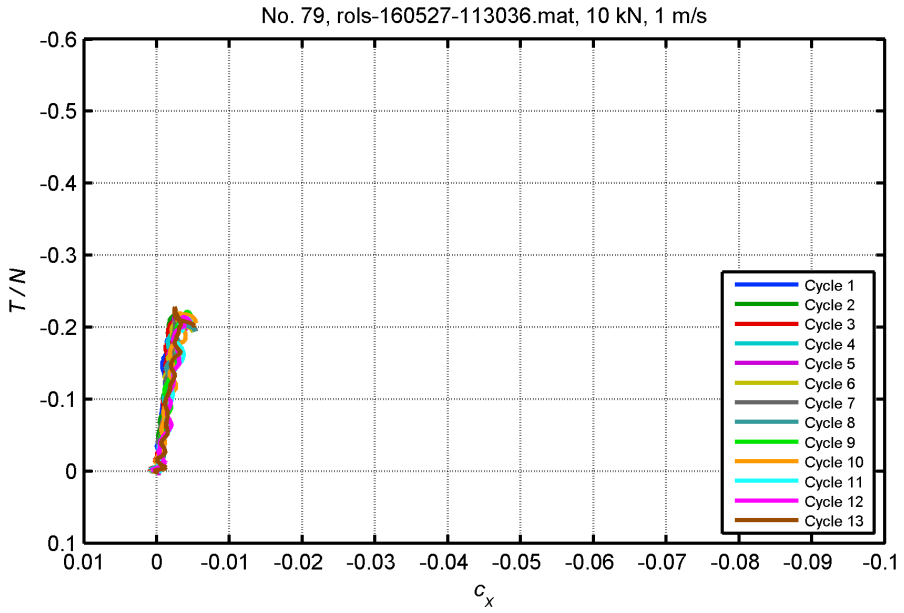

Figure 41: Part 3: Creep curves from bulk water application tests performed under 10 kN normal load at 1 m/s.

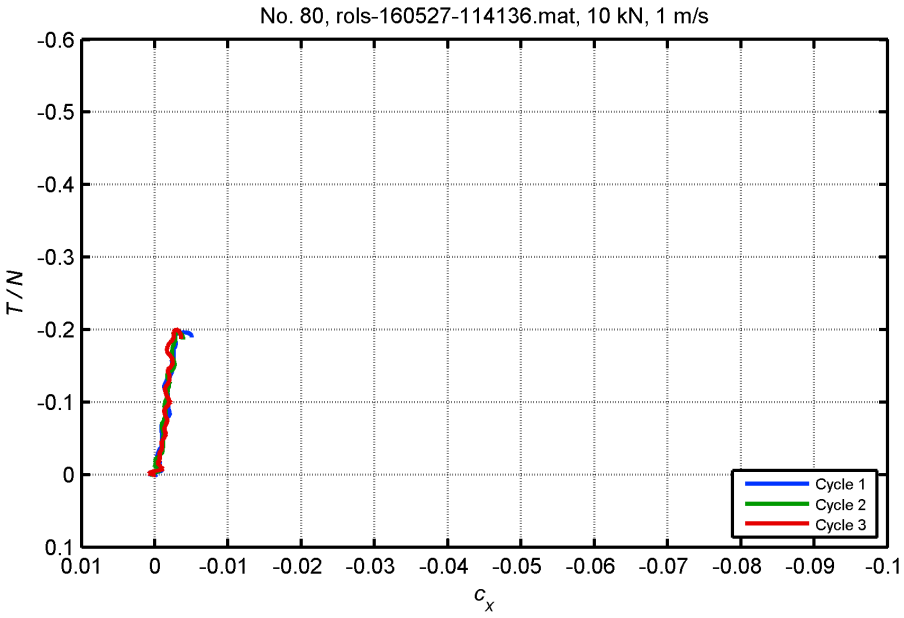

Figure 42: Part 4: Creep curves from bulk water application tests performed under 10 kN normal load at 1 m/s.

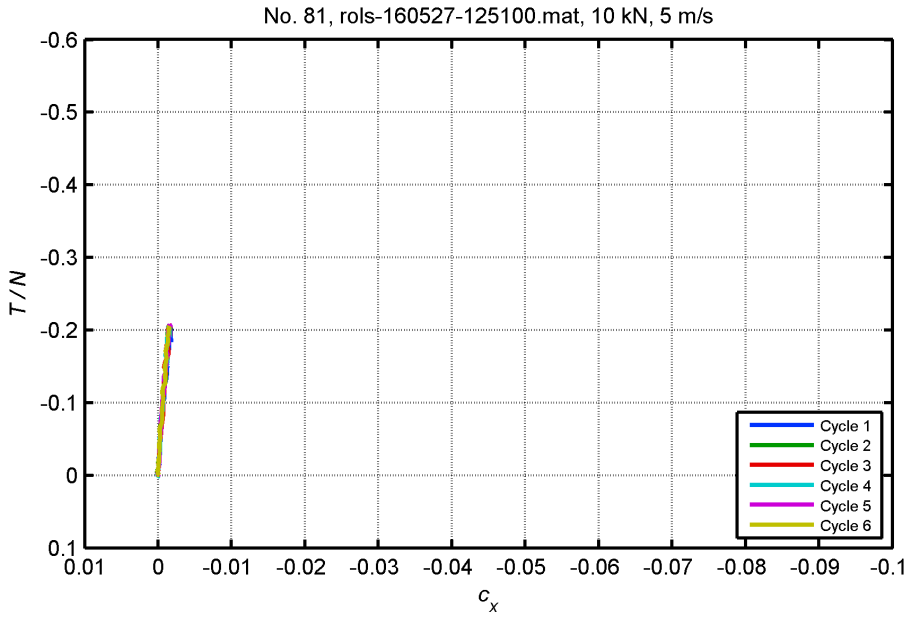

Figure 43: Creep curves from bulk water application tests performed under 10 kN normal load at 5 m/s.

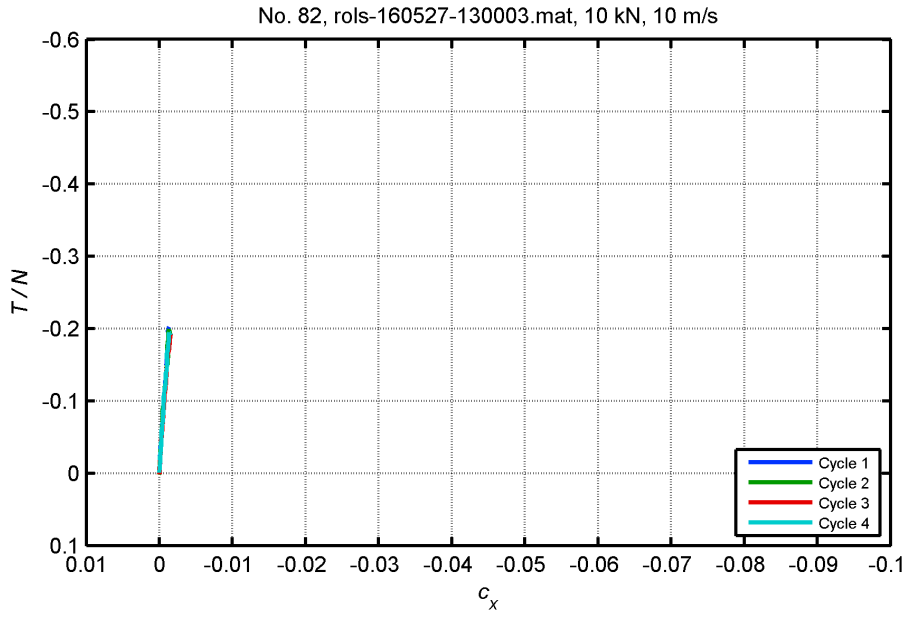

Figure 44: Creep curves from bulk water application tests performed under 10 kN normal load at 10 m/s.

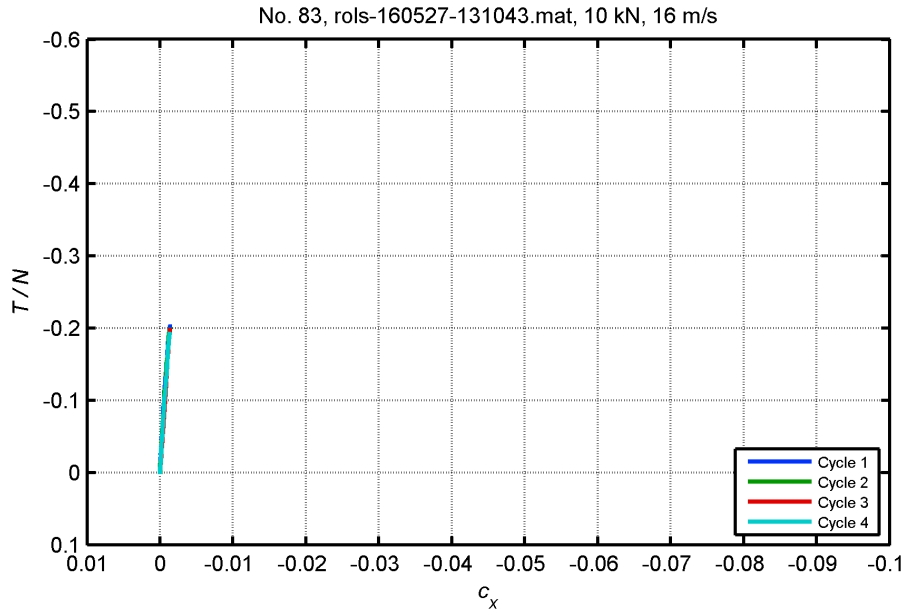

Figure 45: Creep curves from bulk water application tests performed under 10 kN normal load at 16 m/s.

Figures 60 – 61 ran as one continuous test.

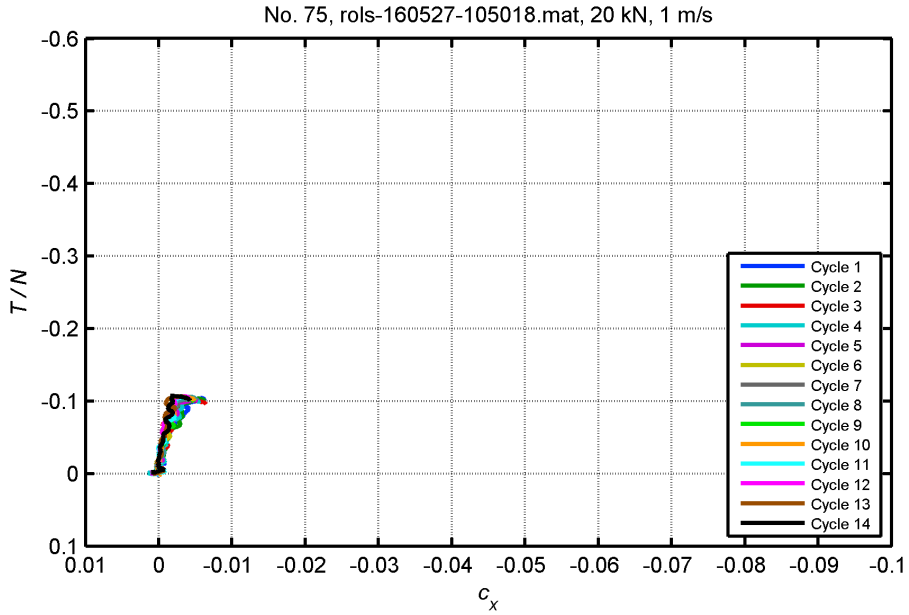

Figure 46: Part 1: Creep curves from bulk water application tests performed under 20 kN normal load at 1 m/s.

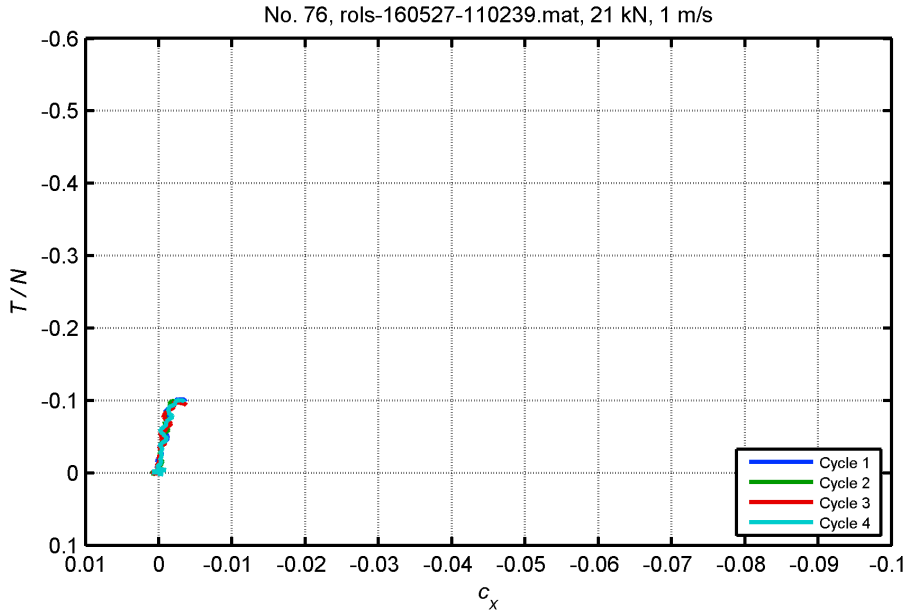

Figure 47: Part 2: Creep curves from bulk water application tests performed under 10 kN normal load at 1 m/s.

Test data from 20 kN at 5, 10 and 16 m/s and all tests at 40 kN not completed due to motor traction limitation.